Biological effects of polyacrylic acid-coated and non-coated superparamagnetic iron oxide nanoparticles in *in vitro* and *in vivo* experimental models

Diana Manuel Mocho de Bastos Couto

Tese do 3ºCiclo de Estudos conducente ao grau de Doutor em Ciências Farmacêuticas na especialidade de Química Farmacêutica e Medicinal apresentada à Faculdade de Farmácia da Universidade do Porto

Thesis of the 3rd Cycle of Studies for obtaining the PhD degree in Pharmaceutical Sciences in the specialty of Pharmaceutical and Medicinal Chemistry submitted to the Faculty of Pharmacy of the University of Porto

Work performed under the supervision of:

Professora Doutora Eduarda das Graças Rodrigues Fernandes

Professor Doutor Félix Dias Carvalho

April 2015

Assinatura do autor,

“Science knows no country, because

knowledge belongs to humanity, and

is the torch which illuminates the world”

Louis Pasteur

To my parents

To my sister

To my nephew Alexandre

ACKNOWLEDGEMENTS

During this period of my life, many were the people that supported me and contributed to my achievements. Although it is impossible to mention and thank to all of these people, I could not leave without thanking to some of them, which revealed to be a true inspiration, a precious help and a source of encouragement to me:

Ao Professor Doutor José Luís Costa Lima, não só por me ter permitido a integração no seu grupo de trabalho, ainda no antigo Departamento de Química Física e, mais recentemente Química Aplicada, como também por ter sempre colocado à minha disposição todos os meios, equipamentos e reagentes que necessitei para a realização deste trabalho. Não queria deixar de agradecer a simpatia com a qual sempre me tratou, os conselhos turísticos que me deu, assim como destacar o seu grande empenho e dedicação no que toca à gestão e ao bom funcionamento do departamento. Por fim, queria agradecer o facto de permitir que todas as deslocações e participações em congressos fossem possíveis.

À Professora Doutora Eduarda Fernandes, por me ter recebido como sua aluna, numa fase inicial de iniciação à investigação e, posteriormente, como aluna de doutoramento. Dona de um grande rigor científico e académico e de um precurso profissional de valor indiscutível, agradeço a transmissão de conhecimentos, assim como a disponibilidade, a prontidão na discussão de resultados e revisão do trabalho e as oportunidades que me concedeu. Agradeço também, como não poderia deixar de ser, a orientação e o facto de sempre ter colocado no meu caminho as pessoas certas no momento certo.

Ao Professor Doutor Félix Carvalho, meu co-orientador, por ter aceitado co-orientar o meu trabalho, enriquecendo-o sempre com as suas ideias preciosas e a sua supervisão rigorosa, fruto de uma experiência profissional vasta e repleta de êxitos. Agradeço a transmissão de conhecimentos, a disponibilidade, a prontidão e o incentivo transmitido ao longo de todo este precurso.

À Marisa Freitas, com quem partilhei o laboratório durante estes quatro anos, um muito obrigado por toda a ajuda dispensada a todos os níveis: pelo acolhimento, pela amizade, pelos conselhos dados, por estar sempre perto quando necessário, pela discussão sempre atempada dos resultados, pela revisão do trabalho, pelas suas opiniões sempre válidas e preciosas, por ter feito tudo o que estava ao alcance dela e ainda mais… Por ter sido, sem dúvida, uma peça chave neste doutoramento…

À Daniela Ribeiro, minha colega de curso e de doutoramento, agradecer todo o companheirismo, disponibilidade, acessibilidade e ajuda sempre prestada ao longo de todo este tempo.

Ao Renan Chisté, pela ajuda prestada, amizade e alegria transmitida ao longo destes 4 anos de doutoramento.

Aos restantes, atuais e antigos, colegas da FRAU (Free Radicals and Antioxidant Unit), um muito obrigada pela amizade, companheirismo e simpatia.

À Engenheira Manuela Barros e Patrícia Monteiro pela simpatia e prontidão em satisfazer as nossas necessidades.

Ao Professor Doutor Agostinho Almeida, assim como à Anne-Sophie Alves, pela valiosa ajuda e contribuição nos ensaios do doseamento de ferro.

À Vera Costa, do Laboratório de Toxicologia, por me ter introduzido ao mundo da experimentação animal, e por o ter feito de uma forma exímia. Um muito obrigado por toda a ajuda prestada em todo o planeamento e execução dos estudos *in vivo* integrantes desta tese, assim como pela revisão do respectivo trabalho.

Aos restantes membros dos Departamentos de Química Aplicada e Toxicologia, agradeço a simpatia, disponibilidade e ajuda sempre prestada.

A los Profesores Doctores M. Arturo Lopez-Quintela, José Rivas y Paulo Freitas, del International Iberian Nanotechnology Laboratory por su contribución en la síntesis y caracterización físicoquímica de las nanopartículas de óxido de hierro, objeto de estudio de esta tesis.

Muchas gracias a Carlos Gonzalez, así como a los otros colegas del International Iberian Nanotechnology Laboratory, por toda la ayuda prestada en los experimentos de caracterización de las nanopartículas.

À Professora Doutora Graça Porto, do Hospital Geral de Santo António, pela sua contribuição para a realização deste trabalho e por ter permitido a obtenção das amostras de sangue, indispensáveis à realização deste.

Às enfermeiras do Hospital Geral de Santo António pela prontidão com que sempre me disponibilizaram as amostras de sangue necessárias à realização deste estudo, assim como que aos dadores de sangue deste mesmo hospital, que generosamente contribuíram para este trabalho com a sua dádiva de sangue.

À Professora Doutora Beatriz Porto, do Instituto de Ciências Biomédicas Abel Salazar, assim como às suas colaboradoras Rosa Sousa e Lara Andrade, por me terem recebido tão bem no seu laboratório de citogenética e me despertarem o interesse pela citogenética, uma área para mim desconhecida até então. Obrigada por toda a ajuda prestada, assim como pela amizade, acessibilidade e pelos bons momentos passados…

À Professora Doutora Paula Silva, do Instituto de Ciências Biomédicas Abel Salazar, pela simpatia, acessibilidade, assim como por toda a ajuda prestada nos ensaios de histologia realizados no âmbito desta tese.

À Doutora Margarida Lima, assim como à Magdalena Leander, do Hospital Geral de Santo António, pela ajuda prestada nos ensaios de citometria de fluxo e por terem colocado à minha disposição não só as instalações e equipamentos do Serviço de Hematologia Clínica, assim como também o seu conhecimento.

Ao Professor Doutor José Alberto Duarte, da Faculdade de Desporto da Universidade do Porto, por toda a simpatia, ajuda, prestabilidade e por ter colocado à minha disposição as instalações do seu laboratório para a realização dos ensaios de histologia que são parte integrante desta tese.

À D. Celeste Resende, da Faculdade de Desposto da Universidade do Porto, por toda a prestabilidade, amizade e pela ajuda valiosa nos ensaios de histologia realizados no âmbito desta tese.

Ao Bruno Silveira pelo apoio gráfico na elaboração da tese.

À Andreia Ferreira, Helena Gonçalves, Sanjay Radia, Vanessa Lima e Paulo Santos, pioneiros no que toca à imigração, por toda a amizade, partilha das vossas experiências de trabalho e/ou doutoramento, encontros e reencontros, em Portugal e no estrangeiro, e incentivo constante… Por me acolherem sempre em vossas casas e por estarem sempre presentes na minha vida mesmo quando estão ausentes.

À Ana Isabel Couto, Daniela Sampaio, Florbela Santos, Joana Magalhães, Joana Sampaio, João Costa, Raquel Magalhães e Raquel Rodrigues, meus grandes amigos e

colegas de curso, por todos os convívios, desabafos, viagens, saídas e muitos outros momentos de diversão.

À Cristiana Jardim, Susana Silva, Cláudio Araújo, João Maia, Ricardos Gonçalves (em duplicado!), André Rebelo, Arlete Capela, Joel Teixeira e Arlindo Gomes, igualmente por me darem o privilégio de ser vossa amiga.

A Aarón, por todo el apoyo incondicional en los buenos y malos momentos.

Aos meus pais, pelas boleias tardias, pelo incentivo constante nos momentos altos e baixos e por me apoiarem sempre incondicionalmente nas decisões mais importantes da minha vida.

À minha irmã por toda a compreensão, por ter sempre uma palavra amiga nos momentos mais difíceis e pelo incentivo e conselhos valiosos. Às minhas primas, tios e restante família, pela motivação sempre transmitida.

Ao meu sobrinho e afilhado Alexandre, nascido pouco antes do início deste doutoramento, por ter crescido com o desenrolar deste: pelas vezes em que esteve ao meu colo a ver-me trabalhar, rindo-se alegremente dos gráficos que ia vendo aparecerem diante do ecrã do computador, pelas vezes que me chamava para as suas brincadeiras, pela alegria que sempre me transmitiu.

À Faculdade de Farmácia da Universidade do Porto, por me ter aceitado como aluna de doutoramento. À Fundação para a Ciência e Tecnologia pelo suporte financeiro e pela bolsa de doutoramento concedida (SFRH/BD/72856/2010), no âmbito do "QREN-POPH-Tipologia 4.1 – Formação Avançada", co-financiado pelo Fundo Social Europeu e pelos fundos nacionais do Ministério da Ciência, Tecnologia e Ensino Superior.


FCT
Fundação para a Ciência e a Tecnologia
MINISTÉRIO DA CIÊNCIA, INOVAÇÃO E DO ENSINO SUPERIOR


POPH
QUALIFICAR É CRESCER.


QUADRO
DE REFERÊNCIA
ESTRATÉGICO
NACIONAL
PORTUGAL 2007.2013


UNIÃO EUROPEIA
Fundo Social Europeu


Governo da República Portuguesa

ABSTRACT

Nanotechnology is in the limelight concerning the development of new therapeutic and diagnostic concepts in all areas of medicine. In this context, iron oxide nanoparticles (IONs) have shown to present a wide scope of applications in biomedicine, namely in magnetic resonance imaging, tissue repair, drug delivery, hyperthermia, transfection, tissue soldering, and as antimicrobial agents. However, their use has generated many concerns among public, scientific and regulatory authorities regarding their long-term impact on human health, as many lines of evidence show that some IONs may have adverse effects on living organisms.

Regarding immune system, the studies assessing the effect of IONs on the cells of this system, namely neutrophils, lymphocytes, monocytes, are scarce and some of them contradictory. Moreover, the toxicity of IONs with some coatings that are described as promising for some biomedical applications, namely polyacrylic acid (PAA), remains to be studied. Therefore, we felt the need to deepen the knowledge existing so far in this area of the immune system.

Our first approach was to evaluate the effects of PAA-coated and non-coated magnetite IONs on human neutrophils, namely their capacity to activate the oxidative burst and to modify their lifespan through necrosis and/or apoptosis. It was demonstrated that PAA-coated and non-coated IONs trigger neutrophils' oxidative burst in a nicotinamide adenine dinucleotide phosphate (NADPH) oxidase dependent manner, and that PAA-coated IONs increase, while non-coated IONs prevent, apoptotic signaling and apoptosis.

The second objective of this dissertation was to assess the effect of PAA-coated and non-coated IONs on their capacity to induce cytokine production [interleukin (IL)-1β, tumor necrosis factor alpha (TNF-α), IL-6, IL-8, interferon gamma (IFN-γ) and IL-10] by *ex-vivo* human blood cells and the pathways involved in this induction. Our results showed that PAA-coated and non-coated IONs are able to induce all the tested cytokines and that activation of transforming growth factor beta-activated kinase (TAK1), p38 mitogen-activated protein kinase (MAPK) and c-Jun-N-terminal kinase (JNK) are involved in this effect.

Subsequently, we studied the ability of PAA-coated and non-coated IONs to induce genotoxicity in human T lymphocytes through influence on cell cycle progression and on the induction of chromosome aberrations, as well as to exert cumulative effect with the iron-dependent genotoxic agent bleomycin (BLM). In this study, we demonstrated that the tested IONs are not genotoxic, do not trigger the cell cycle arrest and do not potentiate the clastogenic effects of BLM in human T lymphocytes.

The *in vitro* studies previously mentioned and performed led us to our last work, a *in vivo* study using male CD-1 mice from Charles River. In this study, we studied the biodistribution as well as the effect of acute intravenous PAA-coated IONs administration in male CD-1 mice, namely their ability to induce pro-inflammatory processes and induce toxicity. The obtained results show that these IONs accumulate mainly in phagocytic cells in the periportal zone of the liver and in splenic red pulp of the spleen and, to a lesser extent, in lung. Moreover, our data put in evidence that, even though PAA-coated IONs do not cause severe organ damage, a light inflammatory process seems to be triggered, as evidenced by an increased neutrophils' and large lymphocytes' frequency in blood and by an accumulation in phagocytes in liver and spleen. The studied IONs also showed to trigger lipid peroxidation in liver tissue; however, they did not produce any alteration in the parameters total glutathione (GSHt), reduced glutathione (GSH) and oxidized glutathione (GSSG) in liver and kidney.

Keywords: Iron oxide nanoparticles; biological effects; inflammation; blood cells; *in vivo* studies.

RESUMO

A nanotecnologia desempenha atualmente um papel preponderante no desenvolvimento de novos métodos terapêuticos e de diagnóstico em todas as áreas da medicina. Neste contexto, as nanopartículas de óxido de ferro (IONs) têm demonstrado apresentar uma grande variedade de aplicações em biomedicina, nomeadamente em ressonância magnética nuclear, reparação tecidular, direcionamento de fármacos, hipertermia, transfeção, fusão tecidular e agentes antimicrobianos. Contudo, a sua utilização tem sido alvo de preocupação por parte das autoridades públicas, científicas e reguladoras relativamente aos possíveis efeitos a longo prazo na saúde humana, pois diversas evidências mostram que algumas IONs podem ter efeitos adversos nos organismos vivos.

No que diz respeito ao sistema imune, os estudos existentes que avaliam o efeito das IONs nas células deste sistema, nomeadamente neutrófilos, linfócitos, monócitos, são escassos e alguns deles até mesmo contraditórios. Adicionalmente, a toxicidade das IONs com alguns revestimentos que são descritos como sendo promissores em algumas aplicações biomédicas, nomeadamente ácido poliacrílico (PAA), não tem sido estudada. Por este motivo, sentimos a necessidade de aprofundar o conhecimento existente até ao momento nesta área do sistema imune.

A nossa primeira abordagem foi avaliar os efeitos das IONs revestidas com PAA e não revestidas, na forma magnetite, em neutrófilos humanos, nomeadamente na sua capacidade de ativar o “burst” oxidativo e de modificar o seu tempo de vida através de fenómenos apoptóticos e necróticos. Foi demonstrado que as IONs revestidas com PAA e não revestidas desencadeiam o “burst” oxidativo dos neutrófilos via ativação da enzima nicotinamida adenina dinucleótido fosfato (NADPH) oxidase, assim como que as IONs revestidas com PAA induzem, enquanto as IONs não revestidas inibem, o processo apoptótico e consequente sinalização.

O segundo objetivo desta dissertação foi avaliar o efeito das IONs revestidas com PAA e não revestidas na sua capacidade de induzir produção de citoquinas [interleuquina (IL)-1β, fator de necrose tumoral alfa (TNF-α), IL-6, IL-8, interferão gama (IFN-γ) e IL-10] pelas células sanguíneas humanas *ex-vivo* e as vias inflamatórias envolvidas nesta indução. Os resultados obtidos revelaram que as IONs revestidas com PAA e não revestidas são capazes de induzir todas as citoquinas testadas e que a activação da

cinase ativada pelo fator de transformação do crescimento beta (TAK1), proteína cinase ativada pelo mitógeno (MAPK) p38 e cinase c-Jun-N-terminal (JNK) estão envolvidas nesta indução.

Seguidamente estudámos a capacidade das IONs revestidas com PAA e não revestidas de induzir genotoxicidade em linfócitos T humanos através da influência na progressão no ciclo celular e na indução de aberrações cromossómicas, assim como da execução de um efeito cumulativo com a bleomicina (BLM), um conhecido agente genotóxico dependente do ferro. Neste estudo, demonstrámos que as IONs testadas não são genotóxicas, não desencadeiam paragem do ciclo celular e não potenciam os efeitos clastogénicos da BLM em linfócitos T humanos.

Os estudos *in vitro* previamente mencionados e executados conduziram-nos ao nosso último trabalho, um estudo *in vivo* no qual recorremos a murganhos machos da estirpe CD-1 da Charles River. Neste estudo, estudámos a distribuição, assim como o efeito da administração aguda e intravenosa de IONs revestidas com PAA em ratinhos CD-1, nomeadamente a sua capacidade de induzir processos pro-inflamatórios e toxicidade. Os resultados obtidos mostram que estas IONs se acumulam principalmente em fagócitos na zona periportal do fígado e na polpa vermelha do baço e, numa menor extensão, no pulmão. Adicionalmente, os nossos dados colocam em evidência o facto de, apesar das IONs revestidas com PAA não aparentarem causar danos orgânicos severos, um processo inflamatório ligeiro parece ser desencadeado, como é evidenciado pelo aumento na frequência de neutrófilos e linfócitos grandes no sangue, assim como pela acumulação em fagócitos no fígado e baço. Estas IONs mostraram também provocar peroxidação lipídica no fígado. Contudo, elas não produziram qualquer alteração em parâmetros como glutationa total (GSHt), glutationa reduzida (GSH) e glutationa oxidada (GSSG) no fígado e no rim.

Palavras-chave Nanopartículas de óxido de ferro; efeitos biológicos; inflamação; células sanguíneas; estudos *in vivo*.

INDEX

CHAPTER III. INTEGRATED DISCUSSION AND CONCLUSIONS

INDEX OF FIGURES

CHAPTER I. GENERAL INTRODUCTION

I.1.1.

I.1.2.

CHAPTER II. ORIGINAL RESEARCH

II.1.

II.2.

II.3.

II.4.

INDEX OF TABLES

CHAPTER I. GENERAL INTRODUCTION

I.1.1.

I.1.2.

CHAPTER II. ORIGINAL RESEARCH

II.3.

II.4.

LIST OF ABBREVIATIONS AND CHEMICAL SYMBOLS

AIF – Apoptosis inducing factor

Akt – Protein kinase B

ALT – Alanine aminotransferase

AP-1 – Activator protein 1

AST – Aspartate aminotransferase

ATF-2 – Activating transcription factor 2

ATP – Adenosine triphosphate

BALF – Bronchoalveolar lavage fluid

BLM – Bleomycin

CK – Creatine kinase

CLIO – Cross-linked iron oxide nanoparticles

CNS – Central nervous system

DHR – Dihydrorhodamine 123

DMSA – 2,3-Dimercaptosuccinic acid

DNA – Deoxyribonucleic acid

DPI – Diphenyleneiodonium chloride

EDTA – Ethylenediamine tetraacetic acid

ERK – Extracellular signal-related kinases

FADD – Fas-associated death domain

FITC – Fluorescein isothiocyanate

GSH – Reduced glutathione

GSHt – Total glutathione

GSSG – Oxidized glutathione

H_2O_2 – Hydrogen peroxide

H&E – Haematoxylin-eosin

$HO^{\bullet}$ – Hydroxyl radical

HOCl – Hypochlorous acid

HPLC – High performance liquid chromatography

IFN-γ – Interferon gamma

IkB – Inhibitor of kB

IL – Interleukin

ION – Iron oxide nanoparticles

i.p. – Intraperitoneal

i.v. – Intravenous

JNK – c-Jun-N-terminal kinase

LDH – Lactate dehydrogenase

M1 – Macrophages subset 1

M2 – Macrophages subset 2

MAPK – Mitogen-activated protein kinase

MAPKKK – MAPK kinases kinases

MCP-1 – Monocyte chemoattractant protein-1

MDA – Malondialdehyde

MION – Monocrystalline iron oxide nanoparticles

MKK – MAPK kinases

MRI – Magnetic resonance imaging

NADH – Reduced β-nicotinamide adenine dinucleotide

NADPH – Nicotinamide adenine dinucleotide phosphate

NF-kB – Nuclear factor kB

$^{\bullet}NO$ – Nitric oxide radical

NP – Nanoparticles

$O_2^{\bullet-}$ – Superoxide radical

$ONOO^-$ – Peroxynitrite anion

PAA – Polyacrylic acid

PBMC – Peripheral blood mononuclear cells

PBS – Phosphate buffer saline

PDTC – Pyrrolidine dithiocarbamate

PEG – Polyethylene glycol

PEI – Polyethylenimine

PI – Propidium iodide

PLL – Poly(L-lysine)

PMA – Phorbol 12-myristate 3-acetate

PTA – Polycationic transfection agents

PVA – Polyvinyl alcohol

PVP – Poly(vinylpyrrolidone)

RES – Reticuloendothelial system

RNS – Reactive nitrogen species

ROS – Reactive oxygen species

SB203580 – 4-[4-Fluorophenyl]-2-[4-methylsulfinylphenyl]-5-[4-pyridyl]1H-imidazole

SEM – Standard error of the mean

SP 600125 – Anthra[1,9-*cd*]pyrazol-6(2H)-one1,9-pyrazoloanthrone

SPION – Superparamagnetic iron oxide nanoparticles

SR – Scavenger receptors

TAK1 – Transforming growth factor beta activated kinase

TCL – Thermally cross linked

TGF-β – Transforming growth factor beta

Th1 – T-Helper lymphocytes 1

Th2 – T-Helper lymphocytes 2

TNF-α – Tumor necrosis factor alpha

USPION – Ultra-small superparamagnetic iron oxide nanoparticles

VSOP – Very small superparamagnetic iron oxide nanoparticles

OUTLINE OF THE DISSERTATION

The present dissertation is structured in three main chapters:

Chapter I – General Introduction

This chapter is divided in two sections:

I.1. Theoretical background

This section is divided in two subsections. The first subsection (I.1.1.) is a review article which provides an update on the different iron oxide nanoparticles and the substances and/or polymers that can be used to coat the iron oxide core, as well as their applications and biological properties, namely their biodistribution in the human organism and their cellular internalization pathways. The second subsection (I.1.2.) is an overview of the toxicological and pro-inflammatory mechanisms of iron oxide nanoparticles.

I.2. General and specific objectives of the dissertation

The general and specific objectives of the dissertation are provided in this section.

Chapter II – Original Research

This chapter is divided in four sections corresponding to submitted and/or published (II.1., II.2., II.3., II.4.) original manuscripts, which resulted from experimental studies performed in order to find an answer to the questions raised in the general and

specific objectives of this thesis. In this chapter, my contribution for all the works performed comprised all the performed studies, except the iron oxide nanoparticles synthesis and characterization.

Chapter III – Integrated Discussion and Conclusions

This chapter is divided in two sections: the first section contains an integrated discussion of the performed studies and the second section contains the general conclusions of the dissertation.

CHAPTER I

GENERAL INTRODUCTION

I.1. Theoretical background

I.1.1. IRON OXIDE NANOPARTICLES: AN INSIGHT INTO THEIR BIOMEDICAL APPLICATIONS

Manuscript accepted for publication in Current Medicinal Chemistry

Iron oxide nanoparticles: an insight into their biomedical applications

Diana Couto[a], Marisa Freitas[a], Félix Carvalho[b*], Eduarda Fernandes[a]*

[a]*UCIBIO-REQUIMTE, Laboratory of Applied Chemistry, Department of Chemical Sciences, Faculty of Pharmacy, University of Porto, Porto, Portugal*
[b]*UCIBIO-REQUIMTE, Laboratory of Toxicology, Department of Biological Sciences, Faculty of Pharmacy, University of Porto, Porto, Portugal*

Corresponding authors:
Eduarda Fernandes, PharmD; PhD
UCIBIO-REQUIMTE, Laboratory of Applied Chemistry
Department of Chemical Sciences
Faculty of Pharmacy, University of Porto, Porto, Portugal
Rua de Jorge Viterbo Ferreira n.º 228, 4050-313 Porto, Portugal
Phone: +351 220428675
Email: egracas@ff.up.pt

Félix Carvalho, PharmD; PhD
UCIBIO-REQUIMTE, Laboratory of Toxicology
Department of Biological Sciences
Faculty of Pharmacy, University of Porto, Porto, Portugal
Rua de Jorge Viterbo Ferreira n.º 228, 4050-313 Porto, Portugal
Phone: +351 220428600
Email: felixdc@ff.up.pt

Abstract

Iron oxide nanoparticles (IONs) are among the most common types of nanoparticles (NPs) used in biomedical applications. IONs can be presented in different forms [e.g. magnetite (Fe_3O_4), hematite (α-Fe_2O_3) and maghemite (γ- Fe_2O_3)], and are usually coated with substances and/or polymers according to the purpose for which they are intended to be used. In recent years, IONs use has been increasing exponentially in many fields of biomedicine, namely in magnetic resonance imaging, cell sorting, tissue repair, induction of hyperthermia and drug delivery, among others. This review aims to provide an update on the different IONs and the substances and/or polymers that can be used to coat the IONs core as well as their applications and biological properties, namely their biodistribution in the human body and their cellular internalization pathways.

Keywords: Biodistribution; biomedical applications; coatings; internalization routes; iron oxide nanoparticles; toxicity.

Contents

1. Introduction

Nanotechnology encompasses structures of 100 nm or smaller that may present several dimensions: nanoscale in one dimension (very thin surface coating), in two dimensions (nanotubes and nanowires) or in three dimensions, known as nanoparticles (NPs), which comprise nanomaterials. Nanomaterials are present in toothpastes, sunscreens, food products and even sanitaryware coatings. Currently, the use of nanomaterials is being extended to multiple areas such as cell labeling, gene delivery, drug targeting, biosensors, chemistry, material science, physics, medicine, microelectronics and hyperthermia therapy [1, 2, 3, 4]

NPs can present different characteristics and be engineered from almost all chemical substances. They have physical and chemical properties that differ from the atom or bulk counterparts and have been recognized to have great potential in several fields due to the unique properties conferred by their surface-area-to-volume ratios [5, 6, 7], namely:

- the ease with which they are captured by the cells;
- avoidance of clearance by the immune system compared to traditional macroscale materials;
- porous structure;
- lower melting points;
- increased light absorption.

Iron oxide nanoparticles (IONs) are among the most common types of NPs used in medical applications. IONs can exist in different forms and are usually coated with substances and/or polymers that are able to confer the expected properties according to the purpose for which they are intended. Their small dimensions make IONs more chemically reactive with particle size being inversely proportional to bioactivity and toxicity [8, 9, 10]. From a health and environmental perspective, this can be harmful if the NPs are toxic or in some way disturb biological functions and lead to undesirable health effects. In particular, people with pre-existing medical conditions are at greater risk [11, 12]. This review aims to provide an update on the different types of IONs and the substances and/or polymers that can be used to coat the IONs core as well as their applications and biological properties, namely their biodistribution in the human body and their internalization pathways into cells.

2. Types of IONs

IONs are particles with dimensions ranging from 1 to 100 nm, composed of iron oxide. IONs consist of a magnetic iron oxide core with a coating of non-magnetic surface chemistry and exist in many forms in nature, namely magnetite (Fe_3O_4), hematite (α-Fe_2O_3) and maghemite (γ-Fe_2O_3) [7, 9].

Magnetite is a mixture of FeO and Fe_2O_3 containing both Fe^{3+} and Fe^{2+} ions, with a cubic inverse spinel structure. It is thermodynamically unstable due to the oxidation of magnetite (from Fe^{2+} into Fe^{3+}) to form maghemite in the presence of moisture, air and light [13, 14, 15, 16, 17]:

$$Fe_3O_4+2H^+ \rightarrow \gamma\text{-}Fe_2O_3+Fe^{2+}+H_2O \quad \text{(Equation 1)}$$

Maghemite NPs (γ-Fe_2O_3) are composed of fully oxidized cubic crystals and are therefore extremely stable under aerobic conditions even when bacteria are present [14, 18].

Hematite (α-Fe_2O_3) is a mineral form of Fe^{3+} oxide presenting a rhombohedral corundum crystal structure. It is considered the most abundant iron oxide polymorph and its iron content is approximately 70%. Due to its application as a pigment, it is one of the most common industrially used forms of iron oxide, apart from magnetite [18, 19, 20, 21].

3. Sizes of IONs

IONs can be classified according to their size which greatly influences their magnetic and biological properties. Ultra-small superparamagnetic iron oxide nanoparticles (USPIONs) are less than 50 nm in diameter and comprise 2-3 nm single crystal iron oxide cores enclosed in a coating that makes them biocompatible. Particles with dimensions larger than 50 nm are denominated superparamagnetic iron oxide nanoparticles (SPIONs) [16, 22, 23, 24].

4. Coatings

Biomedical applications demand that the IONs present uniform chemical and physical properties and for that reason, have high magnetization values with a size lower than 100 nm being essential. The nature of the coating determines the total size of the colloid as well as the biodistribution and biokinetics of SPIONs *in vivo* [25].

Since introduction of the first contrast agents in magnetic resonance imaging (MRI) in the decade of 1980 [26], most of the SPIONs and USPIONs agents have been fabricated with different types of coating material including citrate, dextran, albumin, starch, polyethylene glycol (PEG) and silicones to achieve their dispersion status and uptake selectivity by macrophage or endothelial cells [27, 28]. The carboxylate group is the most common fixation site on an iron oxide core. Other anchoring agents have been researched, such as phosphate, sulfonate and phosphonates, despite their strong affinity towards the core of iron oxide [29, 30]. The utilization of bifunctional phosphonic acid-based coupling agents with polar end groups (-OH,-COOH,-NH_2) not only makes the NPs hydrophilic and stable regarding aggregation, but also conveys functionality on the surface to provide easy access to bioconjugates [31]. These coatings ideally should be nonantigenic and nonimmunogenic, have a high affinity for the iron oxide core and impede opsonization by plasma proteins [32].

The coating of SPIONs is indispensable because it:

- decreases the aggregation tendency of the non-coated NPs (which occurs due to their hydrophobic surfaces with large surface area to volume ratio and their van-der walls and magnetic dipole–dipole attractive forces [7, 33, 34]), thus improving their colloidal stability and dispersibility [35];
- prevents the oxidation of their surface [35], given that non-coated IONs tend to be transformed from magnetite (Fe_3O_4) to maghemite (γ-Fe_2O_3) [13];
- provides a surface for conjugation of targeting ligands and drug molecules such as proteins, antibodies, therapeutic genes, targeting ligands, etc. [13, 35, 36];
- augments blood circulation time by evading clearance from the reticuloendothelial system (RES) [35];
- renders the NPs biocompatible and decreases nonspecific interactions, consequently reducing toxicity [35, 37];
- increases their efficiency of internalization by target cells [35, 37].

4.1. Types of coatings

Diverse groups of coating materials are used to modify magnetic NPs surface chemistry, namely:

- synthetic polymers, such as poly(ethylene-co-vinyl acetate), poly(vinylpyrrolidone) (PVP), poly(lactic-co-glycolic acid) (PLGA), PEG and polyvinyl alcohol (PVA);
- natural polymers, such as dextran, pullulan, gelatin and chitosan;

- organic surfactants, such as dodecylamine, sodium carboxymethylcellulose and sodium oleate;
- inorganic metals, such as gold;
- inorganic oxides, such as carbon and silica;
- bioactive molecules and structures, such as liposomes, lipids, ligands/receptors and peptides [9, 13, 28, 38].

In this review, we refer only to the most relevant coatings described in the literature (figure 1).

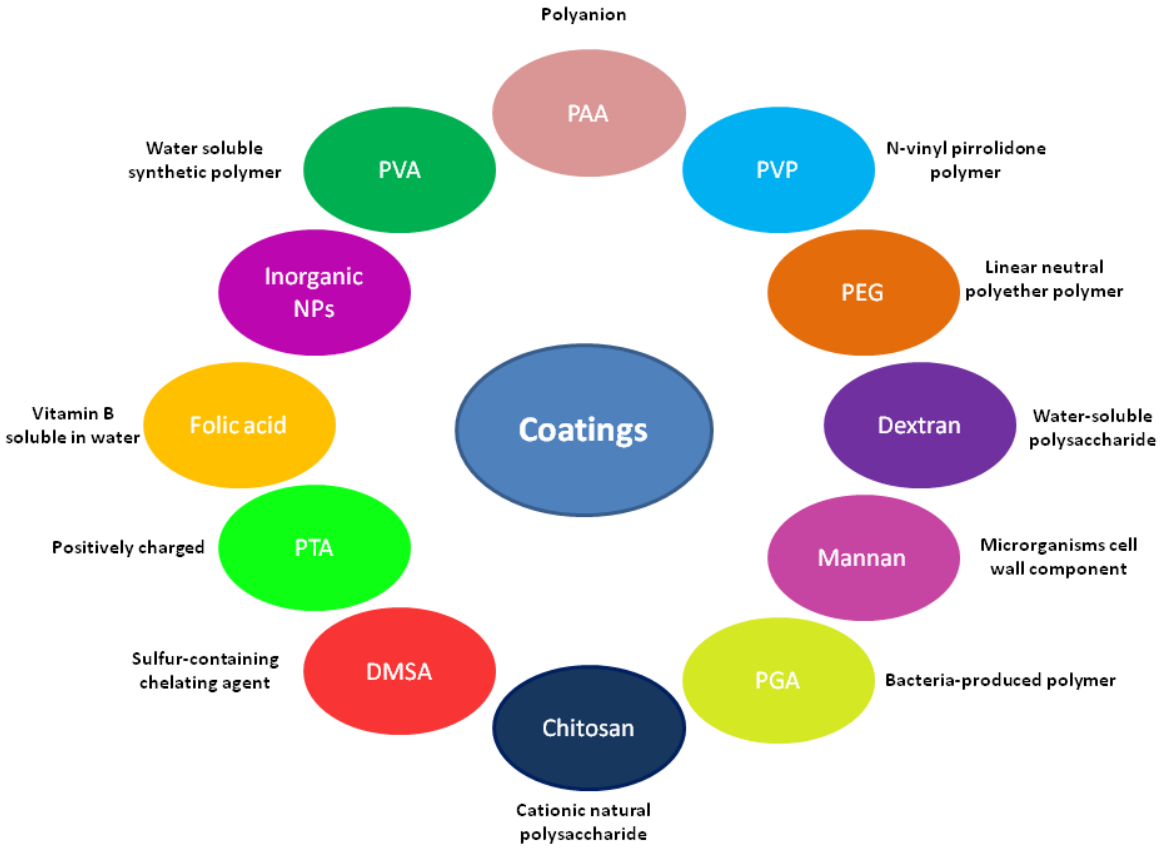

Figure 1. Most widely coatings used in IONs.

4.1.1. Polyvinyl alcohol (PVA)

PVA is a water soluble synthetic polymer that has exceptional emulsifying, film-forming and adhesive properties. Besides the fact that PVA enhances polymer-surface interactions, PVA also forms hydrogen bonds between the polymer chains which results in a hydrogel structure that embeds the NPs and is responsible for steric stabilization above and around the critical polymer concentration. This structure prevents aggregation and

agglomeration of SPIONs [9, 39, 40]. It was reported that PVA has the capacity to bind to proteins through hydrogen-bonding interactions and this may be responsible for a reduced capacity of monocyte-derived human dendritic cells to process antigens, secrete cytokines and stimulate T cells after exposure to PVA-coated magnetic IONs [41, 42].

4.1.2. Poly(vinylpyrrolidone) (PVP)

PVP is a synthetic water-soluble polymer produced from the monomer N-vinyl pyrrolidone. It has non-biodegradable properties, good biocompatibility and a safe, long-standing record in biomedical and pharmaceutical applications. The main benefits of PVP for coating SPIONs are stability and safety in the use of SPIONs [43, 44].

4.1.3. Polyethylene glycol (PEG)

PEG is a linear neutral polyether polymer that can be considered to reduce opsonization because it is hydrophilic, uncharged and non-immunogenic [9, 36]. In addition to steric stabilization of magnetic NPs, PEG non-fouling properties diminish interactions of the NPs with blood proteins permitting PEG-coated NPs to escape recognition by the mononuclear phagocyte system, in this way increasing NPs circulation *in vivo* [45, 46]. PEG-coated NPs are internalized efficiently by cells through amphiphilic affinity to lipid bilayers on plasma membranes and via fluid-phase endocytosis [9].

PEG exhibits low immunogenicity and toxicity. It is excreted through kidneys (for PEG <30 kDa) and feces (for PEG >20 kDa) in an intact form [36].

4.1.4. Polyacrylic acid (PAA)

PAA is a non-toxic polyanion where each repeating unit exhibits a carboxylic acid function [47]. In an aqueous solution at neutral pH, since PAA is a weak organic acid, many of its side chains lose their protons and obtain a negative charge [48]. PAA has been considered an endosomolytic polymer. It has been shown that the addition of PAA to polyethylenimine (PEI)-deoxyribonucleic acid (DNA) transfection complexes not only increased reporter gene expression but also reduced toxicity *in vivo* [49, 50].

4.1.5. Dextran

Dextran has proven to be among the most commonly used coatings and is a water-soluble polysaccharide which has been clinically used for more than half a century.

Many commercially-available contrast agents are coated with dextran or carboxydextran such as Resovist®, Endorem®, Sinerem® and Supravist® [16, 51, 52].

Dextran-coated USPIONs are described as offering beneficial properties in their absorption, biodistribution, biotransformation, metabolism and excretion. These agents have been reported to be rapidly and nonspecifically captured by phagocytic cells and accumulate in the RES such as lymph nodes, Kupffer cells of the liver and spleen [9, 53, 54, 55]. It was reported that after intravenous infusion, approximately 70% of dextran was excreted into urine within a 24 hour period with the remaining 30% retained in the body for a few days [56]. Furthermore dextranase (an intracellular enzyme) cleaves the dextran component and consequently, the iron oxide is solubilized into iron ions, which are gradually incorporated into the hemoglobin pool [57]. However, one important limitation of polysaccharide coatings is that they are structurally unstable in highly acidic environments. Dextran is a huge macromolecule that is continually undergoing conformational changes and completely desorbs from the particle surface. In addition, in dextran-coated NPs, dextran is not strongly bound to the iron oxide core and can be effortlessly detached from the IONs surface, leading to their aggregation and even precipitation under physiological conditions [16, 23, 55]. Consequently, the NPs themselves are internalized very inefficiently given that low molecular-weight dextran is typically captured by fluid phase-mediated endocytosis, which is a fairly inefficient uptake process [23]. It was described that coatings such as mannan, citrate and silica permitted better internalization in macrophages compared to dextran [58, 59, 60]. As such, to guarantee the stability of the polymer coating *in vivo*, cross-linked IONs (CLIO) NPs have been conceived. CLIO NPs are dextran-coated SPIONs where the dextran chains are cross-linked chemically [61].

It was also reported that dextran coating may adsorb several plasma proteins, namely the *C3* component, vitronectin and fibronectin [62]. Additionally, it was described that dextran caused allergic reactions. The fact that anti-dextran antibodies are present in few individuals has been related to the use of dextran coating in some USPIONs. Serious reactions linked to the use of dextrans 40 and 70 as a plasma substitute have been reported for considerable time. These reactions are caused at least in part, by dextran-reactive IgG antibodies [63].

Carboxydextran is a derivative of dextran that has been used equally to coat IONs. It has been suggested that the carboxyl groups which carboxydextran presents, in addition to dextran, might lead to greater affinity to the cell membrane [64]. It was established that SHU555C (an ionic USPIONs with a size of 21 nm and a carboxydextran coating) is considerably better internalized into monocytes *ex vivo* compared to

ferumoxtran-10, which is a non-ionic USPIONs with a dextran coating and size of 20–50 nm [65].

Carboxymethyl-substituted dextran is another anionic dextran derivative that has been used as coating material for biosensors in both commercial and research settings due to the high density of carboxymethyl groups available for chemical conjugations. This coating is cleared from circulation at a low rate (compared to the unmodified form) and exhibits low fouling activity. This derivative also has the advantage of permitting covalent fixation of the polymer to the NPs' surface which is favorable for the colloidal stability of the NPs [66].

4.1.6. Mannan

Mannan is a cell wall component that exists on the surface of microorganisms and consists of D-mannose residues. Mannan in *Saccharomyces cerevisiae* is composed of α-(1,3)-, α-(1,6)- and α-(1,2)-linkages between the two sugar monomers, being water soluble. Its recognition is done by mannan-binding lectins of the complement system and mannose receptors on antigen-presenting cells and RES, while circulating antigen-presenting cells also opsonize the antigen present in circulation and thereafter migrate to the lymph nodes. For this reason, mannan–coated SPIONs may be used as an MRI contrast agent to target macrophages. These NPs are phagocytosed in the liver by Kupffer cells [59].

4.1.7. Poly(*γ*-glutamic acid) (PGA)

PGA is a multifunctional and polyanionic polymer that is biosynthesized by *Bacillus subtilis* through fermentation and consists of repetitive glutamic acid units linked by *γ*-amide linkages between *γ* –carboxyl and *α*-amino groups [67, 68]. It was described that PGA increases antibacterial activity towards *Escherichia coli* [67].

4.1.8. Chitosan

Chitosan is a kind of cationic linear natural polysaccharide whose protonated amino groups can become positively charged under weak acidic conditions [69]. Chitosan is derived and can also be prepared by N-deacetylation of chitin, a poly [(1,4)-N-acetyl-D-glucosamine]. Chitin is, after cellulose, the most abundant natural biopolymer and is removed from the shell of shrimp and crabs [70].

Recently, chitosan has been in the limelight thanks to its outstanding biological properties such as biodegradability, biocompatibility, wound healing and antibacterial activity [69]. It was described that the low molecular-weight chitosan may restrict tumor growth and present anti-transfer activity in tumor-bearing mice by lymphocyte factor activation and immune regulation enhancement [71, 72]. However, the application of chitosan and chitosan-based materials is in some way restricted due to their poor solubility, physical properties, reactivity and consequently, strong inter and intra-molecular hydrogen linking in aqueous medium. Besides, chitosan-coated NPs may be adsorbed onto normal tissues throughout the circulation process *in vivo* due to their good bioadhesive and mucoadhesive characteristics. This is evidently undesirable for a targetted drug delivery system [69, 73, 74].

To overcome these limitations, chemical modifications have been performed with a view to making chitosan derivatives more soluble in water, such as N-carboxymethylchitosan, N-carboxymethylchitosan, O-carboxymethylchitosan, O-sulfatechitosan, N-sulfatechitosan, O-succinyl-chitosan, hydroxypropylchitosan, N-methylene phosphonic chitosan and N-trimethylchitosan, etc. [74, 75]. For example, the small hydrophilic size (<50 nm) of O-carboxymethylchitosans-coated SPIONs and their hydrophilic surface has been reported to significantly ameliorate suspension stabilization, decrease protein absorption and increase SPIONs surface hydrophilicity, thereby avoiding their detection and uptake by mouse macrophage cells [76].

Recently, an association between chitosan and poly(N-isopropylacrylamide) has been described. This is one of the most widely described water-soluble polymers, known for having a lower critical solution temperature (32ºC). Above this temperature, a phase separation occurs. It is also possible to associate monomers with this coating in order to modify the critical solution temperature. This modification may make this coating useful for hyperthermia and drug delivery applications [77, 78, 79]. Given that poly(N-isopropylacrylamide) is non-biodegradable, its association with chitosan renders it degradable in small fragments, which facilitates its removal by renal clearance [80].

4.1.9. Dimercaptosuccinic acid (DMSA)

DMSA is a sulfur-containing chelating agent that is negatively charged. Today, DMSA is injected to patients with the aim of absorbing additional elements in their body. Using DMSA, an anionic coating is produced on the NPs surface which avoids opsonization and their removal by RES of liver and spleen. Consequently, as direct contact with the cells is decreased, their toxic effects are also reduced [9, 81, 82]. DMSA protects NPs from aggregation and due to its negative charge, establishes a strong

interaction with the positively charged regions of the plasma membrane [9]. Moreover, highly negatively charged SPIONs (as in the case of DMSA-coated IONs) interact repulsively with negative domains of the plasma membrane, induce local neutralization and unspecifically adsorb on the cell membrane with subsequent membrane bending and efficient capturing into endosomal compartments [58]. For this reason, DMSA-coated IONs were shown to be internalized by cells to a greater extent than dextran-coated IONs [83].

4.1.10. Inorganic NPs

Inorganic compounds have been used to coat IONs. These compounds can greatly increase the antioxidant properties of non-coated IONs. IONs functionalized with inorganic compounds show great potential for application in biolabeling, catalysis and bioseparation. Coatings with inorganic materials comprise silica, sulfides, metal, non-metal and metal oxides [34]. Additionally, precious metals (namely gold) may be used to offer protection to iron oxide cores against oxidation, given that these metals form highly stable NPs and with low reactivity [9].

4.1.10.1. Silica and aminosilane

Silica (SiO_2) is a coating material that is inert, prevents the aggregation of the iron oxide core in liquid media and increases their chemical stability [60]. Silica-coated NPs are stable and redispersible in aqueous conditions (even when pH changes occur) due to the negative charge of the silica shell and the surface silanol groups that may react with silane and alcohol coupling agents to create dispersions stable in non-aqueous solvents, and offer the ideal anchorage for covalent binding of specific ligands [9, 13, 36]. Silica-coated NPs offer excellent control of interparticle interactions within structures and in solutions by varying the shell thickness. Silica-coated NPs present longer circulation times. Moreover, their hydrophilic and negatively charged surface offers ideal anchorage for covalent binding to ligands, being an exceptional platform for drug delivery [9]. Additionally, silica and other microporous inorganic materials have the advantage of being heat resistant with a high surface area and good mechanical strength. The porosity of silica, which efficiently encapsulates drugs at high concentrations, also allows a controllable drug release over a prescribed period of time at the target site [36].

Aminosilane (SiO_2-NH_2) is a derivative of silica that presents higher cellular labeling efficiency than silica. Under pH 7.4, aminosilane is positively charged and as plasma membranes possess huge negatively charged domains, their cationic surfaces

have been demonstrated to favor cellular internalization [84, 85]. This coating was shown to be effective in increasing survival in animals subjected to the tumor model when used in thermotherapy [86].

4.1.11. Polycationic transfection agents (PTA)

PTA, such as PEI, poly(L-lysine) (PLL) or protamine sulfate have been used to facilitate interaction between the SPIONs and the surface of those cells which present negative charges, and consequently in endosomal absorption [25]. They are also utilized in cell transfection to form electrostatic complexes with the anionic phosphate backbone of DNA [87].

PEI is a synthesized cationic polymer. Due to its positive charge, PEI interacts with anionic proteoglycan at the cell surface, which facilitates the IONs entrance into the cells by endocytosis [88]. It was also reported that PEI interacts in an undetermined way with anionic molecules in the serum as well as with plasma proteins, namely opsonins [89, 90].

Protamines are arginine-rich proteins of low molecular-weight (~4000 Da), purified from the mature testes of fish. Protamine sulfate is a polycationic peptide approved by the Food and Drug Administration (FDA) and is mainly employed as an antidote for heparin anticoagulation [91, 92].

PLL is a synthetic positively charged polymer commonly used to increase cell adhesion to culture dish surfaces. Although its use has still not been accepted in humans, it was reported to be able to bind (through electrostatic interactions) to the dextran coat, modifying the distribution of anionic and cationic surface charges of ferumoxides that can adhere to the cell membrane [93, 94].

4.1.12. Folic acid

Folic acid is a water soluble B vitamin which is synthesized by prokaryotes, plants and yeast to facilitate the digestion, utilization and synthesis of proteins in the body when they are necessary. It is required for red blood cells production and DNA synthesis [95, 96].

Folate-receptor is a folate-binding and glycosylphatidylinositol-anchored protein highly expressed in various types of human tumors, namely colon, ovarian, lung, liver, kidney and breast cancers, where it functions by folate uptake to feed rapidly growing tumor cells in division. In contrast, the folate receptor expression level on other non-tumoral cells is low and only restricted to some epithelial cells [97, 98]. IONs conjugated with folate have the capacity to enter the receptor-expressing cancer cells through folate

receptor-mediated endocytosis and evade nonspecific capture of NPs in normal tissues, producing their apoptotic effect solely in cancer cells [95, 99].

4.2. Toxicity of coatings

Although coatings are beneficial for the above-mentioned reasons, there are increasing reports concerning their toxicity. After NPs core coating, the acute toxicity experimented is ascribed to the physicochemical properties of the NPs surface, which is key for cellular uptake and particle-cell interactions. These properties comprise surface charge, hydrodynamic radius and toxicity inherent to the coating materials [9, 66].

It is known that positively charged SPIONs are usually more toxic due to the fact that positive charges tend to be firmly attached to the cell surface, compared to the anionic NPs. This occurs because the resting cell membrane potential is negative [100]. Following intravenous injection of positively charged SPIONs, nonspecific interactions and unspecific adsorptive endocytosis take place, which results in aggregates formed with plasma proteins and blood cells. Therefore, cationic SPIONs will be more concentrated into the cells than anionic SPIONs. Cell membrane integrity was demonstrated to be more severely damaged and intracellular vesicles contained a higher concentration of SPIONs in the cells exposed to positively charged SPIONs [100]. Hoskins *et al* [101] reported that PEI-coated magnetic IONs decreased the viability of breast cancer (MCF-7), neuroblastoma (SH-SY5Y) and macrophage-like (U937) cell lines respectively. It was also reported that PEI-coated NPs increased reactive oxygen species (ROS) production which resulted in cellular stress [101]. The explanation for these toxic effects is that, by inserting the cationic SPIONs in an acidifying lysosomal compartment, the unsaturated amino groups are able to trap protons that are provided by the proton pump for cationic SPIONs digestion. One Cl^- ion and one water molecule per proton are propagated in the lysosome vesicle. Owing to Coulombic interactions, more protons will be injected into the lysosome which will cause lysosomal swelling and consequent rupture, leading to NPs deposition in the cytoplasm and lysosomal content spillage [102, 103].

Regarding polyethylene oxide (PEO), it was reported that the shortest tails of PEO are more toxic when compared to the longest tails. The shortest 0.75 kD tail triggered chromatin condensation, nuclear blebbing and formation of apoptotic bodies [16]. In the case of PAA, it was reported that PAA-coated IONs markedly reduced cell viability in OCTY mouse cells. Only 16% of cell viability was observed at an iron concentration of 400 µg/mL after 72 hours of culture [104].

5. Magnetization of IONs

Superparamagnetism is a fundamental criteria of magnetic NPs in nanomedicine. This phemomenon arises from competition between thermal fluctuations of magnetic moments of NPs and the ordering effect on such NPs due to an external magnetic field [103].

When an external magnetic field is not present, ferromagnetic materials are not magnetized, given that the magnetization of the ferromagnetic domains is randomly oriented. Contrary to para- and dia- magnetic materials, elimination of the magnetic field will not lead to magnetism loss, but the NPs will still display a remnant magnetization given that the large Weiss domains (regions within a magnetic material which have a uniform magnetization) are still aligned along the original field. When the particles size is smaller than the diameter of the Weiss/ferromagnetic domains (about 30 nm) leading to NPs not showing any magnetic remanence (i.e. restoration of the induced magnetization to zero upon elimination of the external magnetic field), superparamagnetism occurs. Superparamagnetic IONs are the most widely applied NPs in the biomedical field. Each of the NPs may be considered a monomagnet and is regarded as a fully magnetized single Weiss monodomain, which is a direct consequence of the spinel structure of the NPs, permitting strong magnetic coupling and therefore a perfect alignment of the individual magnetic spins. The IONs saturation magnetization diminishes with particule size, which is unfavorable for the efficiency (relaxivity) of the IONs. This decline of saturation magnetization has been ascribed to surface effects, namely spin canting, which is a lack of full alignment of the spins at the surface in high magnetic fields [23, 28, 103, 105].

6. Biodistribution

Biodistribution of IONs and their efficient delivery to a specific tissue depends on their chemical and physical characteristics. NPs may be characterized according to their surface coating, size, surface charge, density, surface hydrophobicity and pH of their suspensions [106]. These properties are particularly relevant and strongly influence blood circulation time, bioavailability and metabolism of the NPs within the body [9, 46]. The coating of IONs plays a relevant role in their biodistribution. Coating materials that restrict or hamper water access to the iron oxide core display significantly lower degradation rates, as demonstrated by the enhanced half-life of these NPs in the liver [107, 108]. The surface charge of SPIONs also plays a key role in their blood half-life. Cationic NPs tend to adhere unspecifically to cells. Strong negative charges result in increased liver uptake [109].

Furthermore, the biodistribution of NPs is influenced by a myriad of factors including the route of administration and the physiological environment to which NPs are introduced [110]. NPs could straightforwardly pass through diverse tissue compartments and move rapidly and freely to target organs [111]. The characteristic biodistribution of NPs is 80–90% in liver, 5–8% in spleen and 1–2% in bone marrow [9].

6.1. Route

Magnetic NPs may be administered into the body via several routes. Although the preferred route for cancer therapy is intravenous injection, other routes are considered effective for drug delivery. For example, in the case of lymphatic targeting, interstitial injections (namely intradermal and subcutaneous) are chosen, since low doses of magnetic NPs reach high accumulation levels in the regional lymph nodes [36].

6.2. Influence of size

Particle size plays a fundamental role in the biodistribution of IONs. In general, larger particles circulate in blood for shorter time periods than smaller particles. It was described that larger particles greater than 200 nm in diameter are usually entrapped by the liver and spleen due to mechanical filtration. IONs over 50 nm are usually captured quickly by the RES in Kupffer cells of the liver and have a restricted uptake in lymph and bone tissues. They are eventually eliminated by the phagocytic cells which results in diminished blood circulation times [9, 112, 113]. Due to their greater half-life, USPIONs can pass through the capillary wall and present more extensive tissue distribution. For this reason, they are readily captured by phagocytic cells, namely the Kupffer cells of the liver, mononuclear T cells and circulating monocytes/macrophages, as well as reactive astrocytes, dendritic cells and microglia inside the brain, and can be found in phagocytic cells in the lymph nodes, bone marrow, liver and spleen. This does not occur with SPIONs, which are found almost exclusively in the liver and spleen [114, 115]. However, smaller NPs of diameters less than 10 nm are quickly eliminated via extravasation and renal clearance. Particles between 10 to 100 nm are consequently ideal for subcutaneous injection and display the most prolonged blood circulation times (in humans of 24 to 36 h and in rats approximately 5 h [116]), having been reported to accumulate in bone marrow, heart, kidney, intestine, spleen and stomach [13, 117]. The ability of these IONs to cross the blood-brain barrier (BBB) and move into the central nervous system (CNS) via the olfactory pathway was also described as well as the ability to penetrate stratum corneum and hair follicles, attaining viable skin epidermis [9, 18]. The NPs in this size interval are

sufficiently small to evade RES and in addition, enter the very small capillaries within the body tissues. For this reason, they may provide the most effective distribution in several tissues [13]. The capture of SPIONs into the RES is associated with protein adsorption on the particle surface and ensuing opsonization. Consequently, decreasing the particle size will reduce NPs phagocytosis, which results in a significant increase in plasma half-life and larger biodistribution [118, 119].

6.3. Half-life

For all IONs, the blood half-life is dose-dependent. This feature is related to a gradual saturation of macrophage capture by the liver or other macrophage-rich organs, namely spleen and bone marrow [28]. The blood half-life of IONs is normally higher in humans than in animals. Although it was described that SPIONs are more appropriate for primary monocytes labeling, USPION are more frequently used for *in vivo* labeling due to their long blood pool half-life: the plasma half-life for USPIONs has been reported to range from 80 minutes to more than 24 hours, compared with only ~2 to 4 hours for standard SPIONs [28, 114, 120]. Ferumoxides interaction time with cells is reported to be approximately 6 minutes *in vivo* compared to 4 h *in vitro* [65]. The large variability in USPIONs circulation time is related to the composition of the surface coating used to stabilize the particle. In general, the extended circulation time for USPIONs derives from the particles not being immediately recognized by phagocytic cells of the RES [114]. Ferumoxtran-10 (15-30 nm) is reported to have a longer blood half-life (around 30 h in humans) without accumulating in specific tissues compared to ferumoxide AMI-25 (120-180 nm) [28].

6.4. Circulation and homeostasis

The destiny of NPs following intravenous administration is defined by their polymer coatings. After injection of NPs into the bloodstream, they are usually opsonized and this step is critical in dictating their outcome. Usually, opsonization makes the NPs recognizable by the RES. The liver macrophages and, to a lesser extent, the macrophages in circulation and of the spleen, play a significant role in the elimination of opsonized NPs [121]. IONs do not extravasate into the interstitium in most tissues. However, some extravasation was observed across the discontinuous endothelium of microvessels in the liver, spleen, lymph nodes and bone marrow [122]. In addition, when NPs are transported to the tumor site through the bloodstream, some extravasation can occur across hyperpermeable microvessels [123]. After clearing by the RES, there is the

possibility that magnetic NPs recirculate in the blood or inflammatory lesions, being transported by membrane vesicles which are released by apoptotic macrophages. Consequently, the vesicular traffic permits a dynamic intercellular redistribution of NPs [124].

Intracellular iron homeostasis involves a tightly regulated balance between the synthesis of transferrin receptors and the synthesis of intracellular ferritin molecules, responsible for cellular iron capture [125, 126]. Clear evidence has now emerged that once the USPIONs are ingested by macrophages, they are dissolved within the lysosomes by a succession of hydrolyzing enzymes with the low pH (~ 4.5) of the lysosome, where this low pH and heme oxygenase divides the iron oxide core into iron ions. These ions are subsequently incorporated into the hemoglobin pool and potentially into other iron requiring proteins such as apoferritin, ferritin and transferrin [36, 115, 127, 128].

When cytoplasmic iron content rises, ferritin synthesis is triggered, which results in the entrapment of toxic iron (Fe^{2+}) into the ferritin molecules [129]. However, it was described that elevated levels of free iron ions from magnetic NPs may trigger a disequilibrium in body homeostasis and lead to aberrant cellular responses including oxidative stress, DNA damage, epigenetic events and inflammatory processes [36].

6.5. Elimination

The efficacy of NPs clearance exerted by RES depends on the chemical composition, size and surface chemistry of the magnetic NPs and may influence mechanisms of particle internalization as well as macrophage activation [9]. The most desirable excretion pathway for IONs is via the kidney (89%) given that this route implies minimal intracellular catabolism and reduces the probability of producing reactive oxygen species (ROS) and therefore, associated toxicity. Renal excretion is considered the safest route of excretion for IONs. However, the hydrodynamic size, shape, surface charge and surface coating of IONs play a key role in the regulation of their renal clearance [28, 35, 130]. The rest of the iron is excreted slowly (84 days) in feces [131]. The presence of γ-Fe_2O_3 NPs in podocytes has been reported, suggesting that they can cross the glomerular basement membrane and consequently, are filtered into the urine. This is also supported by the finding that NPs are present in lysosomes/endocytic vesicles in the cytoplasm of proximal tubular cells [132].

Regarding coating elimination, it has been suggested that the acidic environment of the lysosomal compartment (pH ~ 5.5) may cause the rupture of the dextran shell

(because of the existence of intracellular dextranases in macrophages) and liberate Fe^{3+} from IONs. Sulfatases are also lysosomal enzymes that break a variety of sulfated carbohydrates, being these compounds able to be used as IONs coating [133, 134].

6.6. Differences between normal and cancer cells

Carcinoma and normal cells were shown to have different metabolism regarding iron uptake. Breast carcinoma cell metabolism, for example, is faster than in normal cells. As a result, carcinoma cells necessitate larger amounts of micronutrients (namely iron), which can be evidenced by the increase of transferrin receptors in these cells [135, 136]. Moreover, in fast-growing tumors, neovascularization is habitually deficient and associated with poor lymphatic drainage, which permits increased permeation and retention of therapeutic nanodrugs [137]. However, it was described that SPIONs are not phagocytosed by reticuloendothelial cells in tumoral lymphoid tissues because macrophages are replaced by cancer cells and consequently, these tissues lack reticuloendothelial cells [138, 139].

6.7. Cellular localization

IONs have been described as having cytoplasmic localization in different cells, namely non-coated Fe_3O_4 NPs in HeLa cells [140], DMSA-coated Fe_3O_4 NPs in RAW264.7 cells [141, 142], pullulan-coated Fe_3O_4 NPs in fibroblasts [143] and citrate-coated γ-Fe_2O_3 NPs in THP-1cells [124]. IONs seem to be grouped into clusters in the cytoplasm of the cells, in part around the nucleus and possibly localized in endocytotic vesicles (for example lysosomes) [124, 144, 145]. It was reported that in BEAS-2B cells, IONs are surrounded by mitochondria but do not have the capacity to penetrate them [145]. However, in monocytes NPs are described as entering into the mitochondria, having been found on the membrane and cristae, sometimes filling the matrix [146].

7. Internalization routes

Diverse cellular internalization routes exist which include transcytosis and endocytosis (clathrin-mediated endocytosis, caveolae-mediated endocytosis, phagocytosis and macropinocytosis), among others. It is believed that all of these types of mechanisms are used by cells to internalize several substrates [9, 147].

The cellular internalization routes through which NPs enter into the cells depend on their surface properties which may be characterized according to their

hydrophilic/hydrophobic features, chemistry or surface energy. These surface characteristics determine the means by which NPs adsorb to the cell surfaces and more specifically, dictate the behavior of the cells in contact with them [46]. Size is also determinant for NPs internalization and efficacy of cellular uptake. For NPs in the interval 10–30 nm, diffusion through membrane channels or across plasma membranes may occur [36]. Smaller NPs may also be internalized by pinocytosis while in the case of larger NPs, phagocytosis and receptor-mediated endocytosis seem to be the most common internalization pathways [148]. In phagocytic cells, smaller NPs are often internalized less effectively than larger NPs while in nonphagocytic T-cells, NPs with intermediate sizes were shown to be internalized more effectively than any other size [148].

7.1. Transcytosis

Transcytosis is described as being the vesicular transendothelial transport mechanism. Endothelial vesicles represent the most important mediator of macromolecular transport via the capillary wall and are increased in inflamed tissues [149, 150]. Endothelial transcytosis into the interstitium throughout the body has been described as a mechanism by which IONs uptake can occur. When USPIONs are in the bloodstream, they may cross the endothelium by transcytosis. Thereafter, USPIONs will be taken up by cells through endocytosis or other processes [28]. Transcapillary passage of the NPs through the venules into the medullary sinuses within the lymph nodes has been described, with subsequent phagocytosis by macrophages [151].

7.2. Endocytosis

Most inorganic NPs are captured by cells through the endocytic route. Internalization via endocytosis (the process of capturing macromolecules into cells by including them in membrane vesicles) after cell membrane contact can occur through a variety of mechanisms: clathrin-mediated endocytosis, caveolae-mediated endocytosis, receptor-mediated endocytosis, phagocytosis, pinocytosis and macropinocytosis [152].

In endocytosis, NPs interact with the cell plasma membrane which encloses and traps them into vesicles. These vesicles are denominated early endosomes and are transported via the cytoplasm and fuse sequentially with late endosomes and lysosomes. In this process of cell internalization, NPs meet compartments with various enzymatic activities and continuously decreasing pH, ending up in lysosomes [153, 154]. The endocytic pathway was previously reported for anionic magnetic NPs after interacting with the plasma membrane via electrostatic interactions [124, 155]. It was also described that

PVA-coated SPIONs were endocytozed by monocyte-derived human dendritic cells in a dose-related manner, predominantly via an actin-dependent process [41]. Cellular uptake data showed that the uptake of long-circulating dextran-coated IONs was ever-present in several tumor cells and was not saturable, which suggests that fluid-phase endocytosis rather than receptor-mediated endocytosis is the uptake mechanism [156]. Improved endocytosis strategies may be sought, namely the use of transfection agents, antibody or receptor-mediated delivery or conjugated, cellular translocation signal peptides [4, 103].

7.2.1. Phagocytosis

Phagocytosis is an actin-dependent endocytic mechanism which involves phagocytes such as dendritic cells, macrophages and neutrophils [157]. It is often triggered by particle opsonization and ensuing F-actin-driven pseudopods receptor-mediated activation, which encloses the NPs in a phagosome present in the cytoplasm [158]. It was observed that phagocytic uptake of IONs increases when NPs size increases. USPIONs of sizes varying from 20–50 nm and monocrystalline IONs (MIONs) of 10–20 nm sizes were less efficiently phagocytized than SPIONs between 50–180 nm [115, 159]. Another study reported that phagocytosis was highest in response to 10 nm magnetite particles and minimal in response to 1 μm particles, which is not completely in line with the previous mentioned studies [160].

7.2.2. Macropinocytosis

Macropinocytosis is a highly conserved endocytic process where extracellular fluid and its contents are enclosed into cells through macropinosomes. These are heterogeneous and large vesicles formed through direct actin polymerization near the plasma membrane, causing membrane ruffling [157, 161]. Rejman *et al* [147] demonstrated that efficient uptake of microspheres requires cholesterol in their plasma membrane which can indicate that macropinocytosis is in some way involved in the internalization of larger sized particles. Macropinocytosis, although not ubiquitous, may function in cells other than macrophages. It was described that magnetic NPs can be incorporated into A549 human lung endothelial cells by macropinocytosis [12, 162].

7.2.3. Clathrin-mediated endocytosis

IONs uptake can also occur via clathrin-mediated endocytosis. It is known that some cells (such as macrophages) express clathrin, and clathrin forms clusters at these

NPs capture areas. Clathrin assembly triggers the generation of coated pits of approximately 150 nm. Internalization occurs when the clathrin coating on the plasma membrane creates invaginations in the membrane, leading to clathrin-coated vesicles budding. Following internalization, the clathrin coating is recycled, leading to the fusion of the vesicle with an endosome where the sorting (which is mediated by microtubules) and dissociation of potential receptors takes place. Thereafter, degradation in lysosomes takes place and further transportation to the final destination occurs [142, 163, 164].

Lunov *et al* [165], having detected by transmission electron microscopy (TEM) that SPIONs and USPIONs are incorporated inside vesicles of approximately 100 nm in diameter, used monodansyl cadaverine, which is a specific inhibitor of clathrin-mediated endocytosis, and demonstrated that macrophages capture the carboxydextran-coated NPs though a clathrin-mediated endocytosis mechanism. Yang *et al* [166] using phenylarsine oxide (another inhibitor), reached a similar conclusion with Ferucarbotran. Likewise, Ayala *et al* [66] using dansylcadaverine also showed that carboxymethylsubstituted dextran-coated IONs were internalized using this mechanism. Internalization by this mechanism was attributed in this last case to the formation of a protein corona surrounding NPs. This protein corona is formed through non-specific interactions between serum proteins and NPs that are usually internalized via clathrin-mediated and caveolae-mediated endocytosis [66].

7.2.4. Caveolae-mediated endocytosis

Caveolae (of diameter 50–100 nm) are invaginated, flask-shaped plasma membrane domains which are present in diverse cell types but particularly abundant in endothelial cells. Their structure is sustained by caveolins, which are a family of cholesterol-binding proteins. In addition to caveolin, caveolae are enriched in sphingomyelin, cholesterol and glycosphingolipids [147, 167]. Prijic *et al* [168] suggest that SPIONs uptake by mouse L929 fibroblasts cells, human melanoma SK-MEL-28 cells and human mesothelial MeT-5A cells occurs by caveolae-mediated endocytosis. Moreover, DMSA-coated SPIONs uptake in RAW264.7 cells was also reported to be caveolae-mediated [142]. Likewise, Ayala *et al* [66] using fillipin (which is a specific inhibitor of caveolae-mediated endocytosis), showed that carboxymethylsubstituted dextran-coated IONs were also internalized using this mechanism for the reason outlined above in 7.2.3.

7.2.5. Receptor-mediated endocytosis

7.2.5.1. Transferrin receptor

It has been described that the transferrin receptor is the most important route for iron transport through the capillary endothelium luminal membrane. It is possible that iron passes through the luminal membrane and in the form of Fe^{2+}, enters the interstitial fluid [169]. Chen *et al* [170] hypothesized that gambogic acid loaded on magnetic IONs permeated the cell membrane through binding to the transferrin-binding site of transferrin receptor and endocytosis, which were potential routes for IONs uptake into cells.

7.2.5.2. Scavenger receptor (SR)-A

Among the several receptor types involved in the endocytic process, macrophage SRs are an attractive family which has been thoroughly studied. These receptors were firstly identified as macrophage receptors involved in the recognition of modified lipoproteins. Presently, they comprise a family of eight different pattern recognition receptor subclasses, binding to a diversity of ligands, namely modified low density lipoproteins (LDL), polysaccharides, proteins, RNA and environmental particles, while playing a fundamental role in immunity and host defense [165, 171]. Under physiological conditions, SRs scavenge or clean up cellular debris as well as other similar materials and exert an important role in host defense. Under pathological conditions, SRs intervene in the recruitment, activation and transformation of several cells which may be correlated with the development of atherosclerosis and other disorders provoked by accumulation of the denatured materials, such as Alzheimer disease or multiple sclerosis [172]. It has been described that SPIONs uptake is mediated by SR-A [122, 173]. Raynal *et al* [173] used the SR-A inhibitors fucoidan and polyinosinic acid in competition experiments and observed that there was a dose-related inhibition of ferumoxides uptake, which clearly demonstrates that a SR-A-mediated endocytic pathway is implicated in IONs uptake by macrophages. SPIONs uptake into hepatocytes was also shown to be independent of caveolae, dynamin and clathrin-coated pits and mediated principally by a SR other than SR-A [174].

7.2.5.3. Mac-1 receptor

Another receptor possibly implicated in NPs capture is Mac-1 [175]. Both SPIONs and USPIONs are eliminated from the circulation by mononuclear phagocyte system cells

through adsorptive endocytosis in a monocyte integrin Mac-1 receptor-mediated process, which is also involved in the adhesion of leukocytes, activation of complement and phagocytosis [159]. Von Zur Muhlen *et al* [175] reported that, after human monocytes stimulation with PMA, the capture of Ferumoxtran-10 and amino-PVA-coated USPIONs (with a mean hydrodynamic size of 30 nm) was significantly enhanced for Ferumoxtran-10 and amino-PVA SPIONs but was inhibited by antibodies to Mac-1 (CD11b/CD18) in human monocytes.

7.2.5.4. Other receptors

Mannose receptors are possibly involved in mannan-coated SPIONs uptake. It was described that recognition of mannan-coated SPIONs was efficiently performed by mannose receptors which were expressed on human monocyte-derived macrophages [59]. Also, it was reported that ION coated with folic acid can be internalized by folate receptor, which is useful for tumor imaging [176, 177].

8. NPs available in the market

Currently, a wide range of IONs formulas are available in the market (table 1). Despite the fact that these formulas were initially conceived for imaging lesions in RES organs like spleen, liver and lymph nodes, they have also been used for cell labeling. These formulas differ in surface coating materials and size, which is a determining factor for uptake rate and cell retention [178].

Table **1**. IONs available in the market.

Name	Type	Coating agent	Applications
Ferumoxides Endorem® (Europe) Feridex® (USA, Japan – withdrawn from the market) AMI-25®	SPIONs	Dextran	– liver and spleen imaging [28, 115, 133] – monitorization of dendritic cells in melanoma patients and neural stem cells in traumatic brain injury [179, 180]
Ferucarbotran Resovist® (Europe, America, Japan and Australia – withdrawn from the market in America and Australia) Supravist®	SPIONs (Resovist®) and USPIONs (Supravist®)	Carboxydextran	– imaging of liver and central nervous system tumors [115] – pancreatic islet grafts in type I diabetic patients [181]
Ferumoxytol Feraheme®	USPIONs	Polyglucose sorbitol carboxymethylester	– iron replacement therapy in patients with chronic renal failure [115, 182] – CNS imaging applications [115]
Ferumoxtran-10 Combidex® (USA) Sinerem® (Europe)	USPIONs	Low molecular weight dextran	– Imaging of CNS, lymph node, brain, kidney, osteoarticular tissues, inflammatory cells, atherosclerotic plaques, etc. [57, 115, 122]
Ferumoxsil Lumiren® AMI-121®	USPIONs	Silicone	– bowel imaging [183]
Feruglose Clariscan® (discontinued)	USPIONs	Carbohydratepolyethylene glycol	– MRI angiography [184]
VSOP-C184	USPIONs	Citrate	– MRI [178]

9. Concentration

The ingestion of dietary iron amounts to about 10–30 mg per day in adult humans while the mucosa absorbs approximately 0.6–1.5 mg per day [185]. In therapeutic situations, the IONs concentration may vary according to the IONs formula used as well as the purpose for which they are being used. Table 2 summarises the recommended doses reported in the literature.

Table **2**. Recommended doses of IONs used for medical purposes.

Name	Dose
Resovist®	0.42−0.65 mg Fe/kg (in humans when used for liver-specific magnetic resonance contrast agent) [186]
USPIONs	2.6 mg Fe/kg [187, 188]
Sinerem®	2.6 mg/kg (for MRI detection of human atherosclerotic plaques) [189]
Endorem®	0.588 mg/mL (for liver MRI, intravenously) [190]
Fe_2O_3 NPs	45 µmol Fe/kg (for human MRI in CNS and in carotid atherosclerotic plaque) [57]

10. Applications

Due to their chemical, physical, mechanical and thermal properties, IONs are of high interest for *in vivo* applications.

10.1. Magnetic resonance imaging (MRI)

The advantages of MRI, when compared to other imaging techniques are that it is noninvasive; it provides superior spatial resolution and tissue contrast, principally in soft tissues; it can screen cellular events in living animals *in vivo*; it may be performed repeatedly and continuously in real time; and it does not involve the use of radioactive isotopes [191].

MRI contrast agents are sorted by the several changes in relaxation times after their injection and are divided into two categories. Positive contrast agents (bright on MRI) provoke a decrease in the T1 spin lattice relaxation time (increased signal intensity on T1 weighted images). These agents are usually low molecular weight compounds which contain manganese, gadolinium or iron as their active element. Negative contrast agents (dark on MRI) such as USPIONs typically consist of a crystalline iron oxide core which contains thousands of iron atoms and a polymer shell. These mainly produce spin relaxation effects (local field inhomogeneities), resulting in shorter T2 relaxation times [192]. SPIONs are also mainly used as a T2 contrast agent in MRI although this agent may shorten T1 and T2/T2* relaxation processes [183]. However, to date only few examples have been published where IONs are used as a T1 contrast agent. An important example corresponds to the well-known blood pool contrast agents, which are applied to the imagiology of particular vessel structures in MR angiography and offer a longer blood half-life when compared to the other classes [193, 194, 195].

10.1.1. Labeling and imaging

A huge diversity of SPIONs has been prepared to date and experimented for several preclinical applications, and in clinical trials. Hepatic imaging was the first clinical application for IONs. Several studies have demonstrated that IONs are captured by macrophages to a greater extent than other cell types although most of the cells are possibly capable of capturing them to a certain degree [62, 196]. After intravenous injection, IONs are quickly captured by the Kupffer cells (specialized hepatic macrophages), which results in a decrease in magnetic resonance signal intensity and consequently in hypointense images [28]. It was reported that monocytes are labeled more effectively by utilizing SPIONs rather than USPIONs mainly due to the larger diameter of SPIONs compared to that of USPIONs. However, the long blood pool half-life of USPIONs (greater than 24 hours in humans) makes them the most commonly used ION for *in vivo* labeling [28, 120].

The different composition and size of IONs (which impacts their biodistribution) caters for diverse clinical applications: SPIONs with high macrophage capture are used mainly for liver imaging [28]; USPIONs with extended blood half-life are efficient for macrophage imaging and metastatic lymph node as well as blood pool agents utilizing a T1 sequence for angiography, tumor blood volume and tumor permeability or utilizing a T2/T2* sequence for vessel size index and steady-state cerebral blood volume measurements [28].

IONs administered intravenously have been applied as a MRI contrast agent to analyse liver pathology, namely in the identification and characterization of focal hepatic lesions. They have also been proposed for use in monitoring patients undergoing surgical procedures for focal hepatic malignancies and in the follow-up stage of patients with liver cirrhosis for hepatocellular carcinoma detection [197, 198, 199, 200]. Additionally, they have been used as an *ex vivo* cell labeling agent for diverse types of mammalian cells which after labeling, may be used as *in vivo* MRI probes. IONs have been successfully used to label T cells [201], cancer cells [139], stem cells [58] and dendritic cells [202] as well as detect functional and anatomic renal abnormalities [203, 204, 205].

IONs alone or conjugated with target-specific ligands (namely antibodies or proteins) have been utilized in the selective imaging of tumors *in vivo* as well as for gene delivery and therapy [37]. In fact, one strategy to perform specific and efficient cell labeling with magnetic NPs is to alter the NPs surface by recurring to a ligand, which could be effectively captured by target cells through receptor-mediated endocytosis. A diversity of ligands has been conjugated to NPs surfaces to favor the receptor-mediated endocytosis of the NPs, namely monoclonal antibodies. Targeting agents (for instance, albumin, insulin, transferrin and growth factors, etc.) have been shown to preferentially target the cell surface, given that the receptors for these ligands are usually overexpressed on the mammalian cells surface [13]. For example, it was described that HER2/neu antibody conjugated poly(amino acid)-coated IONs derivatives can be used for breast cancer SKBR-3 cells molecular MR imaging [206].

IONs were also hypothesized as being useful for vascular compartment imaging (magnetic resonance angiography) as in the case of pullulan-modified IONs [143]. Labeling mouse insulinoma cells with IONs is also feasible. Citrate-coated MIONs were described to be internalized in all insulinoma cell lines experimented, although at low concentration [207].

Apart from these applications, SPIONs are intensively explored in neuromedicine because they can cross the BBB [208]. The use of IONs conjugated to a glioblastoma specific antibody in glioblastoma tumors imaging has been described as has the application of IONs in the study of neuroinflammation following stroke [209, 210]. Some studies demonstrated that transplanted oligodendrocyte progenitors [211], neural stem cells [212], Schwann cells [213], olfactory ensheathing cells [213], bone marrow stromal cells [214] and undifferentiated embryonic stem cells [214] can be located using MRI in CNS and non-CNS tissue *in vivo* through intracellular labeling with IONs [215].

IONs have been employed to image inflammatory processes, angiogenesis or atherosclerosis [175, 216]. Small SPIONs were described as being able to navigate through the tight interstitial endothelial pores and have been used in imagiology with

macrophages in *in vivo* studies [159]. It has been demonstrated by experimental research in an atherosclerotic animal model using hyperlipidemic rabbits that USPIONs enter atherosclerotic plaques with an enhanced endothelial permeability and accumulate in atheroma with high macrophage content [217, 218].

SPIONs have also been successfully used to label transplanted cells for *in viv*o monitoring by high resolution MRI [37]. Mesenchymal stem cells also called mesenchymal stromal cells (MSC), have the potential to migrate after systemic transplantation along chemokine gradients to diseased tissues where they engraft and differentiate into the defective cell type and/or induce regenerative processes through paracrine mechanisms [58, 219, 220]. IONs are useful in tracking the transplantation of stem cells and immune cells with the aim of regenerating, repairing or restoring the functionality of diverse tissues or organs. These have been in the limelight for the treatment of a variety of diseases such as cancer, leukemia, muscle damage, neural degenerative diseases, spinal cord injuries, stroke, myocardial infarction and bone fractures. Numerous studies have already demonstrated the *in vivo* tracking of SPIONs-labeled MSC by MRI in various tissues such as brain, liver, kidney, spinal cord, myocardial heart and muscle tissue [58, 219].

IONs may also be useful in the identification of tumor cell apoptosis markers using MRI. Numerous markers can be used to identify apoptotic cells including DNA fragmentation, morphological changes and caspase activation. The flipping of phosphatidylserine from the plasma membrane bilayer inner leaflet to the outer surface is a relatively early event in the apoptotic process, which can be detected by the protein annexin V binding to surface phosphatidylserine [221, 222, 223]. It was reported that a conjugation of annexin V to CLIO enabled the detection of apoptosis with MRI both *in vitro* and *in vivo* [224]. It was also shown that the C2A-GST (domain of synaptotagmin I; glutathione S-transferase) fusion protein could also be used to detect apoptotic tumor cells *in vivo* and *in vitro* in *T*2-weighted MRI experiments, when directly conjugated to SPIONs [221, 225].

10.1.2. Cell sorting

Cell labelling with IONs is an increasingly widespread method for *in vivo* cell separation given that the labelled cells may be detected by MRI. Most recent labelling techniques apply one of these two approaches: 1) engulfment of biocompatible magnetic NPs by receptor-mediated endocytosis, fluid phase endocytosis or phagocytosis or 2) binding of magnetic NPs to the cell surface [13]. The immunomagnetic poly(glycidyl methacrylate) (PGMA)-coated IONs conjugated with a specific monoclonal antibody with

CD4 molecules expressed on CD4+ lymphocytes were reported to be highly efficient and specific in CD4+ lymphocytes separation from whole blood, which can be applied in diverse biomedical applications namely diagnosis, treatment and monitoring of illnesses [226].

10.2. Tissue repair

IONs can be used to promote tissue repair. In fact, they were described (in the presence of the nerve growth factor) to synergistically instigate neurite outgrowth and upregulate a neural specific marker protein [227].

The possibility of using magnetic NPs in osteoporosis treatment has also been reported [228, 229]. The ability of these NPs (principally maghemite) to instantaneously enhance bone density and give rise to a further increase in osteoblast functions at the disease site was underlined. In addition, the magnetic properties of these NPs can be applied to guide drug molecules that were previously attached to the NPs under a magnetic field to targeted bone sites [228, 229].

10.3. Drug delivery

Magnetic NPs were used for the first time as delivery systems for drug delivery in cancer treatment in the late 1970s [168]. The magnetic properties of SPIONs permit their mechanic manipulation by a magnetic field gradient. This capacity of “acting at a distance” in combination with the intrinsic capacity that magnetic fields have to penetrate into human tissue, increases the specificity and selectivity of the therapy, enabling these particles to be conducted or held to a certain place through a magnetic field and heated to induce drug release or generate tissue hyperthermia [123, 230]. Therefore, the main benefits sought through use of nanovectors over simple drugs are: protection of the drug from their natural inhibitors, such as enzymatic degradation; specific and effective delivery of large quantities of therapeutic drugs utilizing biorecognition targets; pharmacokinetic and drug tissue distribution profile control; increased drug absorption into a selected tissue via increased retention effect and permeability; amelioration of intracellular penetration; avoidance of damage to healthy cells when cancer cells are killed and; low toxicity and immunogenicity [231, 232, 233].

SPIONs can work as vehicles for several molecules such as alkylating agents, plant alkaloids, antitumor antibiotics, antimetabolites, cytokines and monoclonal antibodies. Therefore, they function as delivery systems for therapeutic purposes [137, 168, 169]. A potential application is the conjugation of thrombin to IONs for use in the

promotion of wound healing, given that thrombin is necessary for the conversion of fibrinogen to fibrin, whose action is critical and necessary for the early and late stages of wound healing [234].

IONs can be used to solve the problem of lack of sensitivity of tumor cells to cytotoxic drugs, which occurs in tumor treatment. Indeed, some reports have proven the synergistic effect of IONs on the delivery of anticancer drugs [5, 170, 235, 236], namely increasing the accumulation of the drug daunorubicin in leukemia cells. This accumulation could be related to the capacity of the IONs to block glycoprotein P function [237]. Previous investigation has demonstrated that daunorubicin and 5-bromotetrandrine attached to magnetic IONs revealed a considerable cytotoxicity effect on drug resistant leukemia K562/A02 cells [238]. SPIONs and USPIONs can be further modified by incorporation of a photosensitizer that has proven capable of generating singlet oxygen ($^1O_2$), useful in cancer therapy [239].

To achieve drug-targeting, SPIONs are frequently combined with targeting ligands such as antibodies, small molecules or peptides. This will target them for specific sites and allow rapid accumulation of SPIONs as well as the drugs they carry into the regions of interest. Some examples are folic acid, given that the folate receptor is usually overexpressed solely in cancer cells, namely in ovary, breast, kidney, colon and lung, and restricted in normal tissues [4, 97, 98]. Antisense oligonucleotides coupled with silica-coated magnetic IONs are also described as being a significantly attractive targeting delivery system for selective tumor targeting and specific cellular uptake [240]. Recently, Seabra *et al* [241] reported that IONs coated with DMSA or mercaptosuccinic acid may be nitrosated in their thiol groups. This formation of S-nitroso groups on the surface of IONs permits the release of nitric oxide, which can be useful in anticancer therapies.

10.4. Hyperthermia

Hyperthermia is a therapeutic practice that relies on the enhancement of temperature in body tissues with the aim of changing the functionality of the cellular structures [86]. The earliest use of magnetic hyperthermia on tumors was described in 1957 by Gilchrist *et al* [242]. This author showed with *in vitro* assays that 5 mg of 20–100 nm diameter Fe_2O_3 NPs in lymph nodes (47 mg of Fe_2O_3 per gram of tissue) were able to trigger a temperature enhancement of 14 ºC in an alternating magnetic field of 200–240 Oe at 1.2 MHz [242]. However, the first prospective study for biomedical purposes in humans was described only in 1993. In 2010, magnetic hyperthermia trials involving the use of magnetic NPs passed preclinical stages and obtained regulatory authorization as a new clinical therapy denominated thermotherapy [243]. Recently, many IONs have been

developed to be used in hyperthermia, namely γ-Fe_2O_3 NPs coated with L-3,4-dihydroxyphenylalanine (L-DOPA) and *tetra*-methylrhodamine-5/6-isothiocyanate [162].

In this process, heat is produced as a result of magnetic hysteresis loss. When NPs are submitted to a high frequency AC magnetic field, they become heated due to Neel or Brownian relaxation losses in single-domain particles, which results in localized destruction of the cells [9, 35].

This local enhancement in temperature may be applied in medical treatments to destroy tumor cells and this is favored by the fact that cancer cells are more sensitive to abrupt rises in temperature above 43ºC than normal cells [86, 244]. In fact, the increase in temperature alters the performance of many structural and enzymatic cellular proteins, triggering repair enzyme inhibition, as well as alterations in DNA synthesis and conformation, together with alterations in differentiation and cell growth, which may lead to apoptosis. Hyperthermia may also trigger alterations in cell membrane which leads to a fall in transmembrane transport and provokes a destabilization of its potential [86].

Exposure of tumor cells to moderately high temperatures renders them sensitive to radiation and chemotherapy and may diminish their viability, depending on the exposure time and temperature [245]. Apart from killing cancer cells with heat, a host immune response is induced. Nevertheless, conventional hyperthermia systems encompass treatment solely once or twice per week, performed at intervals greater than 48 h to avoid thermotolerance provoked by the expression of heat shock proteins [245]. In addition, it is difficult to heat the local tumor region to the desired temperature without provoking damage in the normal tissue [245]. However, hyperthermia using magnetite NPs has proven to be efficient in animals with different types of tumor, including T-9 rat glioma, B16 mouse melanoma, VX-7 squamous cell carcinoma in rabbit tongue, Os515 hamster osteosarcoma and MM46 mouse mammary carcinoma [245].

10.5. Transfection

Transfection or gene therapy implies the introduction of genetic materials namely small interference RNA, oligonucleotides, plasmid DNA, messenger RNA and double-stranded DNA into tissues or target cells to express knockdown mutated deleterious genes, heterogeneous gene products, and substitute with functional genes. Gene delivery has demonstrated great promise in genetic disease treatments such as thalassemia, cystic fibrosis, influenza A, Huntington's disease, Parkinson's disease, cancer, inherited color blindness, etc. The gene carrier (usually denominated as a vector) is required to transfer the genetic sequences for gene expression into the cellular compartment. Vectors can be generally classified into two groups: nonviral and viral [103, 246, 247].

Magnetofection is a process whereby magnetic NPs linked to DNA are, under the influence of an external magnetic field, transfected into cells [9, 13]. NPs present numerous advantages as gene vectors over viral carriers, namely they:

- do not induce immune responses, since they are not biological materials;
- have limited genotoxicity and cytotoxicity;
- are able to mediate the introduction of foreign genes into the DNA of host chromosomes and consequently, foreign genes are expressed stably;
- have the ability to protect foreign genes from host enzymes and complement;
- may kill or destroy some viruses [248].

NPs cannot effectively label the required cells because of the repulsive electric interaction between the NPs and cell membrane, given that both the SPIONs and cell membrane possess a negatively charged surface. Therefore, a complex composed of SPIONs and transfection agents is frequently used to increase its labeling efficiency. The use of transfection agents is beneficial in transferring SPIONs to the target cells. The commonly used transfection agents such as PLL, lipofectamine, PEI and protamine sulphate are predominantly cationic [87, 103, 249, 250]. Positively charged magnetic NPs are endocytozed in the tight fitting vesicles due to the electrostatic interaction between positive charged magnetic NPs and the anionic cell membrane. Subsequently, the unsaturated amino groups trap the pumped-in-protons by the ATPase located on the endosomal membrane, which conducts to Cl^- ions retention and water molecules in the endosome. When water retention accumulates, swelling and bursting of the endosomes occur which results in the genetic material and magnetic NPs being released into the cytoplasm [103].

Therefore, NPs have the potential to be used in magnetofection. It has been reported that CLIO-Tat may be used to transfect CD34q hematopoietic T cell precursors and offers a suitable combination for effective T lymphocytes loading [251]. CLIO which show polyethylene glycol moiety and covalently linked branched PEI, mediates efficient and rapid transfection in primary vascular human umbilical vein endothelial cells (HUVEC) and effectively inhibits plasminogen activator inhibitor-1 expression which is responsible for several vascular dysfunctions, such as atherosclerosis and vascular inflammation. For this reason, these IONs offer a possible approach to transfect highly sensitive HUVEC [252].

10.6. DNA detection

IONs readily interact with proteins and as such, it is possible to combine several hydrophilic macromolecules (namely peptides and nucleotides) with IONs, which could be applied for highly sensitive detection of the DNA sequence [253, 254].

10.7. Tissue soldering

SPIONs may be used for tissue soldering [108]. For this purpose, their specific size requires an assessment for optimized heating ability given that these SPIONs may be “tuned” with their corresponding electromagnetic frequency, also called Neél and Brownian relaxation [108, 255].

10.8. Biofilm treatment and antibacterial activity

IONs may provide some supplementary advantages for biofilm treatment since iron restriction is intimately connected to the physiological onset of biofilm formation for common pathogenic bacteria, namely *Staphylococcus aureus, S. epidermidis* and *Pseudomonas aeruginosa* [229]. Inhibition of a bacterial colony formation even when the SPIONs concentration is 10 µg/mL has been described [229]. *In vitro* antimicrobial activity of magnetic poly(γ-glutamic acid)-coated NPs was also reported against *S. enteritidis, E. coli* and *S. aureus* [67]. It was also illustrated that IONs may be able to enhance the antibacterial activity of the bacitracin, which results in a lower dosage with a subsequent reduction in side effects associated with the antibiotics [256].

10.9. Vaccine carriers

The potential of IONs as potential vaccine carriers has also been reported. However, further work is being carried out to induce antibody responses *in vivo* [257]. Hu *et al* reported an ocular mucosal administration of IONs containing DNA vaccine pRSC-gD-IL-21 as promising in the inhibition of herpes stromal keratitis due to the efficient transport of plasmid DNA vaccine into target cells [258]. More recently, it was reported that IONs could be linked to polyinosinic-polycytidylic acid, an activator of Toll-like receptors 3 which is described as being a promising adjuvant for vaccines. Given that this receptor is expressed by tumor cells of several cancers, this system could prove an alternative in cancer treatment [259].

10.10. Peroxidase activity

Magnetic IONs were reported to have peroxidase behavior which is an attractive property apart from their superparamagnetism. Since IONs can compete with natural enzymes due to their robustness, ease of preparation and stability in adverse conditions, they may constitute robust, simple, easy-to-make and cost-effective biosensors in the future. For example, the capacity to catalyze the organic substrates oxidation to generate a color change and/or to diminish their toxicity is regularly employed as a detection tool or in the treatment of wastewater [260, 261, 262]. However, one of the most usual peroxidase-relevant applications is related to the oxidation reaction by hydrogen peroxide. Glucose detection is frequent in the laboratory or in clinics and is a common application of peroxidase. IONs also exhibit high sensitivity in glucose detection particles [261].

11. Final notes

IONs (USPIONs, <50 nm and SPIONs, >50 nm) encompass electrical, thermal, mechanical and imaging properties that gain relevance regarding their use in biomedicine. Due to these properties, several commercial formulations of these NPs (namely Ferumoxides, Ferucarbotran, Ferumoxtran-10, among others) have been extensively used in MRI. Tissue repair, drug delivery, hyperthermia and transfection among other biomedical applications mentioned in this review also represent other applications of this type of NPs. The number of applications of IONs is growing exponentially and this growth is estimated to increase endlessly in the future. New types of IONs are coming to market and significant research is being directed towards developing new types of IONs with different sizes and coatings for innovative applications in biomedicine. However, and despite the importance and enormous utility of these NPs in biomedicine, it will be important in the near future to evaluate their safety and the way in which the different types of existing and prospective IONs interact with the human body. Equally important will be the need to create a toxicology database for better control of the less beneficial effects of these NPs.

12. List of Abbreviations

$^1O_2$ – Singlet oxygen

BBB – Blood-brain barrier

C2A-GST – Domain of synaptotagmin I; glutathione S-transferase

CLIO – Cross-linked iron oxide nanoparticles

CNS – Central nervous system

DMSA – Dimercaptosuccinic acid

DNA – Deoxyribonucleic acid

FDA – Food and Drug Administration

HUVEC – Human umbilical vein endothelial cells

IONs – Iron oxide nanoparticles

LDL – Low density lipoproteins

L-DOPA – L-3,4-Dihydroxyphenylalanine

MIONs – Monocrystalline iron oxide nanoparticles

MRI – Magnetic resonance imaging

MSC – Mesenchymal stem cells

NPs – Nanoparticles

PAA – Polyacrylic acid

PEG – Polyethylene glycol

PEI – Polyethylenimine

PEO – Polyethylene oxide

PGMA – Poly(glycidyl methacrylate)

PLGA – Poly(lactic-co-glycolic acid)

PLL – Poly(L-lysine)

PTA – Polycationic transfection agents

PVA – Polyvinyl alcohol

PVP – Poly(vinylpyrrolidone)

RES – Reticuloendothelial system

ROS – Reactive oxygen species

SPIONs – Superparamagnetic iron oxide nanoparticles

SR – Scavenger receptors

TEM – Transmission electron microscopy

USPIONs – Ultra-small superparamagnetic iron oxide nanoparticles

TEM – Transmission electron microscopy

13. Conflicts of Interest

The authors declare that there are no conflicts of interest.

14. Acknowledgements

Diana Couto and Marisa Freitas acknowledge the FCT financial support for the PhD and Pos-doc grants (SFRH/BD/72856/2010 and SFRH/BPD/76909/2011, respectively), in the ambit of “POPH - QREN - Tipologia 4.1 - Formação Avançada” co-sponsored by FSE and national funds of MCTES.

15. References

[1] Azevedo, R.B.; Valois, C.R.; Chaves, S.B.; Silva, J.R.; Garcia, M.P. Leukocyte transepithelial migration in lung induced by DMSA functionalized magnetic nanoparticles. *Cell Adhes. Migr.*, **2011,** *5*(1), 29-33.

[2] Rai, M.K.; Gade, A.K.; Ingle, A.P. In: *A Textbook of Molecular Biotechnology*; Chauhan, A. K.; Varma, A.; I. K. International Publishing House: New Delhi, **2009**; pp 651.

[3] Cai, W.B.; Chen, X.Y. Nanoplatforms for targeted molecular imaging in living subjects. *Small*, **2007,** *3*(11), 1840-1854.

[4] Thanh, N.T.K.; Green, L.A.W. Functionalisation of nanoparticles for biomedical applications. *Nano Today*, **2010,** *5*(3), 213-230.

[5] Lv, G.; He, F.; Wang, X.; Gao, F.; Zhang, G.; Wang, T.; Jiang, H.; Wu, C.; Guo, D.; Li, X.; Chen, B.; Gu, Z. Novel nanocomposite of nano Fe_3O_4 and polylactide nanofibers for application in drug uptake and induction of cell death of leukemia cancer cells. *Langmuir*, **2008,** *24*(5), 2151-2156.

[6] Ma, Y.; Manolache, S.; Denes, F.S.; Thamm, D.H.; Kurzman, I.D.; Vail, D.M. Plasma synthesis of carbon magnetic nanoparticles and immobilization of doxorubicin for targeted drug delivery. *J. Biomater. Sci.- Polym. Ed.*, **2004,** *15*(8), 1033-1049.

[7] Issa, B.; Obaidat, I.M.; Albiss, B.A.; Haik, Y. Magnetic nanoparticles: Surface effects and properties related to biomedicine applications. *Int. J. Mol. Sci.*, **2013,** *14*(11), 21266-21305.

[8] Griffiths, S.M.; Singh, N.; Jenkins, G.J.; Williams, P.M.; Orbaek, A.W.; Barron, A.R.; Wright, C.J.; Doak, S.H. Dextran coated ultrafine superparamagnetic iron oxide nanoparticles: Compatibility with common fluorometric and colorimetric dyes. *Anal. Chem.*, **2011,** *83*(10), 3778-3785.

[9] Shubayev, V.I.; Pisanic, T.R., 2nd; Jin, S. Magnetic nanoparticles for theragnostics. *Adv. Drug Deliv. Rev.*, **2009,** *61*(6), 467-477.

[10] Zhang, W.; Kalive, M.; Capco, D.G.; Chen, Y. Adsorption of hematite nanoparticles onto Caco-2 cells and the cellular impairments: effect of particle size. *Nanotechnology*, **2010,** *21*(35), 355103.

[11] Wilkinson, K.; Ekstrand-Hammarstrom, B.; Ahlinder, L.; Guldevall, K.; Pazik, R.; Kepinski, L.; Kvashnina, K.O.; Butorin, S.M.; Brismar, H.; Onfelt, B.; Osterlund, L.; Seisenbaeva, G.A.; Kessler, V.G. Visualization of custom-tailored iron oxide nanoparticles chemistry, uptake, and toxicity. *Nanoscale*, **2012,** *4*(23), 7383-7393.

[12] Konczol, M.; Ebeling, S.; Goldenberg, E.; Treude, F.; Gminski, R.; Giere, R.; Grobety, B.; Rothen-Rutishauser, B.; Merfort, I.; Mersch-Sundermann, V. Cytotoxicity and genotoxicity of size-fractionated iron oxide (magnetite) in A549 human lung epithelial cells: Role of ROS, JNK, and NF-kB. *Chem. Res. Toxicol.*, **2011,** *24*(9), 1460-1475.

[13] Gupta, A.K.; Gupta, M. Synthesis and surface engineering of iron oxide nanoparticles for biomedical applications. *Biomaterials*, **2005,** *26*(18), 3995-4021.

[14] Auffan, M.; Achouak, W.; Rose, J.; Roncato, M.A.; Chaneac, C.; Waite, D.T.; Masion, A.; Woicik, J.C.; Wiesner, M.R.; Bottero, J.Y. Relation between the redox state of

iron-based nanoparticles and their cytotoxicity toward *Escherichia coli*. *Environ. Sci. Technol.*, **2008,** *42*(17), 6730-6735.

[15] Sorescu, M.; Xu, T.H.; Wise, A.; Diaz-Michelena, M.; McHenry, M.E. Studies on structural, magnetic and thermal properties of xFe_2TiO_4-$(1-x)Fe_3O_4$ ($0 \leq x \leq 1$) pseudo-binary system. *J. Magn. Magn. Mater.*, **2012,** *324*(7), 1453-1462.

[16] Singh, N.; Jenkins, G.J.; Asadi, R.; Doak, S.H. Potential toxicity of superparamagnetic iron oxide nanoparticles (SPION). *Nano Rev.*, **2010,** *1*, 5358.

[17] Goloverda, G.; Jackson, B.; Kidd, C.; Kolesnichenko, V. Synthesis of ultrasmall magnetic iron oxide nanoparticles and study of their colloid and surface chemistry. *J. Magn. Magn. Mater.*, **2009,** *321*(10), 1372-1376.

[18] Wang, Y.; Wang, B.; Zhu, M.T.; Li, M.; Wang, H.J.; Wang, M.; Ouyang, H.; Chai, Z.F.; Feng, W.Y.; Zhao, Y.L. Microglial activation, recruitment and phagocytosis as linked phenomena in ferric oxide nanoparticle exposure. *Toxicol. Lett.*, **2011,** *205*(1), 26-37.

[19] Bhattacharya, K.; Hoffmann, E.; Schins, R.F.; Boertz, J.; Prantl, E.M.; Alink, G.M.; Byrne, H.J.; Kuhlbusch, T.A.; Rahman, Q.; Wiggers, H.; Schulz, C.; Dopp, E. Comparison of micro- and nanoscale Fe^{+3}-containing (hematite) particles for their toxicological properties in human lung cells *in vitro*. *Toxicol. Sci.*, **2012,** *126*(1), 173-182.

[20] Freyria, F.S.; Bonelli, B.; Tomatis, M.; Ghiazza, M.; Gazzano, E.; Ghigo, D.; Garrone, E.; Fubini, B. Hematite nanoparticles larger than 90 nm show no sign of toxicity in terms of lactate dehydrogenase release, nitric oxide generation, apoptosis, and comet assay in murine alveolar macrophages and human lung epithelial cells. *Chem. Res. Toxicol.*, **2012,** *25*(4), 850-861.

[21] Prim, S.R.; Folgueras, M.V.; de Lima, M.A.; Hotza, D. Synthesis and characterization of hematite pigment obtained from a steel waste industry. *J. Hazard. Mater.*, **2011,** *192*(3), 1307-1313.

[22] Uppal, R.; Caravan, P. Targeted probes for cardiovascular MRI. *Future Med. Chem.*, **2010,** *2*(3), 451-470.

[23] Soenen, S.J.; De Cuyper, M. Assessing iron oxide nanoparticle toxicity *in vitro*: current status and future prospects. *Nanomedicine*, **2010,** *5*(8), 1261-1275.

[24] Jander, S.; Schroeter, M.; Saleh, A. Imaging inflammation in acute brain ischemia. *Stroke*, **2007,** *38*(2 Suppl), 642-645.

[25] Babic, M.; Horak, D.; Trchova, M.; Jendelova, P.; Glogarova, K.; Lesny, P.; Herynek, V.; Hajek, M.; Sykova, E. Poly(L-lysine)-modified iron oxide nanoparticles for stem cell labeling. *Bioconjugate Chem.*, **2008,** *19*(3), 740-750.

[26] Stark, D.D.; Weissleder, R.; Elizondo, G.; Hahn, P.F.; Saini, S.; Todd, L.E.; Wittenberg, J.; Ferrucci, J.T. Superparamagnetic iron oxide: Clinical application as a contrast agent for MR imaging of the liver. *Radiology*, **1988,** *168*(2), 297-301.

[27] Cheng, F.Y.; Su, C.H.; Yang, Y.S.; Yeh, C.S.; Tsai, C.Y.; Wu, C.L.; Wu, M.T.; Shieh, D.B. Characterization of aqueous dispersions of Fe_3O_4 nanoparticles and their biomedical applications. *Biomaterials*, **2005,** *26*(7), 729-738.

[28] Corot, C.; Robert, P.; Idee, J.M.; Port, M. Recent advances in iron oxide nanocrystal technology for medical imaging. *Adv. Drug Deliv. Rev.*, **2006,** *58*(14), 1471-1504.

[29] Das, M.; Mishra, D.; Dhak, P.; Gupta, S.; Maiti, T.K.; Basak, A.; Pramanik, P. Biofunctionalized, phosphonate-grafted, ultrasmall iron oxide nanoparticles for combined targeted cancer therapy and multimodal imaging. *Small*, **2009,** *5*(24), 2883-2893.

[30] Adden, N.; Gamble, L.J.; Castner, D.G.; Hoffmann, A.; Gross, G.; Menzel, H. Phosphonic acid monolayers for binding of bioactive molecules to titanium surfaces. *Langmuir*, **2006,** *22*(19), 8197-8204.

[31] Das, M.; Mishra, D.; Maiti, T.K.; Basak, A.; Pramanik, P. Bio-functionalization of magnetite nanoparticles using an aminophosphonic acid coupling agent: new, ultradispersed, iron-oxide folate nanoconjugates for cancer-specific targeting. *Nanotechnology*, **2008,** *19*(41), 415101.

[32] McCarthy, J.R.; Weissleder, R. Multifunctional magnetic nanoparticles for targeted imaging and therapy. *Adv. Drug Deliv. Rev.*, **2008,** *60*(11), 1241-1251.

[33] Sun, C.; Fang, C.; Stephen, Z.; Veiseh, O.; Hansen, S.; Lee, D.; Ellenbogen, R.G.; Olson, J.; Zhang, M. Tumor-targeted drug delivery and MRI contrast enhancement by chlorotoxin-conjugated iron oxide nanoparticles. *Nanomedicine*, **2008,** *3*(4), 495-505.

[34] Wu, W.; He, Q.G.; Jiang, C.Z. Magnetic iron oxide nanoparticles: Synthesis and surface functionalization strategies. *Nanoscale Res. Lett.*, **2008,** *3*(11), 397-415.

[35] Wahajuddin; Arora, S. Superparamagnetic iron oxide nanoparticles: magnetic nanoplatforms as drug carriers. *Int. J. Nanomed.*, **2012,** *7*, 3445-3471.

[36] Kim, J.E.; Shin, J.Y.; Cho, M.H. Magnetic nanoparticles: an update of application for drug delivery and possible toxic effects. *Arch. Toxicol.*, **2012,** *86*(5), 685-700.

[37] Kubinova, S.; Sykova, E. Nanotechnologies in regenerative medicine. *Minim. Invasive Ther. Allied Technol.*, **2010,** *19*(3), 144-156.

[38] Burtea, C.; Laurent, S.; Mahieu, I.; Larbanoix, L.; Roch, A.; Port, M.; Rousseaux, O.; Ballet, S.; Murariu, O.; Toubeau, G.; Corot, C.; Vander Elst, L.; Muller, R.N. *In vitro* biomedical applications of functionalized iron oxide nanoparticles, including those not related to magnetic properties. *Contrast Media Mol. Imaging*, **2011,** *6*(4), 236-250.

[39] Petri-Fink, A.; Chastellain, M.; Juillerat-Jeanneret, L.; Ferrari, A.; Hofmann, H. Development of functionalized superparamagnetic iron oxide nanoparticles for interaction with human cancer cells. *Biomaterials*, **2005,** *26*(15), 2685-2694.

[40] Hassan, C.M.; Peppas, N.A. Structure and applications of poly(vinyl alcohol) hydrogels produced by conventional crosslinking or by freezing/thawing methods. *Adv. Polym. Sci.*, **2000,** *153*, 37-65.

[41] Blank, F.; Gerber, P.; Rothen-Rutishauser, B.; Sakulkhu, U.; Salaklang, J.; De Peyer, K.; Gehr, P.; Nicod, L.P.; Hofmann, H.; Geiser, T.; Petri-Fink, A.; Von Garnier, C. Biomedical nanoparticles modulate specific $CD4^+$ T cell stimulation by inhibition of antigen processing in dendritic cells. *Nanotoxicology*, **2011,** *5*(4), 606-621.

[42] Boyer, C.; Whittaker, M.R.; Bulmus, V.; Liu, J.Q.; Davis, T.P. The design and utility of polymer-stabilized iron-oxide nanoparticles for nanomedicine applications. *NPG Asia Mater.*, **2010,** *2*(1), 23-30.

[43] Reddy, A.M.; Kwak, B.K.; Shim, H.J.; Ahn, C.; Cho, S.H.; Kim, B.J.; Jeong, S.Y.; Hwang, S.J.; Yuk, S.H. Functional characterization of mesenchymal stem cells labeled with a novel PVP-coated superparamagnetic iron oxide. *Contrast Media Mol. Imaging*, **2009,** *4*(3), 118-126.

[44] Lee, H.Y.; Lim, N.H.; Seo, J.A.; Yuk, S.H.; Kwak, B.K.; Khang, G.; Lee, H.B.; Cho, S.H. Preparation and magnetic resonance imaging effect of polyvinylpyrrolidone-coated iron oxide nanoparticles. *J. Biomed. Mater. Res. B Appl. Biomater.*, **2006,** *79B*(1), 142-150.

[45] Huang, C.; Neoh, K.G.; Kang, E.T. Combined ATRP and 'click' chemistry for designing stable tumor-targeting superparamagnetic iron oxide nanoparticles. *Langmuir*, **2012,** *28*(1), 563-571.

[46] Gupta, A.K.; Wells, S. Surface-modified superparamagnetic nanoparticles for drug delivery: Preparation, characterization, and cytotoxicity studies. *IEEE Trans. Nanobiosci.*, **2004,** *3*(1), 66-73.

[47] Roohi, F.; Lohrke, J.; Ide, A.; Schutz, G.; Dassler, K. Studying the effect of particle size and coating type on the blood kinetics of superparamagnetic iron oxide nanoparticles. *Int. J. Nanomed.*, **2012,** *7*, 4447-4458.

[48] Zhang, J.; Dong, G.; Thurber, A.; Hou, Y.; Gu, M.; Tenne, D.A.; Hanna, C.B.; Punnoose, A. Tuning the properties of ZnO, hematite, and Ag nanoparticles by adjusting the surface charge. *Adv. Mater.*, **2012,** *24*(9), 1232-1237.

[49] Stayton, P.S.; El-Sayed, M.E.; Murthy, N.; Bulmus, V.; Lackey, C.; Cheung, C.; Hoffman, A.S. 'Smart' delivery systems for biomolecular therapeutics. *Orthod. Craniofac. Res.*, **2005,** *8*(3), 219-225.

[50] Prijic, S.; Prosen, L.; Cemazar, M.; Scancar, J.; Romih, R.; Lavrencak, J.; Bregar, V.B.; Coer, A.; Krzan, M.; Znidarsic, A.; Sersa, G. Surface modified magnetic nanoparticles for immuno-gene therapy of murine mammary adenocarcinoma. *Biomaterials*, **2012,** *33*(17), 4379-4391.

[51] Ding, J.; Tao, K.; Li, J.; Song, S.; Sun, K. Cell-specific cytotoxicity of dextran-stabilized magnetite nanoparticles. *Colloids Surf. B Biointerfaces*, **2010,** *79*(1), 184-190.

[52] Mehvar, R. Dextrans for targeted and sustained delivery of therapeutic and imaging agents. *J. Control. Release*, **2000,** *69*(1), 1-25.

[53] Feng, J.; Liu, H.; Bhakoo, K.K.; Lu, L.; Chen, Z. A metabonomic analysis of organ specific response to USPIO administration. *Biomaterials*, **2011,** *32*(27), 6558-6569.

[54] Dias, A.M.G.C.; Hussain, A.; Marcos, A.S.; Roque, A.C.A. A biotechnological perspective on the application of iron oxide magnetic colloids modified with polysaccharides. *Biotechnol. Adv.*, **2011,** *29*(1), 142-155.

[55] Papaphilippou, P.; Loizou, L.; Popa, N.C.; Han, A.; Vekas, L.; Odysseos, A.; Krasia-Christoforou, T. Superparamagnetic hybrid micelles, based on iron oxide nanoparticles and well-defined diblock copolymers possessing b-ketoester functionalities. *Biomacromolecules*, **2009,** *10*(9), 2662-2671.

[56] Askari, M.; Fisher, C.; Weniger, F.G.; Bidic, S.; Lee, W.P.A. Anticoagulation therapy in microsurgery: A review. *J. Hand Surg.-Am. Vol.*, **2006,** *31A*(5), 836-846.

[57] Corot, C.; Petry, K.G.; Trivedi, R.; Saleh, A.; Jonkmanns, C.; Le Bas, J.F.; Blezer, E.; Rausch, M.; Brochet, B.; Foster-Gareau, P.; Baleriaux, D.; Gaillard, S.; Dousset, V. Macrophage imaging in central nervous system and in carotid atherosclerotic plaque using ultrasmall superparamagnetic iron oxide in magnetic resonance imaging. *Invest. Radiol.*, **2004,** *39*(10), 619-625.

[58] Andreas, K.; Georgieva, R.; Ladwig, M.; Mueller, S.; Notter, M.; Sittinger, M.; Ringe, J. Highly efficient magnetic stem cell labeling with citrate-coated superparamagnetic iron oxide nanoparticles for MRI tracking. *Biomaterials*, **2012,** *33*(18), 4515-4525.

[59] Vu-Quang, H.; Yoo, M.K.; Jeong, H.J.; Lee, H.J.; Muthiah, M.; Rhee, J.H.; Lee, J.H.; Cho, C.S.; Jeong, Y.Y.; Park, I.K. Targeted delivery of mannan-coated superparamagnetic iron oxide nanoparticles to antigen-presenting cells for magnetic resonance-based diagnosis of metastatic lymph nodes *in vivo*. *Acta Biomater.*, **2011,** *7*(11), 3935-3945.

[60] Kunzmann, A.; Andersson, B.; Vogt, C.; Feliu, N.; Ye, F.; Gabrielsson, S.; Toprak, M.S.; Buerki-Thurnherr, T.; Laurent, S.; Vahter, M.; Krug, H.; Muhammed, M.; Scheynius, A.; Fadeel, B. Efficient internalization of silica-coated iron oxide nanoparticles of different sizes by primary human macrophages and dendritic cells. *Toxicol. Appl. Pharmacol.*, **2011,** *253*(2), 81-93.

[61] Wunderbaldinger, P.; Josephson, L.; Weissleder, R. Crosslinked iron oxides (CLIO): A new platform for the development of targeted MR contrast agents. *Acad. Radiol.*, **2002,** *9*(suppl 2), S304-S306.

[62] Moore, A.; Weissleder, R.; Bogdanov, A., Jr. Uptake of dextran-coated monocrystalline iron oxides in tumor cells and macrophages. *J. Magn. Reson. Imaging*, **1997,** *7*(6), 1140-1145.

[63] Zinderman, C.E.; Landow, L.; Wise, R.P. Anaphylactoid reactions to Dextran 40 and 70: reports to the United States Food and drug administration, 1969 to 2004. *J. Vasc. Surg.*, **2006,** *43*(5), 1004-1009.

[64] Mailander, V.; Lorenz, M.R.; Holzapfel, V.; Musyanovych, A.; Fuchs, K.; Wiesneth, M.; Walther, P.; Landfester, K.; Schrezenmeier, H. Carboxylated superparamagnetic iron oxide particles label cells intracellularly without transfection agents. *Mol. Imaging Biol.*, **2008,** *10*(3), 138-146.

[65] Metz, S.; Bonaterra, G.; Rudelius, M.; Settles, M.; Rummeny, E.J.; Daldrup-Link, H.E. Capacity of human monocytes to phagocytose approved iron oxide MR contrast agents *in vitro*. *Eur. Radiol.*, **2004,** *14*(10), 1851-1858.

[66] Ayala, V.; Herrera, A.P.; Latorre-Esteves, M.; Torres-Lugo, M.; Rinaldi, C. Effect of surface charge on the colloidal stability and *in vitro* uptake of carboxymethyl dextran-coated iron oxide nanoparticles. *J. Nanopart. Res.*, **2013,** *15*(8), 1874.

[67] Inbaraj, B.S.; Kao, T.H.; Tsai, T.Y.; Chiu, C.P.; Kumar, R.; Chen, B.H. The synthesis and characterization of poly(γ -glutamic acid)-coated magnetite nanoparticles and their effects on antibacterial activity and cytotoxicity. *Nanotechnology*, **2011,** *22*(7), 075101.

[68] Xu, H.; Jiang, M.; Li, H.; Lu, D.Q.; Ouyang, P. Efficient production of poly(γ-glutamic acid) by newly isolated Bacillus subtilis NX-2. *Process Biochem.*, **2005,** *40*(2), 519-523.

[69] Riva, R.; Ragelle, H.; des Rieux, A.; Duhem, N.; Jerome, C.; Preat, V. Chitosan and chitosan derivatives in drug delivery and tissue engineering. *Adv. Polym. Sci.*, **2011,** *244*, 19-44.

[70] Reddy, A.M.; Kwak, B.K.; Shim, H.J.; Ahn, C.; Lee, H.S.; Suh, Y.J.; Park, E.S. *In vivo* tracking of mesenchymal stem cells labeled with a novel chitosan-coated superparamagnetic iron oxide nanoparticles using 3.0T MRI. *J. Korean Med. Sci.*, **2010,** *25*(2), 211-219.

[71] Shen, J.M.; Guan, X.M.; Liu, X.Y.; Lan, J.F.; Cheng, T.; Zhang, H.X. Luminescent/magnetic hybrid nanoparticles with folate-conjugated peptide composites for tumor-targeted drug delivery. *Bioconjugate Chem.*, **2012,** *23*, 1010-1021.

[72] Xia, W.S.; Liu, P.; Zhang, J.L.; Chen, J. Biological activities of chitosan and chitooligosaccharides. *Food Hydrocolloids*, **2011,** *25*(2), 170-179.

[73] Qu, J.B.; Shao, H.H.; Jing, G.L.; Huang, F. PEG-chitosan-coated iron oxide nanoparticles with high saturated magnetization as carriers of 10-hydroxycamptothecin:

Preparation, characterization and cytotoxicity studies. *Colloids Surf. B Biointerfaces*, **2013,** *102*, 37-44.

[74] Bhattarai, S.R.; Badahur, K.C.R.; Aryal, S.; Khil, M.S.; Kim, H.Y. N-Acylated chitosan stabilized iron oxide nanoparticles as a novel nano-matrix and ceramic modification. *Carbohydr. Polym.*, **2007,** *69*(3), 467-477.

[75] Kim, S.K.; Venkatesan, J. In: *Chitin and Chitosan Derivatives: Advances in Drug Discovery and Developments*; Kim, S. K.; CRC Press: Florida, **2014**; pp 4-7.

[76] Fan, C.; Gao, W.; Chen, Z.; Fan, H.; Li, M.; Deng, F. Tumor selectivity of stealth multi-functionalized superparamagnetic iron oxide nanoparticles. *Int. J. Pharm.*, **2011,** *404*(1-2), 180-190.

[77] Sundaresan, V.; Menon, J.U.; Rahimi, M.; Nguyen, K.T.; Wadajkar, A.S. Dual-responsive polymer-coated iron oxide nanoparticles for drug delivery and imaging applications. *Int. J. Pharm.*, **2014,** *466*(1-2), 1-7.

[78] Heskins, M.; Guillet, J.E. Solution properties of poly(N-isopropylacrylamide). *J. Macromol. Sci.*, **1968,** *2*(8), 1441-1455.

[79] Campbell, S.B.; Patenaude, M.; Hoare, T. Injectable superparamagnets: Highly elastic and degradable poly(N-isopropylacrylamide)-superparamagnetic iron oxide nanoparticle (SPION) composite hydrogels. *Biomacromolecules*, **2013,** *14*(3), 644-653.

[80] Patenaude, M.; Hoare, T. Injectable, degradable thermoresponsive poly(N-isopropylacrylamide) hydrogels. *ACS Macro Lett.*, **2012,** *1*(3), 409-413.

[81] Noori, A.; Parivar, K.; Modaresi, M.; Messripour, M.; Yousefi, M.H.; Amiri, G.R. Effect of magnetic iron oxide nanoparticles on pregnancy and testicular development of mice. *Afr. J. Biotechnol.*, **2011,** *10*(7), 1221-1227.

[82] Flora, S.J.S.; Pachauri, V. Chelation in metal intoxication. *Int. J. Environ. Res. Public Health*, **2010,** *7*(7), 2745-2788.

[83] Wilhelm, C.; Billotey, C.; Roger, J.; Pons, J.N.; Bacri, J.C.; Gazeau, F. Intracellular uptake of anionic superparamagnetic nanoparticles as a function of their surface coating. *Biomaterials*, **2003,** *24*(6), 1001-1011.

[84] Zhu, X.M.; Wang, Y.X.; Leung, K.C.; Lee, S.F.; Zhao, F.; Wang, D.W.; Lai, J.M.; Wan, C.; Cheng, C.H.; Ahuja, A.T. Enhanced cellular uptake of aminosilane-coated superparamagnetic iron oxide nanoparticles in mammalian cell lines. *Int. J. Nanomed.*, **2012,** *7*, 953-964.

[85] Thorek, D.L.J.; Tsourkas, A. Size, charge and concentration dependent uptake of iron oxide particles by non-phagocytic cells. *Biomaterials*, **2008,** *29*(26), 3583-3590.

[86] Silva, A.C.; Oliveira, T.R.; Mamani, J.B.; Malheiros, S.M.; Malavolta, L.; Pavon, L.F.; Sibov, T.T.; Amaro, E., Jr.; Tannus, A.; Vidoto, E.L.; Martins, M.J.; Santos, R.S.;

Gamarra, L.F. Application of hyperthermia induced by superparamagnetic iron oxide nanoparticles in glioma treatment. *Int. J. Nanomed.*, **2011,** *6*, 591-603.

[87] Dalby, B.; Cates, S.; Harris, A.; Ohki, E.C.; Tilkins, M.L.; Price, P.J.; Ciccarone, V.C. Advanced transfection with Lipofectamine 2000 reagent: primary neurons, siRNA, and high-throughput applications. *Methods*, **2004,** *33*(2), 95-103.

[88] Zhang, S.; He, H.; Lu, W.; Xu, Q.; Zhou, B.; Tang, X. Tracking intrahepatically transplanted islets labeled with Feridex-polyethyleneimine complex using a clinical 3.0-T magnetic resonance imaging scanner. *Pancreas*, **2009,** *38*(3), 293-302.

[89] Petri-Fink, A.; Steitz, B.; Finka, A.; Salaklang, J.; Hofmann, H. Effect of cell media on polymer coated superparamagnetic iron oxide nanoparticles (SPIONs): Colloidal stability, cytotoxicity, and cellular uptake studies. *Eur. J. Pharm. Biopharm.*, **2008,** *68*(1), 129-137.

[90] Neu, M.; Fischer, D.; Kissel, T. Recent advances in rational gene transfer vector design based on poly(ethylene imine) and its derivatives. *J. Gene Med.*, **2005,** *7*(8), 992-1009.

[91] Jasmin; Torres, A.L.; Nunes, H.M.; Passipieri, J.A.; Jelicks, L.A.; Gasparetto, E.L.; Spray, D.C.; Campos de Carvalho, A.C.; Mendez-Otero, R. Optimized labeling of bone marrow mesenchymal cells with superparamagnetic iron oxide nanoparticles and *in vivo* visualization by magnetic resonance imaging. *J. Nanobiotechnology*, **2011,** *9*, 4.

[92] Kadam, S.S.; Mahadik, K.R.; Bothara, K.G. *Principles of Medicinal Chemistry*, 8th ed; Nirali Prakashan: Mumbai, **2007**.

[93] Kalish, H.; Arbab, A.S.; Miller, B.R.; Lewis, B.K.; Zywicke, H.A.; Bulte, J.W.M.; Bryant, L.H.; Frank, J.A. Combination of transfection agents and magnetic resonance contrast agents for cellular imaging: Relationship between relaxivities, electrostatic forces, and chemical composition. *Magn. Reson. Med.*, **2003,** *50*(2), 275-282.

[94] Frank, J.A.; Zywicke, H.; Jordan, E.K.; Mitchell, J.; Lewis, B.K.; Miller, B.; Bryant, L.H.; Bulte, J.W.M. Magnetic intracellular labeling of mammalian cells by combining (FDA-approved) superparamagnetic iron oxide MR contrast agents and commonly used transfection agents. *Acad. Radiol.*, **2002,** *9*(suppl 2), S484-S487.

[95] Chen, T.J.; Cheng, T.H.; Hung, Y.C.; Lin, K.T.; Liu, G.C.; Wang, Y.M. Targeted folic acid-PEG nanoparticles for noninvasive imaging of folate receptor by MRI. *J. Biomed. Mater. Res. Part A*, **2008,** *87*(1), 165-175.

[96] Cichoke, A.C. *The Complete Book of Enzyme Therapy: A pratical guide to using the natural power of enzymes to maximize your health and combat a host of common disorders, ranging from allergies to cardiovascular disease to indigestion*, Penguin Putnam Publishers: New York, **1999**.

[97] Zwicke, G.L.; Mansoori, G.A.; Jeffery, C.J. Utilizing the folate receptor for active targeting of cancer nanotherapeutics. *Nano Rev.*, **2012,** *3*, 18496.

[98] Mahato, R.; Tai, W.Y.; Cheng, K. Prodrugs for improving tumor targetability and efficiency. *Adv. Drug Deliv. Rev.*, **2011,** *63*(8), 659-670.

[99] Liao, Z.; Wang, H.; Lv, R.; Zhao, P.; Sun, X.; Wang, S.; Su, W.; Niu, R.; Chang, J. Polymeric liposomes-coated superparamagnetic iron oxide nanoparticles as contrast agent for targeted magnetic resonance imaging of cancer cells. *Langmuir*, **2011,** *27*(6), 3100-3105.

[100] Hong, S.C.; Lee, J.H.; Lee, J.; Kim, H.Y.; Park, J.Y.; Cho, J.; Han, D.W. Subtle cytotoxicity and genotoxicity differences in superparamagnetic iron oxide nanoparticles coated with various functional groups. *Int. J. Nanomed.*, **2011,** *6*, 3219-3231.

[101] Hoskins, C.; Cuschieri, A.; Wang, L. The cytotoxicity of polycationic iron oxide nanoparticles: Common endpoint assays and alternative approaches for improved understanding of cellular response mechanism. *J. Nanobiotechnology*, **2012,** *10*, 15.

[102] Mahmoudi, M.; Laurent, S.; Shokrgozar, M.A.; Hosseinkhani, M. Toxicity evaluations of superparamagnetic iron oxide nanoparticles: cell "vision" versus physicochemical properties of nanoparticles. *ACS Nano*, **2011,** *5*(9), 7263-7276.

[103] Meng Lin, M.; Kim, H.H.; Kim, H.; Muhammed, M.; Kyung Kim, D. Iron oxide-based nanomagnets in nanomedicine: fabrication and applications. *Nano Rev.*, **2010,** *1*, 4883.

[104] Wan, S.; Huang, J.; Guo, M.; Zhang, H.; Cao, Y.; Yan, H.; Liu, K. Biocompatible superparamagnetic iron oxide nanoparticle dispersions stabilized with poly(ethylene glycol)-oligo(aspartic acid) hybrids. *J. Biomed. Mater. Res. Part A*, **2007,** *80*(4), 946-954.

[105] Topkaya, R.; Akman, O.; Kazan, S.; Aktas, B.; Durmus, Z.; Baykal, A. Surface spin disorder and spin-glass-like behaviour in manganese-substituted cobalt ferrite nanoparticles. *J. Nanopart. Res.*, **2012,** *14*(10), 1156.

[106] Firouznia, K.; Amirmohseni, S.; Guiti, M.; Amanpour, S.; Baitollahi, A.; Kharadmand, A.A.; Mohagheghi, M.A.; Oghabian, M.A. MR relaxivity measurement of iron oxide nano-particles for MR lymphography applications. *Pak. J. Biol. Sci.*, **2008,** *11*(4), 607-612.

[107] Briley-Saebo, K.; Bjornerud, A.; Grant, D.; Ahlstrom, H.; Berg, T.; Kindberg, G.M. Hepatic cellular distribution and degradation of iron oxide nanoparticles following single intravenous injection in rats: implications for magnetic resonance imaging. *Cell Tissue Res.*, **2004,** *316*(3), 315-323.

[108] Schlachter, E.K.; Widmer, H.R.; Bregy, A.; Lonnfors-Weitzel, T.; Vajtai, I.; Corazza, N.; Bernau, V.J.; Weitzel, T.; Mordasini, P.; Slotboom, J.; Herrmann, G.; Bogni, S.; Hofmann, H.; Frenz, M.; Reinert, M. Metabolic pathway and distribution of

superparamagnetic iron oxide nanoparticles: *in vivo* study. *Int. J. Nanomed.*, **2011,** *6*, 1793-1800.

[109] Berry, C.C. Progress in functionalization of magnetic nanoparticles for applications in biomedicine. *J. Phys. D-Appl. Phys.*, **2009,** *42*(22), 224003 (224009pp).

[110] Almeida, J.P.; Chen, A.L.; Foster, A.; Drezek, R. *In vivo* biodistribution of nanoparticles. *Nanomedicine*, **2011,** *6*(5), 815-835.

[111] Zhu, M.T.; Feng, W.Y.; Wang, Y.; Wang, B.; Wang, M.; Ouyang, H.; Zhao, Y.L.; Chai, Z.F. Particokinetics and extrapulmonary translocation of intratracheally instilled ferric oxide nanoparticles in rats and the potential health risk assessment. *Toxicol. Sci.*, **2009,** *107*(2), 342-351.

[112] Stolnik, S.; Illum, L.; Davis, S.S. Long circulating microparticulate drug carriers. *Adv. Drug Deliv. Rev.*, **1995,** *16*(2-3), 195-214.

[113] Barry, S.E. Challenges in the development of magnetic particles for therapeutic applications. *Int. J. Hyperthermia*, **2008,** *24*(6), 451-466.

[114] Elias, A.; Tsourkas, A. Imaging circulating cells and lymphoid tissues with iron oxide nanoparticles. *Hematology Am. Soc. Hematol. Educ. Program.*, **2009**, 720-726.

[115] Weinstein, J.S.; Varallyay, C.G.; Dosa, E.; Gahramanov, S.; Hamilton, B.; Rooney, W.D.; Muldoon, L.L.; Neuwelt, E.A. Superparamagnetic iron oxide nanoparticles: diagnostic magnetic resonance imaging and potential therapeutic applications in neurooncology and central nervous system inflammatory pathologies, a review. *J. Cereb. Blood Flow Metab.*, **2010,** *30*(1), 15-35.

[116] Petry, K.G.; Boiziau, C.; Dousset, V.; Brochet, B. Magnetic resonance imaging of human brain macrophage infiltration. *Neurotherapeutics*, **2007,** *4*(3), 434-442.

[117] Veiseh, O.; Gunn, J.W.; Zhang, M.Q. Design and fabrication of magnetic nanoparticles for targeted drug delivery and imaging. *Adv. Drug Deliv. Rev.*, **2010,** *62*(3), 284-304.

[118] Ma, H.L.; Xu, Y.F.; Qi, X.R.; Maitani, Y.; Nagai, T. Superparamagnetic iron oxide nanoparticles stabilized by alginate: Pharmacokinetics, tissue distribution, and applications in detecting liver cancers. *Int. J. Pharm.*, **2008,** *354*(1-2), 217-226.

[119] Neuberger, T.; Schopf, B.; Hofmann, H.; Hofmann, M.; von Rechenberg, B. Superparamagnetic nanoparticles for biomedical applications: Possibilities and limitations of a new drug delivery system. *J. Magn. Magn. Mater.*, **2005,** *293*(1), 483-496.

[120] Oude Engberink, R.D.; van der Pol, S.M.; Dopp, E.A.; de Vries, H.E.; Blezer, E.L. Comparison of SPIO and USPIO for *in vitro* labeling of human monocytes: MR detection and cell function. *Radiology*, **2007,** *243*(2), 467-474.

[121] Berry, C.C.; Curtis, A.S.G. Functionalisation of magnetic nanoparticles for applications in biomedicine. *J. Phys. D-Appl. Phys.*, **2003,** *36*(13), R198-R206.

[122] Islam, T.; Wolf, G. The pharmacokinetics of the lymphotropic nanoparticle MRI contrast agent ferumoxtran-10. *Cancer Biomark.*, **2009,** *5*(2), 69-73.

[123] Arruebo, M.; Fernandez-Pacheco, R.; Ibarra, M.R.; Santamaria, J. Magnetic nanoparticles for drug delivery. *Nano Today*, **2007,** *2*(3), 22-32.

[124] Luciani, N.; Wilhelm, C.; Gazeau, F. The role of cell-released microvesicles in the intercellular transfer of magnetic nanoparticles in the monocyte/macrophage system. *Biomaterials*, **2010,** *31*(27), 7061-7069.

[125] Pawelczyk, E.; Arbab, A.S.; Pandit, S.; Hu, E.; Frank, J.A. Expression of transferrin receptor and ferritin following ferumoxides-protamine sulfate labeling of cells: implications for cellular magnetic resonance imaging. *NMR Biomed.*, **2006,** *19*(5), 581-592.

[126] Papachristodoulou, D.; Snape, A.; Elliott, W.H.; Elliot, D.C. *Biochemistry & Molecular Biology*, 5th ed.; Oxford: Oxford, **2014**.

[127] Muller, K.; Skepper, J.N.; Posfai, M.; Trivedi, R.; Howarth, S.; Corot, C.; Lancelot, E.; Thompson, P.W.; Brown, A.P.; Gillard, J.H. Effect of ultrasmall superparamagnetic iron oxide nanoparticles (Ferumoxtran-10) on human monocyte-macrophages *in vitro*. *Biomaterials*, **2007,** *28*(9), 1629-1642.

[128] Asokan, A.; Cho, M.J. Exploitation of intracellular pH gradients in the cellular delivery of macromolecules. *J. Pharm. Sci.*, **2002,** *91*(4), 903-913.

[129] Aisen, P.; Enns, C.; Wessling-Resnick, M. Chemistry and biology of eukaryotic iron metabolism. *Int. J. Biochem. Cell Biol.*, **2001,** *33*(10), 940-959.

[130] Hanini, A.; Schmitt, A.; Kacem, K.; Chau, F.; Ammar, S.; Gavard, J. Evaluation of iron oxide nanoparticle biocompatibility. *Int. J. Nanomed.*, **2011,** *6*, 787-794.

[131] Bourrinet, P.; Bengele, H.H.; Bonnemain, B.; Dencausse, A.; Idee, J.M.; Jacobs, P.M.; Lewis, J.M. Preclinical safety and pharmacokinetic profile of ferumoxtran-10, an ultrasmall superparamagnetic iron oxide magnetic resonance contrast agent. *Invest. Radiol.*, **2006,** *41*(3), 313-324.

[132] Iversen, N.K.; Frische, S.; Thomsen, K.; Laustsen, C.; Pedersen, M.; Hansen, P.B.; Bie, P.; Fresnais, J.; Berret, J.F.; Baatrup, E.; Wang, T. Superparamagnetic iron oxide polyacrylic acid coated γ-Fe_2O_3 nanoparticles do not affect kidney function but cause acute effect on the cardiovascular function in healthy mice. *Toxicol. Appl. Pharmacol.*, **2013,** *266*, 276-288.

[133] Kedziorek, D.A.; Muja, N.; Walczak, P.; Ruiz-Cabello, J.; Gilad, A.A.; Jie, C.C.; Bulte, J.W. Gene expression profiling reveals early cellular responses to intracellular magnetic labeling with superparamagnetic iron oxide nanoparticles. *Magn. Reson. Med.*, **2010,** *63*(4), 1031-1043.

[134] Arbab, A.S.; Wilson, L.B.; Ashari, P.; Jordan, E.K.; Lewis, B.K.; Frank, J.A. A model of lysosomal metabolism of dextran coated superparamagnetic iron oxide (SPIO)

nanoparticles: implications for cellular magnetic resonance imaging. *NMR Biomed.*, **2005,** *18*(6), 383-389.

[135] Carneiro, M.L.; Nunes, E.S.; Peixoto, R.C.; Oliveira, R.G.; Lourenco, L.H.; da Silva, I.C.; Simioni, A.R.; Tedesco, A.C.; de Souza, A.R.; Lacava, Z.G.; Bao, S.N. Free rhodium (II) citrate and rhodium (II) citrate magnetic carriers as potential strategies for breast cancer therapy. *J. Nanobiotechnology*, **2011,** *9*, 11.

[136] Kwok, J.C.; Richardson, D.R. The iron metabolism of neoplastic cells: alterations that facilitate proliferation? *Crit. Rev. Oncol. Hemat.*, **2002,** *42*(1), 65-78.

[137] Jain, V.; Jain, S.; Mahajan, S.C. Nanomedicines based drug delivery systems for anti-cancer targeting and treatment. *Curr. Drug Deliv.*, **2014,** *11*.

[138] Lim, S.W.; Kim, H.W.; Jun, H.Y.; Park, S.H.; Yoon, K.H.; Kim, H.S.; Jon, S.; Yu, M.K.; Juhng, S.K. TCL-SPION-enhanced MRI for the detection of lymph node metastasis in murine experimental model. *Acad. Radiol.*, **2011,** *18*(4), 504-511.

[139] Barentsz, J.O.; Futterer, J.J.; Takahashi, S. Use of ultrasmall superparamagnetic iron oxide in lymph node MR imaging in prostate cancer patients. *Eur. J. Radiol.*, **2007,** *63*(3), 369-372.

[140] Khan, J.A.; Mandal, T.K.; Das, T.K.; Singh, Y.; Pillai, B.; Maiti, S. Magnetite (Fe_3O_4) nanocrystals affect the expression of genes involved in the TGF-beta signalling pathway. *Mol. Biosyst.*, **2011,** *7*(5), 1481-1486.

[141] Liu, Y.; Chen, Z.; Gu, N.; Wang, J. Effects of DMSA-coated Fe_3O_4 magnetic nanoparticles on global gene expression of mouse macrophage RAW264.7 cells. *Toxicol. Lett.*, **2011,** *205*(2), 130-139.

[142] Gu, J.; Xu, H.; Han, Y.; Dai, W.; Hao, W.; Wang, C.; Gu, N.; Cao, J. The internalization pathway, metabolic fate and biological effect of superparamagnetic iron oxide nanoparticles in the macrophage-like RAW264.7 cell. *Sci. China Life Sci.*, **2011,** *54*(9), 793-805.

[143] Gupta, A.K.; Gupta, M. Cytotoxicity suppression and cellular uptake enhancement of surface modified magnetic nanoparticles. *Biomaterials*, **2005,** *26*(13), 1565-1573.

[144] Wu, X.; Tan, Y.; Mao, H.; Zhang, M. Toxic effects of iron oxide nanoparticles on human umbilical vein endothelial cells. *Int. J. Nanomed.*, **2010,** *5*, 385-399.

[145] Bhattacharya, K.; Davoren, M.; Boertz, J.; Schins, R.P.; Hoffmann, E.; Dopp, E. Titanium dioxide nanoparticles induce oxidative stress and DNA-adduct formation but not DNA-breakage in human lung cells. *Part. Fibre Toxicol.*, **2009,** *6*, 17.

[146] Katsnelson, B.A.; Privalova, L.I.; Sutunkova, M.P.; Tulakina, L.G.; Pichugova, S.V.; Beykin, J.B.; Khodos, M.J. Interaction of iron oxide Fe_3O_4 nanoparticles and alveolar macrophages *in vivo*. *Bull. Exp. Biol. Med.*, **2012,** *152*(5), 627-629.

[147] Rejman, J.; Oberle, V.; Zuhorn, I.S.; Hoekstra, D. Size-dependent internalization of particles via the pathways of clathrin- and caveolae-mediated endocytosis. *Biochem. J.*, **2004,** *377*(Pt 1), 159-169.

[148] Tang, T.Y.; Muller, K.H.; Graves, M.J.; Li, Z.Y.; Walsh, S.R.; Young, V.; Sadat, U.; Howarth, S.P.; Gillard, J.H. Iron oxide particles for atheroma imaging. *Arterioscler. Thromb. Vasc. Biol.*, **2009,** *29*(7), 1001-1008.

[149] Gellissen, J.; Axmann, C.; Prescher, A.; Bohndorf, K.; Lodemann, K.P. Extra- and intracellular accumulation of ultrasmall superparamagnetic iron oxides (USPIO) in experimentally induced abscesses of the peripheral soft tissues and their effects on magnetic resonance imaging. *Magn. Reson. Imaging*, **1999,** *17*(4), 557-567.

[150] Tuma, P.; Hubbard, A.L. Transcytosis: crossing cellular barriers. *Physiol. Rev.*, **2003,** *83*(3), 871-932.

[151] Sharma, R.; Wendt, J.A.; Rasmussen, J.C.; Adams, K.E.; Marshall, M.V.; Sevick-Muraca, E.M. New horizons for imaging lymphatic function. *Ann. NY Acad. Sci.*, **2008,** *1131*, 13-36.

[152] Verma, A.; Stellacci, F. Effect of surface properties on nanoparticle-cell interactions. *Small*, **2010,** *6*(1), 12-21.

[153] Levy, M.; Wilhelm, C.; Luciani, N.; Deveaux, V.; Gendron, F.; Luciani, A.; Devaud, M.; Gazeau, F. Nanomagnetism reveals the intracellular clustering of iron oxide nanoparticles in the organism. *Nanoscale*, **2011,** *3*(10), 4402-4410.

[154] Pryor, P.R.; Luzio, J.P. Delivery of endocytosed membrane proteins to the lysosome. *Biochim. Biophys. Acta-Mol. Cell Res.*, **2009,** *1793*(4), 615-624.

[155] Billotey, C.; Wilhelm, C.; Devaud, M.; Bacri, J.C.; Bittoun, J.; Gazeau, F. Cell internalization of anionic maghemite nanoparticles: Quantitative effect on magnetic resonance imaging. *Magn. Reson. Med.*, **2003,** *49*(4), 646-654.

[156] Moore, A.; Marecos, E.; Bogdanov, A., Jr.; Weissleder, R. Tumoral distribution of long-circulating dextran-coated iron oxide nanoparticles in a rodent model. *Radiology*, **2000,** *214*(2), 568-574.

[157] El-Sayed, A.; Harashima, H. Endocytosis of gene delivery vectors: From clathrin-dependent to lipid raft-mediated endocytosis. *Mol. Ther.*, **2013,** *21*(6), 1118-1130.

[158] Li, Y.; Chen, Z.W.; Gu, N. *In vitro* biological effects of magnetic nanoparticles. *Chin. Sci. Bull.*, **2012,** *57*(31), 3972-3978.

[159] Beckmann, N.; Cannet, C.; Babin, A.L.; Ble, F.X.; Zurbruegg, S.; Kneuer, R.; Dousset, V. *In vivo* visualization of macrophage infiltration and activity in inflammation using magnetic resonance imaging. *Wiley Interdiscip. Rev. Nanomed. Nanobiotechnol.*, **2009,** *1*(3), 272-298.

[160] Katsnelson, B.; Privalova, L.I.; Kuzmin, S.V.; Degtyareva, T.D.; Sutunkova, M.P.; Yeremenko, O.S.; Minigalieva, I.A.; Kireyeva, E.P.; Khodos, M.Y.; Kozitsina, A.N.; Malakhova, N.A.; Glazyrina, J.A.; Shur, V.Y.; Shishkin, E.I.; Nikolaeva, E.V. Some peculiarities of pulmonary clearance mechanisms in rats after intratracheal instillation of magnetite (Fe_3O_4) suspensions with different particle sizes in the nanometer and micrometer ranges: are we defenseless against nanoparticles? *Int. J. Occup. Environ. Health*, **2010,** *16*(4), 508-524.

[161] Commisso, C.; Davidson, S.M.; Soydaner-Azeloglu, R.G.; Parker, S.J.; Kamphorst, J.J.; Hackett, S.; Grabocka, E.; Nofal, M.; Drebin, J.A.; Thompson, C.B.; Rabinowitz, J.D.; Metallo, C.M.; Vander Heiden, M.G.; Bar-Sagi, D. Macropinocytosis of protein is an amino acid supply route in Ras-transformed cells. *Nature*, **2013,** *497*(7451), 633-638.

[162] Panariti, A.; Lettiero, B.; Alexandrescu, R.; Collini, M.; Sironi, L.; Chanana, M.; Morjan, I.; Wang, D.; Chirico, G.; Miserocchi, G.; Bucci, C.; Rivolta, I. Dynamic investigation of interaction of biocompatible iron oxide nanoparticles with epithelial cells for biomedical applications. *J. Biomed. Nanotechnol.*, **2013,** *9*(9), 1556-1569.

[163] Kendrew, J. *Encyclopaedia of Molecular Biology*, Blackwell Science Ltd.: Oxford, **1994**.

[164] Conner, S.D.; Schmid, S.L. Regulated portals of entry into the cell. *Nature*, **2003,** *422*(6927), 37-44.

[165] Lunov, O.; Zablotskii, V.; Syrovets, T.; Rocker, C.; Tron, K.; Nienhaus, G.U.; Simmet, T. Modeling receptor-mediated endocytosis of polymer-functionalized iron oxide nanoparticles by human macrophages. *Biomaterials*, **2011,** *32*(2), 547-555.

[166] Yang, C.Y.; Tai, M.F.; Lin, C.P.; Lu, C.W.; Wang, J.L.; Hsiao, J.K.; Liu, H.M. Mechanism of cellular uptake and impact of Ferucarbotran on macrophage physiology. *PLoS One*, **2011,** *6*(9), e25524.

[167] Gumbleton, M.; Abulrob, A.N.G.; Campbell, L. Caveolae: An alternative membrane transport compartment. *Pharm. Res.*, **2000,** *17*(9), 1035-1048.

[168] Prijic, S.; Scancar, J.; Romih, R.; Cemazar, M.; Bregar, V.B.; Znidarsic, A.; Sersa, G. Increased cellular uptake of biocompatible superparamagnetic iron oxide nanoparticles into malignant cells by an external magnetic field. *J. Membr. Biol.*, **2010,** *236*(1), 167-179.

[169] Qian, Z.M.; Li, H.Y.; Sun, H.Z.; Ho, K. Targeted drug delivery via the transferrin receptor-mediated endocytosis pathway. *Pharmacol. Rev.*, **2002,** *54*(4), 561-587.

[170] Chen, B.; Liang, Y.; Wu, W.; Cheng, J.; Xia, G.; Gao, F.; Ding, J.; Gao, C.; Shao, Z.; Li, G.; Chen, W.; Xu, W.; Sun, X.; Liu, L.; Li, X.; Wang, X. Synergistic effect of magnetic nanoparticles of Fe_3O_4 with gambogic acid on apoptosis of K562 leukemia cells. *Int. J. Nanomed.*, **2009,** *4*, 251-259.

[171] Murphy, J.E.; Tedbury, P.R.; Homer-Vanniasinkam, S.; Walker, J.H.; Ponnambalam, S. Biochemistry and cell biology of mammalian scavenger receptors. *Atherosclerosis*, **2005,** *182*(1), 1-15.

[172] Yamada, Y.; Doi, T.; Hamakubo, T.; Kodama, T. Scavenger receptor family proteins: roles for atherosclerosis, host defence and disorders of the central nervous system. *Cell. Mol. Life Sci.*, **1998,** *54*(7), 628-640.

[173] Raynal, I.; Prigent, P.; Peyramaure, S.; Najid, A.; Rebuzzi, C.; Corot, C. Macrophage endocytosis of superparamagnetic iron oxide nanoparticles: mechanisms and comparison of ferumoxides and ferumoxtran-10. *Invest. Radiol.*, **2004,** *39*(1), 56-63.

[174] Bae, J.E.; Huh, M.I.; Ryu, B.K.; Do, J.Y.; Jin, S.U.; Moon, M.J.; Jung, J.C.; Chang, Y.; Kim, E.; Chi, S.G.; Lee, G.H.; Chae, K.S. The effect of static magnetic fields on the aggregation and cytotoxicity of magnetic nanoparticles. *Biomaterials*, **2011,** *32*(35), 9401-9414.

[175] von Zur Muhlen, C.; von Elverfeldt, D.; Bassler, N.; Neudorfer, I.; Steitz, B.; Petri-Fink, A.; Hofmann, H.; Bode, C.; Peter, K. Superparamagnetic iron oxide binding and uptake as imaged by magnetic resonance is mediated by the integrin receptor Mac-1 (CD11b/CD18): implications on imaging of atherosclerotic plaques. *Atherosclerosis*, **2007,** *193*(1), 102-111.

[176] Li, J.; Zheng, L.; Cai, H.; Sun, W.; Shen, M.; Zhang, G.; Shi, X. Polyethyleneimine-mediated synthesis of folic acid-targeted iron oxide nanoparticles for *in vivo* tumor MR imaging. *Biomaterials*, **2013,** *34*(33), 8382-8392.

[177] Kumar, M.; Singh, G.; Arora, V.; Mewar, S.; Sharma, U.; Jagannathan, N.R.; Sapra, S.; Dinda, A.K.; Kharbanda, S.; Singh, H. Cellular interaction of folic acid conjugated superparamagnetic iron oxide nanoparticles and its use as contrast agent for targeted magnetic imaging of tumor cells. *Int. J. Nanomed.*, **2012,** *7*, 3503-3516.

[178] Bhirde, A.; Xie, J.; Swierczewska, M.; Chen, X. Nanoparticles for cell labeling. *Nanoscale*, **2011,** *3*(1), 142-153.

[179] de Vries, I.J.M.; Lesterhuis, W.J.; Barentsz, J.O.; Verdijk, P.; van Krieken, J.H.; Boerman, O.C.; Oyen, W.J.G.; Bonenkamp, J.J.; Boezeman, J.B.; Adema, G.J.; Bulte, J.W.M.; Scheenen, T.W.J.; Punt, C.J.A.; Heerschap, A.; Figdor, C.G. Magnetic resonance tracking of dendritic cells in melanoma patients for monitoring of cellular therapy. *Nat. Biotechnol.*, **2005,** *23*(11), 1407-1413.

[180] Zhu, J.H.; Zhou, L.F.; XingWu, F.G. Tracking neural stem cells in patients with brain trauma. *New Engl. J. Med.*, **2006,** *355*(22), 2376-2378.

[181] Toso, C.; Valle, J.P.; Morel, P.; Ris, F.; Demuylder-Mischler, S.; Lepetit-Coiffe, M.; Marangon, N.; Saudek, F.; Shapiro, A.M.J.; Bosco, D.; Berney, T. Clinical magnetic

resonance imaging of pancreatic islet grafts after iron nanoparticle labeling. *Am. J. Transplant.*, **2008,** *8*(3), 701-706.

[182] Jin, R.R.; Lin, B.B.; Li, D.Y.; Ai, H. Superparamagnetic iron oxide nanoparticles for MR imaging and therapy: design considerations and clinical applications. *Curr. Opin. Pharmacol.*, **2014,** *18*, 18-27.

[183] Wang, Y.X.J.; Hussain, S.M.; Krestin, G.P. Superparamagnetic iron oxide contrast agents: physicochemical characteristics and applications in MR imaging. *Eur. Radiol.*, **2001,** *11*(11), 2319-2331.

[184] Kellar, K.E.; Fujii, D.K.; Gunther, W.H.H.; Briley-Saebo, K.; Bjornerud, A.; Spiller, M.; Koenig, S.H. NC100150 injection, a preparation of optimized iron oxide nanoparticles for positive-contrast MR angiography. *J. Magn. Reson. Imaging*, **2000,** *11*(5), 488-494.

[185] Black, J. *Biological Performance of Materials - Fundamentals of Biocompatibility*, 4th ed; CRC Taylor & Francis: Florida, **2006**.

[186] Shen, C.C.; Wang, C.C.; Liao, M.H.; Jan, T.R. A single exposure to iron oxide nanoparticles attenuates antigen-specific antibody production and T-cell reactivity in ovalbumin-sensitized BALB/c mice. *Int. J. Nanomed.*, **2011,** *6*, 1229-1235.

[187] Hudgins, P.A.; Anzai, Y.; Morris, M.R.; Lucas, M.A. Ferumoxtran-10, a superparamagnetic iron oxide as a magnetic resonance enhancement agent for imaging lymph nodes: A phase 2 dose study. *Am. J. Neuroradiol.*, **2002,** *23*(4), 649-656.

[188] Dinniwell, R.; Chan, P.; Czarnota, G.; Haider, M.A.; Jhaveri, K.; Jewett, M.; Fyles, A.; Jaffray, D.; Milosevic, M. Pelvic lymph node topography for radiotherapy treatment planning from ferumoxtran-10 contrast-enhanced magnetic resonance imaging. *Int. J. Radiat. Oncol. Biol. Phys.*, **2009,** *74*(3), 844-851.

[189] Kooi, M.E.; Cappendijk, V.C.; Cleutjens, K.B.; Kessels, A.G.; Kitslaar, P.J.; Borgers, M.; Frederik, P.M.; Daemen, M.J.; van Engelshoven, J.M. Accumulation of ultrasmall superparamagnetic particles of iron oxide in human atherosclerotic plaques can be detected by *in vivo* magnetic resonance imaging. *Circulation*, **2003,** *107*(19), 2453-2458.

[190] Astanina, K.; Simon, Y.; Cavelius, C.; Petry, S.; Kraegeloh, A.; Kiemer, A.K. Superparamagnetic iron oxide nanoparticles impair endothelial integrity and inhibit nitric oxide production. *Acta Biomater.*, **2014,** *10*(11), 4896-4911.

[191] Sundstrom, J.B.; Mao, H.; Santoianni, R.; Villinger, F.; Little, D.M.; Huynh, T.T.; Mayne, A.E.; Hao, E.; Ansari, A.A. Magnetic resonance imaging of activated proliferating rhesus macaque T cells labeled with superparamagnetic monocrystalline iron oxide nanoparticles. *JAIDS*, **2004,** *35*(1), 9-21.

[192] Rabias, I.; Pratsinis, H.; Drossopoulou, G.; Fardis, M.; Maris, T.; Boukos, N.; Tsotakos, N.; Kletsas, D.; Tsilibary, E.; Papavassiliou, G. *In vitro* studies on ultrasmall

superparamagnetic iron oxide nanoparticles coated with gummic acid for T2 MRI contrast agent. *Biomicrofluidics*, **2007,** *1*(4), 44104.

[193] Tromsdorf, U.I.; Bruns, O.T.; Salmen, S.C.; Beisiegel, U.; Weller, H. A highly effective, nontoxic T_1 MR contrast agent based on ultrasmall PEGylated iron oxide nanoparticles. *Nano Lett.*, **2009,** *9*(12), 4434-4440.

[194] Taboada, E.; Rodriguez, E.; Roig, A.; Oro, J.; Roch, A.; Muller, R.N. Relaxometric and magnetic characterization of ultrasmall iron oxide nanoparticles with high magnetization. Evaluation as potential T1 magnetic resonance imaging contrast agents for molecular imaging. *Langmuir*, **2007,** *23*(8), 4583-4588.

[195] Wagner, S.; Schnorr, J.; Pilgrimm, H.; Hamm, B.; Taupitz, M. Monomer-coated very small superparamagnetic iron oxide particles as contrast medium for magnetic resonance imaging - Preclinical *in vivo* characterization. *Invest. Radiol.*, **2002,** *37*(4), 167-177.

[196] Weissleder, R.; Elizondo, G.; Wittenberg, J.; Rabito, C.A.; Bengele, H.H.; Josephson, L. Ultrasmall superparamagnetic iron-oxide - Characterization of a new class of contrast agents for MR imaging. *Radiology*, **1990,** *175*(2), 489-493.

[197] Hagspiel, K.D.; Neidl, K.F.; Eichenberger, A.C.; Weder, W.; Marincek, B. Detection of liver metastases: comparison of superparamagnetic iron oxide-enhanced and unenhanced MR imaging at 1.5 T with dynamic CT, intraoperative US, and percutaneous US. *Radiology*, **1995,** *196*(2), 471-478.

[198] Yamamoto, H.; Yamashita, Y.; Yoshimatsu, S.; Baba, Y.; Hatanaka, Y.; Murakami, R.; Nishiharu, T.; Takahashi, M.; Higashida, Y.; Moribe, N. Hepatocellular carcinoma in cirrhotic livers: detection with unenhanced and iron oxide-enhanced MR imaging. *Radiology*, **1995,** *195*(1), 106-112.

[199] Macarini, L.; Marini, S.; Milillo, P.; Vinci, R.; Ettorre, G.C. Double-contrast MRI (DC-MRI) in the study of the cirrhotic liver: utility of administering Gd-DTPA as a complement to examinations in which SPIO liver uptake and distribution alterations (SPIO-LUDA) are present and in the identification and characterisation of focal lesions. *Radiol. Med.*, **2006,** *111*(8), 1087-1102.

[200] Wang, Y.X. Superparamagnetic iron oxide based MRI contrast agents: Current status of clinical application. *Quant. Imaging Med. Surg.*, **2011,** *1*(1), 35-40.

[201] Garden, O.A.; Reynolds, P.R.; Yates, J.; Larkman, D.J.; Marelli-Berg, F.M.; Haskard, D.O.; Edwards, A.D.; George, A.J. A rapid method for labelling $CD4^+$ T cells with ultrasmall paramagnetic iron oxide nanoparticles for magnetic resonance imaging that preserves proliferative, regulatory and migratory behaviour *in vitro*. *J. Immunol. Methods*, **2006,** *314*(1-2), 123-133.

[202] Kobukai, S.; Baheza, R.; Cobb, J.G.; Virostko, J.; Xie, J.; Gillman, A.; Koktysh, D.; Kerns, D.; Does, M.; Gore, J.C.; Pham, W. Magnetic nanoparticles for imaging dendritic cells. *Magn. Reson. Med.*, **2010,** *63*(5), 1383-1390.

[203] Janic, B.; Iskander, A.S.; Rad, A.M.; Soltanian-Zadeh, H.; Arbab, A.S. Effects of Ferumoxides-protamine sulfate labeling on immunomodulatory characteristics of macrophage-like THP-1 cells. *PLoS One*, **2008,** *3*(6), e2499.

[204] Serkova, N.J.; Renner, B.; Larsen, B.A.; Stoldt, C.R.; Hasebroock, K.M.; Bradshaw-Pierce, E.L.; Holers, V.M.; Thurman, J.M. Renal inflammation: Targeted iron oxide nanoparticles for molecular MR imaging in mice. *Radiology*, **2010,** *255*(2), 517-526.

[205] Choyke, P.L.; Kobayashi, H. Functional magnetic resonance imaging of the kidney using macromolecular contrast agents. *Abdom. Imaging*, **2006,** *31*(2), 224-231.

[206] Yang, H.M.; Park, C.W.; Woo, M.A.; Kim, M.I.; Jo, Y.M.; Park, H.G.; Kim, J.D. HER2/neu antibody conjugated poly(amino acid)-coated iron oxide nanoparticles for breast cancer MR imaging. *Biomacromolecules*, **2010,** *11*, 2866-2872.

[207] Oca-Cossio, J.; Mao, H.; Khokhlova, N.; Kennedy, C.M.; Kennedy, J.W.; Stabler, C.L.; Hao, E.; Sambanis, A.; Simpson, N.E.; Constantinidis, I. Magnetically labeled insulin-secreting cells. *Biochem. Biophys. Res. Commun.*, **2004,** *319*(2), 569-575.

[208] Wang, J.; Chen, Y.; Chen, B.A.; Ding, J.H.; Xia, G.H.; Gao, C.; Cheng, J.A.; Jin, N.; Zhou, Y.; Li, X.M.; Tang, M.; Wang, X.M. Pharmacokinetic parameters and tissue distribution of magnetic Fe_3O_4 nanoparticles in mice. *Int. J. Nanomed.*, **2010,** *5*, 861-866.

[209] Hadjipanayis, C.G.; Machaidze, R.; Kaluzova, M.; Wang, L.; Schuette, A.J.; Chen, H.; Wu, X.; Mao, H. EGFRvIII antibody-conjugated iron oxide nanoparticles for magnetic resonance imaging-guided convection-enhanced delivery and targeted therapy of glioblastoma. *Cancer Res.*, **2010,** *70*(15), 6303-6312.

[210] Nighoghossian, N.; Wiart, M.; Cakmak, S.; Berthezene, Y.; Derex, L.; Cho, T.H.; Nemoz, C.; Chapuis, F.; Tisserand, G.L.; Pialat, J.B.; Trouillas, P.; Froment, J.C.; Hermier, M. Inflammatory response after ischemic stroke - A USPIO-enhanced MRI study in patients. *Stroke*, **2007,** *38*(2), 303-307.

[211] Jenkins, S.I.; Yiu, H.H.P.; Rosseinsky, M.J.; Chari, D.M. Magnetic nanoparticles for oligodendrocyte precursor cell transplantation therapies: progress and challenges. *Mol. Cell. Ther.*, **2014,** *2*, 23.

[212] Ke, Y.Q.; Hu, C.C.; Jiang, X.D.; Yang, Z.J.; Zhang, H.W.; Ji, H.M.; Zhou, L.Y.; Cai, Y.Q.; Qin, L.S.; Xu, R.X. *In vivo* magnetic resonance tracking of Feridex-labeled bone marrow-derived neural stem cells after autologous transplantation in rhesus monkey. *J. Neurosci. Methods*, **2009,** *179*(1), 45-50.

[213] Dunning, M.D.; Lakatos, A.; Loizou, L.; Kettunen, M.; ffrench-Constant, C.; Brindle, K.M.; Franklin, R.J.M. Superparamagnetic iron oxide-labeled Schwann cells and olfactory

ensheathing cells can be traced *in vivo* by magnetic resonance imaging and retain functional properties after transplantation into the CNS. *J. Neurosci.*, **2004,** *24*(44), 9799-9810.

[214] Jendelova, P.; Herynek, V.; Urdzikova, L.; Glogarova, K.; Kroupova, J.; Andersson, B.; Bryja, V.; Burian, M.; Hajek, M.; Sykova, E. Magnetic resonance tracking of transplanted bone marrow and embryonic stem cells labeled by iron oxide nanoparticles in rat brain and spinal cord. *J. Neurosci. Res.*, **2004,** *76*(2), 232-243.

[215] Lepore, A.C.; Walczak, P.; Rao, M.S.; Fischer, I.; Bulte, J.W. MR imaging of lineage-restricted neural precursors following transplantation into the adult spinal cord. *Exp. Neurol.*, **2006,** *201*(1), 49-59.

[216] Kang, H.W.; Torres, D.; Wald, L.; Weissleder, R.; Bogdanov, A.A., Jr. Targeted imaging of human endothelial-specific marker in a model of adoptive cell transfer. *Lab. Invest.*, **2006,** *86*(6), 599-609.

[217] Tang, T.Y.; Howarth, S.P.; Miller, S.R.; Graves, M.J.; Patterson, A.J.; JM, U.K.-I.; Li, Z.Y.; Walsh, S.R.; Brown, A.P.; Kirkpatrick, P.J.; Warburton, E.A.; Hayes, P.D.; Varty, K.; Boyle, J.R.; Gaunt, M.E.; Zalewski, A.; Gillard, J.H. The ATHEROMA (atorvastatin therapy: Effects on reduction of macrophage activity) study. Evaluation using ultrasmall superparamagnetic iron oxide-enhanced magnetic resonance imaging in carotid disease. *J. Am. Coll. Cardiol.*, **2009,** *53*(22), 2039-2050.

[218] Ruehm, S.G.; Corot, C.; Vogt, P.; Cristina, H.; Debatin, J.F. Ultrasmall superparamagnetic iron oxide-enhanced MR imaging of atherosclerotic plaque in hyperlipidemic rabbits. *Acad. Radiol.*, **2002,** *9*, S143-S144.

[219] Chamberlain, G.; Fox, J.; Ashton, B.; Middleton, J. Concise review: Mesenchymal stem cells: Their phenotype, differentiation capacity, immunological features, and potential for homing. *Stem Cells*, **2007,** *25*(11), 2739-2749.

[220] Barry, F.P.; Murphy, J.M. Mesenchymal stem cells: clinical applications and biological characterization. *Int. J. Biochem. Cell Biol.*, **2004,** *36*(4), 568-584.

[221] Jung, H.I.; Kettunen, M.I.; Davletov, B.; Brindle, K.M. Detection of apoptosis using the C2A domain of synaptotagmin I. *Bioconjugate Chem.*, **2004,** *15*(5), 983-987.

[222] Elmore, S. Apoptosis: A review of programmed cell death. *Toxicol. Pathol.*, **2007,** *35*(4), 495-516.

[223] Vermes, I.; Haanen, C.; Steffensnakken, H.; Reutelingsperger, C. A novel assay for apoptosis - Flow cytometric detection of phosphatidylserine expression on early apoptotic cells using fluorescein-labeled annexin-V. *J. Immunol. Methods*, **1995,** *184*(1), 39-51.

[224] Schellenberger, E.A.; Hogemann, D.; Josephson, L.; Weissleder, R. Annexin V-CLIO: A nanoparticle for detecting apoptosis by MRI. *Acad. Radiol.*, **2002,** *9*(suppl 2), S310-S311.

[225] Zhao, M.; Beauregard, D.A.; Loizou, L.; Davletov, B.; Brindle, K.M. Non-invasive detection of apoptosis using magnetic resonance imaging and a targeted contrast agent. *Nat. Med.*, **2001,** *7*(11), 1241-1244.

[226] Pimpha, N.; Chaleawlert-umpon, S.; Chruewkamlow, N.; Kasinrerk, W. Preparation of anti-CD4 monoclonal antibody-conjugated magnetic poly(glycidyl methacrylate) particles and their application on $CD4^+$ lymphocyte separation. *Talanta*, **2011,** *84*(1), 89-97.

[227] Kim, J.A.; Lee, N.; Kim, B.H.; Rhee, W.J.; Yoon, S.; Hyeon, T.; Park, T.H. Enhancement of neurite outgrowth in PC12 cells by iron oxide nanoparticles. *Biomaterials*, **2011,** *32*(11), 2871-2877.

[228] Pareta, R.A.; Taylor, E.; Webster, T.J. Increased osteoblast density in the presence of novel calcium phosphate coated magnetic nanoparticles. *Nanotechnology*, **2008,** *19*(26), 265101.

[229] Taylor, E.N.; Webster, T.J. The use of superparamagnetic nanoparticles for prosthetic biofilm prevention. *Int. J. Nanomed.*, **2009,** *4*, 145-152.

[230] Pankhurst, Q.A.; Connolly, J.; Jones, S.K.; Dobson, J. Applications of magnetic nanoparticles in biomedicine. *J. Phys. D-Appl. Phys.*, **2003,** *36*(13), R167-R181.

[231] Chen, B.A.; Lai, B.B.; Cheng, J.; Xia, G.H.; Gao, F.; Xu, W.L.; Ding, J.H.; Gao, C.; Sun, X.C.; Xu, C.R.; Chen, W.J.; Chen, N.N.; Liu, L.J.; Li, X.M.; Wang, X.M. Daunorubicin-loaded magnetic nanoparticles of Fe_3O_4 overcome multidrug resistance and induce apoptosis of K562-n/VCR cells *in vivo*. *Int. J. Nanomed.*, **2009,** *4*, 201-208.

[232] Ferrari, M. Cancer nanotechnology: Opportunities and challenges. *Nat. Rev. Cancer*, **2005,** *5*(3), 161-171.

[233] Peer, D.; Karp, J.M.; Hong, S.; FaroKHzad, O.C.; Margalit, R.; Langer, R. Nanocarriers as an emerging platform for cancer therapy. *Nat. Nanotechnol.*, **2007,** *2*(12), 751-760.

[234] Ziv-Polat, O.; Topaz, M.; Brosh, T.; Margel, S. Enhancement of incisional wound healing by thrombin conjugated iron oxide nanoparticles. *Biomaterials*, **2010,** *31*(4), 741-747.

[235] Jing, H.; Wang, J.; Yang, P.; Ke, X.; Xia, G.; Chen, B. Magnetic Fe_3O_4 nanoparticles and chemotherapy agents interact synergistically to induce apoptosis in lymphoma cells. *Int. J. Nanomed.*, **2010,** *5*, 999-1004.

[236] Chen, B.A.; Cheng, J.; Shen, M.F.; Gao, F.; Xu, W.L.; Shen, H.L.; Ding, J.H.; Gao, C.; Sun, Q.; Sun, X.C.; Cheng, H.Y.; Li, G.H.; Chen, W.J.; Chen, N.N.; Liu, L.J.; Li, X.M.;

Wang, X.M. Magnetic nanoparticle of Fe_3O_4 and 5-bromotetrandrin interact synergistically to induce apoptosis by daunorubicin in leukemia cells. *Int. J. Nanomed.*, **2009,** *4*(1), 65-71.

[237] Cheng, J.; Wu, W.; Chen, B.A.; Gao, F.; Xu, W.; Gao, C.; Ding, J.; Sun, Y.; Song, H.; Bao, W.; Sun, X.; Xu, C.; Chen, W.; Chen, N.; Liu, L.; Xia, G.; Li, X.; Wang, X. Effect of magnetic nanoparticles of Fe_3O_4 and 5-bromotetrandrine on reversal of multidrug resistance in K562/A02 leukemic cells. *Int. J. Nanomed.*, **2009,** *4*, 209-216.

[238] Wang, J.; Chen, B.; Cheng, J.; Cai, X.; Xia, G.; Liu, R.; Wang, X. Apoptotic mechanism of human leukemia K562/A02 cells induced by magnetic iron oxide nanoparticles co-loaded with daunorubicin and 5-bromotetrandrin. *Int. J. Nanomed.*, **2011,** *6*, 1027-1034.

[239] Lai, C.W.; Wang, Y.H.; Lai, C.H.; Yang, M.J.; Chen, C.Y.; Chou, P.T.; Chan, C.S.; Chi, Y.; Chen, Y.C.; Hsiao, J.K. Iridium-complex-functionalized Fe_3O_4/SiO_2 core/chell nanoparticles: A facile three-in-one system in magnetic resonance imaging, luminescence imaging, and photodynamic therapy. *Small*, **2008,** *4*(2), 218-224.

[240] Shen, H.B.; Long, D.H.; Zhu, L.Z.; Li, X.Y.; Dong, Y.M.; Jia, N.Q.; Zhou, H.Q.; Xin, X.; Sun, Y. Magnetic force microscopy analysis of apoptosis of HL-60 cells induced by complex of antisense oligonucleotides and magnetic nanoparticles. *Biophys. Chem.*, **2006,** *122*(1), 1-4.

[241] Seabra, A.B.; Pasquoto, T.; Ferrarini, A.C.; Santos Mda, C.; Haddad, P.S.; de Lima, R. Preparation, characterization, cytotoxicity, and genotoxicity evaluations of thiolated- and S-nitrosated superparamagnetic iron oxide nanoparticles: Implications for cancer treatment. *Chem. Res. Toxicol.*, **2014,** *27*(7), 1207-1218.

[242] Gilchrist, R.K.; Medal, R.; Shorey, W.D.; Hanselman, R.C.; Parrott, J.C.; Taylor, C.B. Selective inductive heating of lymph nodes. *Ann. Surg.*, **1957,** *146*(4), 596-606.

[243] Asin, L.; Ibarra, M.R.; Tres, A.; Goya, G.F. Controlled cell death by magnetic hyperthermia: Effects of exposure time, field amplitude, and nanoparticle concentration. *Pharm. Res.*, **2012,** *29*(5), 1319-1327.

[244] Quarta, A.; Di Corato, R.; Manna, L.; Ragusa, A.; Pellegrino, T. Fluorescent-magnetic hybrid nanostructures: Preparation, properties, and applications in biology. *IEEE Trans. Nanobiosci.*, **2007,** *6*(4), 298-308.

[245] Ito, A.; Honda, H.; Kobayashi, T. Cancer immunotherapy based on intracellular hyperthermia using magnetite nanoparticles: a novel concept of "heat-controlled necrosis" with heat shock protein expression. *Cancer Immunol. Immunother.*, **2006,** *55*(3), 320-328.

[246] Arsianti, M.; Lim, M.; Marquis, C.P.; Amal, R. Assembly of polyethylenimine-based magnetic iron oxide vectors: Insights into gene delivery. *Langmuir*, **2010,** *26*(10), 7314-7326.

[247] Luo, D.; Saltzman, W.M. Synthetic DNA delivery systems. *Nat. Biotechnol.*, **2000,** *18*(1), 33-37.

[248] Jingting, C.; Huining, L.; Yi, Z. Preparation and characterization of magnetic nanoparticles containing Fe_3O_4-dextran-anti-β-human chorionic gonadotropin, a new generation choriocarcinoma-specific gene vector. *Int. J. Nanomed.*, **2011,** *6*, 285-294.

[249] Wang, X.; Wei, F.; Liu, A.; Wang, L.; Wang, J.C.; Ren, L.; Liu, W.; Tu, Q.; Li, L.; Wang, J. Cancer stem cell labeling using poly(L-lysine)-modified iron oxide nanoparticles. *Biomaterials*, **2012,** *33*(14), 3719-3732.

[250] Kwoh, D.Y.; Coffin, C.C.; Lollo, C.P.; Jovenal, J.; Banaszczyk, M.G.; Mullen, P.; Phillips, A.; Amini, A.; Fabrycki, J.; Bartholomew, R.M.; Brostoff, S.W.; Carlo, D.J. Stabilization of poly-L-lysine/DNA polyplexes for *in vivo* gene delivery to the liver. *Biochim. Biophys. Acta-Gene Struct. Expression*, **1999,** *1444*(2), 171-190.

[251] Lewin, M.; Carlesso, N.; Tung, C.H.; Tang, X.W.; Cory, D.; Scadden, D.T.; Weissleder, R. Tat peptide-derivatized magnetic nanoparticles allow *in vivo* tracking and recovery of progenitor cells. *Nat. Biotechnol.*, **2000,** *18*(4), 410-414.

[252] Namgung, R.; Singha, K.; Yu, M.K.; Jon, S.; Kim, Y.S.; Ahn, Y.; Park, I.K.; Kim, W.J. Hybrid superparamagnetic iron oxide nanoparticle-branched polyethylenimine magnetoplexes for gene transfection of vascular endothelial cells. *Biomaterials*, **2010,** *31*(14), 4204-4213.

[253] Xie, J.; Xu, C.J.; Xu, Z.C.; Hou, Y.L.; Young, K.L.; Wang, S.X.; Pourmond, N.; Sun, S.H. Linking hydrophilic macromolecules to monodisperse magnetite (Fe_3O_4) nanoparticles via trichloro-s-triazine. *Chem. Mat.*, **2006,** *18*(23), 5401-5403.

[254] Xi, D.; Luo, X.P.; Lu, Q.H.; Yao, K.L.; Liu, Z.L.; Ning, Q. The detection of HBV DNA with gold-coated iron oxide nanoparticle gene probes. *J. Nanopart. Res.*, **2008,** *10*(3), 393-400.

[255] Rosensweig, R.E. Heating magnetic fluid with alternating magnetic field. *J. Magn. Magn. Mater.*, **2002,** *252*(1-3), 370-374.

[256] Zhang, W.; Shi, X.; Huang, J.; Zhang, Y.; Wu, Z.; Xian, Y. Bacitracin-conjugated superparamagnetic iron oxide nanoparticles: Synthesis, characterization and antibacterial activity. *Chemphyschem*, **2012,** *13*(14), 3388-3396.

[257] Ho, J.; Al-Deen, F.M.; Al-Abboodi, A.; Selomulya, C.; Xiang, S.D.; Plebanski, M.; Forde, G.M. N,N'-Carbonyldiimidazole-mediated functionalization of superparamagnetic nanoparticles as vaccine carrier. *Colloids Surf. B Biointerfaces*, **2011,** *83*(1), 83-90.

[258] Hu, K.; Dou, J.; Yu, F.; He, X.; Yuan, X.; Wang, Y.; Liu, C.; Gu, N. An ocular mucosal administration of nanoparticles containing DNA vaccine pRSC-gD-IL-21 confers protection against mucosal challenge with herpes simplex virus type 1 in mice. *Vaccine*, **2011,** *29*(7), 1455-1462.

[259] Cobaleda-Siles, M.; Henriksen-Lacey, M.; de Angulo, A.R.; Bernecker, A.; Vallejo, V.G.; Szczupak, B.; Llop, J.; Pastor, G.; Plaza-Garcia, S.; Jauregui-Osoro, M.; Meszaros, L.K.; Mareque-Rivas, J.C. An iron oxide nanocarrier for dsRNA to target lymph nodes and strongly activate cells of the immune system. *Small*, **2014,** *10*(24), 5054-5067.

[260] Gao, L.; Zhuang, J.; Nie, L.; Zhang, J.; Zhang, Y.; Gu, N.; Wang, T.; Feng, J.; Yang, D.; Perrett, S.; Yan, X. Intrinsic peroxidase-like activity of ferromagnetic nanoparticles. *Nat. Nanotechnol.*, **2007,** *2*(9), 577-583.

[261] Liu, Y.; Yu, F. Substrate-specific modifications on magnetic iron oxide nanoparticles as an artificial peroxidase for improving sensitivity in glucose detection. *Nanotechnology*, **2011,** *22*(14), 145704.

[262] Wei, H.; Wang, E. Fe_3O_4 Magnetic nanoparticles as peroxidase mimetics and their applications in H_2O_2 and glucose detection. *Anal. Chem.*, **2008,** *80*(6), 2250-2254.

I.1.2. TOXICOLOGICAL AND PRO-INFLAMMATORY MECHANISMS OF IRON OXIDE NANOPARTICLES

Nanoparticles (NPs) are becoming available in the market with exponential increase. In particular, iron oxide nanoparticles (IONs) have been extensively used for biomedical purposes, namely in magnetic resonance imaging [1,2], tissue repair [3,4], drug delivery [5,6], hyperthermia [7,8], transfection [9,10], tissue soldering [11], antibacterial activity [4], vaccine delivery [12] and peroxidase activity [13,14]. However, and despite all the possible biomedical applications, recent studies report that these IONs are not so innocuous as it was thought before. In fact, the small size of IONs may induce toxic effects that are not observed in their bulk material states due to the increase in surface area per unit mass, ability to cross cell and tissue barriers, and resistance to biodegradation [15,16]. Moreover, IONs can affect cells even when no internalization occurs, through the release of material used as coating agent, which can be toxic, the release of toxic metal ions or by interaction with proteins, leading to the formation of protein–NPs complexes and subsequent aggregation [17,18]. The safety of nanotechnology requires the evaluation of concentration-dependent effects of IONs on cellular function and toxicity, as well as the interactions between IONs and biological structures and the influence of size, morphology and agglomeration [19]. However, it is believed that activation of oxidative stress and inflammatory signaling, leading to apoptosis and genotoxicity are the key paradigm(s) of nanotoxicity [15]. Apart from the potential involvement in Fenton reaction, IONs can cause structural damage to mitochondria, which could potentially result in anomalous functioning of these organels, including altered membrane potential, cytochrome c release, superoxide radical ($O_2^{\bullet-}$) production, and uncoupling of oxidative phosphorylation, which may also contribute to the underlying mechanisms associated with cytotoxicity [20]. Putative toxicity of IONs may become associated with multiple neurodegenerative disorders, including multiple sclerosis, Alzheimer's and Parkinson's diseases that occur due to the generation of free radicals in the brain resulting from iron deposition [15]. It was also described that α-Fe_2O_3 NPs are able to disrupt the adherens junctions of cell lines due to interaction of IONs with membrane proteins and phospholipids [21]. The mechanisms of cytotoxicity and apoptotic death that may be caused by IONs are presented in this part of the introductory chapter.

I.1.2.1. MECHANISMS OF CYTOTOXICITY

The effects of IONs on the viability and/or cytotoxicity of several cells are variable according to the type of IONs, coating, concentration, interaction with different types of cells, and have been described in several studies. The mechanisms behind the IONs cytotoxicity are not completely established and various mechanisms are proposed (figure 1), as discussed in the following chapter.

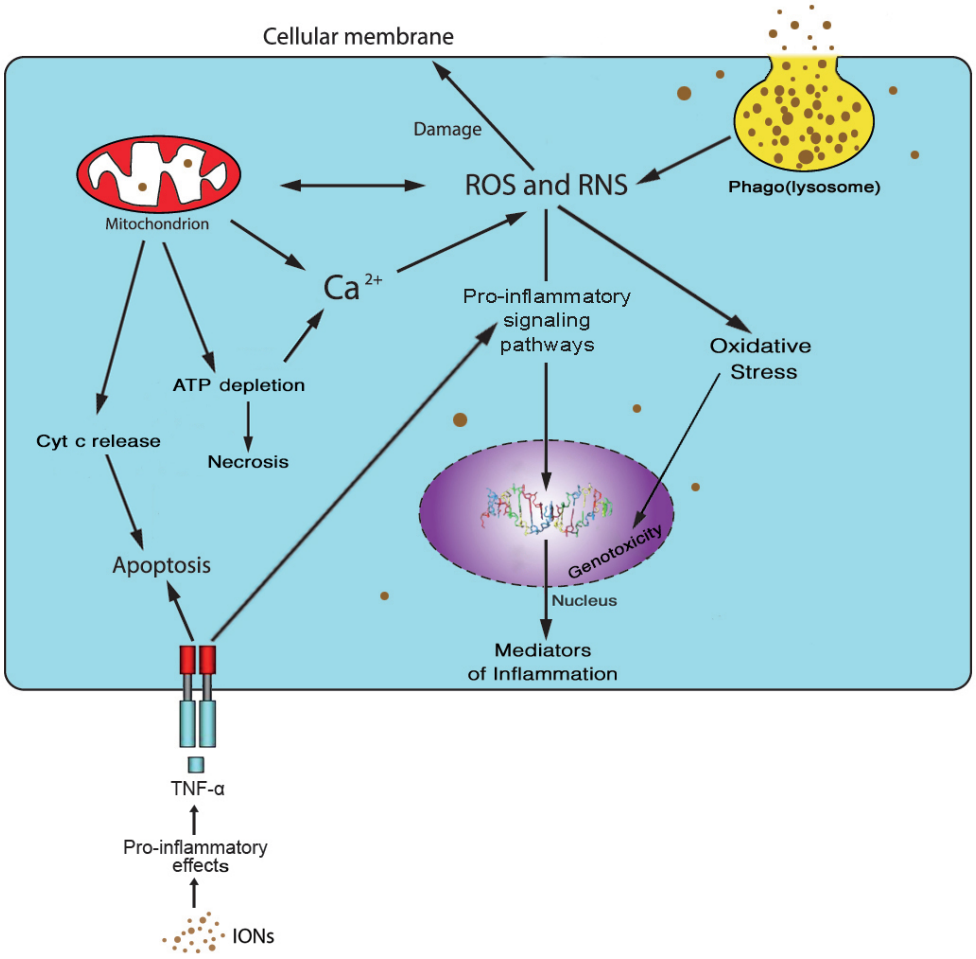

Figure 1. Possible mechanisms underlying the cytotoxic effects of IONs (ATP: Adenosine triphosphate; Cyt c: Cytochrome c; IONs: Iron oxide nanoparticles; RNS: Reactive nitrogen species; ROS: Reactive oxygen species; TNF-α: Tumor necrosis factor α).

I.1.2.1.1. REACTIVE OXYGEN SPECIES, REACTIVE NITROGEN SPECIES AND PEROXIDASE ACTIVITY

ROS are defined as molecules containing one or more oxygen atoms, which are more reactive than molecular oxygen. RNS, mainly peroxynitrite anion ($ONOO^-$), nitrogen dioxide, and its sub-products, derive from reactions between superoxide radical ($O_2^{\bullet-}$) and nitric oxide radical ($^{\bullet}NO$) [22]. It has been reported that the potential mechanism of IONs cytotoxicity involves the formation of ROS such as hydrogen peroxide (H_2O_2), hydroxyl radical ($HO^{\bullet}$), hydroperoxyl radical ($HO_2^{\bullet}$), and $O_2^{\bullet-}$, among others. When produced in abundance, ROS can lead to oxidative stress, given that they disturb the balance between oxidative pressure and antioxidant defense, which results in damage to biomembranes [20] (figure 1). As a good example, exposure of PC12 cells to Fe_3O_4 NPs was shown to induce a significant increase of intracellular ROS, which was associated to the release of cytochrome c from mitochondria, resulting in initiation of the intrinsic apoptosis pathway [23]. In another study, the free radical scavenger edaravone, abolished caspase 3 activation and apoptosis in Kupffer cells of in mice treated with Resovist® [carboxydextran-coated superparamagnetic IONs (SPIONs)] [24].

After internalization, IONs are presumably degraded into iron ions within the lysosomes by hydrolysing enzymes, at low pH. Free iron ions can potentially cross the nuclear or mitochondrial membrane and induce redox cycling and catalytic chemistry via Fenton reaction [$H_2O_2 + Fe^{2+} \rightarrow Fe^{3+} + HO^- + HO^{\bullet}$], the most prevalent source of ROS in biological systems, and thus catalyze the formation of the highly reactive $HO^{\bullet}$ that damages cellular membranes, depolymerizes polysaccharides, causes deoxyribonucleic acid (DNA) strand breaks, inactivates enzymes, and initiates lipid peroxidation [15,20,25]. In Fe_3O_4 NPs, iron is present as a mixture of Fe^{3+} and Fe^{2+} ions, and it is possible that surface Fe^{2+} ions contribute to the Fenton reaction. On the other hand, in Fe_2O_3 NPs, iron ions are mostly in the ferric state; thus maghemite would produce less radicals [26].

IONs are also known to be phagocytosed by neutrophils and other phagocytes. Upon formation of the phagolysosome nicotinamide adenine dinucleotide phosphate (NADPH) oxidases are activated, generating $O_2^{\bullet-}$ and this generation of $O_2^{\bullet-}$ would lead to the production of other ROS. It is also possible that NPs-induced damage of the mitochondria could determine Ca^{2+} release into the cytosol, where Ca^{2+}-dependent enzymes, such as nitric oxide synthase, become activated, resulting in production of $^{\bullet}NO$ and $ONOO^-$ [27,28]

(figure 2). Depending on the type of IONs used, the time at which maximal ROS and RNS levels are generated can vary greatly, from approximately 4 h for citrate-coated IONs to 24–32 h for dextran-coated ones [29].

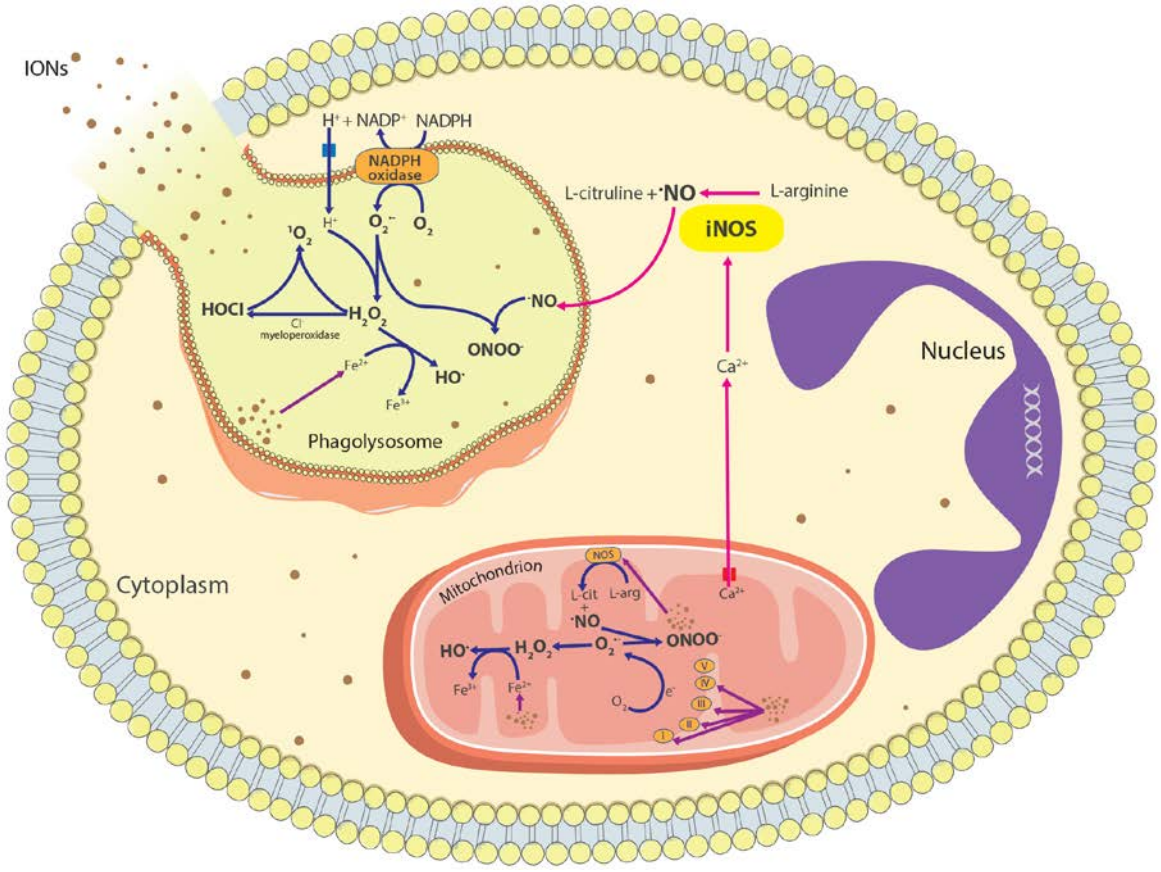

Figure 2. IONs-induced production of ROS and RNS (H_2O_2: Hydrogen peroxide; $HO^{\bullet}$: Hydroxyl radical; HOCl: Hypochlorous acid; iNOS: Inducible nitric oxide synthase; IONs: Iron oxide nanoparticles; NADPH: Nicotinamide adenine dinucleotide phosphate; $^{\bullet}NO$: Nitric oxide radical; NOS: Nitric oxide synthase; $^1O_2$: Singlet oxygen; $O_2^{\bullet-}$: Superoxide radical; $ONOO^-$: Peroxynitrite anion).

There are several studies performed to evaluate the effect of different types of IONs on ROS and RNS production in different types of cells and results indicate that the effect on these cells depends on the different characteristics of the IONs (namely coating, concentration and type of IONs) and the different interaction of these IONs with the different cells and their receptors. For example, Fe_2O_3 NPs was reported to increase ROS production and inhibit catalase in Hep-2 human epithelial cells [30], while FeRex®

(dextran-coated SPIONs) had no effects on ROS production in bone marrow dendritic cells [31]. In these circumstances, detoxifying enzymes such as superoxide dismutase (SOD), catalase and glutathione peroxidase can be produced in order to prevent ROS-induced damage and the extent of ROS production and consequent damage may be dependent on the production of these enzymes, whose expression and activities vary from cell to cell [27].

The techniques used to assess ROS and RNS production may be responsible for the different results reported in the literature. Fe_3O_4 NPs was shown to increase ROS production in human lung cancer A549 cells [32,33], while Guadagnini *et a*l [34] reported that the same IONs did not induce ROS production in the same cell line. The fact that Konczol *et al* [32] and Ahamed *et al* [33] presented contradictory results when compared to the results presented by Guadagnini *et al* [34] may be related to the different probes used: while Konczol *et al* [32] and Ahamed *et al* [33] used dichlorodihydrofluorescein diacetate, a probe that detects H_2O_2, $HO^{\bullet}$, $^{\bullet}NO$ and $ONOO^{-}$, Guadagnini *et al* [34] used hydroethidine, a probe that only detects $O_2^{\bullet-}$ [35].

IONs peroxidase-like activity has as well been described as one of the potential mechanisms involved in the cytotoxicity of IONs. In fact, IONs may catalyze H_2O_2 to react with various intracellular molecules including proteins, lipids, and nucleic acids through peroxidase-like activity, thus causing irreversible cell damage. On the contrary, when IONs have catalase-like activity, they would rather protect cells from oxidative stress through decomposition of H_2O_2 into H_2O and O_2. When IONs are located in lysosomes, the acidic environment contributes to their peroxidase-like activity rather than catalase-like activity [36].

I.1.2.1.2. DISRUPTION OF THE CYTOSKELETON

IONs are described as being capable of affecting the actin cytoskeleton. The cytoskeleton is a dynamic network consisting of actin polymers, microtubules, and associated proteins. Actin, in particular, plays an important role in cell shape, adhesion, and motility. Increasing evidence shows that the actin cytoskeleton is essential to endocytotic processes, including pseudopod extension, phagocytotic engulfment, cell surface remodeling for vesicle formation and movement as well as to the maintenance of

the cell morphology and their effect on signaling pathways monitoring several parameters such as cell death, migration and differentiation [37,38]. It is described that the formation of cytoplasmic vacuoles containing internalized IONs disrupts the cytoskeleton and cell membrane by either chemically or physically impeding actin microfilament formation [39]. In fact, Miller *et al* [40] suggested that NPs could interact with the extracellular domain of integrins (proteins that promote actin assembly) and thereby affect their activation and intracellular signalling cascade. It is reported that IONs affect the morphology and actin cytoskeleton and the formation and maturation of focal adhesion complexes in porcine aorthic endothelial cells [41], human blood outgrowth endothelial cells [42,43], as well as human mesenchymal stem cells [44]. Wu *et al* [45] reported that citrate-coated Fe_3O_4 NPs interfere with the polymerization and depolymetrization of the tubulin in human umbilical vein endothelial cells, and induce disruption of F-actin and microtubules, resulting in a disorganization of the cytoskeleton. Gupta *et al* [46] reported also a rapid disruption of actin and microtubule structures in human fibroblasts as well as Apopa *et al* [47] reported that Fe_2O_3 NPs induced the activation of protein kinase B (Akt) and inhibited glycogen synthase kinase-3β in a phosphoinositide-3-kinase dependent manner in human microascular endothelial cells, which results in microtubule remodeling.

I.1.2.1.3. INTERFERENCE WITH ATP PRODUCTION

IONs were also described as exerting a decrease in ATP production in mitochondria [48]. In fact, it is described that Fe_2O_3 NPs decreased the activity of Mg^{2+}-ATPase in a dose-dependent manner in brains of rats, which may hamper the ATP synthesis and thus lead to mitochondrial disorganization [49]. The same authors also reported that Fe_2O_3 NPs decreased the activities of total, Na^+-K^+, and Ca^{2+}-ATPases in a dose-dependent manner in brains of rats, possibly due to the interaction of these IONs with the enzymes and suggest that the observed decreased in the activity of Na^+-K^+-ATPases may cause alterations in the cell-membrane permeability, presumably resulting in impaired iono-regulatory activity as well as cause an imbalance in cellular functions, while the decrease in the activity of Ca^{2+}-ATPases may conduct to disturbances in numerous cellular processes, such as exocytosis, cell proliferation, gene transcription, cell differentiation, synaptic maturation, neurotransmitter release, intracellular signaling, muscle contraction and cell survival [49].

I.1.2.1.4. PARAMETERS THAT AFFECT THE CYTOTOXICITY OF IRON OXIDE NANOPARTICLES

I.1.2.1.4.1. CELL TYPE

It is important to consider that IONs cytotoxicity depends on diverse parameters. One of them is the cell type. For example, Horie *et al* [50] reported that Fe_2O_3 NPs caused a decrease in the viability of human keratinocyte HaCaT cells, while for similar conditions and concentrations, Sun *et al* [51] reported that Fe_2O_3 NPs did not cause decrease in the viability of human cardiac microvascular endothelial cells. It is also possible to verify that certain cells are more propense to IONs toxicity. For example, in lymphocytes, there are many studies performed that indicate that IONs trigger a decrease in viability [52-54], while most of the authors that studied the effect of IONs on mesenchymal stem cells came to the conclusion that they do not exert cytotoxicity [55-59]. Although there is not any specific explanation for these facts, possible explanations could be the presence of distinct cell surface receptors in these cell types leading to differential downstream signalling events, discrepancy of NPs uptake, differences in the sensitivity of cellular organelles to IONs induced insult (lysosomal/mitochondrial damage), differential handling of NPs after uptake and different inherent capacity to deal with oxidative stress [34]. Noteworthy, for most of the cells, ROS production appeared to be directly related to the quantity of lysosomes formed following SPIONs exposure [60].

I.1.2.1.4.2. COATING OF IONs

The coating used also influence cytotoxity of IONs. In fact, the interaction of the IONs coating with proteins may change their biological reactivities [50], although coatings with known biocompatible compounds do not always exclude an unexpected increase in cytotoxicity or pro-inflammatory response [34]. For example, oleate itself and non-coated Fe_3O_4 NPs were not found to be toxic to TK6 cells and lymphocytes, while oleate-coated Fe_3O_4 NPs were found to be cytotoxic to the same cellular lines [61]. Likewise, Zhu *et al* [62] reported that, while aminosilane, dextran and non-coated SPIONs did not resulted in

decreased cell viability, silica-coated SPIONs decreased cell viability in RAW 264.7 cells. In fact, coordination of the coating agent with the nanostructure influences the entry into or interaction of both the nanostructure and surface chemicals with cells, thereby magnifying any interactions (positive or negative) with cellular components; a second, alternative explanation for this fact is the variance in the effectiveness of the coatings to shield the nanostructures from potentially adverse interactions with cellular components [39,63]. Shen *et al* [64] reported that the cytotoxicity of NPs with amine groups on their surface stems from the strong electrostatic interaction between the positively charged NPs and the negatively charged cell membranes. On the other hand, the absence of cytotoxic effects attributable to poly(L-lysine) (PLL)-Endorem® (dextran-coated SPIONs) could be explained by the delayed release of free iron into the intracellular environment due to the slower degradation of their double-coating [65]. In a similar way, Fan *et al* [66] reported that, while Fe_3O_4 NPs decreased cell viability in hepatic cell line LO2, O-carboxymethyl chitosan-coated Fe_3O_4 NPs, folic acid-carboxymethyl chitosan-coated Fe_3O_4 NPs and dextran-coated SPIONs did not trigger the same effect. In this case, coatings were able to reduce Fe_3O_4 NPs cytotoxicity. For example, it is known that O-carboxymethylchitosan-coated Fe_3O_4 NPs have carboxyl groups that are bound to the surface of Fe_3O_4 by covalent bonds of “O” of the hydrous Fe_3O_4 NPs. These carboxyl groups will confer a negative charge to Fe_3O_4 NPs, which prevents agglomeration by the electrostatic repulsion. Moreover, this coating may increase the surface hydrophilicity, minimizing adherence to cell membranes by hydrophobic interaction, which minimizes phagocytosis [66].

I.1.2.1.4.3. TYPE OF IONs

Several types of IONs can be synthetized, magnetite (Fe_3O_4), hematite (α-Fe_2O_3) and maghemite (γ-Fe_2O_3) being the most common [15,67]. The type of IONs may also influence their cytotoxicity. For example, Karlsson *et al* [68] described that Fe_2O_3 NPs caused a slight decrease in viability of A549 cells, while Fe_3O_4 NPs did not cause the same effect. However, Park *et al* [69] reported that, in a MH-S cell line, Fe_3O_4 NPs caused a greater cell viability decrease than Fe_2O_3 NPs. Likewise, Chen *et al* [36] reported that, while 2,3-dimercaptosuccinic acid (DMSA)-coated γ-Fe_2O_3 NPs are not cytotoxic to human neuronal glioblastoma U251 cells, DMSA-coated Fe_3O_4 NPs decreased cell

viability at a lower concentration in the same cellular line. In Fe_3O_4 NPs, iron is present in the form of Fe^{3+} and Fe^{2+} ions, while in Fe_2O_3 NPs iron is mostly in the form of Fe^{3+} ions [26]. In fact, Fe^{2+} is released into the solution much faster than Fe^{3+} because the bonds between the reduced iron and O_2^- ions of the crystalline lattice are weakened [70]. However, materials only containing Fe^{3+} at the surface, such in the case of Fe_2O_3 NPs, may also release $HO^{\bullet}$ through a Fenton-like reaction that requires previous reduction of Fe^{3+} to Fe^{2+} by endogenous molecules such as ascorbic acid or by reaction of Fe^{3+} and H_2O_2 with $HO_2^{\bullet}$ as the propagating intermediate, which may increase cytotoxicity [70,71].

I.1.2.1.4.4. SOLUBILITY OF IONs

The solubility of IONs has recently been shown to directly affect its cytotoxicity [72]. It is known that the low pH of endosomes/lysosomes can solubilize the iron core within a few days, releasing ferric iron Fe^{3+} into the cytoplasm and consequently the cytotoxicity may increase [73]. However, IONs of extremely low solubility may also be cytotoxic because they will be persistent within the biological system and may provoke a range of long-term effects involving carcinogenic, mutagenic, or teratogenic influence in the organism [72].

I.1.2.1.4.5. SURFACE CHARGE OF IONs

The surface charge of IONs influences their stability as well as the cellular internalization and trafficking pathways, therefore influencing their cytotoxicity [9,74]. It is generally accepted that the NP-protein “corona”, a dynamic layer of proteins and other biomolecules that adsorbs to NP surfaces immediately upon contact with living systems, mediates the interaction of IONs with the cellular machinery [18]. Generally, the surface charges of the IONs are negative due to their interaction with the hydroxyl groups of the water molecules, and these surface charges originate an electric field that attracts counterions [75]. IONs, due to their strong van der Waals forces, have a significant interaction with the surrounding environment, which alters the physical properties of the NPs, depending upon the presence of ionic (salt) and biomolecules in their vicinity, gravitation, diffusion, convection forces, cell type, pH and protein composition, either in

culture media or in body fluids, and the extent of agglomeration [76,77]. Proteins such as albumin, immunoglobulin, fibrinogen, and apolipoproteins were found to play an important role in the agglomeration of IONs [78]. Simberg *et al* [79] reported that IONs have the ability to bind to mouse plasma proteins, namely histidine–proline rich glycoprotein, high molecular weight kininogen, plasma prekallikrein, mannose-binding lectins (MBL), mannose-binding lectin-associated serine proteases, apolipoproteins, beta-2 glycoprotein, clotting factors coagulation factor XI (FXI) and coagulation factor XII (FXII), hemoglobin, hemoglobin-binding hemopexin (proteoglycan-4), vinculin, tubulin-1 and talin-1. The fact that kallikrein, kininogen, FXI and FXII can be bound to IONs surface may potentially initiate the activation of the intrinsic pathway of blood clotting [79].

IONs have also been described as causing disruption of microvilli, through disruption of the adherens junctions [21,80]. In fact, protein fibrillation may occur due to protein-NPs interactions [18]. It was also found that interaction of Fe_3O_4 NPs with amyloid aggregates led to a decrease of the amount of amyloids by depolymerization of amyloid structures and inhibition of lysozyme aggregation [81]. IONs can also disturb the electronic and/or ionic transport chains due to the strong affinity of the NPs for the cell membrane [82]. Therefore, the immediate environment of the NPs (presence of biomolecules, chemical composition, and physiological properties of the liquid in which they are suspended) may modulate their toxicity on the basis of agglomeration, that may depend on the surface chemistry and charge of IONs [77].

It is reported that IONs do not need to enter into the cells to exert cytotoxicity. In the case of non-coated IONs, as they have a negative charge and the cell membrane also has a negative charge, there is a slight electrostatic repulsion between cells and the non-coated-IONs, which influence the interaction between cells and IONs. However, cell membrane receptors have different aminoacid compositions that comprise negative, neutral, and positive charges; therefore, the effect of charge on the interaction between transmembrane receptors or channels and IONs continuously changes according to the type of IONs, coating, surface charge, among many other previously mentioned factors [48,61]. The different charge might also influence the interactions with other compounds present in medium, such as serum proteins, as well as with cell membranes, and thus could have impact on internalization of NPs and toxicity [61].

I.1.2.1.4.6. SIZE OF IONs

IONs size is also a parameter that influences their cytotoxicity. Ying *et al* [52] reported that 50 nm IONs were more toxic than 10 nm IONs to A3 human T lymphocytes. Likewise, Faust *et al* [83] reported that 78 nm α-Fe_2O_3 NPs are more toxic to BeWo b30 plancentary epithelial cell line than 50 nm α-Fe_2O_3 NPs, the 15 nm α-Fe_2O_3 NPs being not toxic to the same cellular line. Larger particles possess larger effective interaction area with more functional groups for accessing to the cell, in comparison with smaller NPs. Within this specific area, there are more functional groups on the individual large particle [52,84]. Larger aggregates, as it occurs in the case of non-coated IONs, are considered more cytotoxic, as they may mechanically damage the cell and also deform the nucleus on the entry into the cell [61,85]. However, it is also reported that smaller NPs are more toxic. This is, probably, due to their large specific surface area and hence larger surface reactivity toward biological systems [86]. According to this theory, Zhang *et al* [21] reported that α-Fe_2O_3 NPs with 26 nm were more cytotoxic to CaCo-2 cells than α-Fe_2O_3 NPs with 53, 76 and 98 nm.

Also, size may influence the uptake of IONs by phagocytic cells. In fact, IONs with dimensions superior to 50 nm are usually phagocytized by cells of the reticuloendothelial system in liver and spleen, being eliminated in a short period of time, while IONs with dimensions inferior to 50 nm are able to move through the capillary wall and be phagocytozed by phagocytic cells that are also in other organs, namely bone marrow and lymph nodes [87,88]. However, when IONs are smaller than 10 nm, they may be eliminated via extravasation and renal clearance [15].

I.1.2.1.4.7. EXPERIMENTAL CONDITIONS

Some erroneous factors derived from the experimental conditions have to be taken into account. The adsorption of the components of the culture media onto IONs induces a starvation state of cells *in vitro*. Thus, the adsorption effect that occurs when cytotoxicity experiments are performed may influence their toxicity *in vitro* [50]. These effects of adsorption are expected to be proeminent when the NPs are smaller, given that the adsorption ability of NP increases as the particle size decreases [50].

It is also important to have into account that the techniques used to determine cytotoxicity can biase the toxicological results obtained. Factors such as exact protocols with respect to the source of cells, the cell number, cell culture medium, and incubation times are all factors of extreme importance for validation of results and to enable comparison between studies [89]. DMSA-coated Fe_3O_4 NPs were reported to decrease cellular viability in RAW 264.7 cells by Liu *et al* [90] when $5x10^4$ cells/mL were used. However, when the same author used $1x10^6$ cells/mL, no cytotoxicity was observed using the same cellular line for the same concentration of the IONs [91]. This evidence shows how the number of cells utilized in the experiments may influence the results obtained, as the number of IONs/cell will vary considerably.

In a similar way, Liu *et al* [23] reported that Fe_3O_4 NPs decreased cell viability in PC12 cells, while Xue *et al* [92] reported the opposite, even at a higher concentration. Again, the different experimental conditions led to different results: although both authors used MTT assay, Liu *et al* used RPMI 1640 cell medium and $1x10^4$ cell/mL, while Xue *et al* used high glucose DMEM culture medium and $2x10^5$ cell/mL. Therefore, all these variables may lead to different results.

In vivo studies also need a careful description, for which animal species, strains, age, sex, methods of applying NPs and vehicles used, will be of main importance. Particularly, for both *in vitro* and *in vivo* toxicology methods, there is a need for the inclusion of the appropriate controls to test possible effects of solvents, adherence of the analyzed proteins to NPs, effects caused by ions released by the NPs, potential contamination of samples, optical interference of the NPs with the method used, and many other factors [89]. As an example, Baratli *et al* [93] reported that while Fe_3O_4 NPs did not show to alter 3-month Wistar rats liver mitochondrial activity the same IONs were able to impair liver mitochondrial activity and the activity of the mitochondrial complexes I, II, III and IV in 18-month rats from the same strain. This fact reflects the importance of age in the toxic effect of IONs. The authors attributed these age differences to the fact that, with the time, the fragility of mitochondria increases, which leads to iron accumulation. As it was previously mentioned, iron accumulation results in $HO^{\bullet}$ formation through Fenton reaction, which may trigger oxidative damage [94] and, consequently, impairment of the mitochondrial complexes. Concerning gender, Srinivas *et al* [95] reported that there is a difference in the recovery of inflammatory and oxidative stress parameters in male and female Wistar rats, namely in the number of neutrophils present in bronchoalveolar lavage fluid (BALF). However, the cause responsible for these differences remains to be elucidated.

Therefore, it is possible to conclude that the final response of a cell to NPs results from a chain of events that depend upon the genetic make-up of the cell, determining the specificity of the intracellular environment (e.g. the spectrum and actual levels of plasma proteins, the activity of repair enzymes, etc.), as well as upon the size and surface chemistry of the given NP. The latter, as reported before, may influence not only the efficiency of IONs internalization, but also the route and speed of their intracellular degradation with the subsequent release of free iron and, last but not least, the choice of particular pathways leading to ROS generation and subsequent damage to biomolecules [65].

The cytotoxic effect of different types of IONs on the several types of cells evaluated so far are summarized in table 1.

Table 1. Toxic effects of IONs in several cell types and tissues.

Type of cell/tissue	Type and concentrations of nanoparticles	Cytotoxic effects
Endothelial cells		
Human endothelial cells	PLL and carboxydextran-coated Fe_2O_3 NPs (50 µg/mL)	Decrease in cell viability [96]
Human endothelial cells	PLL-coated SPIONs (25 µg/mL)	No evidence of cytotoxicity [97]
Human blood outgrowth endothelial cells	Resovist® (600 µg/mL) and Endorem® (400 µg/mL)	Cellular cytoskeleton and morphology were affected [43]
Human microvascular endothelial cells	Fe_2O_3 NPs (50 µg/mL)	No evidence of cytotoxicity [47]
Human cardiac microvascular endothelial cells	Fe_2O_3 NPs (100 µg/mL) and Fe_3O_4 NPs (100 µg/mL)	No evidence of cytotoxicity [51]
Human aortic endothelial cells	DMSA-coated Fe_2O_3 NPs (0.05 mg/mL)	Decrease in cell viability [98]
Human aortic endothelial cells	Fe_3O_4 NPs (100 µg/mL) and Fe_2O_3 NPs (2 µg/mL)	Decrease in cell viability, cytoplasmic vacuolation, mitochondrial swelling and cell death [99]
Human aortic endothelial cells	γ-Fe_2O_3 NPs (50 µg/mL)	No evidence of cytotoxicity [100]
Porcine aortic endothelial cells	Ultra-small SPIONs (USPIONs) (0.5 mg/mL)	Decrease in cell viability and actin cytoskeleton disruption [37]
Porcine aortic endothelial cells	Dextran and polyethylene glycol (PEG)-coated USPIONs (0.5 mg/mL)	No evidence of cytotoxicity [37]
Human umbilical vein endothelial cells	γ-Fe_2O_3 NPs (10 µg/mL)	Long-term toxicity in human endothelial cells by a necrotic process [101]
Human umbilical vein endothelial cells	Citrate-coated Fe_3O_4 NPs (1 mM)	Decrease in cell viability [45]
Human umbilical vein endothelial cells	Citrate-coated Fe_2O_3 NPs (10 mM)	No evidence of cytotoxicity [55]
Human umbilical vein endothelial cells	Thermally cross-linked (TCL) SPIONs (1 mg/mL) and monocrystalline IONs (MION)-47 (1 mg/mL)	No evidence of cytotoxicity [102]
Human umbilical vein endothelial cells	Citric acid-coated IONs (35 µg/mL)	Decrease in cell viability [103]
Murine brain endothelial cell line	Citrate-coated Fe_3O_4 NPs (100 µg/mL)	Decrease in cell viability [104]
Murine brain endothelial cell line	Cross-linked IONs (CLIO) Fe_3O_4 NPs (10 mg/mL)	No evidence of cytotoxicity [104]
Mouse brain-derived microvessel endothelial cell bEnd.3 line	Aminosilane-coated Fe_3O_4 NPs (224 µg/mL) and carboxyaminosilane-coated Fe_3O_4 NPs (224 µg/mL)	No evidence of cytotoxicity [105]
Human cerebral endothelial cells	Oleic acid-coated Fe_3O_4 NPs (75 µg/cm^2)	Decrease in cell viability [106]
Endothelial progenitor cells	Fe_3O_4 NPs (20 µg/mL)	No evidence of cytotoxicity [107]

Table 1. Toxic effects of IONs in several cell types and tissues (continuation).

Type of cell/tissue	Type and concentrations of nanoparticles	Cytotoxic effects
Placentary cells		
Placental choriocarcinoma cell line BeWo b30	Fe_3O_4 NPs (0.12 μg/cm^2) and sodium oleate-coated Fe_3O_4 NPs (0.12 μg/cm^2)	Decrease in cell viability [108]
BeWo placentary epithelial cell line	α-Fe_2O_3 NPs (100 μg/mL)	Decrease in cell viability [83]
Dendritic cells		
Antigen-presenting dendritic cells	Chitosan-coated IONs (200 μg/mL)	Decrease in cell viability [109]
Dendritic cells	Endorem® (400 μg/mL)	Decrease in cell viability [110]
Primary mouse bone marrow-derived dendritic cells	Feridex® (dextran-coated SPIONs) (200 μg/mL)	No evidence of cytotoxicity [31]
Intestinal cells		
CaCo-2 cells	Carboxymethyldextran-coated Fe_3O_4 NPs (0.90 mg/mL)	Decrease in cell viability [111]
CaCo-2 cells	α-Fe_2O_3 NPs (100 μg/mL)	Disruption of microvilli structures [21]
CaCo-2 cells	Fe_2O_3 NPs (10 ppm)	Decrease in microvilli and membrane disruption [80]
Breast cancer and mammary cells		
Breast cancer cell line SKBR3	Poly(aminoacid)-coated Fe_3O_4 NPs (1mg/mL)	No evidence of cytotoxicity [112]
Human ductal breast epithelial tumor T47D cell line	Tetramethylammonium 11-aminoundecanoate-coated Fe_3O_4 NPs (100 μg/mL)	Slight decrease in cell viability [82]
Human breast cancer MCF-7 cells	Folic acid-coated Fe_3O_4 NPs (400 μg/mL)	No evidence of cytotoxicity [113]
Human breast cancer MCF-7 cells	PEG-coated Fe_3O_4 NPs (500 μg/mL)	No evidence of cytotoxicity [114]
Human breast cancer MCF-7 cells	Poly(lactide-co-glycolide)-coated Fe_3O_4 NPs (1 mM) and cellulose-coated Fe_3O_4 NPs (1 mM)	No evidence of cytotoxicity [58]
Human breast cancer MCF-7 cells	Lauric acid-coated Fe_3O_4 NPs (2000 μM)	No evidence of cytotoxicity [115]
Human breast cancer MCF-7 cells	Fe_2O_3 NPs (0.5 mM)	No evidence of cytotoxicity [116]
Human breast cancer MCF-7 cells	Fe_2O_3 NPs (30 μg/mL)	Decrease in cell viability [117]
MDA-MB-435S breast cancer-bearing mouse	Lauric acid-coated Fe_3O_4 NPs (2000 μM)	No evidence of cytotoxicity [115]
Keratinocytes and epidermal cells		
Human keratinocyte HaCaT cells	Fe_2O_3 NPs (100 μg/mL)	Decrease in cell viability [50]
Human melanoma cells (SK-MEL-28)	Silica-coated γ-Fe_2O_3 NPs (200 μg/mL)	Slight decrease in cell viability [9]
Human melanoma cells (SK-MEL-28)	PLL-γ-Fe_2O_3 NPs (10 μg/mL)	No evidence of cytotoxicity [118]
KB (human epidermoid carcinoma) cells	Poly(glycidyl methacrylate*co*-PEG methyl ether methacrylate)-coated Fe_3O_4 NPs (1 mg/mL)	No evidence of cytotoxicity [119]

Table 1. Toxic effects of IONs in several cell types and tissues (continuation).

Type of cell/tissue	Type and concentrations of nanoparticles	Cytotoxic effects
KB (human epidermoid carcinoma) cells	Folic acid-PEG-polyethylenimine (PEI)-coated Fe_3O_4 NPs (100 μg/mL)	No evidence of cytotoxicity [120]
Human epithelial cell line A-431	Fe_3O_4 NPs (25 μg/mL)	Decrease in cell viability [33]
Mouse melanoma cell line B16F10	Dopamine-coated Fe/Fe_3O_4 NPs (10 μg/mL)	Decrease in cell viability [121]
Monocytes and macrophages		
RAW264.7 cells	TCL SPIONs (50 μg/mL) and MION-47 (50 μg/mL)	Reduction in the population of healthy cells and collapse of the mitochondrial membrane potential [102]
RAW 264.7 cells	Aminosilane-coated SPIONs (200 μg/mL)	No evidence of cytotoxicity [62]
RAW 264.7 cells	SPIONs (200 μg/mL)	No evidence of cytotoxicity [62]
RAW 264.7 cells	Dextran-coated SPIONs (200 μg/mL)	No evidence of cytotoxicity [62]
RAW 264.7 cells	Silica-coated SPIONs (10 μg/mL)	Decrease in cell viability [62]
RAW 264.7 cells	Alginate-coated Fe_3O_4 NPs (100 μg/mL)	No evidence of cytotoxicity [122]
RAW 264.7 cells	Pluronic F127-coated Fe_3O_4 NPs (60 μg/mL)	Decrease in cell viability [123]
RAW 264.7 cells	Poly(glycidyl methacrylate*co*-PEG methyl ether methacrylate-coated Fe_3O_4 NPs (1 mg/mL)	No evidence of cytotoxicity [119]
RAW 264.7 cells	DMSA-coated Fe_3O_4 NPs (100 μg/mL)	Decrease in cell viability [90]
RAW 264.7 cells	DMSA-coated Fe_3O_4 NPs (100 μg/mL)	No evidence of cytotoxicity [91]
RAW 264.7 cells	DMSA-coated γ-Fe_2O_3 NPs (50 μg/mL)	No evidence of cytotoxicity [124]
RAW 264.7 cells	γ-Fe_2O_3 NPs (6.25 μg/mL)	Decrease in cell viability and in ATP production and alteration of organelles such as the Golgi apparatus, endoplasmic reticulum, and mitochondria and formation of autophagosome-like vacuoles [48]
RAW 264.7 cells	Ferucarbotran (carboxydextran-coated IONs) (100 μg/mL)	No evidence of cytotoxicity [125]
THP-1 cells	DMSA-coated Fe_3O_4 NPs (100 μg/mL)	No evidence of cytotoxicity [91]
Human monocyte-macrophages	Ferumoxtran-10 (low molecular weight dextran-coated USPIONs) (10 mg/mL)	Decrease in cell viability [126]
Human monocyte derived macrophages	Silica-coated Fe_3O_4 NPs (100 μg/mL)	Decrease in cell viability [127]
U937 Human leukemic monocyte lymphoma cells	Fe_2O_3 NPs (2 μg/mL) and Fe_3O_4 NPs (20 μg/mL)	Decrease in cell viability [99]
Murine macrophage J774 cells	PEG2000-coated Fe_3O_4 NPs (200 μg/mL)	Decrease in cell viability [128]

Table 1. Toxic effects of IONs in several cell types and tissues (continuation).

Type of cell/tissue	Type and concentrations of nanoparticles	Cytotoxic effects
Murine macrophage J774 cells	PEG1100-coated Fe_3O_4 NPs (200 µg/mL) and PEG350-coated Fe_3O_4 NPs (200 µg/mL)	No influence of cytotoxicity [128]
Murine macrophage J774 cells	Tween-80-coated SPIONs (200 µg/mL)	Decrease in cell viability [129]
J774A.1 murine macrophages	High density lipoprotein-coated FeO NPs (4 µg/mL)	No evidence of cytotoxicity [130]
Macrophage cell line J7442	Carbon-coated IONs (10 µg/mL)	Decrease in cell viability [131]
Human macrophages	Resovist® (100 µg/mL) and Supravist® (carboxydextran-coated USPIONs) (0.1 µg/mL)	Decrease in cell viability [132]
Human monocytes	Endorem® (1000 µg/mL) and Sinerem® (low molecular weight dextran-coated USPIONs) (1000 µg/mL)	No evidence of cytotoxicity [133]
Human monocytes	CLIO-680 (100 µg/mL)	No evidence of cytotoxicity [134]
Murine peritoneal macrophages	Resovist® (200 µg/mL)	No evidence of cytotoxicity [135]
Bone marrow-derived macrophages	PEG-coated Fe_3O_4/FeO NPs (0.3 µg/mL)	Decrease in cell viability [136]
Mouse bone marrow-derived macrophages	Fe_3O_4 NPs (200 µg/mL)	No evidence of cytotoxicity [137]
Cardiac cells		
Cardiac-derived stem cells	PLL-coated Ferumoxides (dextran-coated SPIONs) (25 µg/mL)	No evidence of cytotoxicity [138]
Human cardiac myocytes	Carboxyethylsilanetriol-coated SPIONs (8 mg/mL)	Decrease in cell viability [60]
Rat heart	Fe_3O_4 NPs (500 µg/mL)	No alteration of mitochondrial respiratory chain complexes I, II, III and IV activities [139]
Rat heart	GEH121333 (hydroxyphosphonate–PEG-coated Fe_3O_4 NPs) (200 mg/kg)	No evidence of cytotoxicity [140]
Mesenchymal stem cells		
Mesenchymal stem cells	Citrate-coated Fe_2O_3 NPs (10 mM)	No evidence of cytotoxicity [55]
Human mesenchymal stem cells	Feridex® (100 µg/mL), Resovist® (100 µg/mL) and MION-47 (100 µg/mL)	No evidence of cytotoxicity [56]
Human mesenchymal stem cells	Protamine sulfate-coated Feridex IV® (50 µg/mL)	No evidence of cytotoxicity [141]
Human bone marrow-derived mesenchymal stem cells	Poly(vinylpyrrolidone) (PVP)-coated SPIONs (1600 µg/mL) and Feridex IV® (1600 µg/mL)	No evidence of cytotoxicity [142]
Human bone marrow-derived mesenchymal stem cells	Resovist® (400 µg/mL) and chitosan-coated SPIONs (400 µg/mL)	Decrease in cell viability [143]

Table 1. Toxic effects of IONs in several cell types and tissues (continuation).

Type of cell/tissue	Type and concentrations of nanoparticles	Cytotoxic effects
Human bone marrow mesenchymal stromal cells	PLL-coated γ-Fe_2O_3 NPs (15.4 μg/mL), mannose-coated γ-Fe_2O_3 NPs (15.4 μg/mL), PLL-coated Endorem® (15.4 μg/mL), Endorem® (15.4 μg/mL) and γ-Fe_2O_3 NPs (15.4 μg/mL)	Decrease in cell viability [65]
Human amniotic membrane-derived mesenchymal stem cells	Resovist® (28 μg/mL)	Decrease in cell viability and loss of morphology [144]
Mouse mesenchymal stem cells	Protamine-coated Feridex® (25 μg/mL)	No evidence of cytotoxicity [57]
Mouse mesenchymal stem cells	Poly(lactide-co-glycolide)-coated Fe_3O_4 NPs (1 mM) and cellulose-coated Fe_3O_4 NPs (1 mM)	No evidence of cytotoxicity [58]
Rat mesenchymal stem cells	PEI-polyacrylic acid (PAA)-coated Fe_3O_4 NPs (100 μg/mL)	No evidence of cytotoxicity [59]
Pulmonary cells		
Human lung epithelial cells BEAS-2B	Tetramethylammonium hydroxide-coated Fe_3O_4 NPs (6.0 x 10^{12} NP/mL)	No evidence of cytotoxicity [89]
Human lung epithelial cells BEAS-2B	α-Fe_2O_3 NPs (50 μg/mL)	Decrease in cell viability [77]
Human lung epithelial cells BEAS-2B	Fe_2O_3 NPs (50 μg/cm^2)	Decrease in cell viability [145]
Human lung cancer A549 cells	Fe_2O_3 NPs (80 μg/mL)	Decrease in cell viability [68]
Human lung cancer A549 cells	Fe_3O_4 NPs (80 μg/mL)	No evidence of cytotoxicity [68]
Human lung cancer A549 cells	Poly (ethylene oxide)-*block*-poly(γ-methacryloxypropyl trimethoxysilane)-coated IONs (0.5 mg/mL)	No evidence of cytotoxicity [146]
Human lung cancer A549 cells	α-Fe_2O_3 NPs (100 μg/cm^2)	No evidence of cytotoxicity [70]
Human lung cancer A549 cells	Fe_2O_3 NPs (10 mg/mL)	Decrease in cell viability [50]
Human lung cancer A549 cells	Fe_3O_4 NPs (0.5 μg/mL)	Decrease in cell viability [147]
Human lung cancer A549 cells	Fe_3O_4 NPs (200 μg/mL)	Decrease in cell viability [66]
Human lung cancer A549 cells	Carboxyethylsilanetriol-coated SPIONs (114 μg/mL)	Decrease in cell viability [60]
Human lung cancer A549 cells	IONs (25 μg/mL)	Decrease in cell viability and loss of mitochondrial membrane potential [148]
Human lung cancer A549 cells	Fe_3O_4 NPs (25 μg/mL)	Decrease in cell viability [33]
Human lung cancer A549 cells	Sodium oleate-coated Fe_3O_4 NPs (3 μg/cm^2) and Fe_3O_4 NPs (37.5 μg/cm^2)	Decrease in cell viability [34]
Human lung cancer A549 cells	Sodium oleate-coated Fe_3O_4 NPs (0.6 mM), sodium oleate and PEG-coated Fe_3O_4 NPs (0.35 mM), sodium oleate, PEG and poly(lactide-co-glycolic acid)-coated Fe_3O_4 NPs (0.1 mM)	Decrease in cell viability [149]
Human lung cancer A549 cells	Fe_3O_4 NPs (200 μg/cm^2)	Slight loss of mitochondrial membrane potential [32]

Table 1. Toxic effects of IONs in several cell types and tissues (continuation).

Type of cell/tissue	Type and concentrations of nanoparticles	Cytotoxic effects
Human lung fibroblast IMR-90 cells	IONs (100 μg/mL)	No evidence of cytotoxicity [148]
Human lung fibroblast IMR-90 cells	Fe_2O_3 NPs (10 μg/cm^2)	Decrease in cell viability [145]
Rat BALF	Fe_3O_4 NPs (aerosol concentration of 640 mg/m^3 for 4 hours)	Decrease in cell viability [95]
Rat BALF	γ-Fe_2O_3 NPs (90 μg/m^3 for 6 hours during 3 days)	No evidence of cytotoxicity [150]
Rat BALF	γ-Fe_2O_3 NPs (57 μg/m^3 for 6 hours during 3 days)	No evidence of cytotoxicity [151]
Mouse lung alveolar type II (C10) epithelial cells	Carboxy-coated Fe_3O_4 NPs (10 μg/mL)	Decrease in cell viability [152]
Mouse lung alveolar type II (C10) epithelial cells	Amine-coated Fe_3O_4 NPs (200 μg/mL)	No evidence of cytotoxicity [152]
Human lung embryonic HEL 12469 cells	Sodium oleate-coated Fe_3O_4 NPs (0.6 mM), sodium oleate and PEG-coated Fe_3O_4 NPs (0.35 mM), sodium oleate, PEG and poly(lactide-co-glycolic acid)-coated Fe_3O_4 NPs (0.1 mM)	Decrease in cell viability [149]
Human bronchial 16HBE epithelial cells	Sodium oleate-coated Fe_3O_4 NPs (7.5 μg/cm^2) and Fe_3O_4 NPs (15 μg/cm^2)	Decrease in cell viability [34]
Human lung adenocarcinoma ASTC-a-1	PLL-coated SPIONs (50 μg/mL)	Decrease in cell viability [153]
Lewis lung carcinoma cell line	Poly(3-(Trimethoxysilyl)propyl methacrylate -r-PEG monomethyl ether methacylate)-coated Fe_3O_4 NPs (100 μg/10^5 cells)	No evidence of cytotoxicity [154]
Rat lung	Fe_3O_4 NPs (500 μg/mL)	No alteration of mitochondrial respiratory chain complexes I, II, III and IV activities [139]
Osteoblast cells		
Human osteosarcoma (U2OS)	Carbon-coated IONs (100 μg/mL)	Decrease in cell viability [131]
Brain cells		
Human neuronal glioblastoma U251 cells	DMSA-coated γ-Fe_2O_3 NPs (100 μg/mL)	No evidence of cytotoxicity [36]
Human neuronal glioblastoma U251 cells	DMSA-coated Fe_3O_4 NPs (25 μg/mL)	Decrease in cell viability [36]
Human neuronal glioblastoma U251 cells	Tetramethylammonium 11-aminoundecanoate-coated Fe_3O_4 NPs (100 μg/mL)	Decrease in cell viability [82]
Human neuronal glioblastoma U251 cells	Protamine sulfate-coated Feridex IV® (100 μg/mL)	No evidence of cytotoxicity [155]
Human primary glioblastoma cell line U87	Tetramethylammonium 11-aminoundecanoate-coated Fe_3O_4 NPs (100 μg/mL)	No evidence of cytotoxicity [82]

Table 1. Toxic effects of IONs in several cell types and tissues (continuation).

Type of cell/tissue	Type and concentrations of nanoparticles	Cytotoxic effects
U87MG glioblastoma cells	USPIONs (0.03 μmol/mL) and arginine-glycine-aspartic acid-coated USPIONs (0.03 μmol/mL)	No evidence of cytotoxicity [156]
U87MG glioblastoma cells	Fe_3O_4 NPs (25 μg/mL)	Protection from H_2O_2-induced cytotoxicity [157]
Human neural stem cell line HB1F3	Feridex IV® (25 μg/mL), MION-47(25 μg/mL) , CLIO-NH_2 (25 μg/mL) and tat-CLIO (25 μg/mL)	No evidence of cytotoxicity [158]
Neuro-2A mouse neuroblastoma	Fe_3O_4 NPs (200 μg/mL)	No evidence of cytotoxicity [159]
Human glioma cell line D54MG	Tetramethylammonium 11-aminoundecanoate-coated Fe_3O_4 NPs (100 μg/mL)	Decrease in cell viability [82]
Human brain tumor cell G9T/VGH	Tetramethylammonium 11-aminoundecanoate-coated Fe_3O_4 NPs (100 μg/mL)	Decrease in cell viability [82]
Glioma cell line SF126	Tetramethylammonium 11-aminoundecanoate-coated Fe_3O_4 NPs (100 μg/mL)	No evidence of cytotoxicity [82]
Human isolated from brain epithelium U373	Tetramethylammonium 11-aminoundecanoate-coated Fe_3O_4 NPs (100 μg/mL)	No evidence of cytotoxicity [82]
Oligodendroglia OLN-93 cells	DMSA-coated IONs (4 mM)	Loss of the initial bipolar shape and bright intracellular vesicles [160]
Oligodendroglial OLN-93 cells	DMSA-coated IONs (1000 μM)	No evidence of cytotoxicity [161]
BV2 microglial cells	α-Fe_2O_3 NPs (0.2 mmol/L) and γ-Fe_2O_3 NPs (0.2 mmol/L)	Large number of cellular vesicles, proliferation of lysosome, swelling of endoplasmic reticulum and disappearance of mitochondrial cristae [162]
Human brain-derived endothelial cells	Amino polyvinyl alcohol (PVA)-coated SPIONs (200 μg/mL) and Fe_3O_4 NPs (200 μg/mL)	No evidence of cytotoxicity [163]
Human brain-derived endothelial cells	Oleic acid-coated Fe_3O_4 NPs (150 μg/mL)	Decrease in cell viability [163]
C17.2 neural progenitor cells	Resovist® (150 μg/mL) and Endorem® (200 μg/mL)	No evidence of cytotoxicity [43]
Chick cortical neurons	FluidMAG-Amine (aminosilane-coated Fe_3O_4 NPs (100 μg/mL)	No evidence of cytotoxicity [19]
Chick cortical neurons	FluidMAG-D (dextran-coated Fe_3O_4 NPs) (50 μg/mL)	Decrease in cell viability [19]

Table 1. Toxic effects of IONs in several cell types and tissues (continuation).

Type of cell/tissue	Type and concentrations of nanoparticles	Cytotoxic effects
Chick cortical neurons	FluidMAG-PEA (poly-(dimethylamine-co-epichlorhydrin-co-ethylendiamine)-coated Fe_3O_4 NPs) (10 μg/mL)	Decrease in cell viability due to remotion of plasma membrane of the neurons [19]
PC12 cells	Citrate-coated very small SPIONs (VSOP) (400 μg/mL)	Decrease in the formation of intercellular contacts and in the growth of neurites upon nerve growth factor exposure [17]
PC12 cells	Aminopropyltriethoxysilane-coated Fe_3O_4 NPs (100 μg/mL)	Decrease in cell viability [164]
PC12 cells	IONs (40 μg/mL)	Slight decrease in cell viability [165]
PC12 cells	DMSA-coated Fe_2O_3 NPs (1.5 mM)	Decrease in cell viability, decreased ability to respond to nerve growth factor and to generate neuritis, reduction in the formation of actin microfilaments [39]
PC12 cells	Fe_3O_4 NPs (50 μg/mL)	Decrease in cell viability [23]
PC12 cells	Fe_3O_4 NPs (0.5 mg/mL)	No evidence of cytotoxicity [92]
A172 cells	Carboxyethylsilanetriol-coated SPIONs (8 mg/mL)	Decrease in cell viability [60]
BE-2-C brain cells	Carboxyethylsilanetriol-coated SPIONs (4 mg/mL)	Decrease in cell viability [60]
Rat neural progenitor cells	Feridex® (100 μg/mL)	No evidence of cytotoxicity [166]
Rat brain	Fe_3O_4 NPs (500 μg/mL)	No alteration of mitochondrial respiratory chain complexes I, II, III and IV activities [139]
Rat brain	Combidex® (10 mg/kg) (low molecular weight dextran-coated USPION), Ferumoxytol (polyglucose sorbitol carboxymethylester-coated USPIONs) (10 mg/kg) and Feridex IV® (10 mg/kg)	No evidence of cytotoxicity [167]
Rat brain	Fe_2O_3 NPs (1000 mg/kg)	Inhibition of acetylcholinesterase [49]
Mouse hippocampus	α-Fe_2O_3 NPs (130 μg per day for 30 days)	Decrease in the contents of monoamine neurotransmitter and related metabolites [168]

Table 1. Toxic effects of IONs in several cell types and tissues (continuation).

Type of cell/tissue	Type and concentrations of nanoparticles	Cytotoxic effects
Mouse brain	α-Fe_2O_3 NPs (6.5 g/L per day for 40 days) and γ-Fe_2O_3 NPs (6.5 g/L per day for 40 days)	Morphological changes: irregular arrangement of neuron cells or neuronal loss in olfactory bulb, decrease in number of intact neuronal cells in the region I of hippocampus proper, cellular swelling, vacuolar degeneration, nuclear chromatin condensation and fragmentation [162]
Murine microglial cells	Resovist® (50 μg/mL)	No evidence of cytotoxicity [169]
Rat astrocytes	Dextran-coated Fe_3O_4 NPs (500 μg/mL)	No evidence of cytotoxicity [170]
Rat astrocytes	DMSA-coated IONs (1 mM)	Slight decrease in cell viability [171]
Mouse primary astrocytes	Aminosilane-coated Fe_3O_4 NPs (224 μg/mL)	Decrease in cell viability [105]
Mouse primary astrocytes	Carboxyaminosilane-coated Fe_3O_4 NPs (100 μg/mL)	Decrease in cell viability [105]
Mouse primary neurons	Aminosilane-coated Fe_3O_4 NPs (224 μg/mL)	Decrease in cell viability [105]
Mouse primary neurons	Carboxyaminosilane-coated Fe_3O_4 NPs (150 μg/mL)	Decrease in cell viability [105]
Mouse olfactory bulb	α-Fe_2O_3 NPs (130 μg per day for 30 days)	Slightly dilated rough endoplasmic reticulum, degeneration of neurodendron, disruption of membranous structure, and increase of lysosome of nerve cells [168]
Lymphocytes		
Human peripheral lymphocytes	Oleate-coated Fe_3O_4 NPs (75 μg/cm^2)	Decrease in cell viability [61]
A3 human T lymphocytes	Amine-coated IONs (25 μg/mL) and carboxyl-coated IONs (25 μg/mL)	Decrease in cell viability [52]
Jurkat cells	Poly(maleic anhydride-alt-1-octadecene and methoxy-PEG-coated Fe_3O_4 NPs (150 μg/mL)	Decrease in cell viability [54]
Jurkat cells	Carboxyethylsilanetriol-coated SPIONs (8 mg/mL)	Decrease in cell viability [60]
TK6 lymphoblastoid cells	Oleate-coated Fe_3O_4 NPs (45 μg/cm^2)	Decrease in cell viability [61]
Cervical cancer cells		
Human cervical cancer HeLa cells	Polymeric liposomes-coated Fe_3O_4 NPs (1200 μg/mL)	No evidence of cytotoxicity [172]
Human cervical cancer HeLa cells	PLL-coated Ferumoxides (50 μg/mL)	No evidence of cytotoxicity [173]
Human cervical cancer HeLa cells	Fe_3O_4 NPs (10 μg/mL)	Decrease in cell viability [75]

Table 1. Toxic effects of IONs in several cell types and tissues (continuation).

Type of cell/tissue	Type and concentrations of nanoparticles	Cytotoxic effects
Human cervical cancer HeLa cells	Protamine-sulfate Feridex IV® (50 μg/mL)	No evidence of cytotoxicity [141]
Human cervical cancer HeLa cells	Carboxyethylsilanetriol-coated SPIONs (8 mg/mL)	Decrease in cell viability [60]
Human cervical cancer HeLa cells	Dextran-coated Fe_3O_4 NPs (500 μg/mL), aminodextran-coated Fe_3O_4 NPs (500 μg/mL) and DMSA-coated Fe_3O_4 NPs (500 μg/mL)	No evidence of cytotoxicity [174]
Human cervical cancer HeLa cells	Fe_3O_4 NPs (50 μg/mL), arginine and chitosan-coated Fe_3O_4 NPs (50 μg/mL) and arginine and PEG-coated Fe_3O_4 NPs (50 μg/mL)	No evidence of cytotoxicity [175]
Human cervical cancer HeLa cells	Carbon-coated IONs (100 μg/mL)	Decrease in cell viability [131]
Adipose cells		
Human adipose derived stem cells	Protamine sulphate, PEG and dextran-coated γ-Fe_2O_3 NPs (15 mM)	No evidence of cytotoxicity [176]
Rat adipose derived stem cells	Protamine sulphate-coated Ferumoxides (100 μg/mL)	No evidence of cytotoxicity [177]
Pancreatic cells		
Beta-TC-6 cells	PVP-coated SPIONs and Feridex® (200 μg/mL)	No evidence of cytotoxicity [178]
Panc-1 cells	Carboxyethylsilanetriol-coated SPIONs (8 mg/mL)	Slight decrease in cell viability [60]
Capan-2 cells	Carboxyethylsilanetriol-coated SPIONs (8 mg/mL)	Slight decrease in cell viability [60]
Murine insulinoma βTC3	Citrate-coated γ-Fe_2O_3 NPs (20 μg/mL)	No evidence of cytotoxicity [179]
βTC-tet cells	Citrate-coated γ-Fe_2O_3 NPs (20 μg/mL)	No evidence of cytotoxicity [179]
Spleen		
Mouse splenocytes	Resovist® (100 μg/mL)	No evidence of cytotoxicity [180]
Ovarian cells		
Ovarian carcinoma (MLS) cells	USPIONs, arginine-glycine-aspartic acid-coated USPIONs (0.03 μmol/mL)	No evidence of cytotoxicity [156]
Chinese Hamster Ovary (CHO-K1) cells	SPIONs (80 μg/mL)	Decrease in cell viability [181]
Liver cells		
Human hepatocytes	Endorem® (150 μg/mL)	Decrease in cell viability and in albumin production [182]
Human primary hepatocytes	Chitosan and linoleic acid-coated Fe_3O_4 NPs (100 μg/mL)	Slight decrease in cell viability [183]
HepG2 hepatocytes	High density lipoprotein-coated FeO NPs (4 μg/mL)	No evidence of cytotoxicity [130]

Table 1. Toxic effects of IONs in several cell types and tissues (continuation).

Type of cell/tissue	Type and concentrations of nanoparticles	Cytotoxic effects
HepG2 hepatocytes	Carboxyethylsilanetriol-coated SPIONs (8 mg/mL)	Decrease in cell viability [60]
Normal mouse liver NCTC 1469 cell line	Resovist® (0.5 mM)	Decrease in cell viability [184]
Rat liver derived BRL 3A cell line	Fe_3O_4 NPs (250 µg/mL)	Decrease in cell viability [185]
Hepatic cell line LO2	O-carboxymethyl chitosan-coated Fe_3O_4 NPs (1000 µg/mL), folic acid-carboxymethyl chitosan-coated Fe_3O_4 NPs (1000 µg/mL) and dextran-coated Fe_3O_4 NPs (1000 µg/mL)	No evidence of cytotoxicity [66]
Hepatic cell line LO2	Fe_3O_4 NPs (200 µg/mL)	Decrease in cell viability [66]
Mouse liver	Fe_3O_4 NPs (10 mg/kg per day for 1 week)	Cell expansion, liver cords broadening, liver sinuses contraction and hepatic damage [186]
Murine hepatocytes	Fe_2O_3 NPs (250 µg/mL)	Decrease in cell viability [187]
Rat liver	Fe_3O_4 NPs (500 µg/mL)	No alteration of mitochondrial respiratory chain complexes I, II, III and IV activities [139]
Rat liver	Fe_2O_3 NPs (500 mg/kg)	Increase in aspartate aminotransferase (AST), alanine aminotransferase (ALT) and lactate dehydrogenase (LDH) levels [49]
Rat liver	GEH121333 (200 mg/kg)	No evidence of cytotoxicity [140]
Rat liver	Sodium oleate-coated Fe_3O_4 NPs (0.0364 mg/kg)	Diffuse necrosis and mild lipidosis [188]
Fibroblasts		
Human fibroblasts	DMSA-coated γ-Fe_2O_3 NPs (10 µg/L)	Decrease in cell viability and in metabolic mitochondrial activity [189]
Human fibroblasts	MION-47 and TCL SPIONs (1 mg/mL)	No evidence of cytotoxicity [102]
Human fibroblasts	PAA and bacitracin-coated Fe_3O_4 NPs (400 µg/mL)	No evidence of cytotoxicity [190]
Human skin fibroblast	Poly(*γ*–glutamic acid)-coated Fe_3O_4 NPs (1 mg/mL)	No evidence of cytotoxicity [191]
Human diploid fibroblast	Gelatin-coated Fe_3O_4 NPs (600 µg/mL)	No evidence of cytotoxicity [192]
Human diploid fibroblast	Fe_3O_4 NPs (300 µg/mL)	Decrease in cell viability [192]
Mouse fibroblast adhesive cells (L929)	Fe_3O_4 NPs (20 mM)	Decrease in cell viability [193]
Mouse fibroblast adhesive cells (L929)	PVA-coated Fe_3O_4 NPs (80 mM)	No evidence of cytotoxicity [193]
Mouse fibroblast adhesive cells (L929)	Fe_3O_4 NPs (100 mM)	Decrease in cell viability [194]
Mouse fibroblast adhesive cells (L929)	PVA-coated Fe_3O_4 NPs (400 mM)	No evidence of cytotoxicity [194]
Mouse fibroblast adhesive cells (L929)	Alginate-coated Fe_3O_4 NPs (100 µg/mL)	No evidence of cytotoxicity [122]

Table 1. Toxic effects of IONs in several cell types and tissues (continuation).

Type of cell/tissue	Type and concentrations of nanoparticles	Cytotoxic effects
Mouse fibroblast adhesive cells (L929)	Poly(L-lactide)-PEG-poly(L-lactide)-coated Fe_3O_4 NPs (1 mg/mL) and Fe_3O_4 NPs (2 mg/mL)	No evidence of cytotoxicity [195]
Mouse fibroblast adhesive cells (L929)	Dextran-coated SPIONs (1 mg/mL)	Decrease in cell viability [196]
Mouse fibroblast adhesive cells (L929)	Surfactin-coated Fe_3O_4 NPs (400 µg/mL) and rhamnolipid-coated Fe_3O_4 NPs (400 µg/mL)	Decrease in cell viability [197]
Mouse fibroblast adhesive cells (L929)	PEG-coated Fe_3O_4 NPs (400 µg/mL) and dextran-coated Fe_3O_4 NPs (400 µg/mL)	No evidence of cytotoxicity [197]
Mouse fibroblast adhesive cells (L929)	Silica-coated γ-Fe_2O_3 NPs (200 µg/mL)	Slight decrease in cell viability [9]
Telomerase immortalised primary human fibroblasts (h-TERT BJ1)	Fe_3O_4 NPs (50 µg/mL)	Decrease in cell viability [46]
Telomerase immortalised primary human fibroblasts (h-TERT BJ1)	Pullulan-coated Fe_3O_4 NPs (2 mg/mL)	No evidence of cytotoxicity [46]
Telomerase immortalised primary human fibroblasts (h-TERT BJ1)	Lactoferrin and sodium oleate-coated Fe_3O_4 NPs (1 mg/mL) and ceruloplasmin and sodium oleate-coated Fe_3O_4 NPs (1 mg/mL)	No evidence of cytotoxicity [198]
Telomerase immortalised primary human fibroblasts (h-TERT BJ1)	Fe_3O_4 NPs (250 µg/mL)	Decrease in cell viability [198]
Telomerase immortalised primary human fibroblasts (h-TERT BJ1)	Fe_3O_4 NPs (50 µg/mL) and dextran-coated Fe_3O_4 NPs (50 µg/mL)	Decrease in cell viability and cell morphology/cytoskeletal organisation and cell motility changes [199]
Telomerase immortalised primary human fibroblasts (h-TERT BJ1)	Fe_3O_4 NPs (50 µg/mL)	Appearance of vacuoles in the cell body and aberrations on the cell membrane [200]
3T3 cell mouse embryo fibroblast cells	Oleate-coated γ-Fe_2O_3 NPs (0.7 µg/mL)	No evidence of cytotoxicity [201]
3T3 cell mouse embryo fibroblast cells	Poly(glycidyl methacrylate-*co*-PEG methyl ether methacrylate-coated Fe_3O_4 NPs (1 mg/mL)	No evidence of cytotoxicity [119]
3T3 cell mouse embryo fibroblast cells	Silica-coated Fe_3O_4 NPs (1 mg/mL)	No evidence of cytotoxicity [6]
3T3 cell mouse embryo fibroblast cells	Oleic acid-coated Fe_3O_4 NPs (19.7 µg/cm^2)	Decrease in cell viability [202]
3T3 cell mouse embryo fibroblast cells	Fe_3O_4 NPs (316 µg/mL) and Endorem® (316 µg/cm^2)	No evidence of cytotoxicity [202]

Table 1. Toxic effects of IONs in several cell types and tissues (continuation).

Type of cell/tissue	Type and concentrations of nanoparticles	Cytotoxic effects
3T3 cell mouse embryo fibroblast cells	Fe_3O_4 NPs (50 µg/mL), arginine and chitosan-coated Fe_3O_4 NPs (50 µg/mL) and arginine and PEG-coated Fe_3O_4 NPs (50 µg/mL)	No evidence of cytotoxicity [175]
Embryo fibroblast cells (NIH/3T3)	Fe_3O_4 NPs (50 µg/mL)	Decrease in cell viability [203]
Embryo fibroblast cells (NIH/3T3)	PVP-coated Fe_2O_3/Fe_3O_4 NPs (10 mM)	No evidence of cytotoxicity [204]
Embryo fibroblast cells (NIH/3T3)	Fe_2O_3 NPs (100 µg/mL)	Decrease in cell viability, focal adhesion and regulation of actin cytoskeleton, lipid biosynthetic process and the cellular lipid metabolic process alterations [205]
Embryo fibroblast cells (NIH/3T3)	Carbon-coated IONs (100 µg/mL)	Decrease in cell viability [131]
Human lung fibroblast cell line MRC-5	α-Fe_2O_3 NPs (6.25 µg/mL)	Decrease in cell viability [27]
Nasopharingeal cells		
Human nasopharyngeal epidermoid carcinoma cells (KB cells)	Citrate-coated Fe_3O_4 NPs (2 mg/mL)	No evidence of cytotoxicity [206]
Human nasopharyngeal epidermoid carcinoma cells (KB cells)	Acetic anhydride and 3-aminopropyltrimethoxysilane-coated Fe_3O_4 NPs (100 µg/mL)	No evidence of cytotoxicity [64]
Human nasopharyngeal epidermoid carcinoma cells (KB cells)	Succinic anhydride and 3-aminopropyltrimethoxysilane-coated Fe_3O_4 NPs (10 µg/mL) and 3-aminopropyltrimethoxysilane-coated Fe_3O_4 NPs (10 µg/mL)	Decrease in cell viability [64]
Human nasopharyngeal epidermoid carcinoma cells (KB cells)	Pluronic F127 and PAA-coated Fe_3O_4 NPs (1 mg/mL)	No evidence of cytotoxicity [207]
Human nasopharyngeal epidermoid carcinoma cells (KB cells)	Oleic acid and PEG-coated Fe_3O_4 NPs (200 µg/mL)	No evidence of cytotoxicity [208]
Human nasopharyngeal epidermoid carcinoma cells (KB cells)	Fe_3O_4 NPs (100 µg/mL)	Decrease in cell viability [66]
Human nasopharyngeal epidermoid carcinoma cells (KB cells)	O-carboxymethyl chitosan-coated Fe_3O_4 NPs (1 mg/mL) and dextran-coated Fe_3O_4 NPs (1 mg/mL)	No evidence of cytotoxicity [66]
Erythrocytes		
Rabbit erythrocytes	Alginate-coated Fe_3O_4 NPs (570 µg/mL)	No evidence of cytotoxicity [122]
Rat erythrocytes	Fe_2O_3 NPs (500 mg/kg)	Inhibition of acetylcholinesterase [49]
Human erythrocytes	Tetramethylammonium hydroxide-coated Fe_3O_4 NPs (0.1 M)	Increase in hemolysis [209]
Human erythrocytes	Acetic anhydride and 3-aminopropyltrimethoxysilane-coated Fe_3O_4 NPs (400 µg/mL)	No evidence of cytotoxicity [64]

Table 1. Toxic effects of IONs in several cell types and tissues (continuation).

Type of cell/tissue	Type and concentrations of nanoparticles	Cytotoxic effects
Human erythrocytes	Succinic anhydride and 3-aminopropyltrimethoxysilane-coated Fe_3O_4 NPs (400 µg/mL) and 3-aminopropyltrimethoxysilane-coated Fe_3O_4 NPs (400 µg/mL)	Increase in hemolysis [64]
Human erythrocytes	Poly(L-lactide)-PEG-poly(L-lactide)-coated Fe_3O_4 NPs (20 mg/mL) and Fe_3O_4 NPs (20 mg/mL)	Increase in hemolysis [195]
Human erythrocytes	Folic acid-PEG-PEI-coated Fe_3O_4 NPs (400 µg/mL)	No evidence of cytotoxicity [120]
Kidney cells		
Human embryonic kidney 293T cell line	Carboxyethylsilanetriol-coated SPIONs (8 mg/mL)	Decrease in cell viability [60]
Human embryonic kidney 293T cell line	PEI-PAA-coated Fe_3O_4 NPs (200 µg/mL)	No evidence of cytotoxicity [210]
Cos-7 monkey kidney cells	Tetramethylammonium hydroxide-coated Fe_3O_4 NPs (23.05 mM)	No evidence of cytotoxicity [209]
MDCK (canine distal tubule) epithelial cell line	Oleic acid-coated Fe_3O_4 NPs (235 µg/mL)	Decrease in cell viability [211]
LLC-PK (porcine proximal tubule) epithelial cell line	Oleic acid-coated Fe_3O_4 NPs (235 µg/mL)	Decrease in cell viability [211]
Human urinary bladder carcinoma cells UM-UC-3	Poly(ε-caprolactone)-b-poly(propargyl methacrylate-co-poly-(ethylene glycol) methyl ether methacrylate)-coated SPIONs (1 mg/mL)	No evidence of cytotoxicity [212]
Renal NRK cells	Dextran-coated Fe_3O_4 NPs (500 µg/mL)	No evidence of cytotoxicity [170]
Mouse kidney	Fe_3O_4 NPs (5 mg/kg per day for 1 week)	Large reduction of tubular space and extreme edema of epithelial cells in glomeruli [186]
Mouse kidney	PAA-coated γ-Fe_2O_3 NPs (10 mg/kg)	No evidence of cytotoxicity [213]
Rat kidney	Fe_3O_4 NPs (500 µg/mL)	No alteration of mitochondrial respiratory chain complexes I, II, III and IV activities [139]
Rat kidney	Fe_2O_3 NPs (500 mg/kg)	Decrease in AST and ALT levels [49]
Rat kidney	Fe_2O_3 NPs (1000 mg/kg)	Decrease in LDH levels [49]
Rat kidney	GEH121333 (200 mg/kg)	No evidence of cytotoxicity [140]
Muscular cells		
C2C12 cells	Protamine sulfate-coated Feridex® (30 µg/mL)	No evidence of cytotoxicity [214]
Embryonic cells		
Embryonic stem cells	PLL-coated SPIONs (50 µg/mL)	No evidence of cytotoxicity [215]

Table 1. Toxic effects of IONs in several cell types and tissues (continuation).

Type of cell/tissue	Type and concentrations of nanoparticles	Cytotoxic effects
Retina epithelial cells		
ARPE-19 cells	Feraheme® (polyglucose sorbitol carboxymethylester-coated USPIONs) (0.1 mg/mL)	Decrease in metabolic activity [216]
Blood		
Rat serum	Fe_2O_3 NPs (1000 mg/kg)	Increase in AST and LDH levels [49]
Rat serum	Fe_2O_3 NPs (2000 mg/kg)	Increase in ALT levels [49]
Rat blood	Fe_2O_3 NPs (0.8 mg/kg)	Prolongation of prothrombin time and activated partial thromboplastin time and elevation of the average concentration of fibrinogen [217]

Concentrations in parenthesis represent the lowest concentration where an effect was observed. When no effect was observed, concentration in parenthesis represents the highest concentration tested.

I.1.2.2. PROGRAMMED CELL DEATH INDUCED BY IRON OXIDE NANOPARTICLES

Apoptosis is a highly organized process characterized by the progressive activation of precise pathways leading to specific biochemical and morphological alterations, namely cytoplasmatic blebbing, cell shrinking and intense condensation of chromatin in the nucleus [218,219]. Two of those pathways are the mitochondrial-mediated or intrinsic and the receptor-mediated or extrinsic [218]. In both pathways (intrinsic and extrinsic), the initiator caspases (caspase 8 in extrinsic and caspase 9 in intrinsic pathway) activate downstream effector caspases, mainly caspase 3 (cysteine-aspartic acid protease belonging to the family of effector caspases [132]), by proteolytic induction of its inactive zymogen form. Effector caspases cleave cytoplasmic and nuclear components, and promote DNA degradation and cell dismantling, which converges in the demise of the cell [219,220] (figure 3). It was reported that IONs have the ability to induce caspase 3 activation: Resovist® and Supravist® induced caspase 3 activation in human macrophages (greater for Supravist®) [132], Resovist® in mouse hepatic tissues [24], Fe_3O_4 NPs in human hepatoma BEL-7402 cells [221], in PC12 cells [23], in Jurkat cells [222] and in A-431 epithelial and A549 cell lines [33], oleic acid-coated Fe_3O_4 NPs in human hepatoma BEL-7402 cells [221], Fe_2O_3 NPs in human breast cancer MCF-7 cell line [117] and in murine hepatocytes [187], and DMSA-coated Fe_3O_4 NPs and DMSA-coated Fe_2O_3 NPs in rat sciatic nerve [223]. It was also described that Fe_3O_4 NPs enhanced the caspase 3 induction caused by daunorubicin in K562/A02 [224] and gambogic acid in K562 cells [225]. However, it was also reported that citrate-coated VSOP or Resovist® did not cause a measurable increase in caspase 3 activity in THP-1 cells [226].

Caspase 9 was also reported to be affected by IONs. Khan *et al* [227] reported that Fe_3O_4 NPs cause a decrease in the expression of caspase 9, both at ribonucleic acid and protein levels, in HeLa cells. However, Fe_3O_4 NPs induced the activation of caspase 9 in PC12 cells [23], in Jurkat cells [222] and in A-431 epithelial and A549 cell lines [33] and Fe_2O_3 NPs in murine hepatocytes [187].

Regarding caspase 8, Zhang *et al* [228] demonstrated that tetraheptylammonium-coated Fe_3O_4 NPs have the capacity to increase the ability of daunorubucin to induce apoptosis in K562 cells through caspase 8 activation.

One of the earliest indications of apoptosis is the translocation of the membrane phospholipid phosphatidylserine from the inner to the outer leaflet of the plasma membrane. Annexin V has a high affinity for phosphatidylserine and consequently may be used to reveal this phospholipid exposed on the outer surface of cells. This event precedes the loss of membrane integrity, resulting in cell death in the later stages [147]. In fact, after being activated, caspase 3 cleaves and activates Xk-receptor protein 8 (Xkr8). This protein is a scramblase which will be responsible for the translocation of phosphatidylserine to the outer leaflet [229] (figure 3). There are many studies reporting the translocation of phosphatidylserine induced by IONs, namely caused by Resovist® in human macrophages [132], dextran-coated Fe_3O_4 NPs in rat peripheral blood mononuclear cells [170], Fe_3O_4 NPs in human hepatoma BEL-7402 cells [221] and Fe_3O_4 NPs in PC12 cells [23], in human hepatoma BEL-7402 cells [221] and in Jurkat cells [222]. Besides that, some studies demonstrated that Fe_3O_4 NPs have the ability to enhance apoptosis induced by cancer drugs, namely daunorubicin in K562/A02 cells [224,230] and gambogic acid in K562 leukemia cells [225]. Although apoptosis may be beneficial for the killing of cancer cells and in the case of proliferative diseases, such as lymphoproliferative syndrome, IONs-triggered apoptosis also showed to trigger apoptosis in normal cells, which may be detrimental to the organism and harmful to the human health, given that it is known that excessive apoptosis is involved in various ischemia-associated injuries, autoimmune diseases and neurodegenerative diseases [231]. On the other hand, other IONs were not able to induce apoptosis as this was the case of PVA-coated Fe_3O_4 NPs in L929 cells [232], Feridex® in rat neural progenitor cells [166] and γ-Fe_2O_3 NPs in mouse bone marrow dendritic cells [233].

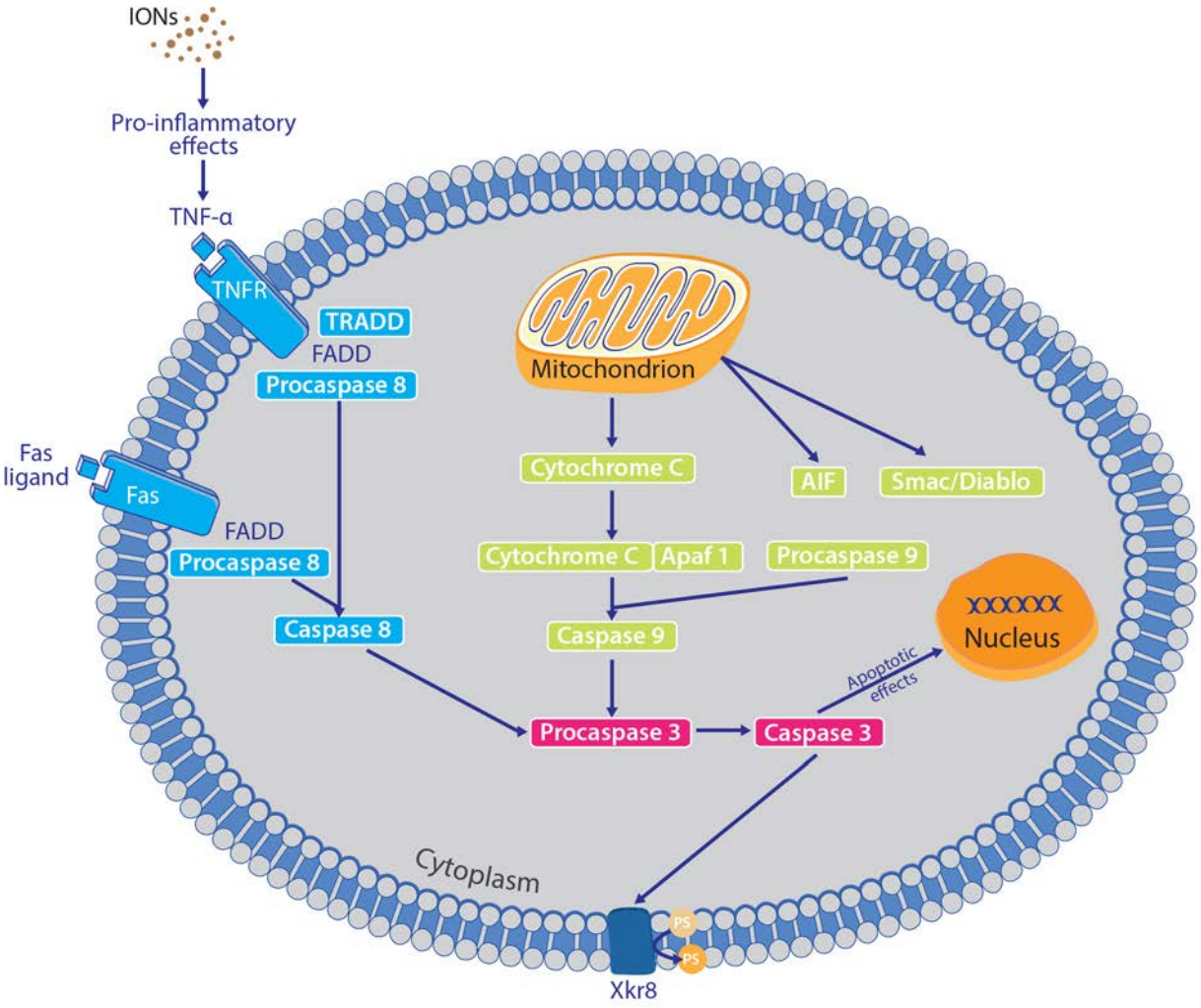

Figure 3. IONs influence on intrinsic and extrinsic apoptotic pathways (AIF: Apoptosis inducing factor; Apaf 1: Apoptotic protease-activating factor 1; FADD: Fas-associated death domain; IONs: Iron oxide nanoparticles; PS: Phosphatidylserine; TNF-α: Tumor necrosis factor α; TNFR: Tumor necrosis factor receptor; TRADD: Tumor necrosis factor receptor associated domain; Xkr8: Xk-receptor protein 8).

I.1.2.2.1. MITOCHONDRIA AND APOPTOTIC-RELATED PROTEINS

As mitochondria and the events that occur in this organelle are intimately linked to apoptosis, it is crucial to evaluate IONs effects in mitochondria. It was observed that Fe_2O_3 NPs and Fe_3O_4 NPs induced mitochondrial swelling, decrease or disappearance of

mitochondrial cristae and vacuolization in human aortic endothelial cells [99] and PLL-coated SPIONs markedly decreased the number of mitochondria and induced mitochondrial swelling in ASTC-a-1 cells [153]. A decrease in mitochondrial membrane potential is usually indicative of cellular apoptosis and has also been described for Fe_3O_4 NPs in A549 cells [32] and in human hepatoma BEL-7402 cells [221], for oleic acid-coated Fe_3O_4 NPs in human hepatoma BEL-7402 cells [221] and for and PLL and carboxydextran-coated Fe_2O_3 NPs in human endothelial cells [96].

IONs are also able to affect survival proteins. It was observed that phosphorylation of Akt, a pro-survival protein, was decreased in γ-Fe_2O_3 NPs exposure to human umbilical vein endothelial cells [101], as well as in Fe_2O_3 NPs exposure to murine hepatocytes [187]. This last author showed that quercetin, a natural antioxidant, was able to revert the decrease in Akt phosphorylation, which demonstrates that apoptosis triggered by IONs may be mediated by ROS [187]. Moreover, the up-regulation of the pro-apoptotic protein Bad triggered by these IONs was also reverted by quercetin [187]. Fe_3O_4 NPs increased the gambogic acid mediated downregulation of the expression of antiapoptotic genes such as Bcl-2 and survivin of K562 cells, whereas the pro-apoptotic protein bax was upregulated [225]. Fe_2O_3 NPs also showed to decrease the level of antiapoptotic protein Bcl-2 in murine hepatocytes, which resulted in mitochondrial membrane potential reduction [187]. Liu *et al* [23] reported also that Fe_3O_4 NPs induced an increase in the Bax/Bcl-2 ratio and a decrease in heat shock proteins 70 and 90 in PC12 cells. Kai *et al* [221] also reported that oleic acid-coated Fe_3O_4 NPs and Fe_3O_4 NPs decreased cytochrome c and increased Bax expression in human hepatoma BEL-7402 cells.

p53 can be also involved in apoptosis, given that its activation leads to the expression of Bax and Noxa, two pro-apoptotic proteins that induce an increase in mitochondrial permeability, leading to the release of cytochrome c, apoptosis inducing factor (AIF) and Diablo/Smac and the consequent mitochondrial apoptotic pathway [218]. Wu *et al* [164,234] reported that aminopropyltriethoxysilane-coated Fe_3O_4 NPs induced p53 gene expression and increased phosphorylation levels of p53 in PC12 cells, and that this activation is associated with increased levels of Bax and decreased levels of Bcl-2. Fe_3O_4 NPs also showed to increase the expression of p53 when in association with adriamycin and daunorubicin in Raji cells [235] and with daunorubicin in K562/A02 cells [224].

However, the opposite was also reported by Huang *et al* [236], reporting slight decreases in p53 expression in Ferucarbotran-labeled human mesenchymal stem cells, as well as it was also reported by Chen *et al* [224] that Fe_3O_4 NPs do not change the

expression of p53 messenger ribonucleic acid (mRNA) in K562/A02 cells. It is possible to conclude that the effect of IONs on p53 activation varies according to the cell which IONs interacts.

c-Jun-N-terminal kinase (JNK) plays a critical role in death receptor-initiated extrinsic- as well as mitochondrial intrinsic-apoptotic pathways. JNK activates apoptotic signaling by the upregulation of pro-apoptotic genes via the transactivation of specific transcription factors or by directly modulating the activities of mitochondrial pro- and anti-apoptotic proteins through distinct phosphorylation events [237]. It is reported that exposure of human macrophages to Resovist® [132] and of PC12 cells to aminopropyltriethoxysilane-coated Fe_3O_4 NPs [164] induces prolonged activation of JNK, leading to apoptosis.

I.1.2.3. GENOTOXICITY

Genotoxins are chemicals or agents that can cause DNA or chromosomal damage [238]. IONs have been extensively described to induce genotoxicity in several types of cells. The exact mechanisms of genotoxic effects of IONs are still unknown. It is suggested that the following factors can potentially affect genotoxicity of nanocarriers: composition, size, molecular weight, particle geometry, and surface charge [181]. This latter, for example, may influence not only the efficiency of SPIONs internalization, but also the route and speed of their intracellular degradation with the subsequent release of free iron and the choice of particular pathways leading to ROS generation and subsequent damage to biomolecules [65].

Genotoxicity can be also indirectly influenced by the interaction between IONs and the culture growth medium, which comprises an array of proteins, nutrients and growth factors. Both *in vitro* and *in vivo*, the IONs-protein corona is a complex transient in nature dependent of extracellular environment, as well as the physicochemical properties of the IONs themselves and the complexes formed between the protein and IONs [239].

Konczol *et al* [32] reported that Fe_3O_4 NPs induced DNA damage in human lung cancer A549 cells that was attenuated by the antioxidants N-acetyl-cysteine and butylated hydroxyanisole. Similarly, dextran-coated γ-Fe_2O_3 NPs induction of DNA damage in human B-lymphoblastoid MCL5 cells was diminished by N-acetylcysteine [239] and Alarifi *et al* [117] attributed the DNA damage triggered by Fe_2O_3 NPs in human breast MCF-7

cell line to the elevated ROS production. It is known that ROS interact with cellular biomolecules such as proteins, membrane lipids and even DNA which could be oxidized, destructured and ultimately became non-functional [33]. In fact, it is thought that the enhanced production of ROS caused by mitochondria or membrane-bound NADPH oxidases in response to their interaction with IONs might be a possible mechanism involved, causing damage to both purine and pyrimidine bases as well as the DNA backbone [32,240]. Moreover, iron ions released from IONs participate in Fenton reaction, originating $HO^{\bullet}$, which is highly reactive, leading to an increase in DNA damage, attacking a multitude of oxidized bases, namely DNA base guanine to form 8-hydroxy-2′-deoxyguanosine adducts, which are known to have mutagenic potential, abasic sites, single and double-strand breaks [33,77,239]. An example of this has been described by Ma *et al* [186]: Fe_3O_4 NPs increased 8-hydroxy-2′-deoxyguanosine adducts in mouse hepatic and renal tissues. RNS are also able to induce DNA damage: $^{\bullet}NO$ can react with $O_2^{\bullet-}$, producing $ONOO^-$, which in turn can generate other RNS to interact with proteins and nucleic acids [241].

The coating and the extent of uptake are described as exerting a determinant role concerning genotoxicity. Singh *et al* [239] stated that cellular internalization of IONs is positively correlated with the induction of genotoxicity. This author also showed that, while dextran-coated γ-Fe_2O_3 NPs induced DNA damage in human B-lymphoblastoid MCL5 cells, γ-Fe_2O_3 NPs, dextran-coated Fe_3O_4 NPs and Fe_3O_4 NPs did not exert the same effect [239]. Similarly, Hong *et al* [242] reported that, in mouse fibroblast adhesive cells (L929), (3-aminopropyl)trimethoxysilane-coated Fe_3O_4 NPs, tetraethyl orthosilicate-(3-aminopropyl)trimethoxysilane-coated Fe_3O_4 NPs and citrate-coated Fe_3O_4 NPs triggered DNA damage, while non-coated Fe_3O_4 NPs and tetraethyl orthosilicate-coated Fe_3O_4 NPs did not exert such effect. The fact that (3-aminopropyl)trimethoxysilane-coated Fe_3O_4 NPs and tetraethyl orthosilicate-(3-aminopropyl)trimethoxysilane-coated Fe_3O_4 NPs induce genotoxicity is probably due to the fact that these positively charged IONs are more concentrated within the cells and enter into the nucleus through the nuclear pore and interact directly with the DNA, which is negatively charged due to its phosphate groups [242]. Citrate-coated Fe_3O_4 NPs are shown to penetrate through nuclear membrane, generating highly reactive $HO^{\bullet}$ in close proximity to DNA, leading to DNA attack [242]. Chen *et al* [195] reported that both poly(L-lactide)–PEG–poly(L-lactide)-coated Fe_3O_4 NPs and Fe_3O_4 NPs increased micronuclei in Chinese Hamster Ovary (CHO-K1) cells, although this increase has been more pronounced in the case of Fe_3O_4 NPs. The authors defend that this polymer coating may reduce the DNA damage caused by the IONs,

affecting the physical presence and/or disturbance of the NPs around the mitotic apparatus [195]. Likewise, Magdolenova *et al* [61] found that oleate-coated Fe_3O_4 NPs induced DNA damage in human peripheral lymphocytes and TK6 lymphoblastoid cells but Fe_3O_4 NPs did not exerted the same effect. Nevertheless, the authors reported that oleate-coated Fe_3O_4 NPs exhibited lower cellular uptake than Fe_3O_4 NPs. This fact proves that augmented IONs internalization is not always synonym of increased genotoxicity. Coating of Fe_3O_4 NPs with oleate was found to change the genotoxic potential of the Fe_3O_4 NPs, probably by inducing changes in features of the IONs related to cellular uptake and binding to extracellular receptors or transmembrane channels [61]. Non-coated IONs have also demonstrated to be cytotoxic: Fe_2O_3 NPs induced DNA damage in human lung fibroblasts IMR-90 cells and human lung epithelial cells BEAS-2B [77,145]. Fe_3O_4 NPs induced DNA damage in human lung cancer A549 cells and human epithelial cell line A-431 [33,68]. In effect, the cells involved and the type of interactions between the cells and ION may be determinant for the genotoxicity.

Besides that, it is also known that genotoxicity may suffer interindividual variations. Novotna *et al* [65] reported that, although PLL-coated γ-Fe_2O_3 NPs, PLL-coated Endorem®, mannose-coated γ-Fe_2O_3 NPs, poly(N,N-dimethylacrylamide)-coated γ-Fe_2O_3 NPs and γ-Fe_2O_3 NPs have induced DNA damage in human bone marrow mesenchymal stromal cells of the two individuals studied, Endorem® only induced DNA damage in one of the individuals, demonstrating not to be genotoxic in the other individual tested.

I.1.2.4. PRO-INFLAMMATORY EFFECTS OF IRON OXIDE NANOPARTICLES

Many studies have been performed in the last few years to evaluate the impact and/or the effect of IONs on the different cells and animal models regarding inflammation [180,243,244]. The interaction between NPs and immune cells and the consequences of such interactions are relevant issues in addressing the potential impact of IONs on inflammatory processes [245]. It is important to remember that the cellular recruitment processes are mediated by a battery of proinflammatory cytokines, including interleukin (IL)-8, IL-6, tumor necrosis factor α (TNF-α), etc. that induce increased microvascular caliber, enhance vascular permeability, leukocyte recruitment, and release of inflammatory mediators (figure 1). This process is of relatively short duration, lasting from several minutes to a few days. However, when inflammation becomes chronic, it can result in tissue destruction and lead to organ dysfunction in pathological situations

[246,247]. IONs have been described as being involved in the different stages of the inflammatory process. Therefore, in this chapter, the effect of IONs on the most relevant inflammatory pathways, as well as in the cytokine production, is reviewed.

I.1.2.4.1. MITOGEN-ACTIVATED PROTEIN KINASE (MAPK) PATHWAY

MAPK signaling pathways relay, amplify and integrate signals from a diverse range of extracellular stimuli, thereby controlling the genomic and physiological response of a cell to changes in the environment. It is a critical link between cell surface signal transduction and nuclear processes, including cell proliferation, differentiation and migration, development, inflammatory response and apoptosis [248]. Mammalian cells express at least four distinctly regulated groups of MAPK, specifically extracellular signal-related kinases (ERK)-1/2, JNK1/2/3, p38 proteins (p38 α/β/γ/δ) and ERK5, which are activated by different MAPK kinases (MKK) [249].

Liu *et al* [90] reported that DMSA-coated Fe_3O_4 NPs activate several members of the MAPK family in RAW264.7 cells. DMSA-coated Fe_2O_3 NPs, however, decreased MAPK-14 (or p38α) expression in human aortic endothelial cells [98], showing the differential responses that may occur when different cells as well as different type of IONs are studied.

ERK1/2 are distributed throughout quiescent cells, but upon stimulation, a significant population of ERK1/2 accumulates in the nucleus. In fact, upon receptor activation, membrane-bound Ras recruits one of the Raf kinases into a complex where it becomes activated. Afterwards, Raf phosphorylates two serine residues on the kinase mitogen protein kinase kinase (MEK) 1 and 2, which in turn activate ERK1/2 by tandem phosphorylation of threonine and tyrosine residues on the dual-specificity motif. While the mechanisms involved in nuclear accumulation of ERK1/2 remain elusive, nuclear retention, dimerization, phosphorylation, and release from cytoplasmic anchors have been shown to play a role. Activated ERK1 and ERK2 phosphorylate numerous substrates in all cellular compartments, including several MKK [250,251]. Moreover, stimulation of inflammatory cells and ROS also triggers protein phosphorylation, where MKK are activated via phosphorylation by MKK kinases (MAPKKK), and these MKK, usually MKK 3 or 6, lead to phosphorylation of p38 MAPK and JNK [252]. JNK and p38 represent one

subgroup of MAPK that is activated primarily by cytokines and exposure to environmental stress. A major target of the these signaling pathways is the activation of the activator protein 1 (AP-1) transcription factor that is mediated, in part, by the phosphorylation of c-Jun and related molecules, such as activating transcription factor 2 (ATF-2) and c-Fos, resulting in the production and secretion of pro-inflammatory cytokines, such as IL-1β and TNF-α [248,252]. AP-1 levels were shown to be increased by dextran-coated Fe_3O_4 NPs in the JB6 P+ murine epidermal cell line [253]. Therefore, in this case and in the most of the cases above mentioned, a pro-inflammatory response is expected to be increased. It is also described that Resovist® significantly induced ERK1/2 and Akt phosphorilation in pancreatic β cells [254]. In fact, ERK1/2 are components of the mechanism by which glucose stimulates insulin gene expression, which is mediated by the activation of transcription factors (pancreatic and duodenal homeobox 1, neurogenic differentiation 1 and E47) [255]. It was also described that PEG-coated Fe_3O_4 NPs increased the phosphorylation of ERK1/2 in PC12 cells in the presence of nerve growth factor [165] and γ-Fe_2O_3 NPs and Fe_3O_4 NPs increased p-ERK levels in RAW 264.7 cells [48]. ERK1 is also essential for regulation of energy homeostasis together with p62 [256] and, for this reason Park *et al* [48] suggest that the increase in p-ERK triggered by γ-Fe_2O_3 NPs was activated for cell survival. Moreover, Resovist® and Supravist®-induced JNK activation in human macrophages was associated with an increase in apoptosis, given that it is known that JNK may lead to formation of the proapoptotic Bid protein [132]. Fe_3O_4 NPs was also shown to activate JNK in a ROS-independent manner in A549 cells [32], although Park *et al* [48] reported that γ-Fe_2O_3 NPs and Fe_3O_4 NPs decrease the levels of p-JNK in RAW 264.7 cells.

I.1.2.4.2. NUCLEAR FACTOR kB (NF-kB) SIGNALING PATHWAY

NF-kB is a pivotal mediator, which is involved in multiple cellular responses. This transcription factor could be activated by a variety of stimuli, including cytokines and ROS, and regulates the transcription of various pro- and inflammatory mediators, namely cytokines (IL-1β, TNF-α, and IL-6), chemokines [IL-8 and macrophage inflammatory protein 2 (MIP-2)], adhesion molecules [vascular cell adhesion molecule 1 (VCAM-1), intercellular adhesion molecule 1 (ICAM-1), and E-selectin], and enzymes [inducible nitric oxide synthase (iNOS)] [32,257,258]. In unstimulated cells, NF-kB is retained in the cytosol by inhibitor of kB (IkB). Stimulation with TNF-α or foreign agents leads to

degradation of IkB which then dissociates from NF-kB enabling it to translocate to the nucleus where it exerts its transcriptional function, increasing the transcription of several cytokines, such as TNF-α, IL-1, IL-6 and IL-8 [32,259]. Zhou *et al* [150] reported a slight increase in NF-kB-DNA binding activity caused by Fe_2O_3 NPs in rat lung. However, Fe_3O_4 NPs did not trigger any alteration on NF-kB activity in rat primary microglia [92], human lung cancer A549 cells [32], occurring a decrease and delay in the IkB degradation in the latter. Therefore, in most of the cases above mentioned, NF-kB does not seem to be an inflammatory pathway largely activated by IONs, as it occurred for MAPK pathways. Consequently, cytokine production triggered by IONs seems to be due to the involvement of other pathways, namely MAPK pathways.

I.1.2.4.3. CYTOKINES

Cytokines are a group of soluble proteins, peptides or glycoproteins regulators of host responses to infection, immune responses, inflammation, and trauma. There are several cytokines that are produced in our organism in the events above mentioned, namely human TNF-α, interferon γ (IFN-γ), IL-1, IL-6, among others [260]. Cytokines may be produced via regulation of transcription factors, namely NF-kB and MAPK pathways as well as due to monocyte/macrophage activation in response to microbial products, which gives rise to the activation of T-cell immunity. Classical activation of macrophages, defined as macrophages subset 1 (M1) activation, may promote the differentiation of T-helper lymphocytes 1 (Th1) cells, whereas macrophages subset 2 (M2) activation could promote T-helper lymphocytes 2 (Th2)-type responses. In both types of responses, there is cytokine production. M1 activation is activated by IFN-γ and characterized by elevated phagocytic ability to kill pathogens, microorganism and tumour cells, elevated expression of major histocompatibility complex (MHC) class II, generation of ROS, and production of the Th1 cytokines, such as IL-12 and TNF-α. M2 macrophages activation down-regulates Th1 responses and stimulates Th2 responses, with production of Th2 cytokines such as IL-4 and IL-6, scavenge debris, and promote angiogenesis, tissue remodelling and repair [261,262].

TNF-α, a pro-inflammatory cytokine, is synthesized and secreted by several types of cells, but especially by macrophages. TNF-α mediates a wide range of biological responses including inflammation, infection, injury, and apoptosis and has a strong anti-tumor effect, markedly inhibiting tumor growth by inducing tumor cell necrosis [263,264].

This cytokine is also involved in IL-6 as well as IL-8 production, being this latter the most potent known chemotactic agent for neutrophils [260,265,266]. Several IONs showed to activate TNF-α, namely Fe_3O_4 NPs in mouse BALF [267] and Resovist® in THP-1 cell line [268].

IFN-γ is a type-II IFN secreted by several immune cells (dendritic cells, Th1, T cells, and natural killer) with anti-viral, anti-tumor, and immunoregulatory effects that can be exerted at several levels. IFN-γ regulates class I and II antigen presentation through the expression of key genes related to MHC class I and II-dependent antigen-presentation [269]. IONs showed to increase this cytokine, namely Fe_3O_4 NPs in mouse peripheral blood [244] and Fe_2O_3 NPs in mouse BALF [270].

IL-1 activates a cascade of cytokine production and induces the production of a broad range of immunomodulatory cytokines. IL-6 is among the mediators regulated by IL-1 and is frequently increased in inflammatory processes [260,271]. In fact, some IONs have shown to activate IL-1β, as it is the case of DMSA-coated Fe_2O_3 NPs in rat sciatic nerve [223], Fe_3O_4 NPs in mouse BALF [267] and citrate-coated γ-Fe_2O_3 NPs in human gingival fibroblasts [272] and also IL-6, as it is the case of dextran-coated Fe_3O_4 NPs in human epidermal keratinocytes [253] and Fe_2O_3 NPs in mouse BALF [270], which demonstrates IONs involvement in pro-inflammatory responses. However, IL-1β may be involved in other mechanisms. In effect, IL-1β released by microglia induces the proliferation of astrocytes, stimulates neovascularization and promotes repair of the central nervous system in brain injury. Wu *et al* [169] showed that Resovist® attenuated IL-1β production in murine microglial cells by suppressing the secretory lysosomal functionality in LPS-stimulated microglia through cathepsin B activity attenuation, which may indicate that IONs promote brain injury.

Transforming growth factor beta (TGF-β) is a large family of cytokines that includes activins, inhibins, bone morphogenetic proteins and nodal and growth differentiation factors. These ligands of the TGF-β signaling pathways bind to a diversity of cell-surface receptors and cause signal transduction through the SMADs [273,274]. TGF-β1 is the most important mediator that influences collagen synthesis and other matrix molecules, activating the gene transcription of collagens I, III, IV, VI, and VII, proteoglycans and matrix metalloproteinases [272,275]. TGF-β activation has been triggered by Fe_3O_4 NPs in mouse BALF [267].

IL-10, as well as IL-4, is a cytokine considered to have an anti-inflammatory role. IL-10 antagonizes a subset of genes activated by Toll-like receptors signaling, such as TNF-α, IL-6, and numerous chemokine mRNA [276]. In fact, some IONs were shown to induce IL-10, inhibiting inflammatory cytokines such IL-1β, IL-6 and IFN-γ. Blank *et al* [277] reported that PVA-coated SPIONs triggered a decrease in IL-1β, IL-6, TNF-α and IFN-γ and increase in IL-10 levels in human monocyte-derived dendritic cells in the presence of LPS and tetanus toxoid [277].

The influence of IONs in cytokine production has been described in other different cell types [95,108,125,278,279]. The studies performed so far indicate that IONs may have several effects on cytokine production, depending on the several factors. In fact, it is known that IONs can modulate cytokine profile and this modulation may be the result of distinct mechanisms of IONs uptake by the cells. Once inside the cell, the fate of the IONs in terms of subcellular location/translocation is different depending on the IONs and on the cell. Consequently, the interactions established between the IONs and the receptors and/or the cellular machinery are different, depending on many factors such as surface charge, coating, type of IONs, among other factors. All these factors may lead to immune-suppression or immune-stimulation, modifying the mode how the antigen is handled in cells [277,280]. The animal model used may also influence the results obtained, determining the regulation of cytokine expression. Siglienti *et al* [281] reported that, in mouse macrophages, Resovist® and SH U 555C (carboxydextran-coated USPIONs) increased IL-10 levels, while in rat macrophages, the same IONs decreased IL-10 and TNF-α levels.

I.1.2.4.4. ION-INDUCED ACTIVATION OF MACROPHAGES AND T CELLS

In inflammation, the major role of monocytes/macrophages is to recognize and eliminate foreign material. For this purpose, they have three major functions: antigen presentation, phagocytosis, and immunomodulation through production of various cytokines and growth factors [89,247]. It is known that NPs in biological fluids and tissues, as other foreign agents, are frequently covered with biological molecules, namely proteins that can facilitate their interaction with monocytes/macrophages, as well as their degradation and clearance from the bloodstream [282,283]. For example, Valois *et al* [282] clearly demonstrated an uptake of DMSA-coated Fe_2O_3 NPs by

monocyte/macrophage cells, indicating that this may be a mechanism of NP clearance used by the lung in order to avoid further damage. It is described that IONs have the potential to modify monocytes' ability to respond to other activating stimuli, as well as to alter monocytes' activity, namely in the recruitment, adhesion and migration into the subendothelial layer of the intima, representing a considerable risk factor for promoting early events in the development of atherosclerosis [99].

T lymphocytes include three major functional subsets: T-helper lymphocytes, T-suppresser lymphocytes, and T-cytotoxic lymphocytes [243]. The immune response depends on the balance of cytokines produced by two Th cell subsets, Th1 and Th2. Th1 cells secrete Th1 cytokines such as IL-2 and INF-γ, promote cytotoxic and inflammatory functions by activating macrophages, natural killer cells and cytotoxic $CD8^+$ T lymphocytes. Th2 cells secrete Th2 cytokines such as IL-4, IL-6 and IL-10, which can trigger the humoral immune mechanism, including antibody production and eosinophil proliferation [284].

There are several studies concerning the role of IONs on T cell activation. In fact, it has been described that magnetic IONs have the ability to generate a significant number of exosomes in the alveolar region of mice. In turn, the immune activation in splenic T cells is simultaneously induced [285]. Fe_3O_4 NPs were shown to increase $CD8^+$ T cells activation and decrease CD4+ T cells activation [267].

When mixed lymphocyte reaction was evaluated, Endorem® revealed an inability to interfere with the dendritic cells activation of the $CD8^+$ T cells [110], $CD4^+$ T cells [286] and protamine sulphate-coated Feridex IV® showed an inability to interfere with the THP-1 cells activation of the $CD4^+$ T cells [287]. However, Pawelczyk *et al* [288] observed, performing the same experiment, suppression of bone marrow stromal cells activation of alloreactive T-cells by protamine sulphate-coated Feridex IV®. Here, the different type of cell may have contributed for the different results.

It was described, by Zhu *et al* [285], that, in ovalbumin-sensitized rats, magnetic IONs have the ability to increase the percentages of Th1 and T-cytotoxic lymphocytes 1, decreasing at the same time the percentages of Th2 and T-cytotoxic lymphocytes 2, which suggest that magnetic IONs are able to skew the immune response toward Th1 responses. Other authors reported that Fe_3O_4 NPs increase Th1 immunity in a greater extent than they increase Th2 immunity [244]. In accordance, Ban *et al* [289] reported that Fe_2O_3 NPs inhibited the ovalbumin-induced Th2 response in mice. Zhu *et al* [261]

reported that IONs-induced exosomes triggered classical peritoneal macrophages activation to M1. Laskar *et al* [278] also reported that Resovist® induces a phenotypic shift of THP1 M2 macrophages towards M1 subtype. Shen *et al* [245], however, showed that Resovist® has a decreasing effect in the ovalbumin-induced production of immunoglobulin G1 and immunoglobulin G2a in mice, which demonstrates the suppressing effect of this IONs on Th2 and Th1 cell type responses, respectively, *in vivo*. The fact that the exposure times were different between this study and other *in vivo* mentioned studies may be the reason for this difference. However, further studies would be necessary to elucidate this question, namely studying the influence of IONs in ovalbumin-induced inflammatory responses at different time points under the same conditions.

I.1.2.5. REFERENCES

[1] Serkova NJ, Renner B, Larsen BA, Stoldt CR, Hasebroock KM, Bradshaw-Pierce EL, et al. Renal inflammation: targeted iron oxide nanoparticles for molecular MR imaging in mice. Radiology 2010;255(2):517-26.

[2] Lim YT, Noh YW, Han JH, Cai QY, Yoon KH, Chung BH. Biocompatible polymer-nanoparticle-based bimodal imaging contrast agents for the labeling and tracking of dendritic cells. Small 2008;4(10):1640-5.

[3] Pareta RA, Taylor E, Webster TJ. Increased osteoblast density in the presence of novel calcium phosphate coated magnetic nanoparticles. Nanotechnology 2008;19(26):265101.

[4] Taylor EN, Webster TJ. The use of superparamagnetic nanoparticles for prosthetic biofilm prevention. Int J Nanomed 2009;4:145-52.

[5] Allard-Vannier E, Cohen-Jonathan S, Gautier J, Herve-Aubert K, Munnier E, Souce M, et al. Pegylated magnetic nanocarriers for doxorubicin delivery: A quantitative determination of stealthiness *in vitro* and *in vivo*. Eur J Pharm Biopharm 2012;81:498-505.

[6] Chen JP, Yang PC, Ma YH, Tu SJ, Lu YJ. Targeted delivery of tissue plasminogen activator by binding to silica-coated magnetic nanoparticle. Int J Nanomed 2012;7:5137-49.

[7] Ito A, Honda H, Kobayashi T. Cancer immunotherapy based on intracellular hyperthermia using magnetite nanoparticles: a novel concept of "heat-controlled necrosis" with heat shock protein expression. Cancer Immunol Immun 2006;55(3):320-8.

[8] Silva AC, Oliveira TR, Mamani JB, Malheiros SM, Malavolta L, Pavon LF, et al. Application of hyperthermia induced by superparamagnetic iron oxide nanoparticles in glioma treatment. Int J Nanomed 2011;6:591-603.

[9] Prijic S, Scancar J, Romih R, Cemazar M, Bregar VB, Znidarsic A, et al. Increased cellular uptake of biocompatible superparamagnetic iron oxide nanoparticles into malignant cells by an external magnetic field. J Membrane Biol 2010;236(1):167-79.

[10] Shi Y, Zhou L, Wang R, Pang Y, Xiao W, Li H, et al. *In situ* preparation of magnetic nonviral gene vectors and magnetofection *in vitro*. Nanotechnology 2010;21(11):115103.

[11] Schlachter EK, Widmer HR, Bregy A, Lonnfors-Weitzel T, Vajtai I, Corazza N, et al. Metabolic pathway and distribution of superparamagnetic iron oxide nanoparticles: *in vivo* study. Int J Nanomed 2011;6:1793-800.

[12] Hu K, Dou J, Yu F, He X, Yuan X, Wang Y, et al. An ocular mucosal administration of nanoparticles containing DNA vaccine pRSC-gD-IL-21 confers protection against mucosal challenge with herpes simplex virus type 1 in mice. Vaccine 2011;29(7):1455-62.

[13] Liu Y, Yu F. Substrate-specific modifications on magnetic iron oxide nanoparticles as an artificial peroxidase for improving sensitivity in glucose detection. Nanotechnology 2011;22(14):145704.

[14] Gao L, Zhuang J, Nie L, Zhang J, Zhang Y, Gu N, et al. Intrinsic peroxidase-like activity of ferromagnetic nanoparticles. Nat Nanotechnol 2007;2(9):577-83.

[15] Shubayev VI, Pisanic TR, 2nd, Jin S. Magnetic nanoparticles for theragnostics. Adv Drug Deliver Rev 2009;61(6):467-77.

[16] Oberdorster G, Oberdorster E, Oberdorster J. Nanotoxicology: An emerging discipline evolving from studies of ultrafine particles. Environ Health Persp 2005;113(7):823-39.

[17] Soenen SJ, De Cuyper M. How to assess cytotoxicity of (iron oxide-based) nanoparticles. A technical note using cationic magnetoliposomes. Contrast Media Mol I 2011;6(3):153-64.

[18] Lynch I, Dawson KA. Protein-nanoparticle interactions. Nano Today 2008;3(1-2):40-47.

[19] Rivet CJ, Yuan Y, Borca-Tasciuc DA, Gilbert RJ. Altering iron oxide nanoparticle surface properties induce cortical neuron cytotoxicity. Chem Res Toxicol 2012;25(1):153-61.

[20] Singh N, Jenkins GJ, Asadi R, Doak SH. Potential toxicity of superparamagnetic iron oxide nanoparticles (SPION). Nano Rev 2010;1:5358.

[21] Zhang W, Kalive M, Capco DG, Chen Y. Adsorption of hematite nanoparticles onto Caco-2 cells and the cellular impairments: effect of particle size. Nanotechnology 2010;21(35):355103.

[22] Frohlich E. Cellular targets and mechanisms in the cytotoxic action of non-biodegradable engineered nanoparticles. Curr Drug Metab 2013;14(9):976-88.

[23] Liu Y, Li X, Bao S, Lu Z, Li Q, Li CM. Plastic protein microarray to investigate the molecular pathways of magnetic nanoparticle-induced nanotoxicity. Nanotechnology 2013;24(17):175501.

[24] Lunov O, Syrovets T, Rocker C, Tron K, Nienhaus GU, Rasche V, et al. Lysosomal degradation of the carboxydextran shell of coated superparamagnetic iron oxide nanoparticles and the fate of professional phagocytes. Biomaterials 2010;31(34):9015-22.

[25] Weinberg ED. Iron loading and disease surveillance. Emerg Infect Dis 1999;5(3):346-52.

[26] Aranda A, Sequedo L, Tolosa L, Quintas G, Burello E, Castell JV, et al. Dichloro-dihydro-fluorescein diacetate (DCFH-DA) assay: A quantitative method for oxidative stress assessment of nanoparticle-treated cells. Toxicol Vitro 2013;27(2):954-63.

[27] Radu M, Munteanu MC, Petrache S, Serban AI, Dinu D, Hermenean A, et al. Depletion of intracellular glutathione and increased lipid peroxidation mediate cytotoxicity of hematite nanoparticles in MRC-5 cells. Acta Biochim Pol 2010;57(3):355-60.

[28] Klotz LO, Sies H. Cellular generation of oxidants: relation to oxidative stress. In: C. Jacob and P. G. Winyard. Redox signaling and regulation in biology and medicine. Weinheim: Wiley-VCH Verlag GmbH; 2009. p. 57-60.

[29] Soenen SJ, De Cuyper M. Assessing cytotoxicity of (iron oxide-based) nanoparticles: an overview of different methods exemplified with cationic magnetoliposomes. Contrast Media Mol I 2009;4(5):207-19.

[30] Fahmy B, Cormier SA. Copper oxide nanoparticles induce oxidative stress and cytotoxicity in airway epithelial cells. Toxicol Vitro 2009;23(7):1365-71.

[31] de Chickera SN, Snir J, Willert C, Rohani R, Foley R, Foster PJ, et al. Labelling dendritic cells with SPIO has implications for their subsequent *in vivo* migration as assessed with cellular MRI. Contrast Media Mol I 2011;6(4):314-27.

[32] Konczol M, Ebeling S, Goldenberg E, Treude F, Gminski R, Giere R, et al. Cytotoxicity and genotoxicity of size-fractionated iron oxide (magnetite) in A549 human lung epithelial cells: Role of ROS, JNK, and NF-kB. Chem Res Toxicol 2011;24(9):1460-75.

[33] Ahamed M, Alhadlaq HA, Alam J, Khan MA, Ali D, Alarafi S. Iron oxide nanoparticle-induced oxidative stress and genotoxicity in human skin epithelial and lung epithelial cell lines. Curr Pharm Des 2013;19(37):6681-90.

[34] Guadagnini R, Moreau K, Hussain S, Marano F, Boland S. Toxicity evaluation of engineered nanoparticles for medical applications using pulmonary epithelial cells. Nanotoxicology 2013;1-8.

[35] Freitas M, Lima JL, Fernandes E. Optical probes for detection and quantification of neutrophils' oxidative burst. A review. Anal Chim Acta 2009;649(1):8-23.

[36] Chen Z, Yin JJ, Zhou YT, Zhang Y, Song L, Song M, et al. Dual enzyme-like activities of iron oxide nanoparticles and their implication for diminishing cytotoxicity. ACS Nano 2012;6(5):4001-12.

[37] Yu M, Huang S, Yu KJ, Clyne AM. Dextran and polymer polyethylene glycol (PEG) coating reduce both 5 and 30 nm iron oxide nanoparticle cytotoxicity in 2D and 3D cell culture. Int J Mol Sci 2012;13(5):5554-70.

[38] Smythe E, Ayscough KR. Actin regulation in endocytosis. J Cell Sci 2006;119(22):4589-98.

[39] Pisanic TR, 2nd, Blackwell JD, Shubayev VI, Finones RR, Jin S. Nanotoxicity of iron oxide nanoparticle internalization in growing neurons. Biomaterials 2007;28(16):2572-81.

[40] Miller IS, Lynch I, Dowling D, Dawson KA, Gallagher WM. Surface-induced cell signaling events control actin rearrangements and motility. J Biomed Mater Res A 2010;93A(2):493-504.

[41] Buyukhatipoglu K, Clyne AM. Superparamagnetic iron oxide nanoparticles change endothelial cell morphology and mechanics via reactive oxygen species formation. J Biomed Mater Res A 2011;96(1):186-95.

[42] Soenen SJ, Nuytten N, De Meyer SF, De Smedt SC, De Cuyper M. High intracellular iron oxide nanoparticle concentrations affect cellular cytoskeleton and focal adhesion kinase-mediated signaling. Small 2010;6(7):832-42.

[43] Soenen SJ, Himmelreich U, Nuytten N, De Cuyper M. Cytotoxic effects of iron oxide nanoparticles and implications for safety in cell labelling. Biomaterials 2011;32(1):195-205.

[44] Andreas K, Georgieva R, Ladwig M, Mueller S, Notter M, Sittinger M, et al. Highly efficient magnetic stem cell labeling with citrate-coated superparamagnetic iron oxide nanoparticles for MRI tracking. Biomaterials 2012;33(18):4515-25.

[45] Wu X, Tan Y, Mao H, Zhang M. Toxic effects of iron oxide nanoparticles on human umbilical vein endothelial cells. Int J Nanomed 2010;5:385-99.

[46] Gupta AK, Gupta M. Cytotoxicity suppression and cellular uptake enhancement of surface modified magnetic nanoparticles. Biomaterials 2005;26(13):1565-73.
[47] Apopa PL, Qian Y, Shao R, Guo NL, Schwegler-Berry D, Pacurari M, et al. Iron oxide nanoparticles induce human microvascular endothelial cell permeability through reactive oxygen species production and microtubule remodeling. Part Fibre Toxicol 2009;6:1.
[48] Park EJ, Umh HN, Kim SW, Cho MH, Kim JH, Kim Y. ERK pathway is activated in bare-FeNPs-induced autophagy. Arch Toxicol 2014;88(2):323-36.
[49] Kumari M, Rajak S, Singh SP, Murty US, Mahboob M, Grover P, et al. Biochemical alterations induced by acute oral doses of iron oxide nanoparticles in Wistar rats. Drug Chem Toxicol 2013;36(3):296-305.
[50] Horie M, Nishio K, Fujita K, Endoh S, Miyauchi A, Saito Y, et al. Protein adsorption of ultrafine metal oxide and its influence on cytotoxicity toward cultured cells. Chem Res Toxicol 2009;22(3):543-53.
[51] Sun J, Wang S, Zhao D, Hun FH, Weng L, Liu H. Cytotoxicity, permeability, and inflammation of metal oxide nanoparticles in human cardiac microvascular endothelial cells: cytotoxicity, permeability, and inflammation of metal oxide nanoparticles. Cell Biol Toxicol 2011;27(5):333-42.
[52] Ying E, Hwang HM. *In vitro* evaluation of the cytotoxicity of iron oxide nanoparticles with different coatings and different sizes in A3 human T lymphocytes. Sci Total Environ 2010;408(20):4475-81.
[53] Garden OA, Reynolds PR, Yates J, Larkman DJ, Marelli-Berg FM, Haskard DO, et al. A rapid method for labelling $CD4^+$ T cells with ultrasmall paramagnetic iron oxide nanoparticles for magnetic resonance imaging that preserves proliferative, regulatory and migratory behaviour *in vitro*. J Immunol Methods 2006;314(1-2):123-33.
[54] Khandhar AP, Ferguson RM, Simon JA, Krishnan KM. Tailored magnetic nanoparticles for optimizing magnetic fluid hyperthermia. J Biomed Mater Res A 2012;100(3):728-37.
[55] Silva AK, Wilhelm C, Kolosnjaj-Tabi J, Luciani N, Gazeau F. Cellular transfer of magnetic nanoparticles via cell microvesicles: Impact on cell tracking by magnetic resonance imaging. Pharm Res 2012;29(5):1392-403.
[56] Kim HS, Oh SY, Joo HJ, Son KR, Song IC, Moon WK. The effects of clinically used MRI contrast agents on the biological properties of human mesenchymal stem cells. NMR Biomed 2010;23(5):514-22.
[57] Jasmin, Torres AL, Nunes HM, Passipieri JA, Jelicks LA, Gasparetto EL, et al. Optimized labeling of bone marrow mesenchymal cells with superparamagnetic iron oxide

nanoparticles and *in vivo* visualization by magnetic resonance imaging. J Nanobiotechnology 2011;9:4.

[58] Nkansah MK, Thakral D, Shapiro EM. Magnetic poly(lactide-co-glycolide) and cellulose particles for MRI-based cell tracking. Magn Reson Med 2011;65(6):1776-85.

[59] Cao B, Qiu P, Mao C. Mesoporous iron oxide nanoparticles prepared by polyacrylic acid etching and their application in gene delivery to mesenchymal stem cells. Microsc Res Techniq 2013;76(9):936-41.

[60] Laurent S, Burtea C, Thirifays C, Hafeli UO, Mahmoudi M. Crucial ignored parameters on nanotoxicology: the importance of toxicity assay modifications and "cell vision". PLoS One 2012;7(1):e29997.

[61] Magdolenova Z, Drlickova M, Henjum K, Runden-Pran E, Tulinska J, Bilanicova D, et al. Coating-dependent induction of cytotoxicity and genotoxicity of iron oxide nanoparticles. Nanotoxicology 2013;1-13.

[62] Zhu XM, Wang YX, Leung KC, Lee SF, Zhao F, Wang DW, et al. Enhanced cellular uptake of aminosilane-coated superparamagnetic iron oxide nanoparticles in mammalian cell lines. Int J Nanomed 2012;7:953-64.

[63] Hoshino A, Fujioka K, Oku T, Suga M, Sasaki YF, Ohta T, et al. Physicochemical properties and cellular toxicity of nanocrystal quantum dots depend on their surface modification. Nano Lett 2004;4(11):2163-69.

[64] Shen M, Cai H, Wang X, Cao X, Li K, Wang SH, et al. Facile one-pot preparation, surface functionalization, and toxicity assay of APTS-coated iron oxide nanoparticles. Nanotechnology 2012;23(10):105601.

[65] Novotna B, Jendelova P, Kapcalova M, Rossner P, Jr., Turnovcova K, Bagryantseva Y, et al. Oxidative damage to biological macromolecules in human bone marrow mesenchymal stromal cells labeled with various types of iron oxide nanoparticles. Toxicol Lett 2012;210(1):53-63.

[66] Fan C, Gao W, Chen Z, Fan H, Li M, Deng F. Tumor selectivity of stealth multi-functionalized superparamagnetic iron oxide nanoparticles. Int J Pharm 2011;404(1-2):180-90.

[67] Issa B, Obaidat IM, Albiss BA, Haik Y. Magnetic nanoparticles: Surface effects and properties related to biomedicine applications. Int J Mol Sci 2013;14(11):21266-305.

[68] Karlsson HL, Cronholm P, Gustafsson J, Moller L. Copper oxide nanoparticles are highly toxic: A comparison between metal oxide nanoparticles and carbon nanotubes. Chem Res Toxicol 2008;21(9):1726-32.

[69] Park EJ, Umh HN, Choi DH, Cho MH, Choi W, Kim SW, et al. Magnetite- and maghemite-induced different toxicity in murine alveolar macrophage cells. Arch Toxicol 2014;88(8):1607-18.

[70] Freyria FS, Bonelli B, Tomatis M, Ghiazza M, Gazzano E, Ghigo D, et al. Hematite nanoparticles larger than 90 nm show no sign of toxicity in terms of lactate dehydrogenase release, nitric oxide generation, apoptosis, and comet assay in murine alveolar macrophages and human lung epithelial cells. Chem Res Toxicol 2012;25(4):850-61.

[71] Perez-Benito JF. Iron(III)-hydrogen peroxide reaction: Kinetic evidence of a hydroxyl-mediated chain mechanism. J Phys Chem A 2004;108(22):4853-58.

[72] Brunner TJ, Wick P, Manser P, Spohn P, Grass RN, Limbach LK, et al. *In vitro* cytotoxicity of oxide nanoparticles: Comparison to asbestos, silica, and the effect of particle solubility. Environ Sci Technol 2006;40(14):4374-81.

[73] Skotland T, Sontum PC, Oulie I. *In vitro* stability analyses as a model for metabolism of ferromagnetic particles (Clariscan^{TM}), a contrast agent for magnetic resonance imaging. J Pharmaceut Biomed 2002;28(2):323-29.

[74] Harush-Frenkel O, Rozentur E, Benita S, Altschuler Y. Surface charge of nanoparticles determines their endocytic and transcytotic pathway in polarized MDCK cells. Biomacromolecules 2008;9(2):435-43.

[75] Calmon MF, de Souza AT, Candido NM, Raposo MI, Taboga S, Rahal P, et al. A systematic study of transfection efficiency and cytotoxicity in HeLa cells using iron oxide nanoparticles prepared with organic and inorganic bases. Colloids Surf B Biointerfaces 2012;100:177-84.

[76] Teeguarden JG, Hinderliter PM, Orr G, Thrall BD, Pounds JG. Particokinetics *in vitro*: Dosimetry considerations for *in vitro* nanoparticle toxicity assessments. Toxicol Sci 2007;95(2):300-12.

[77] Bhattacharya K, Hoffmann E, Schins RF, Boertz J, Prantl EM, Alink GM, et al. Comparison of micro- and nanoscale Fe^{+3}-containing (hematite) particles for their toxicological properties in human lung cells *in vitro*. Toxicol Sci 2012;126(1):173-82.

[78] Saptarshi SR, Duschl A, Lopata AL. Interaction of nanoparticles with proteins: relation to bio-reactivity of the nanoparticle. J Nanobiotechnology 2013;11:26.

[79] Simberg D, Park JH, Karmali PP, Zhang WM, Merkulov S, McCrae K, et al. Differential proteomics analysis of the surface heterogeneity of dextran iron oxide nanoparticles and the implications for their *in vivo* clearance. Biomaterials 2009;30(23-24):3926-33.

[80] Kalive M, Zhang W, Chen Y, Capco DG. Human intestinal epithelial cells exhibit a cellular response indicating a potential toxicity upon exposure to hematite nanoparticles. Cell Biol Toxicol 2012;28(5):343-68.

[81] Bellova A, Bystrenova E, Koneracka M, Kopcansky P, Valle F, Tomasovicova N, et al. Effect of Fe_3O_4 magnetic nanoparticles on lysozyme amyloid aggregation. Nanotechnology 2010;21(6):065103.

[82] Ankamwar B, Lai TC, Huang JH, Liu RS, Hsiao M, Chen CH, et al. Biocompatibility of Fe_3O_4 nanoparticles evaluated by *in vitro* cytotoxicity assays using normal, glia and breast cancer cells. Nanotechnology 2010;21(7):75102.

[83] Faust JJ, Zhang W, Chen Y, Capco DG. Alpha-Fe_2O_3 elicits diameter-dependent effects during exposure to an *in vitro* model of the human placenta. Cell Biol Toxicol 2014;30(1):31-53.

[84] Yin H, Too HP, Chow GM. The effects of particle size and surface coating on the cytotoxicity of nickel ferrite. Biomaterials 2005;26(29):5818-26.

[85] Di Virgilio AL, Reigosa M, Arnal PM, de Mele MFL. Comparative study of the cytotoxic and genotoxic effects of titanium oxide and aluminium oxide nanoparticles in Chinese hamster ovary (CHO-K1) cells. J Hazard Mater 2010;177(1-3):711-18.

[86] Lachance B, Hamzeh M, Sunahara GI. Environmental fate and ecotoxicology of nanomaterials. In: I. Malsch and C. Emond. Nanotechnology and human health. Florida: CRC Press Taylor & Francis Group; 2014. p. 196.

[87] Weinstein JS, Varallyay CG, Dosa E, Gahramanov S, Hamilton B, Rooney WD, et al. Superparamagnetic iron oxide nanoparticles: diagnostic magnetic resonance imaging and potential therapeutic applications in neurooncology and central nervous system inflammatory pathologies, a review. J Cerebr Blood F Met 2010;30(1):15-35.

[88] Barry SE. Challenges in the development of magnetic particles for therapeutic applications. Int J Hyperther 2008;24(6):451-66.

[89] Pfaller T, Colognato R, Nelissen I, Favilli F, Casals E, Ooms D, et al. The suitability of different cellular *in vitro* immunotoxicity and genotoxicity methods for the analysis of nanoparticle-induced events. Nanotoxicology 2010;4(1):52-72.

[90] Liu Y, Chen Z, Gu N, Wang J. Effects of DMSA-coated Fe_3O_4 magnetic nanoparticles on global gene expression of mouse macrophage RAW264.7 cells. Toxicol Lett 2011;205(2):130-9.

[91] Liu YX, Chen ZP, Wang JK. Systematic evaluation of biocompatibility of magnetic Fe_3O_4 nanoparticles with six different mammalian cell lines. J Nanopart Res 2011;13(1):199-212.

[92] Xue Y, Wu J, Sun J. Four types of inorganic nanoparticles stimulate the inflammatory reaction in brain microglia and damage neurons *in vitro*. Toxicol Lett 2012;214(2):91-8.
[93] Baratli Y, Charles AL, Wolff V, Ben Tahar L, Smiri L, Bouitbir J, et al. Age modulates Fe_3O_4 nanoparticles liver toxicity: dose-dependent decrease in mitochondrial respiratory chain complexes activities and coupling in middle-aged as compared to young rats. Biomed Res Int 2014;2014:474081.
[94] Fariss MW, Chan CB, Patel M, Van Houten B, Orrenius S. Role of mitochondria in toxic oxidative stress. Mol Interv 2005;5(2):94-111.
[95] Srinivas A, Rao PJ, Selvam G, Goparaju A, Murthy PB, Reddy PN. Oxidative stress and inflammatory responses of rat following acute inhalation exposure to iron oxide nanoparticles. Hum Exp Toxicol 2012;31(11):1113-31.
[96] Yang FY, Yu MX, Zhou Q, Chen WL, Gao P, Huang Z. Effects of iron oxide nanoparticle labeling on human endothelial cells. Cell Transplant 2012;21(9):1805-20.
[97] Zhou Q, Yang KR, Gao P, Chen WL, Yang DY, Liang MJ, et al. An experimental study on MR imaging of atherosclerotic plaque with SPIO marked endothelial cells in a rabbit model. J Magn Reson Imaging 2011;34(6):1325-32.
[98] Ge G, Wu H, Xiong F, Zhang Y, Guo Z, Bian Z, et al. The cytotoxicity evaluation of magnetic iron oxide nanoparticles on human aortic endothelial cells. Nanoscale Res Lett 2013;8(1):215.
[99] Zhu MT, Wang B, Wang Y, Yuan L, Wang HJ, Wang M, et al. Endothelial dysfunction and inflammation induced by iron oxide nanoparticle exposure: Risk factors for early atherosclerosis. Toxicol Lett 2011;203(2):162-71.
[100] Kennedy IM, Wilson D, Barakat AI. Uptake and inflammatory effects of nanoparticles in a human vascular endothelial cell line. Res Rep Health Eff Inst 2009;136:3-32.
[101] Hanini A, Schmitt A, Kacem K, Chau F, Ammar S, Gavard J. Evaluation of iron oxide nanoparticle biocompatibility. Int J Nanomed 2011;6:787-94.
[102] Li M, Kim HS, Tian L, Yu MK, Jon S, Moon WK. Comparison of two ultrasmall superparamagnetic iron oxides on cytotoxicity and MR imaging of tumors. Theranostics 2012;2(1):76-85.
[103] Cochran DB, Wattamwar PP, Wydra R, Hilt JZ, Anderson KW, Eitel RE, et al. Suppressing iron oxide nanoparticle toxicity by vascular targeted antioxidant polymer nanoparticles. Biomaterials 2013;34(37):9615-22.
[104] Dan M, Scott DF, Hardy PA, Wydra RJ, Hilt JZ, Yokel RA, et al. Block copolymer cross-linked nanoassemblies improve particle stability and biocompatibility of superparamagnetic iron oxide nanoparticles. Pharm Res 2013;30(2):552-61.

[105] Sun Z, Yathindranath V, Worden M, Thliveris JA, Chu S, Parkinson FE, et al. Characterization of cellular uptake and toxicity of aminosilane-coated iron oxide nanoparticles with different charges in central nervous system-relevant cell culture models. Int J Nanomed 2013;8:961-70.

[106] Kenzaoui BH, Bernasconi CC, Guney-Ayra S, Juillerat-Jeanneret L. Induction of oxidative stress, lysosome activation and autophagy by nanoparticles in human brain-derived endothelial cells. Biochem J 2012;441:813-21.

[107] Sun JH, Zhang YL, Nie CH, Qian SP, Yu XB, Xie HY, et al. *In vitro* labeling of endothelial progenitor cells isolated from peripheral blood with superparamagnetic iron oxide nanoparticles. Mol Med Rep 2012;6(2):282-6.

[108] Correia Carreira S, Walker L, Paul K, Saunders M. The toxicity, transport and uptake of nanoparticles in the *in vitro* BeWo b30 placental cell barrier model used within NanoTEST. Nanotoxicology 2013; DOI: 10.3109/17435390.2013.833317.

[109] Schwarz S, Wong JE, Bornemann J, Hodenius M, Himmelreich U, Richtering W, et al. Polyelectrolyte coating of iron oxide nanoparticles for MRI-based cell tracking. Nanomedicine 2012;8(5):682-91.

[110] Verdijk P, Scheenen TW, Lesterhuis WJ, Gambarota G, Veltien AA, Walczak P, et al. Sensitivity of magnetic resonance imaging of dendritic cells for *in vivo* tracking of cellular cancer vaccines. Int J Cancer 2007;120(5):978-84.

[111] Rodriguez-Luccioni HL, Latorre-Esteves M, Mendez-Vega J, Soto O, Rodriguez AR, Rinaldi C, et al. Enhanced reduction in cell viability by hyperthermia induced by magnetic nanoparticles. Int J Nanomed 2011;6:373-80.

[112] Yang HM, Park CW, Woo MA, Kim MI, Jo YM, Park HG, et al. HER2/neu Antibody conjugated poly(amino acid)-coated iron oxide nanoparticles for breast cancer MR imaging. Biomacromolecules 2010;11:2866-72.

[113] Kumar M, Singh G, Arora V, Mewar S, Sharma U, Jagannathan NR, et al. Cellular interaction of folic acid conjugated superparamagnetic iron oxide nanoparticles and its use as contrast agent for targeted magnetic imaging of tumor cells. Int J Nanomed 2012;7:3503-16.

[114] Choi JY, Lee SH, Na HB, An K, Hyeon T, Seo TS. *In vitro* cytotoxicity screening of water-dispersible metal oxide nanoparticles in human cell lines. Bioproc Biosyst Eng 2010;33(1):21-30.

[115] Yan C, Wu Y, Feng J, Chen W, Liu X, Hao P, et al. Anti-αvβ3 antibody guided three-step pretargeting approach using magnetoliposomes for molecular magnetic resonance imaging of breast cancer angiogenesis. Int J Nanomed 2013;8:245-55.

[116] Aljarrah K, Mhaidat NM, Al-Akhras MA, Aldaher AN, Albiss B, Aledealat K, et al. Magnetic nanoparticles sensitize MCF-7 breast cancer cells to doxorubicin-induced apoptosis. World J Surg Oncol 2012;10:62.

[117] Alarifi S, Ali D, Alkahtani S, Alhader MS. Iron oxide nanoparticles induce oxidative stress, DNA damage, and caspase activation in the human breast cancer cell line. Biol Trace Elem Res 2014;159(1-3):416-24.

[118] Sundstrom T, Daphu I, Wendelbo I, Hodneland E, Lundervold A, Immervoll H, et al. Automated tracking of nanoparticle-labeled melanoma cells improves the predictive power of a brain metastasis model. Cancer Res 2013;73(8):2445-56.

[119] Huang C, Neoh KG, Kang ET. Combined ATRP and 'click' chemistry for designing stable tumor-targeting superparamagnetic iron oxide nanoparticles. Langmuir 2012;28(1):563-71.

[120] Li J, Zheng L, Cai H, Sun W, Shen M, Zhang G, et al. Polyethyleneimine-mediated synthesis of folic acid-targeted iron oxide nanoparticles for *in vivo* tumor MR imaging. Biomaterials 2013;34(33):8382-92.

[121] Balivada S, Rachakatla RS, Wang H, Samarakoon TN, Dani RK, Pyle M, et al. A/C magnetic hyperthermia of melanoma mediated by iron(0)/iron oxide core/shell magnetic nanoparticles: a mouse study. BMC Cancer 2010;10:119.

[122] Ma HL, Qi XR, Ding WX, Maitani Y, Nagai T. Magnetic targeting after femoral artery administration and biocompatibility assessment of superparamagnetic iron oxide nanoparticles. J Biomed Mater Res A 2008;84(3):598-606.

[123] Gonzales M, Mitsumori LM, Kushleika JV, Rosenfeld ME, Krishnan KM. Cytotoxicity of iron oxide nanoparticles made from the thermal decomposition of organometallics and aqueous phase transfer with Pluronic F127. Contrast Media Mol I 2010;5(5):286-93.

[124] Gu JL, Xu HF, Han YH, Dai W, Hao W, Wang CY, et al. The internalization pathway, metabolic fate and biological effect of superparamagnetic iron oxide nanoparticles in the macrophage-like RAW264.7 cell. Sci China Life Sci 2011;54(9):793-805.

[125] Hsiao JK, Chu HH, Wang YH, Lai CW, Chou PT, Hsieh ST, et al. Macrophage physiological function after superparamagnetic iron oxide labeling. NMR Biomed 2008;21(8):820-9.

[126] Muller K, Skepper JN, Posfai M, Trivedi R, Howarth S, Corot C, et al. Effect of ultrasmall superparamagnetic iron oxide nanoparticles (Ferumoxtran-10) on human monocyte-macrophages *in vitro*. Biomaterials 2007;28(9):1629-42.

[127] Kunzmann A, Andersson B, Vogt C, Feliu N, Ye F, Gabrielsson S, et al. Efficient internalization of silica-coated iron oxide nanoparticles of different sizes by primary human macrophages and dendritic cells. Toxicol Appl Pharm 2011;253(2):81-93.

[128] Tromsdorf UI, Bruns OT, Salmen SC, Beisiegel U, Weller H. A highly effective, nontoxic T_1 MR contrast agent based on ultrasmall PEGylated iron oxide nanoparticles. Nano Lett 2009;9(12):4434-40.

[129] Naqvi S, Samim M, Abdin M, Ahmed FJ, Maitra A, Prashant C, et al. Concentration-dependent toxicity of iron oxide nanoparticles mediated by increased oxidative stress. Int J Nanomed 2010;5:983-9.

[130] Skajaa T, Cormode DP, Jarzyna PA, Delshad A, Blachford C, Barazza A, et al. The biological properties of iron oxide core high-density lipoprotein in experimental atherosclerosis. Biomaterials 2011;32(1):206-13.

[131] Mendes RG, Koch B, Bachmatiuk A, El-Gendy AA, Krupskaya Y, Springer A, et al. Synthesis and toxicity characterization of carbon coated iron oxide nanoparticles with highly defined size distributions. BBA-Gen Subjects 2013;1840(1):160-69.

[132] Lunov O, Syrovets T, Buchele B, Jiang X, Rocker C, Tron K, et al. The effect of carboxydextran-coated superparamagnetic iron oxide nanoparticles on c-Jun N-terminal kinase-mediated apoptosis in human macrophages. Biomaterials 2010;31(19):5063-71.

[133] Oude Engberink RD, van der Pol SM, Dopp EA, de Vries HE, Blezer EL. Comparison of SPIO and USPIO for *in vitro* labeling of human monocytes: MR detection and cell function. Radiology 2007;243(2):467-74.

[134] Settles M, Etzrodt M, Kosanke K, Schiemann M, Zimmermann A, Meier R, et al. Different capacity of monocyte subsets to phagocytose iron-oxide nanoparticles. PLoS One 2011;6(10):e25197.

[135] Yeh CH, Hsiao JK, Wang JL, Sheu F. Immunological impact of magnetic nanoparticles (Ferucarbotran) on murine peritoneal macrophages. J Nanopart Res 2010;12(1):151-60.

[136] Lak A, Dieckhoff J, Ludwig F, Scholtyssek JM, Goldmann O, Lunsdorf H, et al. Highly stable monodisperse PEGylated iron oxide nanoparticle aqueous suspensions: a nontoxic tracer for homogeneous magnetic bioassays. Nanoscale 2013;5(23):11447-55.

[137] Kodali V, Littke MH, Tilton SC, Teeguarden JG, Shi L, Frevert CW, et al. Dysregulation of macrophage activation profiles by engineered nanoparticles. ACS Nano 2013;7(8):6997-7010.

[138] Terrovitis J, Stuber M, Youssef A, Preece S, Leppo M, Kizana E, et al. Magnetic resonance imaging overestimates Ferumoxide-labeled stem cell survival after transplantation in the heart. Circulation 2008;117(12):1555-62.

[139] Baratli Y, Charles AL, Wolff V, Ben Tahar L, Smiri L, Bouitbir J, et al. Impact of iron oxide nanoparticles on brain, heart, lung, liver and kidneys mitochondrial respiratory chain complexes activities and coupling. Toxicol Vitro 2013;27(8):2142-48.

[140] Shi Q, Pisani LJ, Lee YK, Messing S, Ansari C, Bhaumik S, et al. Evaluation of the novel USPIO GEH121333 for MR imaging of cancer immune responses. Contrast Media Mol I 2013;8(3):281-8.

[141] Pawelczyk E, Arbab AS, Pandit S, Hu E, Frank JA. Expression of transferrin receptor and ferritin following ferumoxides-protamine sulfate labeling of cells: implications for cellular magnetic resonance imaging. NMR Biomed 2006;19(5):581-92.

[142] Reddy AM, Kwak BK, Shim HJ, Ahn C, Cho SH, Kim BJ, et al. Functional characterization of mesenchymal stem cells labeled with a novel PVP-coated superparamagnetic iron oxide. Contrast Media Mol I 2009;4(3):118-26.

[143] Reddy AM, Kwak BK, Shim HJ, Ahn C, Lee HS, Suh YJ, et al. *In vivo* tracking of mesenchymal stem cells labeled with a novel chitosan-coated superparamagnetic iron oxide nanoparticles using 3.0T MRI. J Korean Med Sci 2010;25(2):211-9.

[144] Zeng G, Wang G, Guan F, Chang K, Jiao H, Gao W, et al. Human amniotic membrane-derived mesenchymal stem cells labeled with superparamagnetic iron oxide nanoparticles: the effect on neuron-like differentiation *in vitro*. Mol Cell Biochem 2011;357(1-2):331-41.

[145] Bhattacharya K, Davoren M, Boertz J, Schins RP, Hoffmann E, Dopp E. Titanium dioxide nanoparticles induce oxidative stress and DNA-adduct formation but not DNA-breakage in human lung cells. Part Fibre Toxicol 2009;6:17.

[146] Chen H, Wang L, Yeh J, Wu X, Cao Z, Wang YA, et al. Reducing non-specific binding and uptake of nanoparticles and improving cell targeting with an antifouling PEO-b-PγMPS copolymer coating. Biomaterials 2010;31(20):5397-407.

[147] Choi SJ, Oh JM, Choy JH. Toxicological effects of inorganic nanoparticles on human lung cancer A549 cells. J Inorg Biochem 2009;103(3):463-71.

[148] Khan MI, Mohammad A, Patil G, Naqvi SA, Chauhan LK, Ahmad I. Induction of ROS, mitochondrial damage and autophagy in lung epithelial cancer cells by iron oxide nanoparticles. Biomaterials 2012;33(5):1477-88.

[149] Mesarosova M, Ciampor F, Zavisova V, Koneracka M, Ursinyova M, Kozics K, et al. The intensity of internalization and cytotoxicity of superparamagnetic iron oxide

nanoparticles with different surface modifications in human tumor and diploid lung cells. Neoplasma 2012;59(5):584-97.

[150] Zhou YM, Zhong CY, Kennedy IM, Pinkerton KE. Pulmonary responses of acute exposure to ultrafine iron particles in healthy adult rats. Environ Toxicol 2003;18(4):227-35.

[151] Zhou YM, Zhong CY, Kennedy IM, Leppert VJ, Pinkerton KE. Oxidative stress and NFkB activation in the lungs of rats: a synergistic interaction between soot and iron particles. Toxicol Appl Pharm 2003;190(2):157-69.

[152] Sharma G, Kodali V, Gaffrey M, Wang W, Minard KR, Karin NJ, et al. Iron oxide nanoparticle agglomeration influences dose rates and modulates oxidative stress-mediated dose-response profiles *in vitro*. Nanotoxicology 2014;8(6):663-75.

[153] Yu MX, Chen WL, Zhou Q, Gao P. Study on ASTC-a-1 cells labeled with superparamagnetic iron oxide and its magnetic resonance imaging. Exp Biol Med 2010;235(9):1053-61.

[154] Lee H, Lee E, Kim do K, Jang NK, Jeong YY, Jon S. Antibiofouling polymer-coated superparamagnetic iron oxide nanoparticles as potential magnetic resonance contrast agents for *in vivo* cancer imaging. J Am Chem Soc 2006;128(22):7383-9.

[155] Janic B, Rad AM, Jordan EK, Iskander AS, Ali MM, Varma NR, et al. Optimization and validation of FePro cell labeling method. PLoS One 2009;4(6):e5873.

[156] Kiessling F, Huppert J, Zhang C, Jayapaul J, Zwick S, Woenne EC, et al. RGD-labeled USPIO inhibits adhesion and endocytotic activity of a_vb_3-integrin-expressing glioma cells and only accumulates in the vascular tumor compartment. Radiology 2009;253(2):462-9.

[157] Pal A, Singh A, Nag TC, Chattopadhyay P, Mathur R, Jain S. Iron oxide nanoparticles and magnetic field exposure promote functional recovery by attenuating free radical-induced damage in rats with spinal cord transection. Int J Nanomed 2013;8:2259-72.

[158] Song M, Moon WK, Kim Y, Lim D, Song IC, Yoon BW. Labeling efficacy of superparamagnetic iron oxide nanoparticles to human neural stem cells: Comparison of Ferumoxides, monocrystalline iron oxide, cross-linked iron oxide (CLIO)-NH_2 and tat-CLIO. Korean J Radiol 2007;8(5):365-71.

[159] Jeng HA, Swanson J. Toxicity of metal oxide nanoparticles in mammalian cells. J Environ Sci Health A Tox Hazard Subst Environ Eng 2006;41(12):2699-711.

[160] Hohnholt MC, Dringen R. Iron-dependent formation of reactive oxygen species and glutathione depletion after accumulation of magnetic iron oxide nanoparticles by oligodendroglial cells. J Nanopart Res 2011;13(12):6761-74.
[161] Hohnholt MC, Geppert M, Dringen R. Treatment with iron oxide nanoparticles induces ferritin synthesis but not oxidative stress in oligodendroglial cells. Acta Biomater 2011;7(11):3946-54.
[162] Wang Y, Wang B, Zhu MT, Li M, Wang HJ, Wang M, et al. Microglial activation, recruitment and phagocytosis as linked phenomena in ferric oxide nanoparticle exposure. Toxicol Lett 2011;205(1):26-37.
[163] Kenzaoui BH, Bernasconi CC, Hofmann H, Juillerat-Jeanneret L. Evaluation of uptake and transport of ultrasmall superparamagnetic iron oxide nanoparticles by human brain-derived endothelial cells. Nanomedicine 2012;7(1):39-53.
[164] Wu J, Ding T, Sun J. Neurotoxic potential of iron oxide nanoparticles in the rat brain striatum and hippocampus. Neurotoxicology 2013;34(243-53.
[165] Kim JA, Lee N, Kim BH, Rhee WJ, Yoon S, Hyeon T, et al. Enhancement of neurite outgrowth in PC12 cells by iron oxide nanoparticles. Biomaterials 2011;32(11):2871-7.
[166] Chen CC, Ku MC, D MJ, Lai JS, Hueng DY, Chang C. Simple SPION incubation as an efficient intracellular labeling method for tracking neural progenitor cells using MRI. PLoS One 2013;8(2):e56125.
[167] Muldoon LL, Sandor M, Pinkston KE, Neuwelt EA. Imaging, distribution, and toxicity of superparamagnetic iron oxide magnetic resonance nanoparticles in the rat brain and intracerebral tumor. Neurosurgery 2005;57(4):785-96; discussion 85-96.
[168] Wang B, Feng WY, Zhu MT, Wang Y, Wang M, Gu YQ, et al. Neurotoxicity of low-dose repeatedly intranasal instillation of nano- and submicron-sized ferric oxide particles in mice. J Nanopart Res 2009;11(1):41-53.
[169] Wu HY, Chung MC, Wang CC, Huang CH, Liang HJ, Jan TR. Iron oxide nanoparticles suppress the production of IL-1beta via the secretory lysosomal pathway in murine microglial cells. Part Fibre Toxicol 2013;10(1):46.
[170] Ding J, Tao K, Li J, Song S, Sun K. Cell-specific cytotoxicity of dextran-stabilized magnetite nanoparticles. Colloids Surf B Biointerfaces 2010;79(1):184-90.
[171] Geppert M, Hohnholt MC, Nurnberger S, Dringen R. Ferritin up-regulation and transient ROS production in cultured brain astrocytes after loading with iron oxide nanoparticles. Acta Biomater 2012;8(10):3832-9.

[172] Liao Z, Wang H, Lv R, Zhao P, Sun X, Wang S, et al. Polymeric liposomes-coated superparamagnetic iron oxide nanoparticles as contrast agent for targeted magnetic resonance imaging of cancer cells. Langmuir 2011;27(6):3100-5.

[173] Arbab AS, Bashaw LA, Miller BR, Jordan EK, Lewis BK, Kalish H, et al. Characterization of biophysical and metabolic properties of cells labeled with superparamagnetic iron oxide nanoparticles and transfection agent for cellular MR imaging. Radiology 2003;229(3):838-46.

[174] Villanueva A, Canete M, Roca AG, Calero M, Veintemillas-Verdaguer S, Serna CJ, et al. The influence of surface functionalization on the enhanced internalization of magnetic nanoparticles in cancer cells. Nanotechnology 2009;20(11):115103.

[175] Hasan Hussein-Al-Ali S, Arulselvan P, Fakurazi S, Hussein MZ, Dorniani D. Arginine-chitosan- and arginine- polyethylene glycol-conjugated superparamagnetic nanoparticles: Preparation, cytotoxicity and controlled-release. J Biomater Appl 2014;29(2):186-98.

[176] Lalande C, Miraux S, Derkaoui SM, Mornet S, Bareille R, Fricain JC, et al. Magnetic resonance imaging tracking of human adipose derived stromal cells within three-dimensional scaffolds for bone tissue engineering. Eur Cells Mater 2011;21:341-54.

[177] Wang L, Deng J, Wang J, Xiang B, Yang T, Gruwel M, et al. Superparamagnetic iron oxide does not affect the viability and function of adipose-derived stem cells, and superparamagnetic iron oxide-enhanced magnetic resonance imaging identifies viable cells. Magn Reson Imaging 2009;27(1):108-19.

[178] Zhang B, Jiang B, Chen Y, Huang H, Xie Q, Kang M, et al. Detection of viability of transplanted beta cells labeled with a novel contrast agent - polyvinylpyrrolidone-coated superparamagnetic iron oxide nanoparticles by magnetic resonance imaging. Contrast Media Mol I 2012;7(1):35-44.

[179] Oca-Cossio J, Mao H, Khokhlova N, Kennedy CM, Kennedy JW, Stabler CL, et al. Magnetically labeled insulin-secreting cells. Biochem Biophys Res Co 2004;319(2):569-75.

[180] Shen CC, Liang HJ, Wang CC, Liao MH, Jan TR. A role of cellular glutathione in the differential effects of iron oxide nanoparticles on antigen-specific T cell cytokine expression. Int J Nanomed 2011;6:2791-8.

[181] Shah V, Taratula O, Garbuzenko OB, Patil ML, Savla R, Zhang M, et al. Genotoxicity of different nanocarriers: Possible modifications for the delivery of nucleic acids. Curr Drug Discov Tech 2013;10(1):8-15.

[182] Puppi J, Mitry RR, Modo M, Dhawan A, Raja K, Hughes RD. Use of a clinically approved iron oxide MRI contrast agent to label human hepatocytes. Cell Transplant 2011;20(6):963-75.

[183] Lee CM, Jeong HJ, Kim SL, Kim EM, Kim DW, Lim ST, et al. SPION-loaded chitosan-linoleic acid nanoparticles to target hepatocytes. Int J Pharm 2009;371(1-2):163-9.

[184] Bae JE, Huh MI, Ryu BK, Do JY, Jin SU, Moon MJ, et al. The effect of static magnetic fields on the aggregation and cytotoxicity of magnetic nanoparticles. Biomaterials 2011;32(35):9401-14.

[185] Hussain SM, Hess KL, Gearhart JM, Geiss KT, Schlager JJ. *In vitro* toxicity of nanoparticles in BRL 3A rat liver cells. Toxicol Vitro 2005;19(7):975-83.

[186] Ma P, Luo Q, Chen J, Gan Y, Du J, Ding S, et al. Intraperitoneal injection of magnetic Fe_3O_4-nanoparticle induces hepatic and renal tissue injury via oxidative stress in mice. Int J Nanomed 2012;7:4809-18.

[187] Sarkar A, Sil PC. Iron oxide nanoparticles mediated cytotoxicity via PI3K/AKT pathway: Role of quercetin. Food Chem Toxicol 2014;71:106-15.

[188] Volkovova K, Ulicna O, Kucharska J, Handy R, Staruchova M, Kebis A, et al. Health effects of selected nanoparticles *in vivo*: Liver function and hepatotoxicity following intravenous injection of titanium dioxide and Na-oleate coated iron oxide nanoparticles in rodents. Nanotoxicology 2013; DOI:10.3109/17435390.2013.815285.

[189] Auffan M, Decome L, Rose J, Orsiere T, De Meo M, Briois V, et al. *In vitro* interactions between DMSA-coated maghemite nanoparticles and human fibroblasts: A physicochemical and cyto-genotoxical study. Environ Sci Technol 2006;40(14):4367-73.

[190] Zhang W, Shi X, Huang J, Zhang Y, Wu Z, Xian Y. Bacitracin-conjugated superparamagnetic iron oxide nanoparticles: Synthesis, characterization and antibacterial activity. Chemphyschem 2012;13(14):3388-96.

[191] Inbaraj BS, Kao TH, Tsai TY, Chiu CP, Kumar R, Chen BH. The synthesis and characterization of poly(γ-glutamic acid)-coated magnetite nanoparticles and their effects on antibacterial activity and cytotoxicity. Nanotechnology 2011;22(7):075101.

[192] Gaihre B, Hee Lee Y, Khil MS, Yi HK, Kim HY. *In-vitro* cytotoxicity and cell uptake study of gelatin-coated magnetic iron oxide nanoparticles. J Microencapsul 2011;28(4):240-7.

[193] Mahmoudi M, Simchi A, Vali H, Imani M, Shokrgozar MA, Azadmanesh K, et al. Cytotoxicity and cell cycle effects of bare and poly(vinyl alcohol)-coated iron oxide nanoparticles in mouse fibroblasts. Adv Eng Mater 2009;11(12):B243-B50.

[194] Mahmoudi M, Simchi A, Imani M. Cytotoxicity of uncoated and polyvinyl alcohol coated superparamagnetic iron oxide nanoparticles. J Phys Chem C 2009;113(22):9573-80.

[195] Chen AZ, Lin XF, Wang SB, Li L, Liu YG, Ye L, et al. Biological evaluation of Fe_3O_4-poly(L-lactide)-poly(ethylene glycol)-poly(L-lactide) magnetic microspheres prepared in supercritical CO_2. Toxicol Lett 2012;212(1):75-82.

[196] Easo SL, Mohanan PV. Dextran stabilized iron oxide nanoparticles: Synthesis, characterization and *in vitro* studies. Carbohyd Polym 2013;92(1):726-32.

[197] Sangeetha J, Thomas S, Arutchelvi J, Doble M, Philip J. Functionalization of iron oxide nanoparticles with biosurfactants and biocompatibility studies. J Biomed Nanotechnol 2013;9(5):751-64.

[198] Gupta AK, Curtis ASG. Lactoferrin and ceruloplasmin derivatized superparamagnetic iron oxide nanoparticles for targeting cell surface receptors. Biomaterials 2004;25(15):3029-40.

[199] Berry CC, Wells S, Charles S, Aitchison G, Curtis AS. Cell response to dextran-derivatised iron oxide nanoparticles post internalisation. Biomaterials 2004;25(23):5405-13.

[200] Berry CC, Charles S, Wells S, Dalby MJ, Curtis ASG. The influence of transferrin stabilised magnetic nanoparticles on human dermal fibroblasts in culture. Int J Pharm 2004;269(1):211-25.

[201] Bakandritsos A, Zboril R, Bouropoulos N, Kallinteri P, Favretto ME, Parker TL, et al. The preparation of magnetically guided lipid based nanoemulsions using self-emulsifying technology. Nanotechnology 2010;21(5):055104.

[202] Harris G, Palosaari T, Magdolenova Z, Mennecozzi M, Gineste JM, Saavedra L, et al. Iron oxide nanoparticle toxicity testing using high throughput analysis and high content imaging. Nanotoxicology 2013; DOI:10.3109/17435390.2013.816797.

[203] Meenach SA, Anderson AA, Suthar M, Anderson KW, Hilt JZ. Biocompatibility analysis of magnetic hydrogel nanocomposites based on poly(N-isopropylacrylamide) and iron oxide. J Biomed Mater Res A 2009;91(3):903-9.

[204] Lee HY, Lim NH, Seo JA, Yuk SH, Kwak BK, Khang G, et al. Preparation and magnetic resonance imaging effect of polyvinylpyrrolidone-coated iron oxide nanoparticles. J Biomed Mater Res B Appl Biomater 2006;79(1):142-50.

[205] Li S, Wang H, Qi Y, Tu J, Bai Y, Tian T, et al. Assessment of nanomaterial cytotoxicity with SOLiD sequencing-based microRNA expression profiling. Biomaterials 2011;32(34):9021-30.

[206] Liu J, Sun Z, Deng Y, Zou Y, Li C, Guo X, et al. Highly water-dispersible biocompatible magnetite particles with low cytotoxicity stabilized by citrate groups. Angew Chem Int Ed Engl 2009;48(32):5875-9.

[207] Lin JJ, Chen JS, Huang SJ, Ko JH, Wang YM, Chen TL, et al. Folic acid-Pluronic F127 magnetic nanoparticle clusters for combined targeting, diagnosis, and therapy applications. Biomaterials 2009;30(28):5114-24.

[208] Chen YJ, Tao J, Xiong F, Zhu JB, Gu N, Geng KK. Characterization and *in vitro* cellular uptake of PEG coated iron oxide nanoparticles as MRI contrast agent. Pharmazie 2010;65(7):481-6.

[209] Cheng FY, Su CH, Yang YS, Yeh CS, Tsai CY, Wu CL, et al. Characterization of aqueous dispersions of Fe_3O_4 nanoparticles and their biomedical applications. Biomaterials 2005;26(7):729-38.

[210] Sun SL, Lo YL, Chen HY, Wang LF. Hybrid polyethylenimine and polyacrylic acid-bound iron oxide as a magnetoplex for gene delivery. Langmuir 2012;28(7):3542-52.

[211] Halamoda Kenzaoui B, Chapuis Bernasconi C, Juillerat-Jeanneret L. Stress reaction of kidney epithelial cells to inorganic solid-core nanoparticles. Cell Biol Toxicol 2013;29(1):39-58.

[212] Huang C, Neoh KG, Xu L, Kang ET, Chiong E. Polymeric nanoparticles with encapsulated superparamagnetic iron oxide and conjugated cisplatin for potential bladder cancer therapy. Biomacromolecules 2012;13(8):2513-20.

[213] Iversen NK, Frische S, Thomsen K, Laustsen C, Pedersen M, Hansen PB, et al. Superparamagnetic iron oxide polyacrylic acid coated γ-Fe_2O_3 nanoparticles do not affect kidney function but cause acute effect on the cardiovascular function in healthy mice. Toxicol Appl Pharm 2013;266:276-88.

[214] Sadek H, Latif S, Collins R, Garry MG, Garry DJ. Use of ferumoxides for stem cell labeling. Regen Med 2008;3(6):807-16.

[215] Au KW, Liao SY, Lee YK, Lai WH, Ng KM, Chan YC, et al. Effects of iron oxide nanoparticles on cardiac differentiation of embryonic stem cells. Biochem Biophys Res Co 2009;379(4):898-903.

[216] Grottone GT, Loureiro RR, Covre J, Rodrigues EB, Gomes JA. ARPE-19 cell uptake of small and ultrasmall superparamagnetic iron oxide. Curr Eye Res 2014;39(4):403-10.

[217] Zhu MT, Feng WY, Wang B, Wang TC, Gu YQ, Wang M, et al. Comparative study of pulmonary responses to nano- and submicron-sized ferric oxide in rats. Toxicology 2008;247(2-3):102-11.

[218] Chen F, Shi X. Intracellular signal transduction of cells in response to carcinogenic metals. Crit Rev Oncol Hemat 2002;42(1):105-21.

[219] Franco R, Sanchez-Olea R, Reyes-Reyes EM, Panayiotidis MI. Environmental toxicity, oxidative stress and apoptosis: menage a trois. Mutat Res 2009;674(1-2):3-22.

[220] Kroemer G, Galluzzi L, Brenner C. Mitochondrial membrane permeabilization in cell death. Physiol Rev 2007;87(1):99-163.

[221] Kai W, Xiaojun X, Ximing P, Zhenqing H, Qiqing Z. Cytotoxic effects and the mechanism of three types of magnetic nanoparticles on human hepatoma BEL-7402 cells. Nanoscale Res Lett 2011;6:480.

[222] Namvar F, Rahman HS, Mohamad R, Baharara J, Mahdavi M, Amini E, et al. Cytotoxic effect of magnetic iron oxide nanoparticles synthesized via seaweed aqueous extract. Int J Nanomed 2014;9:2479-88.

[223] Kim Y, Kong SD, Chen LH, Pisanic TR, 2nd, Jin S, Shubayev VI. *In vivo* nanoneurotoxicity screening using oxidative stress and neuroinflammation paradigms. Nanomedicine 2013;9(7):1057-66.

[224] Chen BA, Cheng J, Shen MF, Gao F, Xu WL, Shen HL, et al. Magnetic nanoparticle of Fe_3O_4 and 5-bromotetrandrin interact synergistically to induce apoptosis by daunorubicin in leukemia cells. Int J Nanomed 2009;4(1):65-71.

[225] Chen B, Liang Y, Wu W, Cheng J, Xia G, Gao F, et al. Synergistic effect of magnetic nanoparticles of Fe_3O_4 with gambogic acid on apoptosis of K562 leukemia cells. Int J Nanomed 2009;4:251-9.

[226] Ludwig A, Poller WC, Westphal K, Minkwitz S, Lattig-Tunnemann G, Metzkow S, et al. Rapid binding of electrostatically stabilized iron oxide nanoparticles to THP-1 monocytic cells via interaction with glycosaminoglycans. Basic Res Cardiol 2013;108(2):328.

[227] Khan JA, Mandal TK, Das TK, Singh Y, Pillai B, Maiti S. Magnetite (Fe_3O_4) nanocrystals affect the expression of genes involved in the TGF-beta signalling pathway. Mol Biosyst 2011;7(5):1481-6.

[228] Zhang G, Lai BB, Zhou YY, Chen BA, Wang XM, Lu Q, et al. Fe_3O_4 nanoparticles with daunorubicin induce apoptosis through caspase 8-PARP pathway and inhibit K562 leukemia cell-induced tumor growth *in vivo*. Nanomedicine 2011;7(5):595-603.

[229] Suzuki J, Denning DP, Imanishi E, Horvitz HR, Nagata S. Xk-Related protein 8 and CED-8 promote phosphatidylserine exposure in apoptotic cells. Science 2013;341(6144):403-06.

[230] Chen BA, Dai YY, Wang XM, Zhang RY, Xu WL, Shen HL, et al. Synergistic effect of the combination of nanoparticulate Fe_3O_4 and Au with daunomycin on K562/A02 cells. Int J Nanomed 2008;3(3):343-50.

[231] Elmore S. Apoptosis: A review of programmed cell death. Toxicol Pathol 2007;35(4):495-516.

[232] Mahmoudi M, Shokrgozar MA, Simchi A, Imani M, Milani AS, Stroeve P, et al. Multiphysics flow modeling and *in vitro* toxicity of iron oxide nanoparticles coated with poly(vinyl alcohol). J Phys Chem C 2009;113(39):2322-31.

[233] Su H, Mou Y, An Y, Han W, Huang X, Xia G, et al. The migration of synthetic magnetic nanoparticle labeled dendritic cells into lymph nodes with optical imaging. Int J Nanomed 2013;8:3737-44.

[234] Wu J, Sun J. Investigation on mechanism of growth arrest induced by iron oxide nanoparticles in PC12 cells. J Nanosci Nanotechnol 2011;11(12):11079-83.

[235] Jing H, Wang J, Yang P, Ke X, Xia G, Chen B. Magnetic Fe_3O_4 nanoparticles and chemotherapy agents interact synergistically to induce apoptosis in lymphoma cells. Int J Nanomed 2010;5:999-1004.

[236] Huang DM, Hsiao JK, Chen YC, Chien LY, Yao M, Chen YK, et al. The promotion of human mesenchymal stem cell proliferation by superparamagnetic iron oxide nanoparticles. Biomaterials 2009;30(22):3645-51.

[237] Dhanasekaran DN, Reddy EP. JNK signaling in apoptosis. Oncogene 2008;27(48):6245-51.

[238] Phillips DH, Arlt VM. Genotoxicity: damage to DNA and its consequences. EXS 2009;99:87-110.

[239] Singh N, Jenkins GJ, Nelson BC, Marquis BJ, Maffeis TG, Brown AP, et al. The role of iron redox state in the genotoxicity of ultrafine superparamagnetic iron oxide nanoparticles. Biomaterials 2012;33(1):163-70.

[240] Martinez GR, Loureiro AP, Marques SA, Miyamoto S, Yamaguchi LF, Onuki J, et al. Oxidative and alkylating damage in DNA. Mutat Res 2003;544(2-3):115-27.

[241] Wink DA, Mitchell JB. Chemical biology of nitric oxide: Insights into regulatory, cytotoxic, and cytoprotective mechanisms of nitric oxide. Free Radical Bio Med 1998;25(4-5):434-56.

[242] Hong SC, Lee JH, Lee J, Kim HY, Park JY, Cho J, et al. Subtle cytotoxicity and genotoxicity differences in superparamagnetic iron oxide nanoparticles coated with various functional groups. Int J Nanomed 2011;6:3219-31.

[243] Wang J, Chen B, Jin N, Xia G, Chen Y, Zhou Y, et al. The changes of T lymphocytes and cytokines in ICR mice fed with Fe_3O_4 magnetic nanoparticles. Int J Nanomed 2011;6:605-10.

[244] Chen BA, Jin N, Wang J, Ding J, Gao C, Cheng J, et al. The effect of magnetic nanoparticles of Fe_3O_4 on immune function in normal ICR mice. Int J Nanomed 2010;5:593-9.

[245] Shen CC, Wang CC, Liao MH, Jan TR. A single exposure to iron oxide nanoparticles attenuates antigen-specific antibody production and T-cell reactivity in ovalbumin-sensitized BALB/c mice. Int J Nanomed 2011;6:1229-35.

[246] Rahman I. Oxidative stress, transcription factors and chromatin remodelling in lung inflammation. Biochem Pharmacol 2002;64(5-6):935-42.

[247] Beckmann N, Cannet C, Babin AL, Ble FX, Zurbruegg S, Kneuer R, et al. *In vivo* visualization of macrophage infiltration and activity in inflammation using magnetic resonance imaging. Wiley Interdiscip Rev Nanomed Nanobiotechnol 2009;1(3):272-98.

[248] Weston CR, Davis RJ. The JNK signal transduction pathway. Curr Opin Cell Biol 2007;19(2):142-49.

[249] Johnson GL, Lapadat R. Mitogen-activated protein kinase pathways mediated by ERK, JNK, and p38 protein kinases. Science 2002;298(5600):1911-12.

[250] Cagnol S, Chambard JC. ERK and cell death: Mechanisms of ERK-induced cell death-apoptosis, autophagy and senescence. FEBS J 2010;277(1):2-21.

[251] Roux PP, Blenis J. ERK and p38 MAPK-activated protein kinases: a family of protein kinases with diverse biological functions. Microbiol Mol Biol R 2004;68(2):320-44.

[252] Clark AR, Dean JL. The p38 MAPK pathway in rheumatoid arthritis: A sideways look. Open Rheumatol J 2012;6:209-19.

[253] Murray AR, Kisin E, Inman A, Young SH, Muhammed M, Burks T, et al. Oxidative stress and dermal toxicity of iron oxide nanoparticles *in vitro*. Cell Biochem Biophys 2013;67(2):461-76.

[254] Kim HS, Tian L, Lin S, Cha JH, Jung HS, Park KS, et al. Magnetic labeling of pancreatic β-cells modulates the glucose- and insulin-induced phosphorylation of ERK1/2 and AKT. Contrast Media Mol I 2013;8(1):20-6.

[255] Khoo S, Griffen SC, Xia Y, Baer RJ, German MS, Cobb MH. Regulation of insulin gene transcription by ERK1 and ERK2 in pancreatic β cells. J Biol Chem 2003;278(35):32969-77.

[256] Lee SJ, Pfluger PT, Kim JY, Nogueiras R, Duran A, Pages G, et al. A functional role for the p62-ERK1 axis in the control of energy homeostasis and adipogenesis. Embo Rep 2010;11(3):226-32.

[257] Tak PP, Firestein GS. NF-kB: a key role in inflammatory diseases. J Clin Invest 2001;107(1):7-11.

[258] Chuang KH, Peng YC, Chien HY, Lu ML, Du HI, Wu YL. Attenuation of LPS-induced lung inflammation by glucosamine in rats. Am J Respir Cell Mol Biol 2013;49(6):1110-19.

[259] Gomes A, Fernandes E, Lima JL, Mira L, Corvo ML. Molecular mechanisms of anti-inflammatory activity mediated by flavonoids. Curr Med Chem 2008;15(16):1586-605.

[260] Dinarello CA. Proinflammatory cytokines. Chest 2000;118(2):503-08.

[261] Zhu M, Tian X, Song X, Li Y, Tian Y, Zhao Y, et al. Nanoparticle-induced exosomes target antigen-presenting cells to initiate Th_1-type immune activation. Small 2012;8(18):2841-8.

[262] Martinez FO, Sica A, Mantovani A, Locati M. Macrophage activation and polarization. Front Biosci-Landmrk 2008;13:453-61.

[263] van Horssen R, ten Hagen TLM, Eggermont AMM. TNF-α in cancer treatment: Molecular insights, antitumor effects, and clinical utility. Oncologist 2006;11(4):397-408.

[264] Baud V, Karin M. Signal transduction by tumor necrosis factor and its relatives. Trends Cell Biol 2001;11(9):372-77.

[265] Baggiolini M, Clarklewis I. Interleukin-8, a chemotactic and inflammatory cytokine. FEBS Lett 1992;307(1):97-101.

[266] Craig R, Larkin A, Mingo AM, Thuerauf DJ, Andrews C, McDonough PM, et al. p38 MAPK and NF-kB collaborate to induce interleukin-6 gene expression and release. Evidence for a cytoprotective autocrine signaling pathway in a cardiac myocyte model system. J Biol Chem 2000;275(31):23814-24.

[267] Park EJ, Kim H, Kim Y, Yi J, Choi K, Park K. Inflammatory responses may be induced by a single intratracheal instillation of iron nanoparticles in mice. Toxicology 2010;275(1-3):65-71.

[268] Laskar A, Ghosh M, Khattak SI, Li W, Yuan XM. Degradation of superparamagnetic iron oxide nanoparticle-induced ferritin by lysosomal cathepsins and related immune response. Nanomedicine 2012;7(5):705-17.

[269] Schroder K, Hertzog PJ, Ravasi T, Hume DA. Interferon-γ: an overview of signals, mechanisms and functions. J Leukocyte Biol 2004;75(2):163-89.

[270] Ban M, Langonne I, Huguet N, Goutet M. Effect of submicron and nano-iron oxide particles on pulmonary immunity in mice. Toxicol Lett 2012;210(3):267-75.

[271] Tosato G, Jones KD. Interleukin-1 induces interleukin-6 production in peripheral-blood monocytes. Blood 1990;75(6):1305-10.

[272] Naveau A, Smirnov P, Menager C, Gazeau F, Clement O, Lafont A, et al. Phenotypic study of human gingival fibroblasts labeled with superparamagnetic anionic nanoparticles. J Periodontol 2006;77(2):238-47.

[273] Horiguchi M, Ota M, Rifkin DB. Matrix control of transforming growth factor-β function. J Biochem 2012;152(4):321-29.

[274] Massague J, Hata A, Liu F. TGF-β signalling through the Smad pathway. Trends Cell Biol 1997;7(5):187-92.

[275] Watson RS, Gouze E, Levings PP, Bush ML, Kay JD, Jorgensen MS, et al. Gene delivery of TGF-β1 induces arthrofibrosis and chondrometaplasia of synovium *in vivo*. Lab Invest 2010;90(11):1615-27.

[276] Murray PJ. The primary mechanism of the IL-10-regulated anti inflammatory response is to selectively inhibit transcription. P Natl Acad Sci USA 2005;102(24):8686-91.

[277] Blank F, Gerber P, Rothen-Rutishauser B, Sakulkhu U, Salaklang J, De Peyer K, et al. Biomedical nanoparticles modulate specific $CD4^+$ T cell stimulation by inhibition of antigen processing in dendritic cells. Nanotoxicology 2011;5(4):606-21.

[278] Laskar A, Eilertsen J, Li W, Yuan XM. SPION primes THP1 derived M2 macrophages towards M1-like macrophages. Biochem Biophys Res Co 2013;441(4):737-42.

[279] Wilkinson K, Ekstrand-Hammarstrom B, Ahlinder L, Guldevall K, Pazik R, Kepinski L, et al. Visualization of custom-tailored iron oxide nanoparticles chemistry, uptake, and toxicity. Nanoscale 2012;4(23):7383-93.

[280] Pusic K, Aguilar Z, McLoughlin J, Kobuch S, Xu H, Tsang M, et al. Iron oxide nanoparticles as a clinically acceptable delivery platform for a recombinant blood-stage human malaria vaccine. Faseb J 2012;27(3):1153-66.

[281] Siglienti I, Bendszus M, Kleinschnitz C, Stoll G. Cytokine profile of iron-laden macrophages: Implications for cellular magnetic resonance imaging. J Neuroimmunol 2006;173(1-2):166-73.

[282] Valois CR, Braz JM, Nunes ES, Vinolo MA, Lima EC, Curi R, et al. The effect of DMSA-functionalized magnetic nanoparticles on transendothelial migration of monocytes in the murine lung via a β2 integrin-dependent pathway. Biomaterials 2010;31(2):366-74.

[283] Gupta AK, Gupta M. Synthesis and surface engineering of iron oxide nanoparticles for biomedical applications. Biomaterials 2005;26(18):3995-4021.

[284] Mosmann TR, Sad S. The expanding universe of T-cell subsets: Th1, Th2 and more. Immunol Today 1996;17(3):138-46.
[285] Zhu M, Li Y, Shi J, Feng W, Nie G, Zhao Y. Exosomes as extrapulmonary signaling conveyors for nanoparticle-induced systemic immune activation. Small 2012;8(3):404-12.
[286] Tavare R, Sagoo P, Varama G, Tanriver Y, Warely A, Diebold SS, et al. Monitoring of *in vivo* function of superparamagnetic iron oxide labelled murine dendritic cells during anti-tumour vaccination. PLoS One 2011;6(5):e19662.
[287] Janic B, Iskander AS, Rad AM, Soltanian-Zadeh H, Arbab AS. Effects of Ferumoxides-protamine sulfate labeling on immunomodulatory characteristics of macrophage-like THP-1 cells. PLoS One 2008;3(6):e2499.
[288] Pawelczyk E, Jordan EK, Balakumaran A, Chaudhry A, Gormley N, Smith M, et al. *In vivo* transfer of intracellular labels from locally implanted bone marrow stromal cells to resident tissue macrophages. PLoS One 2009;4(8):e6712.
[289] Ban M, Langonne I, Huguet N, Guichard Y, Goutet M. Iron oxide particles modulate the ovalbumin-induced Th2 immune response in mice. Toxicol Lett 2013;216(1):31-9.

CHAPTER I

GENERAL INTRODUCTION

I.2. General and specific objectives of the dissertation

The main objective of this dissertation was to assess the biological effects of PAA-coated and non-coated magnetite IONs in *in vitro* and *in vivo* experimental models. For this purpose we evaluated the effects of these IONs on human leukocytes, as well as on other blood cells, *in vitro*, namely on the induction of oxidative burst, death and pro-inflammatory pathways and genotoxicity, as well as the effects of PAA-coated IONs *in vivo* concerning their pro-inflammatory and toxicological effects in male CD-1 mice.

The following specific objectives were established:

- To evaluate the effects of PAA-coated and non-coated IONs on human neutrophils, namely their capacity to activate the oxidative burst and to modify their lifespan through necrosis and/or apoptosis;
- To evaluate the ability of PAA-coated and non-coated IONs to induce cytokine production (IL-1β, TNF-α, IL-6, IL-8, IFN-γ and IL-10) by *ex-vivo* human blood cells and assess the pathways (p38 MAPK, JNK and NF-kB) involved in this induction;
- To evaluate the ability of PAA-coated and non-coated IONs to induce genotoxicity in human T lymphocytes through influence on cell cycle progression and on the induction of chromosome aberrations;
- To evaluate the ability of PAA-coated and non-coated IONs to exert cumulative effect with the iron-dependent genotoxic agent BLM in human T lymphocytes;
- To evaluate the biodistribution of PAA-coated IONs in male CD-1 mice after intravenous administration;
- To evaluate the effect of acute intravenous PAA-coated IONs administration on male CD-1 mice, namely their ability to induce pro-inflammatory processes and induce liver and kidney toxicity.

CHAPTER II

ORIGINAL RESEARCH

II.1. INTERACTION OF POLYACRYLIC ACID COATED AND NON-COATED IRON OXIDE NANOPARTICLES WITH HUMAN NEUTROPHILS

Reprinted from Toxicology Letters

Toxicology Letters 225 (2014) 57–65

Contents lists available at ScienceDirect

Toxicology Letters

journal homepage: www.elsevier.com/locate/toxlet

Interaction of polyacrylic acid coated and non-coated iron oxide nanoparticles with human neutrophils

Diana Couto[a], Marisa Freitas[a], Vânia Vilas-Boas[b], Irene Dias[a], Graça Porto[c], M. Arturo Lopez-Quintela[d], José Rivas[e], Paulo Freitas[e], Félix Carvalho[b], Eduarda Fernandes[a,*]

[a] REQUIMTE, Laboratory of Applied Chemistry, Department of Chemical Sciences, Faculty of Pharmacy, University of Porto, Porto, Portugal
[b] REQUIMTE, Laboratory of Toxicology, Department of Biological Sciences, Faculty of Pharmacy, University of Porto, Porto, Portugal
[c] Service of Clinical Hematology, Santo António Hospital, Porto, Portugal
[d] Laboratory of Nanotechnology and Magnetism, Institute of Technological Research, IIT, University of Santiago de Compostela (USC), Santiago de Compostela, Spain
[e] International Iberian Nanotechnology Laboratory, Braga, Portugal

HIGHLIGHTS

- Polyacrylic acid-coated iron oxide nanoparticles increase neutrophils' apoptosis.
- Non-coated iron oxide nanoparticles prevent neutrophils' apoptosis.
- Both nanoparticles trigger neutrophils' oxidative burst by NADPH oxidase activation.

ARTICLE INFO

Article history:
Received 30 August 2013
Received in revised form
17 November 2013
Accepted 18 November 2013
Available online 26 November 2013

Keywords:
Nanotoxicology
Oxidative burst
Apoptosis
Human neutrophils
Iron oxide nanoparticles
Polyacrylic acid coating

ABSTRACT

Iron oxide nanoparticles (ION), with different coatings and sizes, have attracted extensive interest in the last years to be applied in drug delivery, cancer therapy and as contrast agents in imagiologic techniques such as magnetic resonance imaging. However, the safety of these nanoparticles is still not completely established, particularly to host defense systems that are usually recruited for their clearance from the body. In this paper, given the importance of neutrophils in the immune response of the organism to nanoparticles, the effect of polyacrylic acid (PAA)-coated and non-coated ION on human neutrophils was evaluated *in vitro*, namely their capacity to activate the oxidative burst and to modify their lifespan. The obtained results showed that the studied PAA-coated and non-coated ION triggered neutrophils' oxidative burst in a NADPH oxidase dependent manner, and that PAA-coated ION increased — while non-coated ION prevented — apoptotic signaling and apoptosis. These effects may have important clinical implications in biomedical applications of ION.

1. Introduction

Nanotechnology is nowadays at the forefront in the development of new therapeutic and diagnostic tools in all areas of medicine (Shubayev et al., 2009). A good example of nanotechnology applications is brought by the use of iron oxide nanoparticles (ION), due to their multifunctional properties, conferred by their small size, superparamagnetism, and biocompatibility (Mou et al., 2011). In fact, ION have the potential to be extensively used for the improvement of site-specific drug delivery to cells, tissues, or even organs, as well as in the enhancement of magnetic resonance imaging contrast, hyperthermia treatments in cancer therapy, magnetofection, stem cell therapy and gene delivery (Hong et al., 2011; Muller et al., 2007; Naqvi et al., 2010; Shubayev et al., 2009). To prevent the precipitation of iron oxide cores, ION for medical imaging are always coated with a layer of protective and biocompatible colloid, usually a polymer that acts as a steric and/or electrostatic stabilizer (Roohi et al., 2012). In particular, the polyacrylic acid (PAA) coating is an aqueous soluble polymer with a high density of reactive functional groups that make it very attractive in biomedicine, mainly due to its capability to form flexible polymer chain-protein complexes trough electrostatic, hydrogen bonding or hydrophobic interactions (Pineiro-Redondo et al., 2011).

* Corresponding author. Tel.: +351 220428675.
E-mail address: egracas@ff.up.pt (E. Fernandes).

0378-4274/$ – see front matter © 2013 Elsevier Ireland Ltd. All rights reserved.
http://dx.doi.org/10.1016/j.toxlet.2013.11.020

Surface coating and size affect biodistribution, plasma half-life, and extent of cellular uptake of nanoparticles (Muller et al., 2007; Roohi et al., 2012). *In vivo*, large ION (comprised between 60 and 100 nm) are rapidly phagocytosed by cells of the reticuloendothelial system in the liver and spleen, having thereby a short blood half-life. On the other hand, small ION (<60 nm) are not readily phagocytosed, which results in a longer plasma half-life and higher availability to other cells and organs of the immune system (Matsushita et al., 2011; Muller et al., 2007). Although ION may represent extremely useful tools in biomedicine, there are still few studies assessing their possible effects in the above mentioned host defense systems that are usually recruited for their clearance from the body. It was previously reported that ION have the ability to decrease the monocytes' viability (Zhu et al., 2011), as well as to induce the production of reactive oxygen species (ROS) on macrophages and decrease their viability, through apoptosis, in a concentration-dependent manner (Lunov et al., 2010a,b; Naqvi et al., 2010). However, the effect of ION on neutrophils is still to be clarified, this being the purpose of the present study.

Human neutrophils are the most abundant leukocytes in blood and constitute the first line of innate host defense against pathogens and associated acute inflammations (Bockmann et al., 2001; Fadeel et al., 1998; Freitas et al., 2008). Neutrophils are mobilized to the sites of invasion or inflammation, ingesting pathogens into phagosomes (Fadeel et al., 1998; Freitas et al., 2009a,b, 2008). The phagosome fuses with neutrophilic cytoplasmatic granules containing cytotoxic enzymes, namely lysosomal enzymes, as well as NAPDH oxidase and myeloperoxidase, which are responsible for the oxidative burst and consequent generation of ROS (Brasen et al., 2010; Fadeel et al., 1998; Freitas et al., 2009a,b, 2008). While these events are important for the elimination of pathogens, it is not clear how these cells cope with ION, and which consequences ION have on their lifespan.

Neutrophils have a short lifespan that is regulated by the onset of apoptosis. In fact, apoptosis in mature neutrophils is a constitutive process that results in a rapid turnover of the circulating neutrophil population [(5×10^{10} neutrophils per day are released from bone marrow (Goncalves et al., 2010)] with a $t_{1/2}$ of 5 to 6 h *in vivo* and 24 to 36 h *in vitro* (Watson et al., 1998). This process is essential for the normal resolution of inflammation in tissues, because it culminates in the recognition and clearance of the apoptotic neutrophils by macrophages (Rowe et al., 2002). While it has been postulated that these cells undergo apoptosis spontaneously (Goncalves et al., 2010; Rowe et al., 2002), external factors may influence this process, as we have previously shown (Freitas et al., 2013a), and therefore the influence of the different nanoparticles in this process requires further investigation.

Necrosis is an unorganized process associated with extensive damage, resulting in an intense inflammatory response. In neutrophils, this process may occur due to a lack of intracellular adenosine triphosphate (ATP), necessary to apoptosis. Due to the energy-consumptive oxidative burst and consequent depletion of intracellular ATP stores, these cells may be unable to maintain cellular homeostasis and membrane integrity, occurring an influx of water and extracellular ions. This influx will trigger the intracellular organelles and the whole cell swelling, with all the cellular contents being released into the extracellular fluid and surrounding tissues (Kroemer et al., 2007; Turina et al., 2005).

Considering the lack of knowledge on the activation of neutrophils and modulation of their lifespan by ION, the aim of this work was to evaluate the effects of ION in magnetite form (polyacrylic acid (PAA)-coated and non-coated) on human neutrophils, namely their capacity to activate the oxidative burst and to modify their lifespan through necrosis and/or apoptosis.

2. Materials and methods

2.1. Materials

Human venous blood was obtained from healthy human volunteers from Hospital de Santo António (Porto, Portugal). Histopaque 1077, histopaque 1119, Dulbecco's phosphate buffer saline, without calcium chloride and magnesium chloride (PBS) [2.68 mM KCl, 0.14 M NaCl, 1.21 mM KH_2PO_4, 8.10 mM Na_2HPO_4], RPMI 1640 medium, L-glutamine, penicillin, streptomycin, trypan blue solution 0.4%, phorbol 12-myristate 3-acetate (PMA), dihydrorhodamine 123 (DHR), diphenyleneiodonium chloride (DPI), *N*-acetyl-Ile-Glu-Thr-Asp-*p*-nitroanilide, *N*-acetyl-Asp-Glu-Val-Asp-*p*-nitroanilide, Ac-Leu-Glu-His-Asp-*p*-nitroanilide, potassium phosphate, phenlymethylsulfonyl fluoride, leupeptin, pepstatin, HEPES and ethylenediamine tetraacetic acid (EDTA) were obtained from Sigma Chemical Co (St Louis, USA). β-Nicotinamide adenine dinucleotide reduced dipotassium salt (NADH), sodium pyruvate, CHAPS, triton™ X-100, dithiothreitol, ferrous chloride, ferric chloride, NH_4OH, KCl and polyacrylic acid PAA (average M_w 1800) were obtained from Sigma-Aldrich (St Louis, USA). Hemacolor® was obtained from Merck (Darmstadt, Germany). (±)-Nutlin-3 was acquired from Cayman (Michigan, USA). Sucrose was obtained from Mallinckrodt Chemical Works (St Louis, USA). Annexin-V-FLUOS Staining Kit was obtained from Roche Diagnostics GmbH (Mannheim, Germany). Nuclear Extract Kit and TransAM™ p53 Transcription Factor Assay Kits were acquired from Active Motif (La Hulpe, Belgium).

2.2. Methods

2.2.1. Synthesis of iron oxide nanoparticles

ION "non-coated" magnetite particles were prepared following previous well-known procedures with some modifications (Massart et al., 1995). In brief, the procedure is based on the chemical co-precipitation of a mixture of Fe(II) and Fe(III) chloride salts (molar ratio 2:1) using NH_4OH in a degassed 1 M KCl aqueous solution at 60 °C. The dark precipitate was washed several times with deoxygenated water, and finally the particles were stored at pH 9.6 (well-above their isoelectric point: 6.5). For the PAA-coated particles, PAA (25% w/w with respect to the Fe(II) salt) was added to the reaction medium.

2.2.2. Characterization of iron oxide nanoparticles

Non-coated and PAA-coated ION were characterized using transmission electron microscopy (TEM) (Hitachi H-7000, Japan). Determination of the hydrodynamic size and zeta potential of the nanoparticles in water suspensions, in function of pH and [NaCl], as well as in the medium used for the studies on human neutrophils [RPMI 1640 (pH = 7.4) supplemented with 10% fetal bovine serum, 2 mM L-glutamine, 100 U/mL penicillin and 0.1 mg/mL streptomycin] were made using a nanoparticle analyzer SZ-100 (HORIBA Scientific) (DPSS laser 532 nm). Before the dilutions, ION were sonicated for 5 min in order to avoid the formation of aggregates before the preparation of the samples.

2.2.3. Isolation of human neutrophils by the gradient density centrifugation method

Following informed consent, venous blood was collected from healthy human volunteers by antecubital venipuncture, into vacuum tubes with K_3EDTA. The isolation of human neutrophils was performed by the gradient density centrifugation method as previously reported in (Freitas et al., 2008). RPMI 1640 supplemented with 10% fetal bovine serum, 2 mM L-glutamine, 100 U/mL penicillin and 0.1 mg/mL streptomycin was the incubation medium used.

2.2.4. Measurement of neutrophils' oxidative burst

The measurement of neutrophils' oxidative burst was performed by fluorescence, by monitoring the oxidation of DHR to rhodamine 123 by neutrophil-generated reactive species (Freitas et al., 2009a,b). Neutrophils (3×10^6 mL^{-1}) were incubated for 24 h with PAA-coated and non-coated ION (4, 20 and 100 μg/mL) and DHR (10 μM) at 37 °C. At the end of this incubation period, cells were centrifuged (400*g*, 5 min at 20 °C) and the supernatant was discarded. The pellets were resuspended in 300 μL RPMI 1640 medium and the fluorescence was measured in a microplate reader ($\lambda_{excitation}$ = 485 nm and $\lambda_{emission}$ = 520 nm). PMA was used as positive control. Simultaneously it was performed an experiment where the neutrophils were incubated with ION (20 and 100 μg/mL), DPI (20 μM) and DHR (10 μM).

2.2.5. Evaluation of cellular necrosis

2.2.5.1. Trypan blue assay. Trypan blue assay was performed according to (Freitas et al., 2010). Neutrophils (2×10^6 mL^{-1}) were incubated with PAA-coated and non-coated ION (4, 20 and 100 μg/mL) for 24 h, at 37 °C. At the end of the incubation period, 20 μL aliquots of neutrophil suspensions were added to an equal volume of 0.4% trypan blue in a microtube and gently mixed. After 2 min on ice, the neutrophil number and viability (viable cells excluding trypan blue) were determined. This dye enters in the necrotic cells, staining them blue, while the living cells remain discoloured.

2.2.5.2. Lactate dehydrogenase (LDH) leakage assay. LDH leakage was performed according to (Freitas et al., 2010). This release is directly related to the cellular membrane disruption and, consequently, cellular death. Neutrophils (2×10^6 mL^{-1}) were incubated with PAA-coated and non-coated ION (4, 20 and 100 μg/mL) for 24 h at 37 °C. At the end of the incubation period, cells were centrifuged (6500*g*, 2 min at 4 °C) and the supernatant was collected. Simultaneously it was performed a control assay with sonicated cells in order to determine the total LDH. LDH activity was determined by following the rate of oxidation of NADH at 340 nm.

2.2.6. Evaluation of apoptosis

2.2.6.1. Evaluation of apoptosis by morphology. Evaluation of apoptosis by morphology was performed according to (Saldanha-Gama et al., 2010). Neutrophils (1×10^6 mL^{-1}) were incubated with PAA-coated and non-coated ION (4, 20 and 100 μg/mL) for 16 and 24 h at 37 °C. At the end of these incubation periods, cells were centrifuged in a microscopic slide (Cytospin, 300 rpm, 6 min at room temperature), stained with Hemacolor®, and counted under light microscopy to determine the proportion of cells showing characteristic apoptotic morphology (round and dark nucleus that results from the chromatin condensation occurring in apoptosis, signaled with arrows). At least 400 cells were counted per slide.

2.2.6.2. Evaluation of apoptosis by flow cytometry. Apoptotic neutrophils were analysed by flow cytometry after simultaneous staining with annexin-V labeled with fluorescein and propidium iodide, according to (Sladek et al., 2005). Annexin-V is a Ca^{2+}-phospholipid-binding protein that has a high affinity for phosphatidylserine and propidium iodide is impermeant to live cells and apoptotic cells, but stains dead cells with red fluorescence, tightly binding to the nucleic acids in the cell. The commercial Annexin-V-FLUOS Staining Kit (Roche Diagnostics GmbH, Mannheim Germany) was used according to the manufacturer's instructions. Neutrophils (1×10^6 mL^{-1}) were incubated with PAA-coated and non-coated ION (4, 20 and 100 μg/mL) for 16 h, at 37 °C. At the end of the incubation period, cells were centrifuged (400*g*, 5 min at 20 °C) and the supernatant was discarded. Pellets were resuspended in 1 mL of PBS and centrifuged (200*g*, 5 min at 20 °C). After centrifugation, pellets were resuspended in 100 μL of annexin-V and were incubated for 15 min in the dark. After incubation, samples were centrifuged (200*g*, 5 min at 20 °C) and the pellet was resuspended in 300 μL PBS and 3 μL propidium iodide.

Fluorescence signals for each sample were collected using a Becton Dickinson FACSCalibur™ flow cytometer (Becton Dickinson, Inc., Mountain View, CA, USA) equipped with a 488 nm argon-ion laser, as described in Freitas et al. (2013b).

2.2.7. Evaluation of pro-apoptotic signalling

2.2.7.1. p53-DNA binding. Neutrophils (8×10^6 mL^{-1}) were incubated with PAA-coated and non-coated ION (4, 20 and 100 μg/mL) for 24 h at 37 °C. At the end of this incubation period, neutrophils' desoxyribonucleic acid (DNA) was extracted using a Nuclear Extract Kit (Active Motif) according to manufacturer's instructions, with slight modifications. In order to obtain a more efficient nuclear extraction, sonication (4 cycles, 12 s) was performed to disrupt neutrophils' nuclear membrane before centrifugation (14,000*g*, 10 min 4 °C). Cell lysates were diluted to 3.5 μg total protein with lysis buffer and used for the p53 determination. For this purpose, TransAM™ p53 Transcription Factor Assay Kit was used according to manufacturer's instructions, as described in Thompson et al. (2004). (±)-Nutlin-3 was used as positive control.

2.2.7.2. Measurement of caspases 3, 8 and 9 activities. Neutrophils (10×10^6 mL^{-1}) were incubated with PAA-coated and non-coated ION (4, 20 and 100 μg/mL) for 16 and 24 h at 37 °C. At the end of these incubation periods, cells were centrifuged (400*g*, 5 min at 20 °C) and the supernatant was discarded. Pellets were resuspended in 100 μL of lysis buffer (10 mM potassium phosphate, 1 mM EDTA, 0.5% Triton X-100, 2 mM phenlymethylsulfonyl fluoride, 3 μg/mL aprotinin, 10 μg/mL leupeptin, 10 μg/mL pepstatin, and 10 mM dithiothreitol). After incubation for 20 min on ice, samples were centrifuged at 18,000*g* for 20 min, at 20 °C. An aliquot of each sample (50 μL) was diluted to a final volume of 250 μL in assay buffer consisting of 50 mM HEPES, 10% sucrose, 0.1% CHAPS, and 10 mM dithiothreitol supplemented with 100 μM of the colorimetric caspase-3, 8 or 9 substrates (*N*-acetyl-Asp-Glu-Val-Asp-*p*-nitroanilide, *N*-acetyl-Ile-Glu-Thr-Asp-*p*-nitroanilide and Ac-Leu-Glu-His-Asp-*p*-nitroanilide, respectively). Samples were incubated for 120 min at 37 °C and the absorbance was measured at 405 nm (Weinmann et al., 1999).

2.2.8. Statistical analysis

Statistics were calculated using GraphPad Prism™ (version 5.0; GraphPad Software). The results are expressed as the mean ± SEM (from at least four individual experiments). Statistical comparison between groups was performed using the one-way analysis of variance, followed by Bonferroni's post hoc test. The values of p lower than 0.05 were considered as statistically significant.

3. Results

3.1. Characterization of iron oxide nanoparticles

Both PAA-coated and non-coated ION particles have a similar size distribution, with a mean particle size of 9.9 ± 2.3 nm and 10.1 ± 2.4 nm (Mean ± SD) for the non-coated and PAA-coated ION, respectively (Figs. 1 and 2 of Appendices A and B). Although non-coated (without polymer) ION nanoparticles may be stable in water, they easily agglomerate by changing the pH (due to the change of the surface charge) or increasing the ionic strength (due to the shielding of surface charge). In fact, non-coated particles are only stable at basic pHs, and are already destabilized at pHs below ≈9 (surface charge ≈< −25 mV). However, PAA-coated particles are perfectly stable at neutral and even at slightly acid pHs (above ≈6)

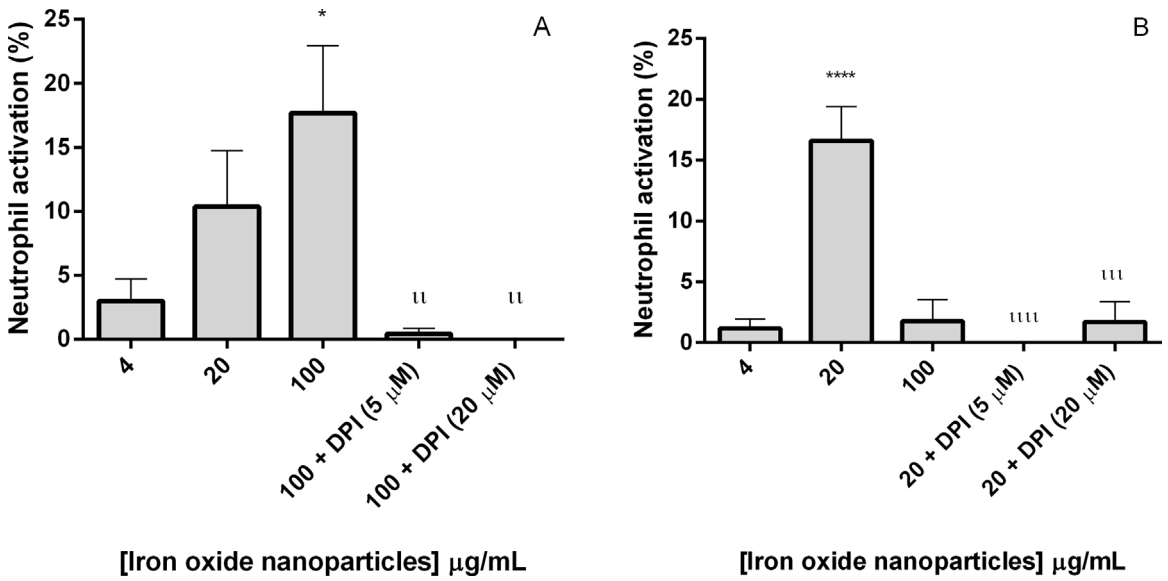

Fig. 1. Neutrophils' oxidative burst in cells exposed to (A) PAA-coated ION (4–100 μg/mL) and (B) non-coated ION (4–100 μg/mL) in the absence and presence of DPI, at 37 °C for 24 h. $^{*}p < 0.05$ and $^{****}p < 0.0001$ comparatively to control (without ION), $^{u}p < 0.01$ comparatively to 100 μg/mL PAA-coated ION and $^{uu}p < 0.001$ and $^{uuu}p < 0.0001$ comparatively to 20 μg/mL non-coated ION. Data are expressed as percentage of neutrophil activation. Values are given as mean ± SEM ($n \geq 4$).

(Fig. 3 of Appendices A and B). Concerning the stability is associated with the ionic strength, it was observed again that non-coated particles are destabilized already at NaCl concentrations ≈0.1 mM, while PAA-coated particles need ≈0.01 M to be destabilized (Fig. 4 of Appendices A and B). When the ION were dispersed in RPMI 1640 medium, the large hydrodynamic sizes observed and the fact that zeta potential was approximately 0 mV indicates that both types of nanoparticles tend to agglomerate when resuspended in this medium, though in much higher intensity in the case of non-coated ION (Fig. 5 of Appendices A and B).

3.2. Effect of ION on neutrophils' oxidative burst

Neutrophils' oxidative burst was assessed using the probe DHR (10 μM) in neutrophils exposed to PAA-coated and non-coated ION (4–100 μg/mL) and ION with DPI (20 μM) at 37 °C for 24 h (Fig. 1A and 1B). The neutrophils' oxidative burst was observed in the presence of both ION. This effect followed a concentration-dependent manner for PAA-coated nanoparticles, but in the case of non-coated ION, it occurred in a concentration-independent manner, having achieved the maximum activation at 20 μg/mL. The activation of oxidative burst triggered by both ION was approximately 20 times lower than positive control PMA (396 ± 49%). However, it was considered statistically significant, as it can be seen in Fig. 1A and B. Activation was blocked in the presence of DPI (20 μM), which means that the neutrophils' oxidative burst observed in the presence of both nanoparticles is due to NADPH oxidase activation.

3.3. Effect of ION on neutrophils' death by necrosis

No effect was found for any of the PAA-coated and non-coated ION (4–100 μg/mL) both at the trypan blue and LDH leakage assays (data not shown), which demonstrates that the ION studied do not seem to disrupt the cellular membrane at the present experimental conditions.

3.4. Effect of ION on neutrophils' death by apoptosis

3.4.1. Apoptosis evaluated by morphology

As it can be observed in 2A and B and 3B, the percentage of apoptotic cells increased in the presence of PAA-coated ION relatively to control (without ION), in a concentration-dependent manner.

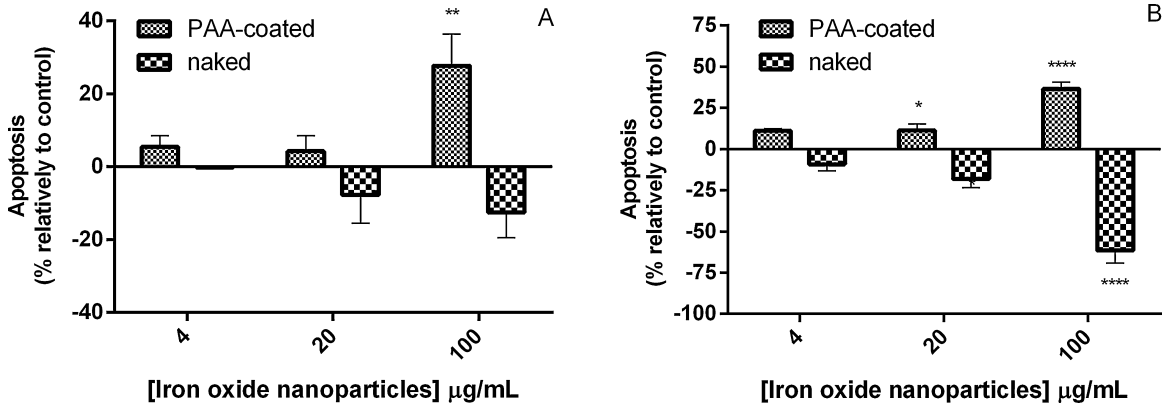

Fig. 2. Neutrophils' apoptosis assessed by microscopic morphology after exposure to PAA-coated and non-coated ION (4–100 μg/mL) at 37 °C: (A) 16 h and (B) 24 h. $^{*}p < 0.05$, $^{**}p < 0.01$ and $^{****}p < 0.0001$ comparatively to control (without ION). Data are expressed as percentage of apoptosis relatively to control. Values are given as mean ± SEM ($n \geq 4$).

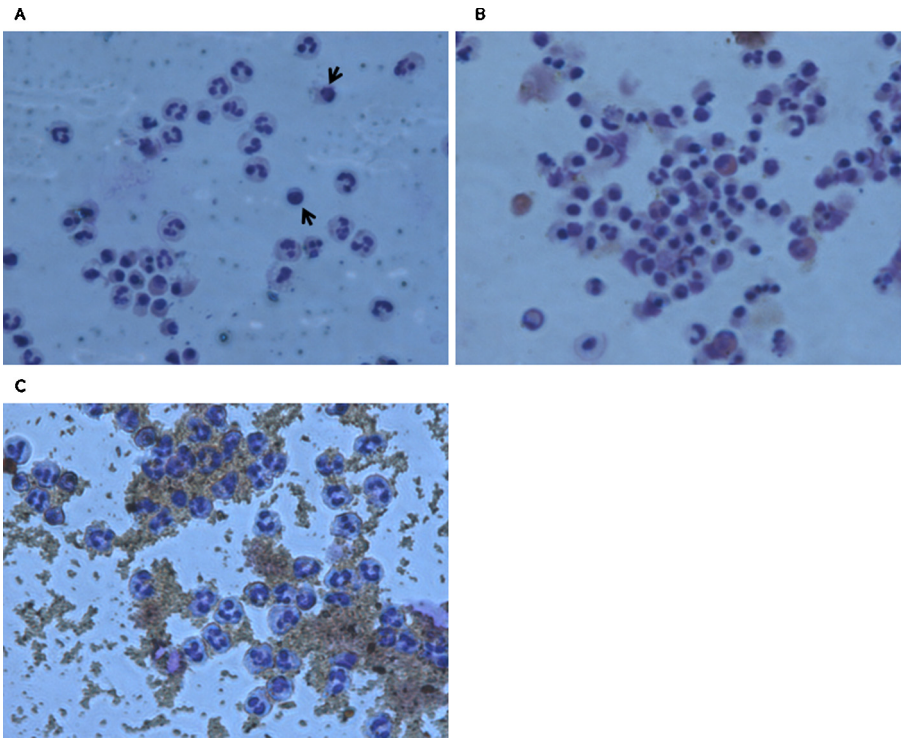

Fig. 3. Neutrophils' apoptosis assessed by microscopic morphology at 16 h: without ION (A), with 100 μg/mL PAA-coated ION (B) and 100 μg/mL non-coated ION (C) (amplification 40×). Arrowheads indicate apoptotic neutrophils.

On the contrary, the percentage of apoptotic cells decreased in the presence of non-coated ION (2A and B and 3C), which indicates that these nanoparticles exert the opposite effect of PAA-coated ION, having the capacity of protecting neutrophils from apoptosis.

3.4.2. Apoptosis evaluated by flow cytometry

It was verified that the proportion of annexin-V(+)/PI(−) cells increased in the presence of PAA-coated ION, in a concentration-dependent manner (4A and 5B). This demonstrates, once again, that PAA-coated ION cause acceleration of apoptotic death. On the contrary, the proportion of annexin-V(+)/PI(−) cells decreased in the presence of non-coated ION, in a concentration-dependent manner (4B and 5C). This result is in agreement with the previous results that demonstrate that this type of nanoparticles is able to protect neutrophils from apoptosis.

3.5. Apoptotic signalling

3.5.1. p53-DNA binding

Regarding PAA-coated ION, a marked heterogeneity was observed among subjects, evidencing two different groups of individuals' neutrophils: one of the groups (non-responders) did not present any increase in p53 activity in the presence of the nanoparticles, when compared to the control; the other group (responders) presented a significant increase in p53 activity in the presence of these nanoparticles, well evidenced for the concentrations of 20

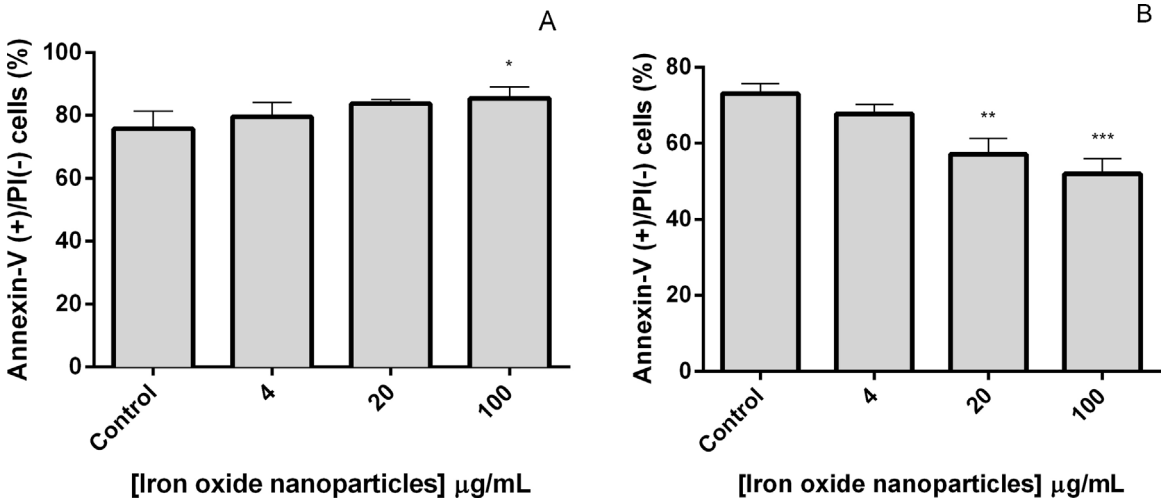

Fig. 4. Neutrophils' apoptosis assessed by flow cytometry after exposure to (A) PAA-coated ION (4–100 μg/mL) and (B) non-coated ION (4–100 μg/mL) at 37 °C for 16 h. $^{*}p < 0.05$, $^{**}p < 0.01$ and $^{***}p < 0.001$ comparatively to control. Data are expressed as percentage of annexin-V(+)/PI(−) cells. Values are given as mean ± SEM ($n \geq 4$).

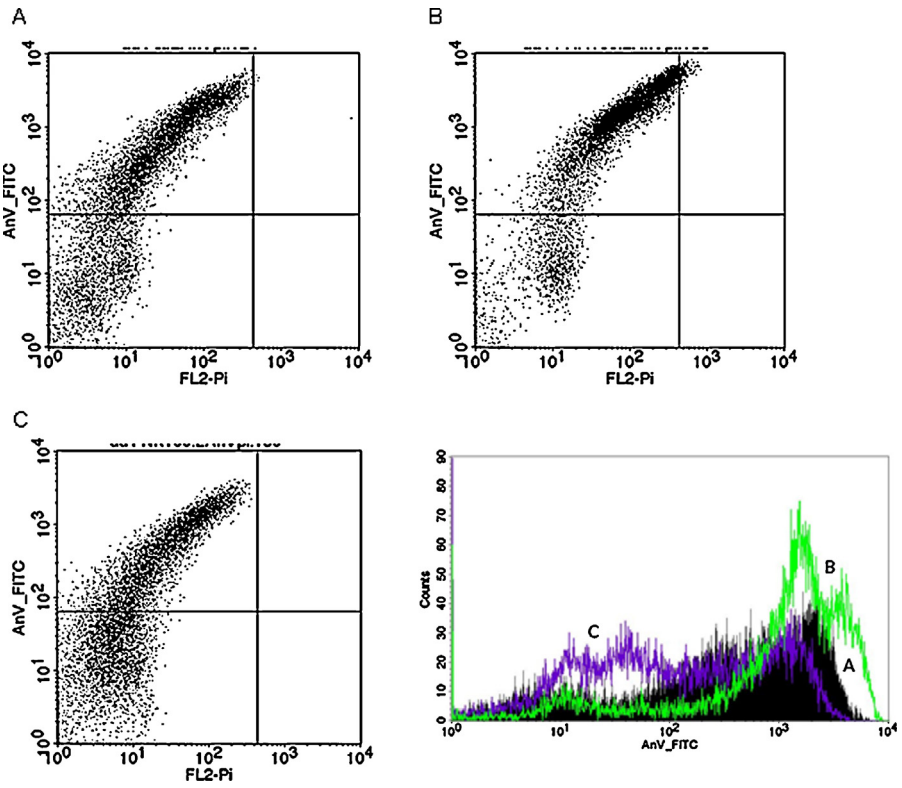

Fig. 5. Flow cytometric analysis of annexin V binding assay. Neutrophils incubated at 37 °C for 16 h without ION (A—black area) and with 100 μg/mL PAA-coated (B—green curve) and non-coated (C—blue curve) ION. (For interpretation of the references to color in this figure legend, the reader is referred to the web version of this article.)

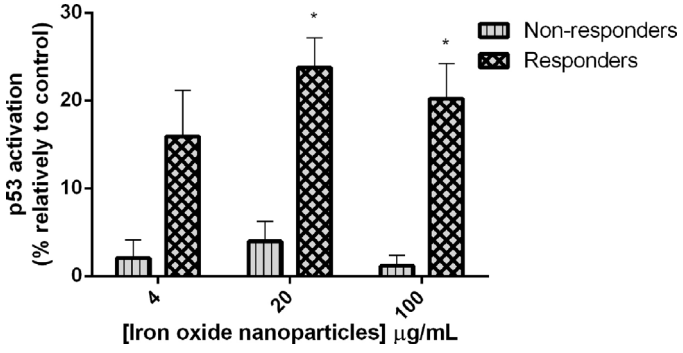

Fig. 6. p53 activation in neutrophils exposed to PAA-coated ION (4–100 μg/mL) at 37 °C for 24 h. *$p < 0.05$ comparatively to control (without ION). Data are expressed as percentage of p53 activation relatively to control. Values are given as mean ± SEM ($n \geq 4$).

and 100 μg/mL (Fig. 6). Non-coated ION did not influence p53 activity (data not shown).

3.5.2. *Measurement of caspases 3, 8 and 9 activities*

Concerning PAA-coated ION, it was observed that caspases 3, 8 and 9 activities were increased in the presence of ION, in a concentration-dependent manner (7A and B, 8A and 9A and B). For the non-coated ION, the opposite effect was observed for caspases 3 and 9, given that these nanoparticles exhibited the ability to inhibit caspases 3 and 9 activity, comparatively to control (without ION) (7A and B and 9A and B). However, they did not alter the caspase 8 activity comparatively to control (data not shown). These results are in agreement with those obtained in the evaluation of apoptosis.

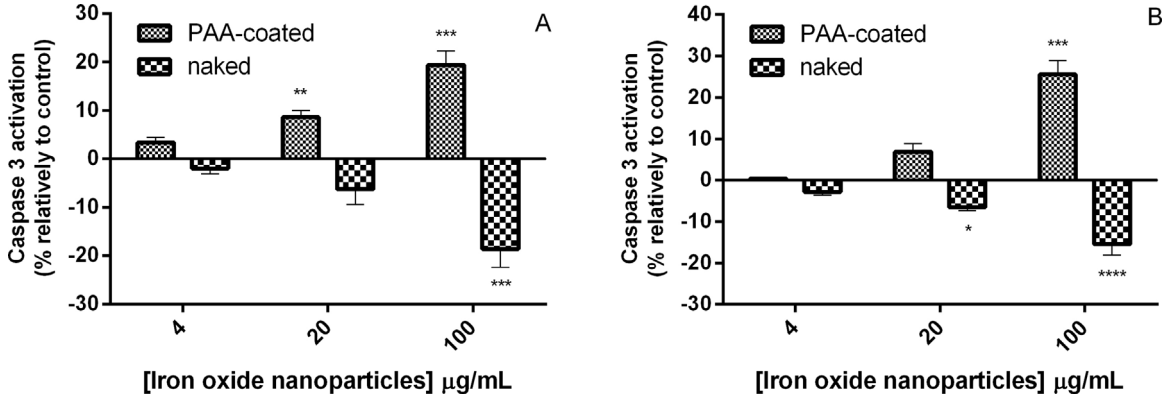

Fig. 7. Caspase 3 activity in neutrophils exposed to PAA-coated and non-coated ION (4–100 μg/mL) at 37 °C: (A) 16 h and (B) 24 h. *$p < 0.05$, **$p < 0.01$, ***$p < 0.001$ comparatively to control (without ION). Data are expressed as percentage of caspase 3 activation relatively to control. Values are given as mean ± SEM ($n \geq 4$).

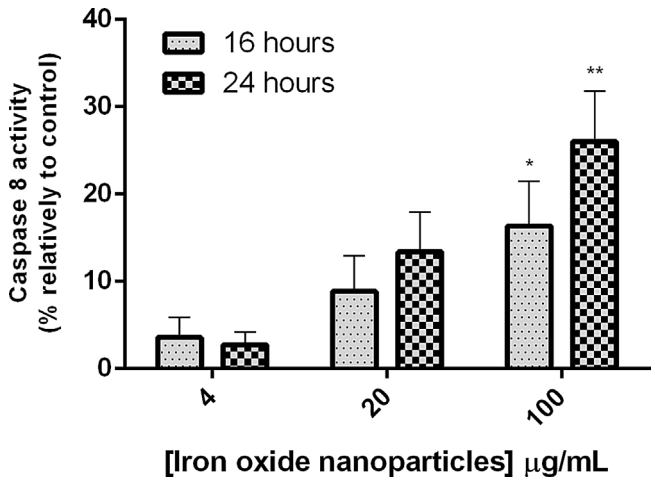

Fig. 8. Caspase 8 activity in neutrophils exposed to PAA-coated ION (4–100 μg/mL) at 37 °C for 16 and 24 h. $^{*}p < 0.05$ and $^{**}p < 0.01$ comparatively to control. Data are expressed as percentage of caspase 8 activation relatively to control (without ION). Values are given as mean ± SEM ($n \geq 4$).

4. Discussion

This work was undertaken to evaluate the putative capacity of PAA-coated and non-coated ION to activate the oxidative burst in human neutrophils and to modify their lifespan *in vitro*. It was clearly evidenced that both ION studied were able to trigger neutrophils' oxidative burst and that PAA-coated ION increased, while non-coated ION decreased, apoptotic signaling and apoptosis.

Neutrophil's oxidative burst occurred in a concentration-dependent manner following exposure to PAA-coated ION. For non-coated ION, the highest neutrophil activation was observed for 20 μg/mL, probably due to NADPH oxidase inhibition at the higher concentration tested (100 μg/mL). In both cases, the observed oxidative burst was reverted in the presence of a NADPH oxidase inhibitor (DPI), which demonstrates the full involvement of NADPH oxidase activation in the observed effect. This enzyme reduces molecular oxygen to superoxide radical $\left(O_2^{-}\cdot\right)$ in the presence of NADPH. After $O_2^{-}\cdot$ production, other ROS, namely hydrogen peroxide (H_2O_2), hypochlorous acid (HOCl), hydroxyl radical ($HO^{\bullet}$) and singlet oxygen ($^1O_2$), and RNS, particularly nitric oxide ($^{\bullet}NO$) and peroxynitrite anion ($ONOO^{-}$), are formed in cascade (Brasen et al., 2010; Freitas et al., 2009a,b), which characterizes the neutrophils' oxidative burst. Although the interaction of PAA-coated ION with neutrophils is reported for the first time in the present study, ION with other types of coatings have been shown to promote ROS production in other cell types. Bae et al. (2011), using 2′,7′-dichlorofluorescein diacetate (DCFH-DA), demonstrated that carboxydextran-coated ION increased intracellular levels of ROS in mouse hepatocytes, and Lunov et al. (2010a,b) demonstrated that carboxydextran-coated superparamagnetic ION induced a time-dependent ROS production in human macrophages. Choi et al. (2009) also showed that anionic clay layered ION caused an increase in ROS production in human lung cancer A549 cells. On the other hand, Karlsson et al. (2008) observed, also using DCFH-DA, that non-coated ION do not potentiate the ROS production in A549 type II lung epithelial cells. Since the concentrations tested were similar in these different studies, it is important to highlight that the ION effects can be distinct according to the type of coating, or the type of cells tested. While neutrophils, monocytes and macrophages may react to ION through the activation of NADPH oxidase, as shown in the present study for neutrophils, other mechanisms may also be involved in the production of ROS. Shubayev et al. (2009) hypothesized that ION induce redox cycling and catalytic chemistry *via* Fenton reaction. Our study did not ascertain the intervention of ION in this reaction. Nevertheless, once NADPH oxidase is activated, the cascade of ROS and RNS production succeeds, and $HO^{\bullet}$ is expected to be generated through the Fenton reaction.

The formation of ROS and RNS, and ensuing oxidative stress may intervene in apoptotic pathways, namely through the activation of the mitochondrial apoptotic pathway (Franco et al., 2009). In fact, there are reports concerning the ability of ROS and RNS to interfere directly in apoptosis through mitochondrial membrane permeabilization and cytochrome c release, as well as in Jun N-terminal protein kinase (JNK) activation (Circu and Aw, 2010; Huang et al., 2008). Another pathway involving ROS and RNS is through direct activation of p53 (Sharma et al., 2012). It is thought that ROS and RNS-induced DNA damage may trigger p53 activation (Simbula et al., 2007). Phosphorylation in response to DNA damage enhances the interaction of p300 and PCAF with p53, thereby leading to p53 acetylation and consequent activation (Sakaguchi et al., 1998). Therefore, these two pathways may be connected to each other. In fact, the activation of p53 triggers the expression of Bax and Noxa, two pro-apoptotic proteins that induce an increase in mitochondrial permeability, leading to the release of cytochrome c, apoptosis inducing factor (AIF) and Diablo/Smac and the consequent mitochondrial apoptotic pathway (Chen and Shi, 2002). Besides the above rationale, the expression of pro-apoptotic proteins and/or the decrease in anti-apoptotic proteins may be activated by several other factors and/or stimuli. For example, Miyake et al. (2012) stated that rapamycin induces p53-independent mitochondrial apoptosis by decreasing anti-apoptotic proteins.

In the present study, p53 activation by PAA-coated ION was demonstrated, for the first time, in part of the subjects tested. In line

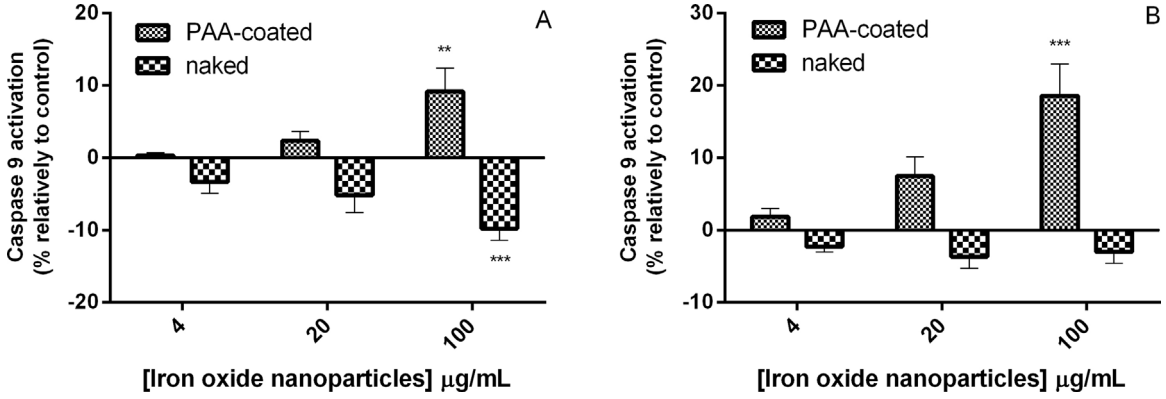

Fig. 9. Caspase 9 activity in neutrophils exposed to PAA-coated and non-coated ION (4–100 μg/mL) at 37 °C: (A) 16 h and (B) 24 h. $^{**}p < 0.01$ and $^{***}p < 0.001$ comparatively to control (without ION). Data are expressed as percentage of caspase 9 activation relatively to control. Values are given as mean ± SEM ($n \geq 4$).

with these results, Wu et al. (2012) and Wu and Sun (2011) have reported before that non-coated ION induced p53 gene expression and increased phosphorylation levels of p53 in PC12 cells, and that this activation is associated with increased levels of Bax and decreased levels of Bcl-2. On the other hand, the opposite was also reported by Huang et al. (2009), in which it was referred slight decreases in p53 expression in ferucarbotran-labeled human mesenchymal stem cells, and it was also reported that ION do not change the expression of p53 mRNA in K562/A02 cells (Chen et al., 2009). While this activation may represent a link, as described above, between ROS and an apoptotic pathway, the truth is that p53 did not demonstrate to be essential for neutrophil activation in our study, given that apoptosis activation occurred for all donors tested with PAA-coated ION, while p53 activation occurred only for one group (named responders).

In this study, the proportion of apoptotic cells was increased in the presence of PAA-coated ION, in a concentration-dependent manner. However, the results obtained with these ION seem to be more evident for the morphologic assay, comparatively to the flow cytometry assay. This happens because, when cells are annexin V+, this means that phosphatidylserine was translocated to the outer cell membrane leaflet, an event that occurs during apoptotic process (Lunov et al., 2010a,b). Thus, it is possible that some of the cells have already initiated the process of apoptosis, even in control, although they do not present the characteristic apoptotic morphology when they are counted on the morphologic assay, presenting already the phosphatidylserine on the outer side of the membrane leaflet. Therefore, annexin V+ control cells is approximately 80% and, consequently, the increase after treatment with PAA-coated ION will not be so evident as it is in cytospin assay. Nevertheless, it is evident that these ION have the ability to accelerate a natural feature of neutrophils that correspond to a short lifespan mediated by apoptosis. In contrast, in the presence of non-coated ION, the proportion of apoptotic cells decreased in a concentration-dependent manner. Likewise, Lunov et al. (2010a,b) reported that exposure of macrophages to carboxydextran-coated superparamagnetic ION triggered translocation of phosphatidylserine to the outer cell membrane leaflet, indicating increased apoptosis. Choi et al. (2009) also reported that non-coated ION triggered the same in human lung cancer A549 cells. On the other hand, it was previously reported a lack of effect of non-coated ION on mature mouse dendritic cells' apoptosis (Mou et al., 2011). Once again, it is important to highlight that the effect of ION is not necessarily the same in different types of cells, namely in what concerns to the production of reactive species and ensuing apoptotic signaling.

For a better clarification of the apoptotic pathways involved in the observed pro- and anti-apoptotic effects, caspases 3, 8 and 9 activities were assessed. It was observed that the activities of caspases 3, 8 and 9 were increased in the presence of PAA-coated ION, in a concentration-dependent manner. Given that caspase 8 is involved in the extrinsic apoptotic pathway and caspase 9 is involved in the mitochondrial apoptotic pathway (Chen and Shi, 2002; Franco et al., 2009; Letuve et al., 2002), these data suggest that PAA-coated ION interfere with both apoptotic pathways, promoting the apoptosis acceleration by both pathways. Regarding caspase 3, as this is one of the effector caspases, intervening in a late apoptosis stage, common to mitochondrial and extrinsic pathways, its increase just corroborates the activation of signaling caspases. Caspase 3 activity increase was previously shown to be triggered by carboxydextran-coated ION in a mouse liver cell line (NCTC 1469) (Bae et al., 2011). Likewise, Lunov et al. (2010a,b) reported that carboxydextran-coated superparamagnetic ION and ultrasmall superparamagnetic ION increased the caspase 3 activity in human macrophages. Dilnawaz et al. (2012) also reported an increase in caspases 3 and 9 activation caused by transferring-conjugated curcumin-loaded superparamagnetic ION in the leukemic cell line K562. It was also found by Zhang et al. (2011) that tetraheptylammonium-coated ION have the capacity to increase the ability of daunorubucin to induce apoptosis in K562 cells through caspase 8 activation, which is in accordance to our results. These results suggest that coating may be important for the activation of apoptotic signaling, by maintaining ION dispersed, though the type of coating may not have an important role in the final effect, though this assumption needs further evaluation. For non-coated ION, it was observed that these nanoparticles exhibit the capacity to inhibit caspases 3 and 9 activation, explaining why these nanoparticles induce a delay in the apoptotic process. These results are in accordance with Khan et al. (2011), which showed that non-coated ION reduced caspase 9 activity in HeLa cells. The fact that non-coated ION inhibited caspases 3 and 9 but did not interfere with caspase 8 demonstrates that these nanoparticles only inhibited the mitochondrial apoptotic pathway, not interfering with the extrinsic apoptotic pathway. Although, at the present stage, the mechanism(s) involved could not be determined, this is an important finding to be considered upon exposure to ION in the workplace and in the environment.

This study also shows that none of the studied ION studied seem to alter neutrophils' lifespan by necrosis. These results are in agreement with the studies of Karlsson et al. (2008), which demonstrated that non-coated ION did not influence cellular necrosis in cultured A549 type II lung epithelial cells. Furthermore, Wang et al. (2009) performed a study in order to assess the dextran-coated ION effect on rat adipose-derived stem cells, reaching the same conclusions. Hussain et al. (2005) used the LDH leakage methodology and stated that the non-coated ION do not produce cytotoxicity up to the concentration of 100 μg/mL in BRL 3A RAT liver cells. However, for similar concentrations, Choi et al. (2009) reported that non-coated ION cause an increase in LDH leakage in human lung cancer A549 cells, which means that these nanoparticles can have different toxicologic mechanisms, according to the cells they are in contact with.

Concerning the limitations of the present study, the fact that it was performed *in vitro* does not consider the interaction existing between different cells that occur *in vivo*. Therefore, the factors produced by adjacent cells that occur *in vivo* and may influence the mode how different physiological processes occur, namely apoptosis and neutrophil activation, are not taken into account in this study. Another factor that cannot be studied *in vitro* is the bone marrow and macrophage response to a smaller neutrophils' lifespan, and therefore how a new equilibrium may be reached *in vivo*. The concentrations used in our study do not seem to constitute a limitation, since they are in accordance with the ones used in therapeutic applications: for magnetic resonance imaging, the concentration usually used is around 45 μmol Fe/kg, which is about the concentration of 70 μg/mL (for 50 kg human weight and 5000 mL human blood volume) (Apopa et al., 2009).

5. Conclusion

In this study it was evaluated the ability of PAA-coated and non-coated ION to induce oxidative burst in human neutrophils and to influence the respective death trends. The obtained results show that both ION induce oxidative burst through NAPDH-oxidase activation. It was also shown that, while necrosis was not affected, PAA-coated ION accelerate the apoptotic death of human neutrophils by the mitochondrial and extrinsic pathways. p53 revealed not to be essential to this effect. However, for some donors, PAA-coated ION showed to be able to activate p53. Non-coated ION showed to inhibit the mitochondrial pathway, not interfering with the extrinsic pathway.

Though these effects still need to be confirmed *in vivo*, the observed effects may have important clinical implications in the

event of their use for the improvement of site-specific drug or gene delivery, in magnetic resonance imaging contrast, hyperthermia treatments in cancer therapy, magnetofection, and stem cell therapy.

Conflict of interest statement

None declared.

Acknowledgments

Authors declare no conflicts of interest concerning the present study. Diana Couto and Vânia Vilas-Boas acknowledge the FCT financial support for the Ph.D. grants (SFRH/BD/72856/2010 and SFRH/BD/82556/2011, respectively) and Marisa Freitas for her Pos-doc grant (SFRH/BPD/76909/2011), in the ambit of "POPH–QREN—Tipologia 4.1—Formação Avançada" co-sponsored by FSE and national funds of MCTES. The authors greatly acknowledge the financial support given by Reitoria da Universidade do Porto and Santander Totta for Projectos IJUP 2011.

Appendix A. Supplementary data

Supplementary data associated with this article can be found, in the online version, at http://dx.doi.org/10.1016/j.toxlet.2013.11.020.

References

Apopa, P.L., et al., 2009. Iron oxide nanoparticles induce human microvascular endothelial cell permeability through reactive oxygen species production and microtubule remodeling. Part. Fibre Toxicol. 6, 1.
Bae, J.E., et al., 2011. The effect of static magnetic fields on the aggregation and cytotoxicity of magnetic nanoparticles. Biomaterials 32 (35), 9401–9414.
Bockmann, S., et al., 2001. Delay of neutrophil apoptosis by the neuropeptide substance P: involvement of caspase cascade. Peptides 22 (4), 661–670.
Brasen, J.C., et al., 2010. On the mechanism of oscillations in neutrophils. Biophys. Chem. 148 (1-3), 82–92.
Chen, B., et al., 2009. Magnetic nanoparticle of Fe_3O_4 and 5-bromotetrandrin interact synergistically to induce apoptosis by daunorubicin in leukemia cells. Int. J. Nanomed. 4, 65–71.
Chen, F., Shi, X., 2002. Intracellular signal transduction of cells in response to carcinogenic metals. Crit. Rev. Oncol. Hematol. 42 (1), 105–121.
Choi, S.J., et al., 2009. Toxicological effects of inorganic nanoparticles on human lung cancer A549 cells. J. Inorg. Biochem. 103 (3), 463–471.
Circu, M.L., Aw, T.Y., 2010. Reactive oxygen species, cellular redox systems, and apoptosis. Free Radical Biol. Med. 48 (6), 749–762.
Dilnawaz, F., et al., 2012. Transferrin-conjugated curcumin-loaded superparamagnetic iron oxide nanoparticles induce augmented cellular uptake and apoptosis in K562 cells. Acta Biomater. 8 (2), 704–719.
Fadeel, B., et al., 1998. Involvement of caspases in neutrophil apoptosis: regulation by reactive oxygen species. Blood 92 (12), 4808–4818.
Franco, R., et al., 2009. Environmental toxicity, oxidative stress and apoptosis: menage a trois. Mutat. Res. Genet. Toxicol. Environ. Mutagen. 674 (1-2), 3–22.
Freitas, M., et al., 2013a. Nickel induces apoptosis in human neutrophils. Biometals 26 (1), 13–21.
Freitas, M., et al., 2013b. Acetaminophen prevents oxidative burst and delays apoptosis in human neutrophils. Toxicol. Lett. 219 (2), 170–177.
Freitas, M., et al., 2010. Nickel induces oxidative burst, NF-kappaB activation and interleukin-8 production in human neutrophils. J. Biol. Inorg. Chem. 15 (8), 1275–1283.
Freitas, M., et al., 2009a. Optical probes for detection and quantification of neutrophils' oxidative burst: a review. Anal. Chim. Acta 649 (1), 8–23.
Freitas, M., et al., 2008. Isolation and activation of human neutrophils in vitro. The importance of the anticoagulant used during blood collection. Clin. Biochem. 41 (7–8), 570–575.
Freitas, M., et al., 2009b. Optimization of experimental settings for the analysis of human neutrophils oxidative burst in vitro. Talanta 78 (4–5), 1476–1483.
Goncalves, D.M., et al., 2010. Activation of human neutrophils by titanium dioxide (TiO_2) nanoparticles. Toxicol. In Vitro 24 (3), 1002–1008.
Hong, S.C., et al., 2011. Subtle cytotoxicity and genotoxicity differences in superparamagnetic iron oxide nanoparticles coated with various functional groups. Int. J. Nanomed. 6, 3219–3231.
Huang, D.M., et al., 2009. The promotion of human mesenchymal stem cell proliferation by superparamagnetic iron oxide nanoparticles. Biomaterials 30 (22), 3645–3651.
Huang, J., et al., 2008. Reactive oxygen species mediate oridonin-induced HepG2 apoptosis through p53, MAPK, and mitochondrial signaling pathways. J. Pharmacol. Sci. 107 (4), 370–379.
Hussain, S.M., et al., 2005. In vitro toxicity of nanoparticles in BRL 3A rat liver cells. Toxicol. In Vitro 19 (7), 975–983.
Karlsson, H.L., et al., 2008. Copper oxide nanoparticles are highly toxic: a comparison between metal oxide nanoparticles and carbon nanotubes. Chem. Res. Toxicol. 21 (9), 1726–1732.
Khan, J.A., et al., 2011. Magnetite (Fe_3O_4) nanocrystals affect the expression of genes involved in the TGF-beta signalling pathway. Mol.Biosyst. 7 (5), 1481–1486.
Kroemer, G., et al., 2007. Mitochondrial membrane permeabilization in cell death. Physiol. Rev. 87 (1), 99–163.
Letuve, S., et al., 2002. Critical role of mitochondria, but not caspases, during glucocorticosteroid-induced human eosinophil apoptosis. Am. J. Respir. Cell Mol. Biol. 26 (5), 565–571.
Lunov, O., et al., 2010a. The effect of carboxydextran-coated superparamagnetic iron oxide nanoparticles on c-Jun N-terminal kinase-mediated apoptosis in human macrophages. Biomaterials 31 (19), 5063–5071.
Lunov, O., et al., 2010b. Lysosomal degradation of the carboxydextran shell of coated superparamagnetic iron oxide nanoparticles and the fate of professional phagocytes. Biomaterials 31 (34), 9015–9022.
Massart, R., et al., 1995. Preparation and properties of monodisperse magnetic fluids. J. Magn. Magn. Mater. 149 (1-2), 1–5.
Matsushita, T., et al., 2011. Inflammatory imaging with ultrasmall superparamagnetic iron oxide. Magn. Reson. Imaging 29 (2), 173–178.
Miyake, N., et al., 2012. Rapamycin induces p53-independent apoptosis through the mitochondrial pathway in non-small cell lung cancer cells. Oncol. Rep. 28 (3), 848–854.
Mou, Y., et al., 2011. Influence of synthetic superparamagnetic iron oxide on dendritic cells. Int. J. Nanomed. 6, 1779–1786.
Muller, K., et al., 2007. Effect of ultrasmall superparamagnetic iron oxide nanoparticles (Ferumoxtran-10) on human monocyte-macrophages in vitro. Biomaterials 28 (9), 1629–1642.
Naqvi, S., et al., 2010. Concentration-dependent toxicity of iron oxide nanoparticles mediated by increased oxidative stress. Int. J. Nanomed. 5, 983–989.
Pineiro-Redondo, Y., et al., 2011. The influence of colloidal parameters on the specific power absorption of PAA-coated magnetite nanoparticles. Nanoscale Res. Lett. 6 (1), 383.
Roohi, F., et al., 2012. Studying the effect of particle size and coating type on the blood kinetics of superparamagnetic iron oxide nanoparticles. Int. J. Nanomed. 7, 4447–4458.
Rowe, S.J., et al., 2002. Caspase-1-deficient mice have delayed neutrophil apoptosis and a prolonged inflammatory response to lipopolysaccharide-induced acute lung injury. J. Immunol. 169 (11), 6401–6407.
Sakaguchi, K., et al., 1998. DNA damage activates p53 through a phosphorylation-acetylation cascade. Genes Dev. 12 (18), 2831–2841.
Saldanha-Gama, R.F., et al., 2010. Alpha(9)beta(1) integrin engagement inhibits neutrophil spontaneous apoptosis: involvement of Bcl-2 family members. Biochim. Biophys. Acta, Mol. Cell Res. 1803 (7), 848–857.
Sharma, V., et al., 2012. Zinc oxide nanoparticles induce oxidative DNA damage and ROS-triggered mitochondria mediated apoptosis in human liver cells (HepG2). Apoptosis 17 (8), 852–870.
Shubayev, V.I., et al., 2009. Magnetic nanoparticles for theragnostics. Adv. Drug Deliv. Rev. 61 (6), 467–477.
Simbula, G., et al., 2007. Increased ROS generation and p53 activation in alpha-lipoic acid-induced apoptosis of hepatoma cells. Apoptosis 12 (1), 113–123.
Sladek, Z., et al., 2005. Neutrophil apoptosis during experimentally induced Staphylococcus aureus mastitis. Vet. Res. 36 (4), 629–643.
Thompson, T., et al., 2004. Phosphorylation of p53 on key serines is dispensable for transcriptional activation and apoptosis. J. Biol. Chem. 279 (51), 53015–53022.
Turina, M., et al., 2005. Endotoxin inhibits apoptosis but induces primary necrosis in neutrophils. Inflammation 29 (1), 55–63.
Wang, L., et al., 2009. Superparamagnetic iron oxide does not affect the viability and function of adipose-derived stem cells, and superparamagnetic iron oxide-enhanced magnetic resonance imaging identifies viable cells. Magn. Reson. Imaging 27 (1), 108–119.
Watson, R.W., et al., 1998. The IL-1 beta-converting enzyme (caspase-1) inhibits apoptosis of inflammatory neutrophils through activation of IL-1 beta. J. Immunol. 161 (2), 957–962.
Weinmann, P., et al., 1999. Bcl-Xl- and Bax-alpha-mediated regulation of apoptosis of human neutrophils via caspase-3. Blood 93 (9), 3106–3115.
Wu, J., et al., 2012. Neurotoxic potential of iron oxide nanoparticles in the rat brain striatum and hippocampus. Neurotoxicology 34, 243–253.
Wu, J., Sun, J., 2011. Investigation on mechanism of growth arrest induced by iron oxide nanoparticles in PC12 cells. J. Nanosci. Nanotechnol. 11 (12), 11079–11083.
Zhang, G., et al., 2011. Fe_3O_4 nanoparticles with daunorubicin induce apoptosis through caspase 8-PARP pathway and inhibit K562 leukemia cell-induced tumor growth in vivo. Nanomedicine 7 (5), 595–603.
Zhu, M.T., et al., 2011. Endothelial dysfunction and inflammation induced by iron oxide nanoparticle exposure: risk factors for early atherosclerosis. Toxicol. Lett. 203 (2), 162–171.

Appendix A. Supplementary data

The following are the supplementary data to this article:

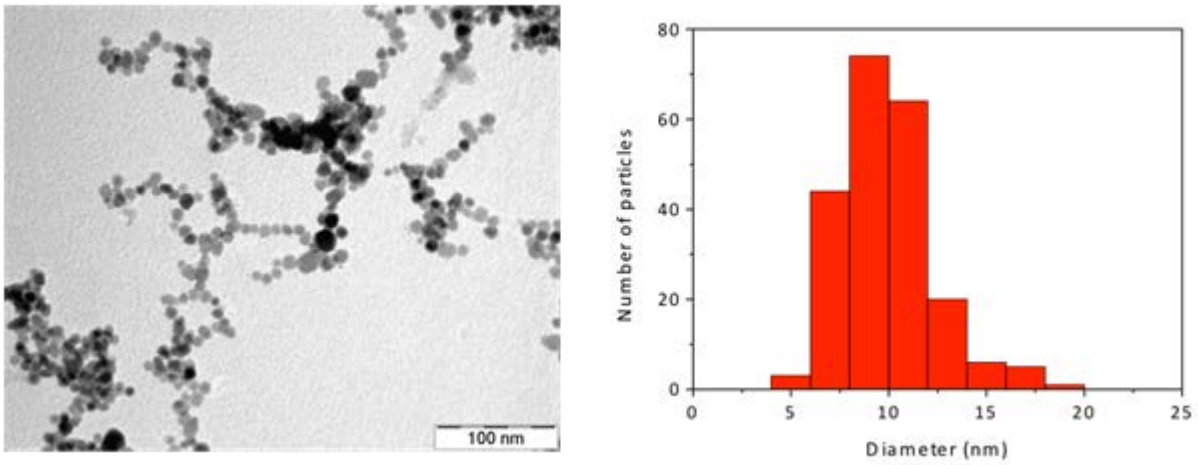

Figure 1 Supplementary: TEM image and size distribution for non-coated ION particles dispersion with a mean particle size (± standard deviation) of 9.9±2.3 nm.

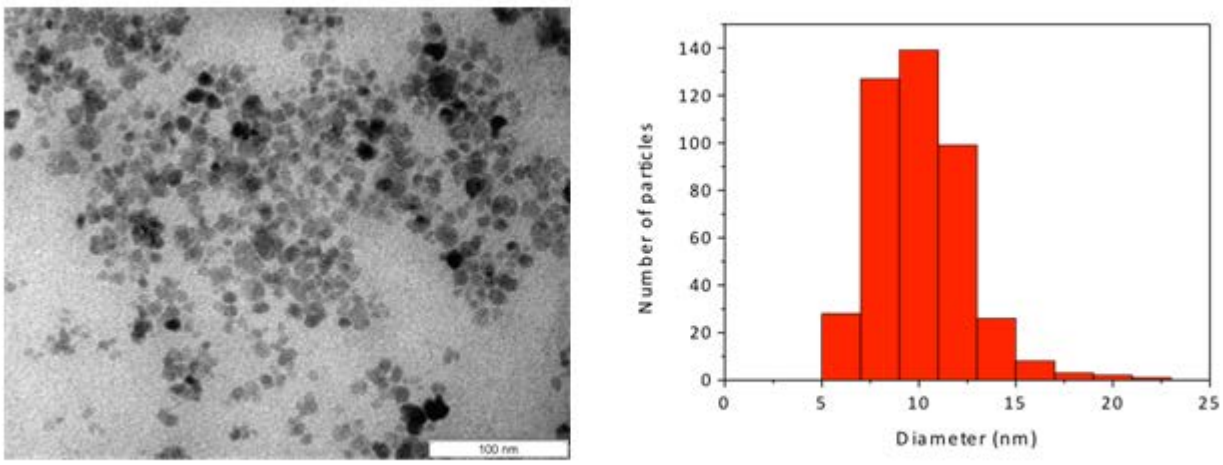

Figure 2 Supplementary: TEM image and size distribution for PAA-coated ION particles dispersion with a mean particle size (± standard deviation) of 10.1±2.4 nm.

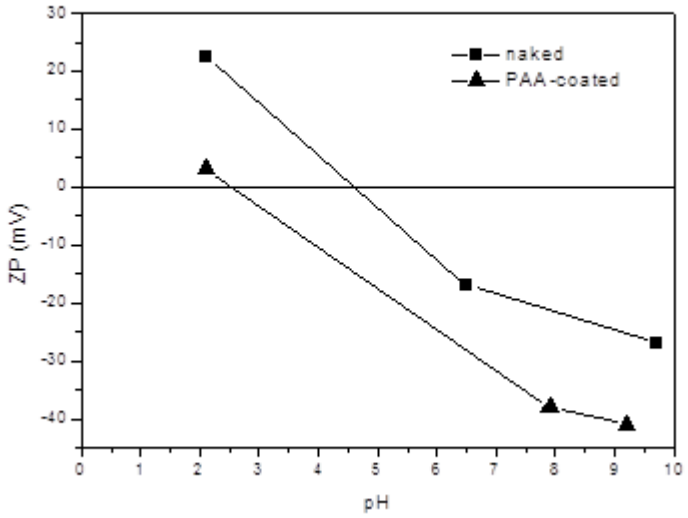

Figure 3 Supplementary: pH dependence of the surface charge for the non-coated and PAA-coated ION particles dispersed in water.

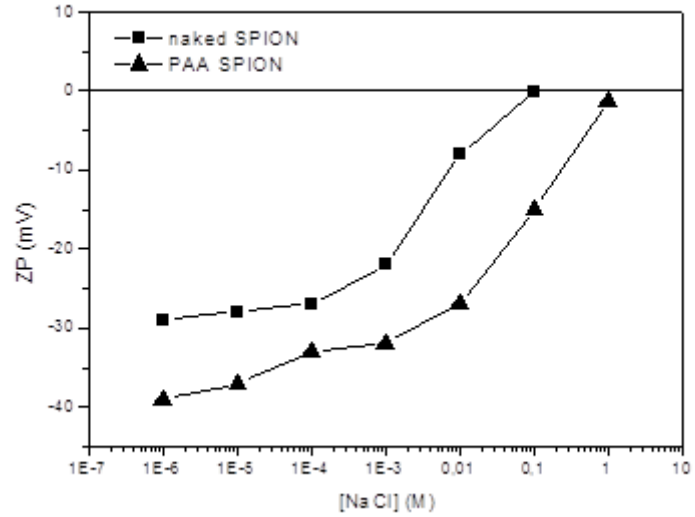

Figure 4 Supplementary: [NaCl] dependence of the surface charge for the non-coated and PAA-coated ION particles dispersed in water.

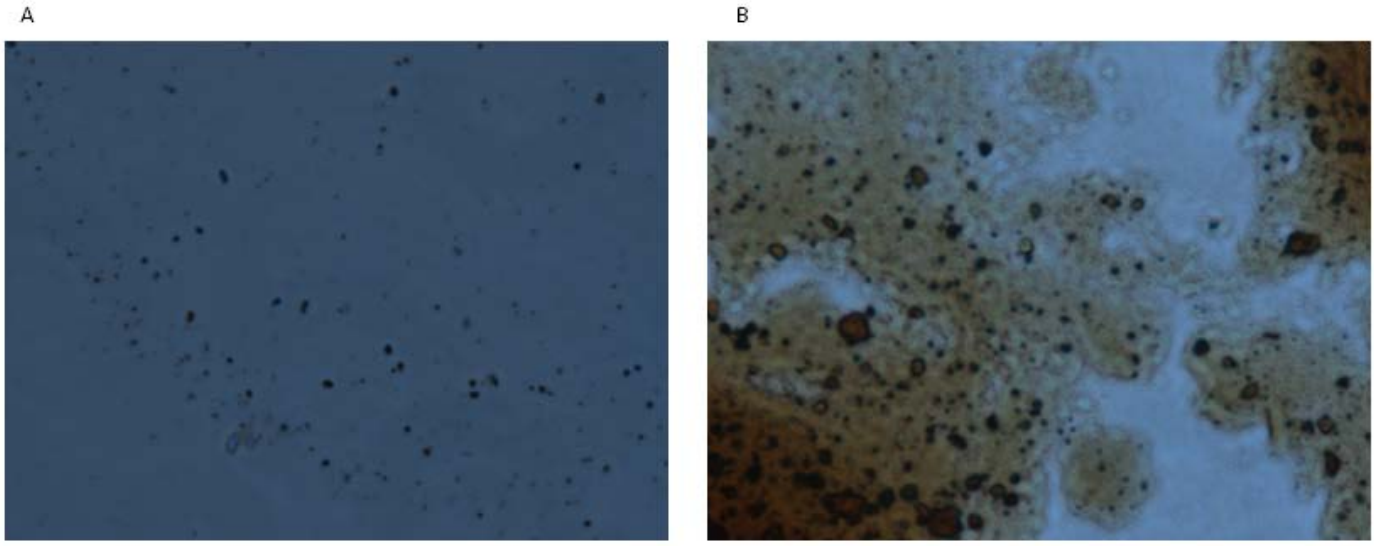

Figure 5 Supplementary: ION dispersed in RPMI 1640 medium: (A) PAA-coated ION and (B) non-coated ION.

II.2. POLYACRYLIC ACID-COATED AND NON-COATED IRON OXIDE NANOPARTICLES INDUCE CYTOKINE ACTIVATION IN HUMAN BLOOD CELLS THROUGH TAK1, p38 MAPK AND JNK PRO-INFLAMMATORY PATHWAYS

Reprinted from Archives of Toxicology

Arch Toxicol
DOI 10.1007/s00204-014-1325-4

NANOTOXICOLOGY

Polyacrylic acid-coated and non-coated iron oxide nanoparticles induce cytokine activation in human blood cells through TAK1, p38 MAPK and JNK pro-inflammatory pathways

Diana Couto · Marisa Freitas · Graça Porto · M. Arturo Lopez-Quintela · José Rivas · Paulo Freitas · Félix Carvalho · Eduarda Fernandes

Received: 13 April 2014 / Accepted: 21 July 2014

Abstract Iron oxide nanoparticles (ION) can have a wide scope of applications in biomedicine, namely in magnetic resonance imaging, tissue repair, drug delivery, hyperthermia, transfection, tissue soldering, and as antimicrobial agents. The safety of these nanoparticles, however, is not completely established, namely concerning their effect on immune system and inflammatory pathways. The aim of this study was to evaluate the in vitro effect of polyacrylic acid (PAA)-coated ION and non-coated ION on the production of six cytokines [interleukin 1 beta (IL-1β), tumor necrosis factor alpha (TNF-α), interleukin 6 (IL-6), interleukin 8 (IL-8), interferon gamma (IFN-γ) and interleukin 10 (IL-10)] by human peripheral blood cells, and to determine the inflammatory pathways involved in this production. The obtained results showed that PAA-coated and non-coated ION were able to induce all the tested cytokines and that activation of transforming growth factor beta (TGF-β)-activated kinase (TAK1), p38 mitogen-activated protein kinases (p38 MAPK) and c-Jun N-terminal kinases (JNK) were involved in this effect.

Keywords Iron oxide nanoparticles · Human blood cells · Inflammation · Cytokines · Interleukins

D. Couto · M. Freitas · E. Fernandes (✉)
REQUIMTE, Laboratory of Applied Chemistry, Department of Chemical Sciences, Faculty of Pharmacy, University of Porto, Porto, Portugal
e-mail: egracas@ff.up.pt

G. Porto
Service of Clinical Hematology, Santo António Hospital, Porto, Portugal

M. A. Lopez-Quintela
Laboratory of Nanotechnology and Magnetism, Institute of Technological Research, University of Santiago de Compostela, Santiago de Compostela, Spain

J. Rivas · P. Freitas
International Iberian Nanotechnology Laboratory, Braga, Portugal

F. Carvalho (✉)
REQUIMTE, Laboratory of Toxicology, Department of Biological Sciences, Faculty of Pharmacy, University of Porto, Porto, Portugal
e-mail: felixdc@ff.up.pt

Introduction

Owing to their unique physico-chemical properties, nanomaterials have been recognized as promising candidates for starting a new revolution in science and technology (Ahamed et al. 2013; Comfort et al. 2013). Iron oxide nanoparticles (ION) are among the nanoparticles (NP) with higher potential in biomedical applications, namely for magnetic resonance imaging (Beckmann et al. 2009; Janic et al. 2008; Lim et al. 2008; Serkova et al. 2010), tissue repair (Pareta et al. 2008; Taylor and Webster 2009), drug delivery (Chen et al. 2012; Prijic et al. 2010), hyperthermia (Giustini et al. 2011; Ito et al. 2006), transfection (Gupta and Gupta 2005; Prijic et al. 2010; Shi et al. 2010), tissue soldering (Schlachter et al. 2011), and as antimicrobial agents (Hu et al. 2011; Taylor and Webster 2009).

To prevent the precipitation of iron oxide cores, ION for medical imaging are always coated with a layer of protective and biocompatible colloid, usually a polymer that acts as a steric and/or electrostatic stabilizer (Roohi et al. 2012). The more frequently applied coatings are dextran (e.g., Endorem® and Feridex®) (Kedziorek et al. 2010; Kumar et al. 2012; Weinstein et al. 2010), carboxydextran (e.g., Resovist® and Supravist®) (Corot et al. 2006; Lunov et al.

Published online: 10 August 2014

2010; Weinstein et al. 2010) and silicone (e.g., Lumiren® and AMI-121®) (Kumar et al. 2012), among others. Recently, the use of polyacrylic acid (PAA) has also been described in the literature for use in gene delivery (Cao et al. 2013; Sun et al. 2012), as well as in liver and kidney imaging (Iversen et al. 2013). PAA is an aqueous soluble polymer with a high density of reactive functional groups that make it very attractive in biomedicine, mainly due to its capability to form flexible polymer chain–protein complexes trough electrostatic, hydrogen bonding or hydrophobic interactions (Pineiro-Redondo et al. 2011).

In spite of the potential importance of ION in the biomedical field, there are still few studies performed so far evaluating the effect of these NP on the inflammatory process. We have recently shown that PAA-coated and non-coated ION trigger neutrophils' oxidative burst in a NADPH oxidase dependent manner, and that PAA-coated ION increase while non-coated ION prevent apoptotic signaling and apoptosis in these cells (Couto et al. 2014). More generally, previous studies have reported that ION may induce an increase in the number of inflammatory cells (Kim et al. 2013; Shen et al. 2011a; Valois et al. 2010; Zhu et al. 2008) and it has been described that ION are able to induce cytokine production in some cell types, namely γ-Fe_2O_3 NP, which was shown to increase tumor necrosis factor alpha (TNF-α) levels in RAW264.7 cells (Park et al. 2014), Fe_3O_4 NP, which increased interleukin 2 (IL-2), interleukin 6 (IL-6) and interferon gamma (IFN-γ) levels in mice lymph node cell cultures (Ban et al. 2012) and Resovist® (carboxydextran-coated Fe_3O_4/Fe_2O_3 NP), which increased TNF-α and interleukin 10 (IL-10) levels in the THP-1 cell line (Laskar et al. 2012). There are also some studies regarding the effect of ION on inflammatory pathways, namely dimercaptosuccinic acid-coated Fe_3O_4 NP, which activated JAK/STAT pathway in RAW264.7 cells (Liu et al. 2011), and Resovist® and Supravist® (carboxydextran-coated Fe_3O_4/Fe_2O_3 NP), which induced c-Jun N-terminal kinases (JNK) activation in human macrophages (Lunov et al. 2010). These studies have been performed under tightly controlled experimental conditions, using only one cell type and do not reflect the in vivo conditions in which the intercellular communication networks play an important role in inflammatory processes.

The human whole blood assay has been successfully used for the study of inflammatory processes involving the production of cytokines and the involved pathways (Hornef et al. 1995; Hussain et al. 2002; Jabs et al. 1996; Myrianthefs et al. 2003) and therefore seems to be a good model for screening the pro-inflammatory effects of xenobiotics, although, to the best of our knowledge, this model was never used before for NP. The aim of this study was to evaluate the effect of ION in magnetite form (PAA-coated and non-coated) on their capacity to induce cytokine production (interleukin 1 beta (IL-1β), TNF-α, IL-6, interleukin 8 (IL-8), IFN-γ and IL-10) by ex vivo human blood cells and by which pathways (p38 MAPK, JNK and NF-kB).

Materials and methods

Materials

Human venous blood was collected from healthy human volunteers from Hospital de Santo António (Porto, Portugal), following informed consent. RPMI 1640 medium, L-glutamine, penicillin, streptomycin, 4-[4-fluorophenyl]-2-[4-methylsulfinylphenyl]-5-[4-pyridyl]1H-imidazole (SB 203580), anthra[1,9-*cd*]pyrazol-6(2*H*)-one 1,9-pyrazoloanthrone (SP 600125), curcumin, pyrrolidine dithiocarbamate (PDTC), 5Z-7-oxozeaenol and lipopolysaccharides from Escherichia coli 026:B6 (LPS) were obtained from Sigma Chemical Co (St Louis, USA). Ferrous chloride, ferric chloride, NH_4OH, KCl and PAA (average M_w 1,800) were obtained from Sigma-Aldrich (St Louis, USA). Multi-Analyte ELISArray Human Kit was obtained from Qiagen® (Boston, USA). Non-coated and PAA-coated ION were obtained from Nanogap (Santiago de Compostela, Spain), and their preparation and physico-chemical characterization was performed as reported before (Couto et al. 2014). Briefly, ION "non-coated" magnetite particles preparation was based on the chemical co-precipitation of a mixture of Fe(II) and Fe(III) chloride salts (molar ratio 2:1) using NH_4OH in a degassed 1 M KCl aqueous solution at 60 °C. The dark precipitate was washed several times with deoxygenated water, and finally, the particles were stored at pH 9.6 (well above their isoelectric point: 6.5). For the PAA-coated NP, PAA [25 % w/w with respect to the Fe(II) salt] was added to the reaction medium. PAA-coated and non-coated ION were characterized using transmission electron microscopy (TEM) (Hitachi H-7000, Japan). Determination of the hydrodynamic size and zeta potential of the studied NP, in RPMI 1640 suspensions, was performed using a nanoparticle analyzer SZ-100 (HORIBA Scientific) (DPSS laser 532 nm). Both PAA-coated and non-coated ION have a similar size distribution, with a mean particle size of 9.9 ± 2.3 nm and 10.1 ± 2.4 nm (mean ± SD) for the non-coated and PAA-coated ION, respectively. However, when the ION were dispersed in RPMI 1640 medium, large hydrodynamic sizes [3,941 ± 101 nm and 1,963 ± 148 nm (mean ± SEM) for the non-coated and PAA-coated ION, respectively], and low zeta potentials [−11.13 ± 2.83 and −2.30 ± 2.4 mV (mean ± SEM) for the non-coated and PAA-coated ION, respectively] were observed, which indicates that both types of NP tend to agglomerate when resuspended in RPMI 1640 medium, though in much higher intensity in the case of non-coated ION. Before dilutions,

ION were sonicated for 5 min in order to avoid the formation of aggregates before the preparation of the samples.

Methods

Whole blood assay

The whole blood assay was performed according to (Myrianthefs et al. 2003) in order to determine the amount of cytokines produced in response to ION. Heparinized blood collected from healthy human volunteers was diluted 10 times in RPMI 1640 culture medium and incubated at 37 °C in a 5 % CO_2 atmosphere for 24 h with PAA-coated and non-coated ION (0.4, 1.5 and 4 μg/mL). These concentrations are within those usually attained in biomedical applications [up to 70 μg/mL (Apopa et al. 2009)]. After this incubation period, the content of each well was transferred to Eppendorf tubes, centrifuged (600g, 5 min, 20 °C) and the supernatants were collected and stored at −20 °C until subsequent measurements. Cytokine (IL-1β, TNF-α, IL-6, IL-8, IFN-γ and IL-10) levels in the supernatant were evaluated using an ELISA kit according to manufacturer's instructions (Multi-Analyte ELISArray Human Kit, Qiagen®). Simultaneously, blood samples were incubated with PAA-coated and non-coated ION (4 μg/mL) and with each one of the following inhibitors: SB 203580 (p38 MAPK inhibitor) (5 μM) (Windheim et al. 2007), SP 600125 (25 μM) (JNK inhibitor) (Chowdhury et al. 2008), curcumin [activator protein 1 (AP-1) inhibitor] (1 μM) (Han et al. 2002), PDTC (NF-kB inhibitor) (10 μM) (Zhang et al. 2011) and 5Z-7-oxozeaenol (TAK1 inhibitor) (1 μM) (Windheim et al. 2007). The inhibitors were incubated with the blood for 30 min before the addition of ION, for 24 h. LPS (2.5 μg/mL) (Hornef et al. 1995; Hussain et al. 2002) was used as positive control.

Statistical analysis

Statistics were calculated using GraphPad Prism™ (version 6.0; GraphPad Software). The results are expressed as the mean ± SEM (from at least four individual experiments). Statistical comparison between groups was performed using the one-way analysis of variance, followed by Bonferroni's post hoc test. p values lower than 0.05 were considered as statistically significant.

Results

Cytokine production (IL-1β, TNF-α, IL-6, IL-8, IFN-γ and IL-10) was assessed by ELISA after incubation of PAA-coated and non-coated ION (0.4, 1.5 and 4 μg/mL) with heparinized blood for 24 h at 37 °C. As can be observed in Figs. 1a, b, 2a, b, 3a, b, 4a, b, 5a, b, 6a, b, both ION were able to increase the production of the six studied cytokines, in the following decreasing order of extent, for PAA-coated ION IL-6 > IL-8 > TNF-α > IFN-γ > IL-1β > IL-10 and for the non-coated ION IL-8 > IL-6 > IL-1β > IFN-γ > TNF-α > IL-10. The effect was seen, in most of the cases, in a concentration-dependent manner, being always statistically significant for the highest concentration tested (4 μg/mL). Additionally, LPS (2.5 μg/mL), used as positive control, showed a strenuous activation of all the cytokines tested (data not shown).

At this point, for a better integration of the obtained results, it is important to reflect on the possible pathways involved in cytokine production. Stimulation of inflammatory cells, such as neutrophils, macrophages, and T lymphocytes initiates a rapid cascade of protein phosphorylation, where MAPK kinases (MKK) are activated by MKK kinases (MAPKKK). One of the MAPKKK seems to correspond to transforming growth factor beta (TGF-β)-activated kinase (TAK1). When TAK1 is activated, usually by TGF-β, IL-1, TNF-α, or by a pro-inflammatory stimulus, a generation of K63-linked polyubiquitin chains occurs, serving as scaffolds for the oligomerization of TAK1. This oligomerization is dependent upon the TAK1 binding proteins, which possess polyubiquitin binding domains. TAK1 proteins that are brought together at polyubiquitin chains are hypothesized to phosphorylate and activate one another. They are then competent for activation of MKK 3, 6 and other kinases, resulting in p38 MAPK and JNK activation (Clark and Dean 2012; Craig et al. 2000; Noubade et al. 2007). MAPK are involved in many aspects of immune responses, including initiation of innate immunity, activation of adaptive immunity, and termination of immune responses through cell death and regulatory T cells (Pasquinelli et al. 2013). The p38 MAPK is a ubiquitous, highly conserved protein kinase that plays an important role in the inflammatory response (Bachstetter et al. 2011; Clark and Dean 2012; Noubade et al. 2007; Pasquinelli et al. 2013; Stambe et al. 2003). The JNK are also members of the MAPK family. The classical JNK pathway is equally activated following the exposure of cells to extracellular stresses and a diversity of stimuli (Guma and Firestein 2012; Kim et al. 2006). TAK1, as well as kinases from inhibitor of kB (IkB) kinase family (IKK), can also activate NF-kB pathway. NF-kB is comprised of two subunits (p65 and p50) that are retained in the cytoplasm in their inactive form by virtue of their interaction with the IkB and is one of the most important inducible transcription factors whose modulation triggers a cascade of signaling events (Craig et al. 2000; Gomes et al. 2008; Rhodus et al. 2005).

Considering the above, we used several inhibitors to ascertain the pathways involved in the production of cytokines: p38 MAPK inhibitor (SB 203580), JNK inhibitor

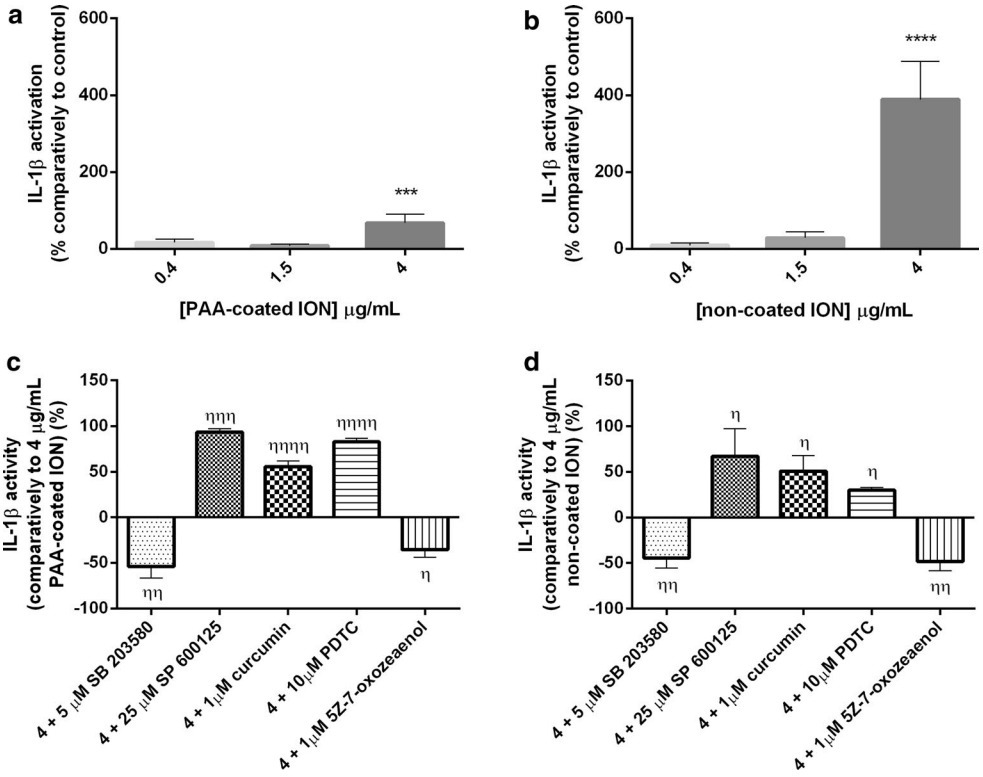

Fig. 1 IL-1β activation following exposure to: **a** PAA-coated ION (0.4–4 μg/mL), **b** non-coated ION (0.4–4 μg/mL), **c** PAA-coated ION (4 μg/mL) in the presence of inhibitors and **d** non-coated ION (4 μg/mL) in the presence of inhibitors, at 37 °C, for 24 h. $^{****}p < 0.0001$ and $^{***}p < 0.001$ when compared to control (without ION) and $^{\eta\eta\eta\eta}p < 0.0001$, $^{\eta\eta\eta}p < 0.001$ $^{\eta\eta}p < 0.01$ and $^{\eta}p < 0.05$ when compared to control (ION 4 μg/mL). Values are given as mean ± SEM ($n \geq 4$)

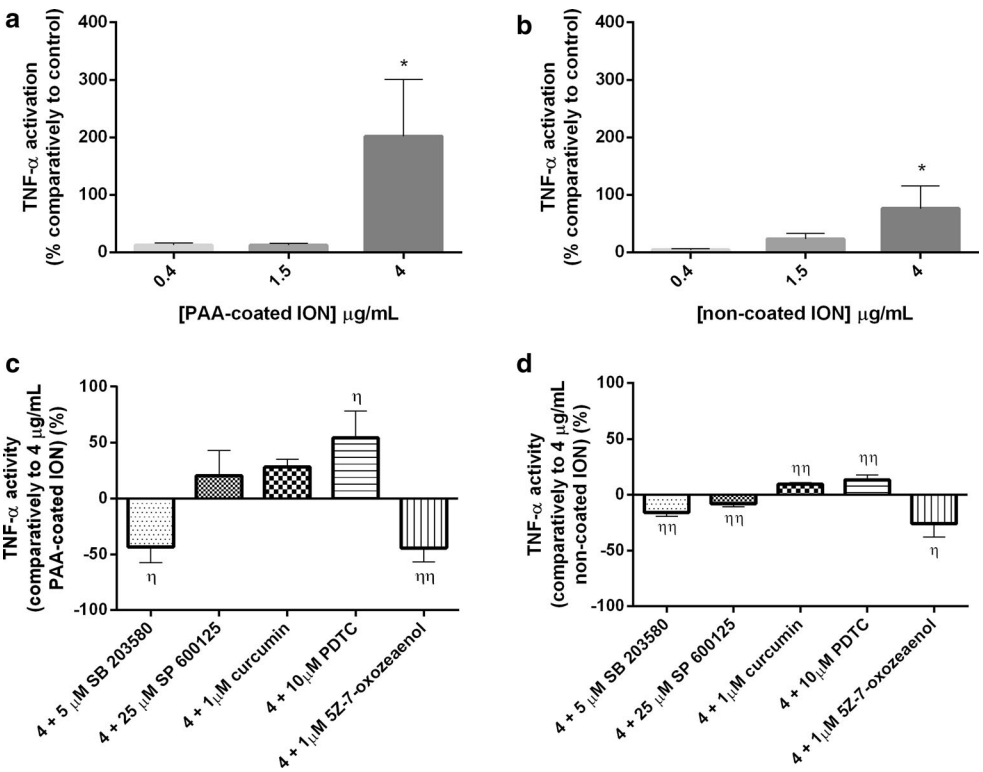

Fig. 2 TNF-α activation following exposure to: **a** PAA-coated ION (0.4–4 μg/mL), **b** non-coated ION (0.4–4 μg/mL), **c** PAA-coated ION (4 μg/mL) in the presence of inhibitors and **d** non-coated ION (4 μg/mL) in the presence of inhibitors, at 37 °C, for 24 h. $^{*}p < 0.05$ when compared to control (without ION) and $^{\eta\eta}p < 0.01$ and $^{\eta}p < 0.05$ when compared to control (ION 4 μg/mL). Values are given as mean ± SEM ($n \geq 4$)

(SP 600125), AP-1 inhibitor (curcumin), NF-kB inhibitor (PDTC) and TAK1 inhibitor (5Z-7-oxozeaenol). Inhibitors, by themselves, did not change cytokine production in the whole blood (data not shown). It was verified that SB 203580 and 5Z-7-oxozeaenol decreased or inhibited the production of all the ION-induced cytokines tested for both

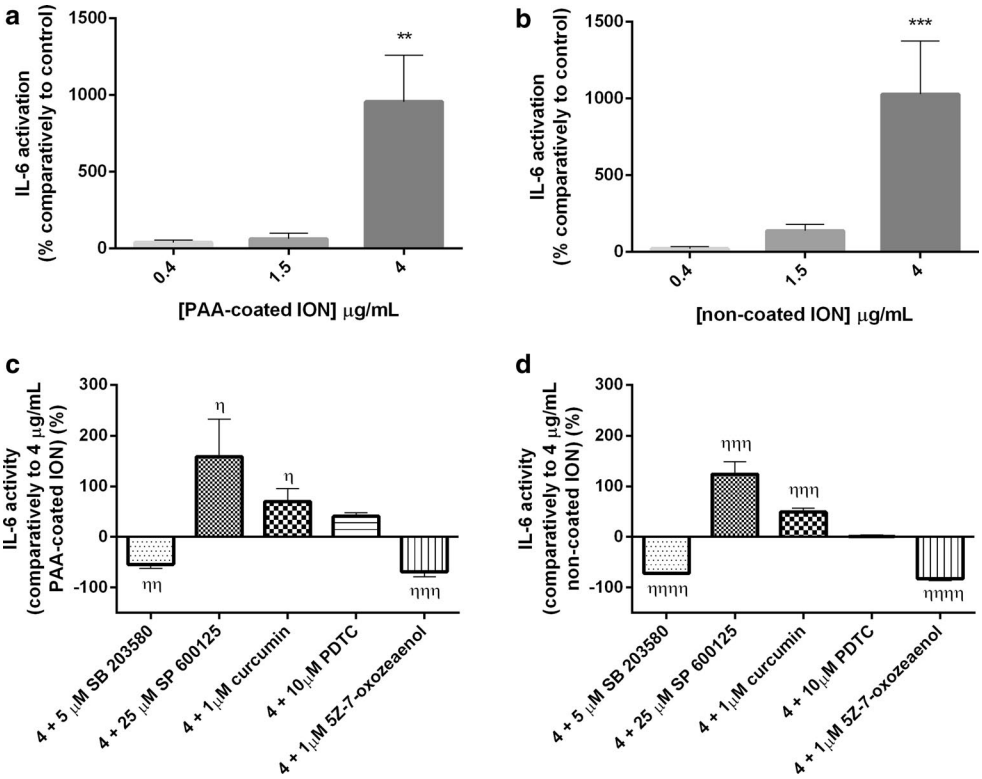

Fig. 3 IL-6 activation following exposure to: **a** PAA-coated ION (0.4–4 µg/mL), **b** non-coated ION (0.4–4 µg/mL), **c** PAA-coated ION (4 µg/mL) in the presence of inhibitors and **d** non-coated ION (4 µg/mL) in the presence of inhibitors, at 37 °C, for 24 h. $^{***}p < 0.001$ and $^{**}p < 0.01$ when compared to control (without ION) and $^{\eta\eta\eta\eta}p < 0.0001$, $^{\eta\eta\eta}p < 0.001$, $^{\eta\eta}p < 0.01$ and $^{\eta}p < 0.05$ when compared to control (ION 4 µg/mL). Values are given as mean ± SEM ($n \geq 4$)

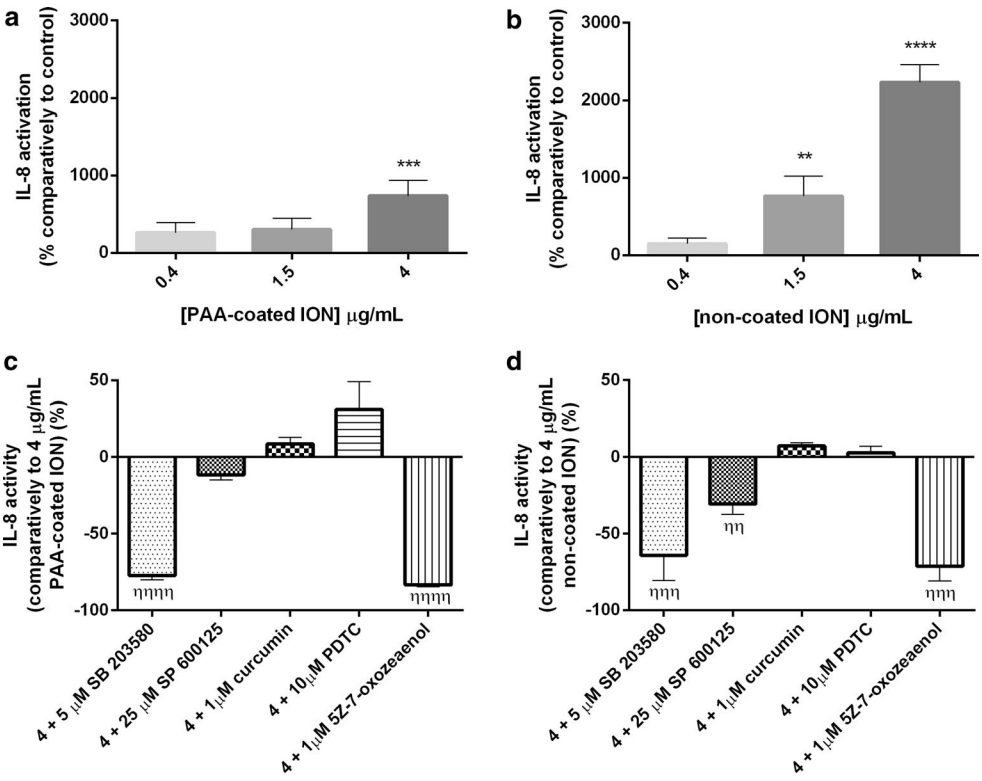

Fig. 4 IL-8 activation following exposure to: **a** PAA-coated ION (0.4–4 µg/mL), **b** non-coated ION (0.4–4 µg/mL), **c** PAA-coated ION (4 µg/mL) in the presence of inhibitors and **d** non-coated ION (4 µg/mL) in the presence of inhibitors, at 37 °C, for 24 h. $^{****}p < 0.0001$, $^{***}p < 0.001$ and $^{**}p < 0.01$ when compared to control (without ION) and $^{\eta\eta\eta\eta}p < 0.0001$, $^{\eta\eta\eta}p < 0.001$ and $^{\eta\eta}p < 0.01$ when compared to control (ION 4 µg/mL). Values are given as mean ± SEM ($n \geq 4$)

types of ION (Figs. 1c, d, 2c, d, 3c, d, 4c, d, 5c, d, 6c, d). This fact shows that PAA-coated ION and non-coated ION increase the production of cytokines through activation of p38 MAPK and TAK1. SP 600125 was equally able to decrease IFN-γ production for both ION (Fig. 5c, d) and also decreased non-coated ION-induced TNF-α and IL-8

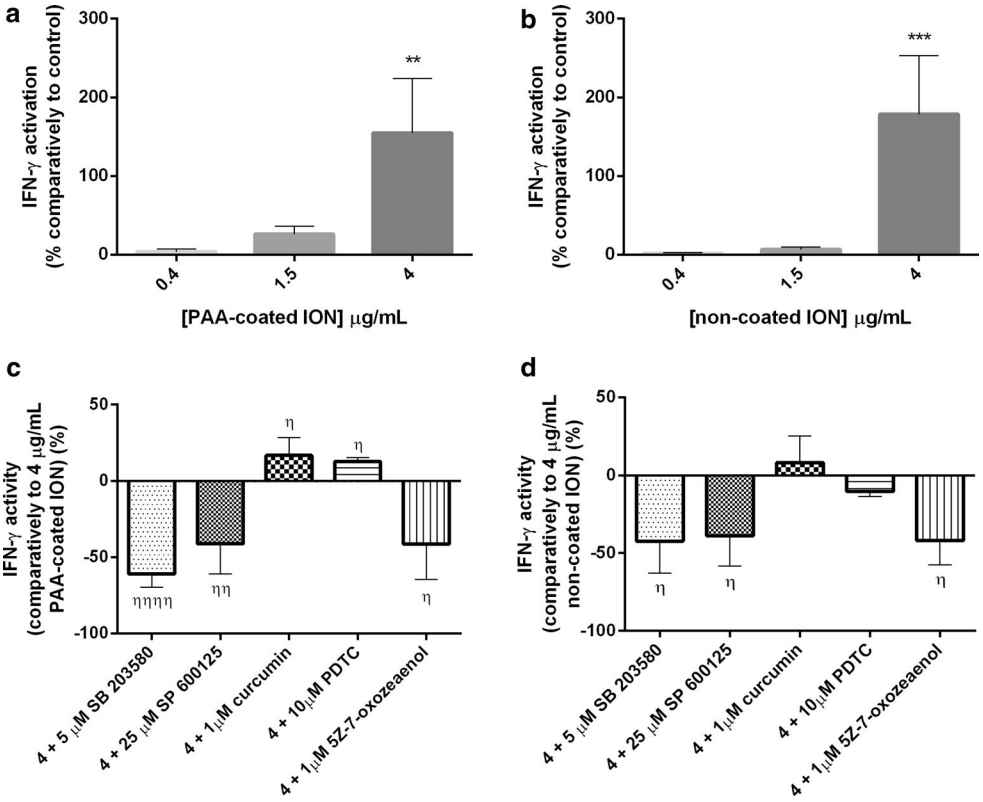

Fig. 5 IFN-γ activation following exposure to: **a** PAA-coated ION (0.4–4 μg/mL), **b** non-coated ION (0.4–4 μg/mL), **c** PAA-coated ION (4 μg/mL) in the presence of inhibitors and **d** non-coated ION (4 μg/mL) in the presence of inhibitors, at 37 °C, for 24 h. $^{***}p < 0.001$ and $^{**}p < 0.01$ when compared to control (without ION) and $^{\eta\eta\eta\eta}p < 0.0001$, $^{\eta\eta}p < 0.01$ and $^{\eta}p < 0.05$ when compared to control (ION 4 μg/mL). Values are given as mean ± SEM ($n \geq 4$)

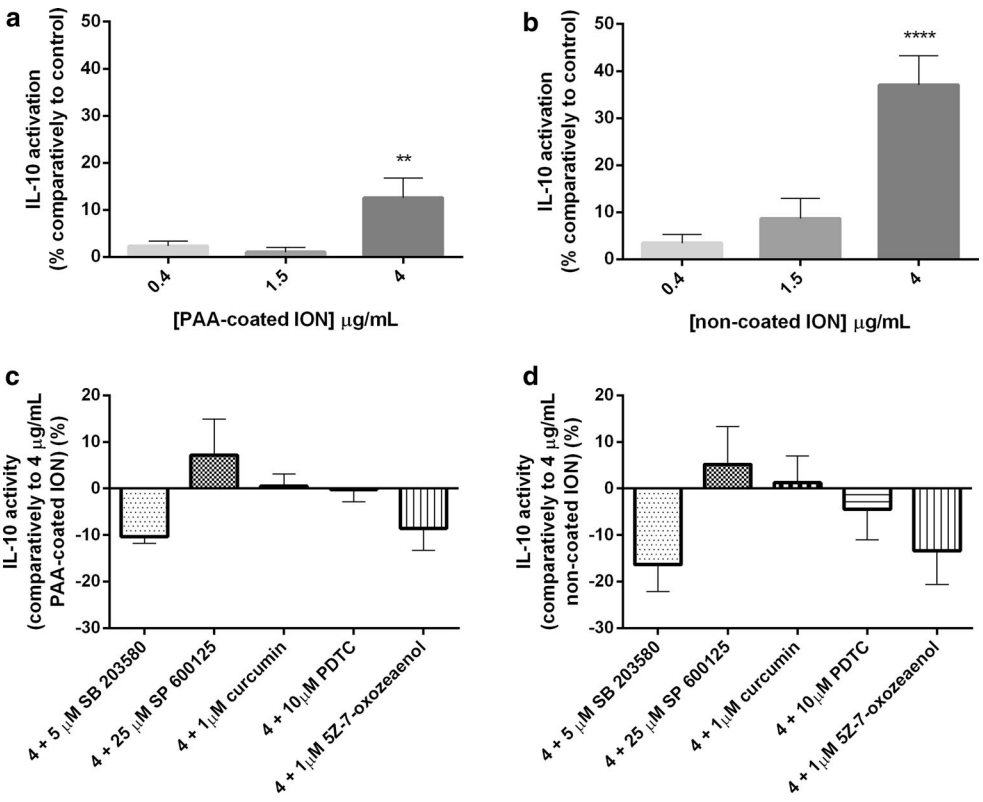

Fig. 6 IL-10 activation following exposure to: **a** PAA-coated ION (0.4–4 μg/mL), **b** non-coated ION (0.4–4 μg/mL), **c** PAA-coated ION (4 μg/mL) in the presence of inhibitors and **d** non-coated ION (4 μg/mL) in the presence of inhibitors, at 37 °C, for 24 h. $^{****}p < 0.0001$ and $^{**}p < 0.01$ when compared to control (without ION). Values are given as mean ± SEM ($n \geq 4$)

production (Figs. 2d, 4d), which means that JNK pathway is involved in the TNF-α and IL-8 production stimulated by non-coated ION, as well as IFN-γ production stimulated by PAA-coated and non-coated ION. However, in the presence of SP 600125, IL-1β and IL-6 production increased for both types of ION tested (Figs. 1c, d, 3c, d). Additionally, in the presence of curcumin, IL-1β and IL-6 production increased for both types of tested ION (Figs. 1c, d, 3c, d), TNF-α production increased for non-coated ION (Fig. 2d) and IFN-γ production increased for PAA-coated ION (Fig. 5c). In the presence of PDTC, IL-1β and TNF-α production increased for both types of ION (Figs. 1c, d, 2c, d) and IFN-γ production increased for PAA-coated ION (Fig. 5c).

Discussion

This work was undertaken with the aim of evaluating the ability of PAA-coated and non-coated ION to induce the production of cytokines in the human whole blood cells in vitro and to identify the pathways involved in this effect. It was clearly evidenced that both types of ION are able to induce the production of all the tested cytokines (IL-1β, TNF-α, IL-6, IL-8, IFN-γ and IL-10), in most of the cases, in a concentration-dependent manner, although at different extents for each one. These cytokines are known to mediate inflammatory reactions, as indicated by cytokines produced and/or associated with Th1 cells, as IFN-γ, TNF-α, IL-1β and IL-8, and also by their involvement in B-cell activation and differentiation (Th2), as IL-6 and IL-10 (Chizzolini et al. 1997; Rhodus et al. 2007; Yang et al. 1998). Of note, ION have been previously shown to induce the production and release of cytokines by Th1 cells, while their influence on Th2 cells remains uncertain. For example, Zhu et al. described that, in ovalbumin-sensitized rats, magnetic ION have the ability to increase the percentages of Th1 and T-cytotoxic-cell type 1, decreasing at the same time the percentages of Th2 and T-cytotoxic-cell type 2, which suggest that magnetic ION are able to skew the immune response toward Th1 responses (Zhu et al. 2012) and it was also reported that Fe_3O_4 NP increase Th1 immunity in much greater extent than they increase Th2 immunity (Chen et al. 2010; Shen et al. 2011b). In the present study, we observed that, concerning Th2 cytokines, although IL-10 is just slightly increased comparatively to control, IL-6 is greatly increased by ION, being the most activated cytokine for PAA-coated ION and the second most activated for non-coated ION. Accordingly, it was previously described an increase in IL-10 production by C57BL/6 J mice peritoneal macrophages (Siglienti et al. 2006) and THP-1 cells (Laskar et al. 2012) after exposure to Resovist®, as well as it was described an increase in TNF-α, IL-6 and IL-1β production in the presence of IFN-γ (Yeh et al. 2010) by murine macrophages after exposure to Resovist®.

Regarding the pathways involved in the ION-induced cytokine production, we demonstrate here, for the first time, that SB 203580 and 5Z-7-oxozeaenol decreased or inhibited the production of all the ION-induced cytokines tested for both types of ION, which reveals that PAA-coated and non-coated ION have the ability to activate p38 MAPK and TAK1, increasing this way the production of cytokines. Given that TAK1 is competent for activation of MKK 3, 6 and other kinases, its activation indirectly results in p38 MAPK and JNK activation (Clark and Dean 2012; Craig et al. 2000). Moreover, TAK1 has also the ability to activate the NF-kB pathway (Craig et al. 2000), and therefore, this pathway is also indirectly activated. Concerning p38 MAPK, this protein was shown to be activated by both types of ION. Once p38 MAPK is activated, it is translocated to the nucleus, where it phosphorylates and activates nuclear transcription factors members of the AP-1 family, such as activating transcription factor 2 (ATF-2) and c-Fos, resulting in the production and secretion of pro-inflammatory cytokines, such as IL-1β and TNF-α (Bachstetter et al. 2011; Clark and Dean 2012; Kim et al. 2006; Noubade et al. 2007; Pasquinelli et al. 2013; Stambe et al. 2003). Therefore, it became evident the reason why both ION were able to induce an increase in the levels of these two cytokines. It is also known that IL-1β is a potent activator of IL-6 synthesis and p38 MAPK has been shown to be a central signaling pathway that controls IL-6 mRNA stability (Mavropoulos et al. 2013; Miyazawa et al. 1998; Patil et al. 2004). TNF-α has also been shown to induce IL-6 production (Craig et al. 2000). IL-8, the most potent known chemotactic agent for neutrophils (Bhattacharyya et al. 2011; Dauletbaev et al. 2011) is also greatly up-regulated upon exposure to IL-1β or TNF-α, the early response cytokines (Dauletbaev et al. 2011; Kim et al. 2006). Therefore, after p38 MAPK activation and consequent activation of the ATF-2 and c-Fos, IL-1β and TNF-α will be produced and, subsequently, these cytokines will induce the production of other cytokines, namely IL-6 and IL-8. IL-10, a cytokine considered to have an anti-inflammatory role, showed to be also induced by IL-1 and TNF-α (Foey et al. 1998). IL-10 is reported to inhibit monocyte production of IL-1 and TNF-α, which suggests that these three cytokines form an autoregulatory feedback loop (Foey et al. 1998). In our study, for both ION, the amount of IL-1β and TNF-α produced was considerably superior to the amount of IL-10 produced, and for this reason, this feedback loop was not evidenced.

The production and release of IFN-γ represents an early and critical event in the immune response to intracellular pathogens that influences both innate and acquired immune responses (Mavropoulos et al. 2005). p38 MAPK

is required for the induction of IFN-γ gene and the mechanisms by which p38 MAPK may participate in the transcriptional activation of IFN-γ are through ATF-2 activation or cAMP response element-binding protein (CREB) phosphorylation (Fukushima et al. 2005; Mavropoulos et al. 2005; Pasquinelli et al. 2013; Rincon et al. 1998). Therefore, as p38 MAPK was directly activated by both types of ION and indirectly activated due to TAK1 activation, this fact indicates that the increase in IFN-γ production is mediated through this pathway, involving p38 MAPK-induced ATF-2 and CREB activation.

SP 600125 (JNK inhibitor) was able to decrease IFN-γ production for both ION and also decreased non-coated ION-induced TNF-α and IL-8 production. These facts show the involvement of JNK in non-coated ION-induced TNF-α and IL-8 production, as well as PAA-coated and non-coated ION-induced IFN-γ production. In accordance, it was previously described that Fe_3O_4 NP activate JNK in a ROS-independent manner (Konczol et al. 2011) and that Resovist® and Supravist® induce JNK activation in human macrophages (Lunov et al. 2010). In our study, ION seem to activate JNK pathway directly, since the inhibition of JNK results in the diminution of IFN-γ, IL-8 and TNF-α production, and indirectly, given that TAK1 activation not only results in the p38 MAPK activation, but also in JNK activation. After JNK activation, they subsequently phosphorylate a variety of substrates, namely c-Fos and ATF-2, similarly to p38 MAPK, and additionally c-Jun, which will result in the transcription of the cytokine genes previously mentioned for p38 MAPK, such as TNF-α and IFN-γ (Guma and Firestein 2012; Kim et al. 2006; Mavropoulos et al. 2013; Rhodus et al. 2005; Shen et al. 2005; Stambe et al. 2003; Yang et al. 1998).

On the other hand, in the presence of SP 600125, the IL-1β and IL-6 production increased for both types of ION tested. In the presence of curcumin [activator protein 1 (AP-1) inhibitor], the IL-1β and IL-6 production increased for both types of ION tested, the TNF-α production increased for non-coated ION and the IFN-γ production increased for PAA-coated ION. In the presence of PDTC (NF-kB inhibitor), the IL-1β and TNF-α production increased for both types of ION and the IFN-γ production increased for PAA-coated ION. Nevertheless, this does not mean that JNK, NF-kB and AP-1 family are not involved in ION-induced cytokine production. As previously mentioned, the fact that JNK inhibition decreases the production of some cytokines shows the involvement of this pathway in ION-induced cytokine production. Moreover, p38 MAPK and JNK

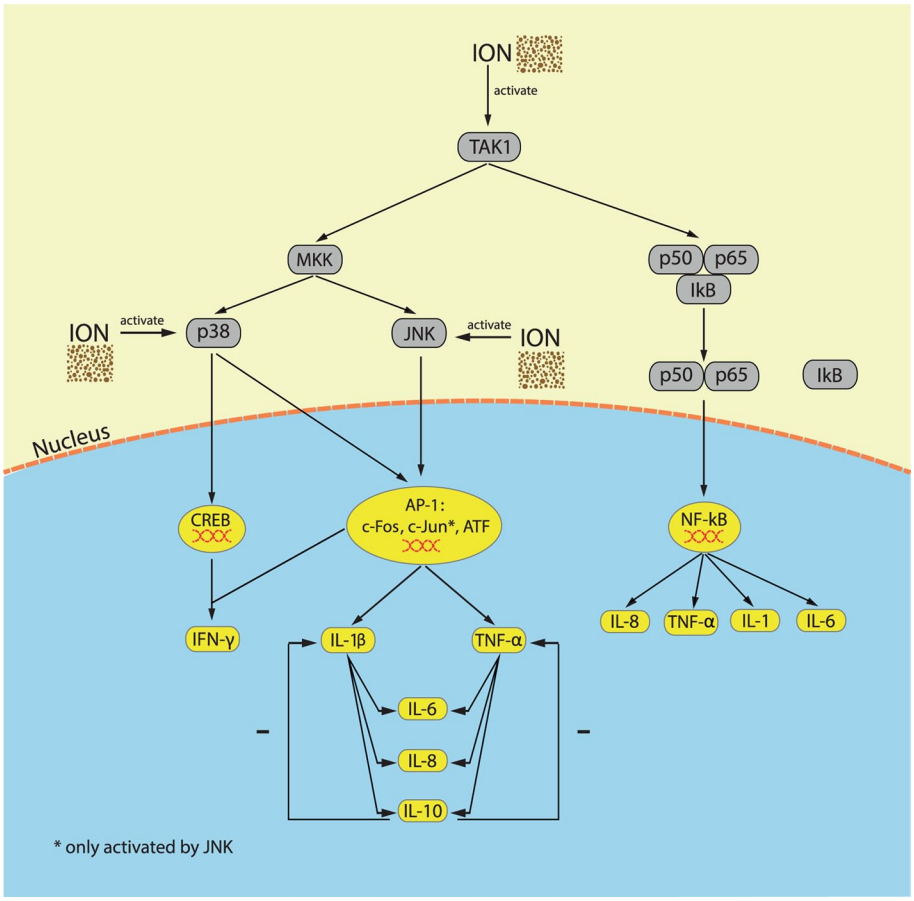

Fig. 7 Inflammatory pathways triggered by the studied PAA-coated and non-coated ION

pathways activate some members of AP-1 family that led to the production of the above mentioned cytokines (Bachstetter et al. 2011; Clark and Dean 2012; Noubade et al. 2007; Pasquinelli et al. 2013; Stambe et al. 2003) and, additionally, TAK1 also activates IKK, which phosphorylates IkB and consequently activates NF-kB, increasing the transcription of TNF-α, IL-1, IL-6 and IL-8 (Craig et al. 2000; Gomes et al. 2008; Rhodus et al. 2005; Shen et al. 2005). However, as Clark and Dean (2012) stated, in the presence of inhibitors of these pathways, a negative feedback mechanism may occur, thereby enhancing or prolonging TAK1 activation. Consequently, this may be an explanation for the fact that the cytokine induction is increased in the presence of JNK, AP-1 family and NF-kB inhibitors, e.g., in the presence of a NF-kB inhibitor, the TAK1 will activate p38 MAPK and/or JNK more effectively and, consequently, the production of some cytokines may be further increased. Concerning the limitations of the present study, the fact that this study was performed in vitro does not allow evaluating the interaction and the effect that this increase in cytokines production may have in the different organs and cells of the organism. Therefore, an in vivo study is essential to further study these aspects.

Conclusion

The results obtained in the present study help to unveil the mechanisms involved in the effects of ION in the MAPK and NF-kB inflammatory pathways. As depicted in Fig. 7, both types of ION were shown to directly activate TAK1, p38 MAPK and JNK pathways. The activation of these pathways results in the production of IFN-γ, as well as in the production of IL-1β and TNF-α, that will stimulate the IL-6, IL-8 and IL-10 production. Additionally, the activation of TAK1 results equally in NF-kB activation, and consequently, the transcription and resultant production of IL-8, TNF-α, IL-1 and IL-6 will take place.

Though these effects still need to be confirmed in vivo, the mentioned effects are indicative that ION may induce inflammation and suggest that appropriate anti-inflammatory prophylaxis may be sought when they are used in their diverse biomedical applications.

Acknowledgments Diana Couto acknowledges the Fundação para a Ciência e Tecnologia (FCT) financial support for the PhD grant (SFRH/BD/72856/2010) and Marisa Freitas for her Pos-doc grant (SFRH/BPD/76909/2011), in the ambit of "POPH–QREN–Tipologia 4.1–Formação Avançada" co-sponsored by FSE and national funds of MCTES. The authors greatly acknowledge the financial support given by Reitoria da Universidade do Porto and Santander Totta for Projectos IJUP 2011.

Conflict of interest Authors declare no conflicts of interest concerning the present study.

References

Ahamed M, Alhadlaq HA, Alam J, Khan MA, Ali D, Alarafi S (2013) Iron oxide nanoparticle-induced oxidative stress and genotoxicity in human skin epithelial and lung epithelial cell lines. Curr Pharm Des 19:6681–6690

Apopa PL, Qian Y, Shao R, Guo NL, Schwegler-Berry D, Pacurari M, Porter D, Shi X, Vallyathan V, Castranova V, Flynn DC (2009) Iron oxide nanoparticles induce human microvascular endothelial cell permeability through reactive oxygen species production and microtubule remodeling. Part Fibre Toxicol 6:1

Bachstetter AD, Xing B, de Almeida L, Dimayuga ER, Watterson DM, Van Eldik LJ (2011) Microglial p38alpha MAPK is a key regulator of proinflammatory cytokine up-regulation induced by toll-like receptor (TLR) ligands or beta-amyloid (Abeta). J Neuroinflamm 8:79

Ban M, Langonne I, Huguet N, Goutet M (2012) Effect of submicron and nano-iron oxide particles on pulmonary immunity in mice. Toxicol Lett 210:267–275

Beckmann N, Cannet C, Babin AL, Ble FX, Zurbruegg S, Kneuer R, Dousset V (2009) In vivo visualization of macrophage infiltration and activity in inflammation using magnetic resonance imaging. Wiley Interdiscip Rev Nanomed Nanobiotechnol 1:272–298

Bhattacharyya S, Gutti U, Mercado J, Moore C, Pollard HB, Biswas R (2011) MAPK signaling pathways regulate IL-8 mRNA stability and IL-8 protein expression in cystic fibrosis lung epithelial cell lines. Am J Physiol Lung Cell Mol Physiol 300:L81–L87

Cao B, Qiu P, Mao C (2013) Mesoporous iron oxide nanoparticles prepared by polyacrylic acid etching and their application in gene delivery to mesenchymal stem cells. Microsc Res Tech 76:936–941

Chen BA, Jin N, Wang J, Ding J, Gao C, Cheng J, Xia G, Gao F, Zhou Y, Chen Y, Zhou G, Li X, Zhang Y, Tang M, Wang X (2010) The effect of magnetic nanoparticles of Fe(3)O(4) on immune function in normal ICR mice. Int J Nanomed 5:593–599

Chen JP, Yang PC, Ma YH, Tu SJ, Lu YJ (2012) Targeted delivery of tissue plasminogen activator by binding to silica-coated magnetic nanoparticle. Int J Nanomed 7:5137–5149

Chizzolini C, Chicheportiche R, Burger D, Dayer JM (1997) Human Th1 cells preferentially induce interleukin (IL)-1beta while Th2 cells induce IL-1 receptor antagonist production upon cell/cell contact with monocytes. Eur J Immunol 27:171–177

Chowdhury TT, Salter DM, Bader DL, Lee DA (2008) Signal transduction pathways involving p38 MAPK, JNK, NFkappaB and AP-1 influences the response of chondrocytes cultured in agarose constructs to IL-1beta and dynamic compression. Inflamm Res 57:306–313

Clark AR, Dean JL (2012) The p38 MAPK pathway in rheumatoid arthritis: a sideways look. Open Rheumatol J 6:209–219

Comfort KK, Maurer EI, Hussain SM (2013) The biological impact of concurrent exposure to metallic nanoparticles and a static magnetic field. Bioelectromagnetics 34:500–511

Corot C, Robert P, Idee JM, Port M (2006) Recent advances in iron oxide nanocrystal technology for medical imaging. Adv Drug Deliv Rev 58:1471–1504

Couto D, Freitas M, Vilas-Boas V, Dias I, Porto G, Lopez-Quintela MA, Rivas J, Freitas P, Carvalho F, Fernandes E (2014) Interaction of polyacrylic acid coated and non-coated iron oxide nanoparticles with human neutrophils. Toxicol Lett 225:57–65

Craig R, Larkin A, Mingo AM, Thuerauf DJ, Andrews C, McDonough PM, Glembotski CC (2000) p38 MAPK and NF-kappa B collaborate to induce interleukin-6 gene expression and release. Evidence for a cytoprotective autocrine signaling pathway in a cardiac myocyte model system. J Biol Chem 275:23814–23824

Dauletbaev N, Eklove D, Mawji N, Iskandar M, Di Marco S, Gallouzi IE, Lands LC (2011) Down-regulation of cytokine-induced

interleukin-8 requires inhibition of p38 mitogen-activated protein kinase (MAPK) via MAPK phosphatase 1-dependent and -independent mechanisms. J Biol Chem 286:15998–16007

Foey AD, Parry SL, Williams LM, Feldmann M, Foxwell BM, Brennan FM (1998) Regulation of monocyte IL-10 synthesis by endogenous IL-1 and TNF-alpha: role of the p38 and p42/44 mitogen-activated protein kinases. J Immunol 160:920–928

Fukushima N, Nishiura Y, Nakamura T, Yamada Y, Kohno S, Eguchi K (2005) Involvement of p38 MAPK signaling pathway in IFN-gamma and HTLV-I expression in patients with HTLV-I-associated myelopathy/tropical spastic paraparesis. J Neuroimmunol 159:196–202

Giustini AJ, Ivkov R, Hoopes PJ (2011) Magnetic nanoparticle biodistribution following intratumoral administration. Nanotechnology 22:345101

Gomes A, Fernandes E, Lima JL, Mira L, Corvo ML (2008) Molecular mechanisms of anti-inflammatory activity mediated by flavonoids. Curr Med Chem 15:1586–1605

Guma M, Firestein GS (2012) c-Jun N-terminal kinase in inflammation and rheumatic diseases. Open Rheumatol J 6:220–231

Gupta AK, Gupta M (2005) Synthesis and surface engineering of iron oxide nanoparticles for biomedical applications. Biomaterials 26:3995–4021

Han SS, Keum YS, Seo HJ, Surh YJ (2002) Curcumin suppresses activation of NF-kappaB and AP-1 induced by phorbol ester in cultured human promyelocytic leukemia cells. J Biochem Mol Biol 35:337–342

Hornef MW, Wagner HJ, Kruse A, Kirchner H (1995) Cytokine production in a whole-blood assay after Epstein-Barr virus infection in vivo. Clin Diagn Lab Immunol 2:209–213

Hu K, Dou J, Yu F, He X, Yuan X, Wang Y, Liu C, Gu N (2011) An ocular mucosal administration of nanoparticles containing DNA vaccine pRSC-gD-IL-21 confers protection against mucosal challenge with herpes simplex virus type 1 in mice. Vaccine 29:1455–1462

Hussain R, Kaleem A, Shahid F, Dojki M, Jamil B, Mehmood H, Dawood G, Dockrell HM (2002) Cytokine profiles using whole-blood assays can discriminate between tuberculosis patients and healthy endemic controls in a BCG-vaccinated population. J Immunol Methods 264:95–108

Ito A, Honda H, Kobayashi T (2006) Cancer immunotherapy based on intracellular hyperthermia using magnetite nanoparticles: a novel concept of "heat-controlled necrosis" with heat shock protein expression. Cancer Immunol Immun 55:320–328

Iversen NK, Frische S, Thomsen K, Laustsen C, Pedersen M, Hansen PB, Bie P, Fresnais J, Berret JF, Baatrup E, Wang T (2013) Superparamagnetic iron oxide polyacrylic acid coated γ-Fe2O3 nanoparticles do not affect kidney function but cause acute effect on the cardiovascular function in healthy mice. Toxicol Appl Pharm 266:276–288

Jabs WJ, Wagner HJ, Neustock P, Kluter H, Kirchner H (1996) Immunologic properties of Epstein-Barr virus-seronegative adults. J Infect Dis 173:1248–1251

Janic B, Iskander AS, Rad AM, Soltanian-Zadeh H, Arbab AS (2008) Effects of ferumoxides-protamine sulfate labeling on immunomodulatory characteristics of macrophage-like THP-1 cells. PLoS ONE 3:e2499

Kedziorek DA, Muja N, Walczak P, Ruiz-Cabello J, Gilad AA, Jie CC, Bulte JW (2010) Gene expression profiling reveals early cellular responses to intracellular magnetic labeling with superparamagnetic iron oxide nanoparticles. Magn Reson Med 63:1031–1043

Kim YM, Reed W, Wu W, Bromberg PA, Graves LM, Samet JM (2006) Zn2+-induced IL-8 expression involves AP-1, JNK, and ERK activities in human airway epithelial cells. Am J Physiol Lung Cell Mol Physiol 290:L1028–L1035

Kim Y, Kong SD, Chen LH, Pisanic TR 2nd, Jin S, Shubayev VI (2013) In vivo nanoneurotoxicity screening using oxidative stress and neuroinflammation paradigms. Nanomedicine 9:1057–1066

Konczol M, Ebeling S, Goldenberg E, Treude F, Gminski R, Giere R, Grobety B, Rothen-Rutishauser B, Merfort I, Mersch-Sundermann V (2011) Cytotoxicity and genotoxicity of size-fractionated iron oxide (magnetite) in A549 human lung epithelial cells: role of ROS, JNK, and NF-kB. Chem Res Toxicol 24:1460–1475

Kumar M, Singh G, Arora V, Mewar S, Sharma U, Jagannathan NR, Sapra S, Dinda AK, Kharbanda S, Singh H (2012) Cellular interaction of folic acid conjugated superparamagnetic iron oxide nanoparticles and its use as contrast agent for targeted magnetic imaging of tumor cells. Int J Nanomed 7:3503–3516

Laskar A, Ghosh M, Khattak SI, Li W, Yuan XM (2012) Degradation of superparamagnetic iron oxide nanoparticle-induced ferritin by lysosomal cathepsins and related immune response. Nanomedicine 7:705–717

Lim YT, Noh YW, Han JH, Cai QY, Yoon KH, Chung BH (2008) Biocompatible polymer-nanoparticle-based bimodal imaging contrast agents for the labeling and tracking of dendritic cells. Small 4:1640–1645

Liu Y, Chen Z, Gu N, Wang J (2011) Effects of DMSA-coated Fe3O4 magnetic nanoparticles on global gene expression of mouse macrophage RAW264.7 cells. Toxicol Lett 205:130–139

Lunov O, Syrovets T, Buchele B, Jiang X, Rocker C, Tron K, Nienhaus GU, Walther P, Mailander V, Landfester K, Simmet T (2010) The effect of carboxydextran-coated superparamagnetic iron oxide nanoparticles on c-Jun N-terminal kinase-mediated apoptosis in human macrophages. Biomaterials 31:5063–5071

Mavropoulos A, Sully G, Cope AP, Clark AR (2005) Stabilization of IFN-gamma mRNA by MAPK p38 in IL-12- and IL-18-stimulated human NK cells. Blood 105:282–288

Mavropoulos A, Rigopoulou EI, Liaskos C, Bogdanos DP, Sakkas LI (2013) The role of p38 MAPK in the aetiopathogenesis of psoriasis and psoriatic arthritis. Clin Dev Immunol 2013:569751

Miyazawa K, Mori A, Miyata H, Akahane M, Ajisawa Y, Okudaira H (1998) Regulation of interleukin-1beta-induced interleukin-6 gene expression in human fibroblast-like synoviocytes by p38 mitogen-activated protein kinase. J Biol Chem 273:24832–24838

Myrianthefs P, Karatzas S, Venetsanou K, Grouzi E, Evagelopoulou P, Boutzouka E, Fildissis G, Spiliotopoulou I, Baltopoulos G (2003) Seasonal variation in whole blood cytokine production after LPS stimulation in normal individuals. Cytokine 24:286–292

Noubade R, Milligan G, Zachary JF, Blankenhorn EP, del Rio R, Rincon M, Teuscher C (2007) Histamine receptor H1 is required for TCR-mediated p38 MAPK activation and optimal IFN-gamma production in mice. J Clin Invest 117:3507–3518

Pareta RA, Taylor E, Webster TJ (2008) Increased osteoblast density in the presence of novel calcium phosphate coated magnetic nanoparticles. Nanotechnology 19:265101

Park EJ, Umh HN, Kim SW, Cho MH, Kim JH, Kim Y (2014) ERK pathway is activated in bare-FeNPs-induced autophagy. Arch Toxicol 88:323–336

Pasquinelli V, Rovetta AI, Alvarez IB, Jurado JO, Musella RM, Palmero DJ, Malbran A, Samten B, Barnes PF, Garcia VE (2013) Phosphorylation of mitogen-activated protein kinases contributes to interferon γ production in response to mycobacterium tuberculosis. J Infect Dis 207:340–350

Patil C, Zhu X, Rossa C Jr, Kim YJ, Kirkwood KL (2004) p38 MAPK regulates IL-1beta induced IL-6 expression through mRNA stability in osteoblasts. Immunol Invest 33:213–233

Pineiro-Redondo Y, Banobre-Lopez M, Pardinas-Blanco I, Goya G, Lopez-Quintela MA, Rivas J (2011) The influence of colloidal parameters on the specific power absorption of PAA-coated magnetite nanoparticles. Nanoscale Res Lett 6:383

Prijic S, Scancar J, Romih R, Cemazar M, Bregar VB, Znidarsic A, Sersa G (2010) Increased cellular uptake of biocompatible superparamagnetic iron oxide nanoparticles into malignant cells by an external magnetic field. J Membr Biol 236:167–179

Rhodus NL, Cheng B, Myers S, Bowles W, Ho V, Ondrey F (2005) A comparison of the pro-inflammatory, NF-kappa B-dependent cytokines: TNF-alpha, IL-1-alpha, IL-6, and IL-8 in different oral fluids from oral lichen planus patients. Clin Immunol 114:278–283

Rhodus NL, Cheng B, Ondrey F (2007) Th1/Th2 cytokine ratio in tissue transudates from patients with oral lichen planus. Mediators Inflamm 2007:19854

Rincon M, Enslen H, Raingeaud J, Recht M, Zapton T, Su MS, Penix LA, Davis RJ, Flavell RA (1998) Interferon-gamma expression by Th1 effector T cells mediated by the p38 MAP kinase signaling pathway. EMBO J 17:2817–2829

Roohi F, Lohrke J, Ide A, Schutz G, Dassler K (2012) Studying the effect of particle size and coating type on the blood kinetics of superparamagnetic iron oxide nanoparticles. Int J Nanomed 7:4447–4458

Schlachter EK, Widmer HR, Bregy A, Lonnfors-Weitzel T, Vajtai I, Corazza N, Bernau VJ, Weitzel T, Mordasini P, Slotboom J, Herrmann G, Bogni S, Hofmann H, Frenz M, Reinert M (2011) Metabolic pathway and distribution of superparamagnetic iron oxide nanoparticles: in vivo study. Int J Nanomed 6:1793–1800

Serkova NJ, Renner B, Larsen BA, Stoldt CR, Hasebroock KM, Bradshaw-Pierce EL, Holers VM, Thurman JM (2010) Renal inflammation: targeted iron oxide nanoparticles for molecular MR imaging in mice. Radiology 255:517–526

Shen J, Sakaida I, Uchida K, Terai S, Okita K (2005) Leptin enhances TNF-alpha production via p38 and JNK MAPK in LPS-stimulated kupffer cells. Life Sci 77:1502–1515

Shen CC, Liang HJ, Wang CC, Liao MH, Jan TR (2011a) A role of cellular glutathione in the differential effects of iron oxide nanoparticles on antigen-specific T cell cytokine expression. Int J Nanomed 6:2791–2798

Shen CC, Wang CC, Liao MH, Jan TR (2011b) A single exposure to iron oxide nanoparticles attenuates antigen-specific antibody production and T-cell reactivity in ovalbumin-sensitized BALB/c mice. Int J Nanomed 6:1229–1235

Shi Y, Zhou L, Wang R, Pang Y, Xiao W, Li H, Su Y, Wang X, Zhu B, Zhu X, Yan D, Gu H (2010) In situ preparation of magnetic nonviral gene vectors and magnetofection in vitro. Nanotechnology 21:115103

Siglienti I, Bendszus M, Kleinschnitz C, Stoll G (2006) Cytokine profile of iron-laden macrophages: implications for cellular magnetic resonance imaging. J Neuroimmunol 173:166–173

Stambe C, Atkins RC, Tesch GH, Kapoun AM, Hill PA, Schreiner GF, Nikolic-Paterson DJ (2003) Blockade of p38alpha MAPK ameliorates acute inflammatory renal injury in rat anti-GBM glomerulonephritis. J Am Soc Nephrol 14:338–351

Sun SL, Lo YL, Chen HY, Wang LF (2012) Hybrid polyethylenimine and polyacrylic acid-bound iron oxide as a magnetoplex for gene delivery. Langmuir 28:3542–3552

Taylor EN, Webster TJ (2009) The use of superparamagnetic nanoparticles for prosthetic biofilm prevention. Int J Nanomed 4:145–152

Valois CR, Braz JM, Nunes ES, Vinolo MA, Lima EC, Curi R, Kuebler WM, Azevedo RB (2010) The effect of DMSA-functionalized magnetic nanoparticles on transendothelial migration of monocytes in the murine lung via a beta2 integrin-dependent pathway. Biomaterials 31:366–374

Weinstein JS, Varallyay CG, Dosa E, Gahramanov S, Hamilton B, Rooney WD, Muldoon LL, Neuwelt EA (2010) Superparamagnetic iron oxide nanoparticles: diagnostic magnetic resonance imaging and potential therapeutic applications in neurooncology and central nervous system inflammatory pathologies, a review. J Cereb Blood Flow Metab 30:15–35

Windheim M, Lang C, Peggie M, Plater LA, Cohen P (2007) Molecular mechanisms involved in the regulation of cytokine production by muramyl dipeptide. Biochem J 404:179–190

Yang DD, Conze D, Whitmarsh AJ, Barrett T, Davis RJ, Rincon M, Flavell RA (1998) Differentiation of CD4 + T cells to Th1 cells requires MAP kinase JNK2. Immunity 9:575–585

Yeh CH, Hsiao JK, Wang JL, Sheu F (2010) Immunological impact of magnetic nanoparticles (Ferucarbotran) on murine peritoneal macrophages. J Nanopart Res 12:151–160

Zhang JJ, Xu ZM, Zhang CM, Dai HY, Ji XQ, Wang XF, Li C (2011) Pyrrolidine dithiocarbamate inhibits nuclear factor-kB pathway activation, and regulates adhesion, migration, invasion and apoptosis of endometriotic stromal cells. Mol Hum Reprod 17:175–181

Zhu MT, Feng WY, Wang B, Wang TC, Gu YQ, Wang M, Wang Y, Ouyang H, Zhao YL, Chai ZF (2008) Comparative study of pulmonary responses to nano- and submicron-sized ferric oxide in rats. Toxicology 247:102–111

Zhu M, Li Y, Shi J, Feng W, Nie G, Zhao Y (2012) Exosomes as extrapulmonary signaling conveyors for nanoparticle-induced systemic immune activation. Small 8:404–412

II.3. POLYACRYLIC ACID COATED AND NON-COATED IRON OXIDE NANOPARTICLES ARE NOT GENOTOXIC TO HUMAN T LYMPHOCYTES

Reprinted from Toxicology Letters

Toxicology Letters 234 (2015) 67–73

Contents lists available at ScienceDirect

Toxicology Letters

journal homepage: www.elsevier.com/locate/toxlet

Polyacrylic acid coated and non-coated iron oxide nanoparticles are not genotoxic to human T lymphocytes

Diana Couto [a], Rosa Sousa [b], Lara Andrade [b], Magdalena Leander [c], M. Arturo Lopez-Quintela [d], José Rivas [e], Paulo Freitas [e], Margarida Lima [c], Graça Porto [c], Beatriz Porto [b], Félix Carvalho [f,*], Eduarda Fernandes [a,**]

[a] UCIBIO/REQUIMTE, Laboratory of Applied Chemistry, Department of Chemical Sciences, Faculty of Pharmacy, University of Porto, Porto, Portugal
[b] Laboratory of Cytogenetics, Department of Microscopy, Institute of Biomedical Sciences Abel Salazar (ICBAS), University of Porto, Porto, Portugal
[c] Service of Clinical Hematology, Santo António Hospital, Porto, Portugal
[d] Laboratory of Nanotechnology and Magnetism, Institute of Technological Research, IIT, University of Santiago de Compostela (USC), Spain
[e] International Iberian Nanotechnology Laboratory, Braga, Portugal
[f] UCIBIO/REQUIMTE, Laboratory of Toxicology, Department of Biological Sciences, Faculty of Pharmacy, University of Porto, Porto, Portugal

HIGHLIGHTS

- The genotoxicity of oxide nanoparticles (ION) was evaluated in human T lymphocytes.
- Polyacrylic acid-coated and non-coated ION were studied and revealed no genotoxicity.
- The tested ION do not influence bleomycin-induced genotoxicity in human T lymphocytes.

GRAPHICAL ABSTRACT

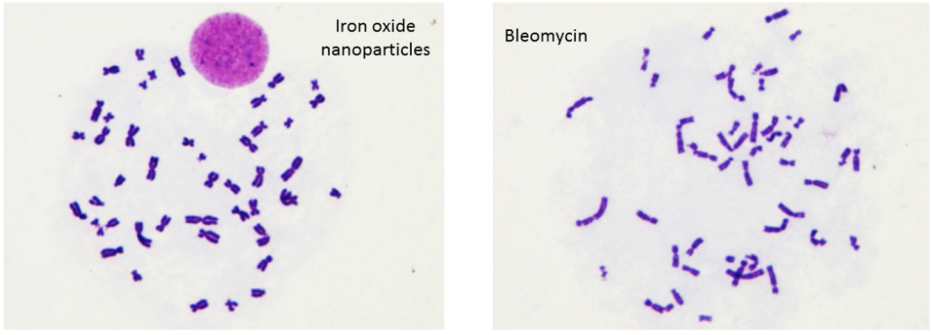

Polyacrylic acid-coated and non-coated iron oxide nanoparticles do not induce genotoxicity in human lymphocytes nor exacerbate bleomycin-induced genotoxicity

ARTICLE INFO

Article history:
Received 2 November 2014
Received in revised form 31 January 2015
Accepted 11 February 2015
Available online 12 February 2015

Keywords:
Iron oxide nanoparticles
Bleomycin
Genotoxicity
Human T lymphocytes
Cell cycle

ABSTRACT

The use of iron oxide nanoparticles (ION) for diagnostic and therapeutic purposes requires a clear favorable risk-benefit ratio. This work was performed with the aim of studying the ability of polyacrylic acid (PAA)-coated and non-coated ION to induce genotoxicity in human T lymphocytes. For that purpose, their influence on cell cycle progression and on the induction of chromosome aberrations was evaluated. Blood samples collected from healthy human donors were exposed to PAA-coated and non-coated ION, at different concentrations, for 48 h. The obtained results showed that, for all culture conditions, the tested ION are not genotoxic and do not influence the cell cycle arrest. Their possible cumulative effect with the iron-dependent genotoxic agent BLM was also evaluated. Blood samples collected from healthy human donors were exposed to ION, at different concentrations, for 48 h, in the presence of a pre-determined toxic concentration of BLM. The obtained results showed that, for all culture conditions, the tested ION do not potentiate the clastogenic effects of BLM.

* Corresponding author at: Rua de Jorge Viterbo Ferreira n° 228, 4050-313 Porto, Portugal. Tel.: +351 220428600.
** Corresponding author at: Rua de Jorge Viterbo Ferreira nº 228, 4050-313 Porto, Portugal. Tel.: +351 220428675.
E-mail addresses: felixdc@ff.up.pt (F. Carvalho), egracas@ff.up.pt (E. Fernandes).

http://dx.doi.org/10.1016/j.toxlet.2015.02.010
0378-4274/

1. Introduction

Nowadays, the amount of iron oxide nanoparticles (ION) used in the diverse biomedical applications is significant. In fact, there are several formulations available in the market including ION in the formulation, namely Endorem®, Resovist®, Combidex®, among others (Azoulay et al., 2008; Kedziorek et al., 2010; Kumar et al., 2012; Lunov et al., 2010). However, despite the considerable use of ION worldwide, their safety is still an important matter of debate. Some studies point that ION may be cytotoxic, stimulating the production of reactive oxygen and nitrogen species (ROS and RNS) (Hoskins et al., 2012; Hsiao et al., 2008; Kenzaoui et al., 2012; Naqvi et al., 2010) and triggering loss of viability in varied cell lines (Cochran et al., 2013; Ge et al., 2013; Schwarz et al., 2012; Yu et al., 2012). Using human neutrophils, we have also demonstrated that polyacrylic acid (PAA)-coated and non-coated ION activate oxidative burst, leading to the sustained production of ROS (Couto et al., 2014). These last results emphasize the potential involvement of cells from the human innate defense system in the deleterious effects of ION.

One of the possible implications of sustained production of high levels of ROS and RNS is oxidative stress-related deoxyribonucleic acid (DNA) damage (AshaRani et al., 2009; Schwartz and Rotter, 1998; Shackelford et al., 1999) and, accordingly, some reports in the literature have already shown that ION may induce DNA damage, namely Fe_2O_3 nanoparticles (NP) in human lung fibroblasts IMR 90 cells (Bhattacharya et al., 2009, 2012) and oleate-coated Fe_3O_4 NP in human peripheral lymphocytes (Magdolenova et al., 2013). In conditions of oxidative stress and/or in the presence of xenobiotics that cause DNA damage, cells have the ability to arrest cell cycle in G1 and G2 to allow adequate functioning of DNA repair systems and prevent the propagation of damage to the resulting daughter cells (AshaRani et al., 2009; Malumbres and Barbacid, 2009; Shackelford et al., 1999). Concerning ION, previous studies reported that γ-Fe_2O_3 NP and Fe_3O_4 NP increase the proportion of cells in G1 phase of the cell cycle in RAW 264.7 cells (Park et al., 2014b), and in cells from the mouse bronchoalveolar lavage fluid (Park et al., 2010). Fe_3O_4 NP also induce G2/M arrest in PC12 cells (Wu et al., 2012) and decrease the number of cells in S phase in mouse bronchoalveolar lavage fluid (Park et al., 2010).

Given that PAA has been increasingly described as a promising coating for ION used in several applications, namely in gene delivery (Cao et al., 2013; Sun et al., 2012) and in liver and kidney imaging (Iversen et al., 2013), and that PAA-coated and non-coated ION seem to activate ROS production, it is of paramount importance to assess its potential genotoxicity. In the present study, we evaluated the effect of PAA-coated and non-coated ION on human T lymphocytes, as these cells may be involved in the immune response to the administration of ION (Katsnelson et al., 2010; Park et al., 2010; Shen et al., 2011; Valois et al., 2010; Zhu et al., 2008). Moreover, they have the important role of stimulating macrophage and B-lymphocyte activities mainly via production of regulatory cytokines (Newsholme, 2001) and present a high rate of division, being therefore possible target cells for the deleterious effects of pro-oxidant agents with potential genotoxic effects (Lialiaris et al., 2008; Zhang et al., 2008). Noteworthy, it is known that these cells are highly susceptible to the genotoxicity of bleomycin (BLM), a well-known iron-dependent clastogenic agent, by formation of a ternary complex with Fe^{2+} and oxygen, which binds to DNA, inducing double strand breaks that result in chromosome breaks, gaps, dicentric chromosomes, rings and radial figures (Jaloszynski et al., 1997; Mir et al., 1996; Paika and Krishan, 1973; Vernole et al., 1998). Notably, BLM has also been shown to exert a synergistic effect with other xenobiotics concerning genotoxic promotion (Lee et al., 2004; Poli et al., 2002), and it is therefore of additional interest to study the clastogenic effects of BLM in the presence of ION.

Considering the above rationale, the present work was performed with the aim of studying the ability of PAA-coated and non-coated ION to induce genotoxicity in human T lymphocytes. For that purpose, their influence on cell cycle progression and on the induction of chromosome aberrations was evaluated. Their possible cumulative effect with the iron-dependent genotoxic agent BLM was further studied.

2. Materials and methods

2.1. Materials

Venous blood was collected by antecubital venipuncture from healthy human blood donors at Hospital de Santo António (Porto, Portugal), following informed consent. Lyophilized BLM sulphate 15,000 UI was obtained from TEVA Pharmaceutical Industries Ltd. (Israel). RPMI 1640 medium, Dulbecco's phosphate buffer saline, without calcium chloride and magnesium chloride (PBS) [2.68 mM KCl, 0.14 M NaCl, 1.21 mM KH_2PO_4, 8.10 mM Na_2HPO_4], L-glutamine, fetal bovine serum, penicillin, streptomycin and histopaque 1077 were obtained from Sigma Chemical Co. (St Louis, USA). Ferrous chloride, ferric chloride, NH_4OH, KCl and PAA (average M_w 1800) were obtained from Sigma–Aldrich (St Louis, USA). Phytohaemagglutinin and colcemid were obtained from Gibco (Invitrogen Corporation, USA). Acetic acid, methanol, Türk's solution and Giemsa's azur eosin methylene blue solution were obtained from Merck (Darmstadt, Germany). Mouse anti-human CD3 monoclonal antibodies conjugated with fluorescein isothiocyanate (FITC) and Coulter® DNA Prep™ Reagents Kit were obtained from Beckman Coulter (Hialeah, FL, USA). Polyclonal rabbit anti-mouse immunoglobulins conjugated with FITC were obtained from Dako A/S (Glostrup, Denmark).

ION non-coated and PAA-coated magnetite particles were obtained from Nanogap (Santiago de Compostela, Spain), and their preparation and physico-chemical characterization was performed as reported before (Couto et al., 2014). Briefly, preparation of "non-coated" ION was based on the chemical co-precipitation of a mixture of Fe(II) and Fe(III) chloride salts (molar ratio 2:1) using NH_4OH in a degassed 1 M KCl aqueous solution at 60 °C. The dark precipitate was washed several times with deoxygenated water, and finally the particles were stored at pH 9.6 (well above their isoelectric point: 6.5). For the PAA-coated ION, PAA [25% w/w with respect to the Fe(II) salt] was added to the reaction medium. PAA-coated and non-coated ION were characterized using transmission electron microscopy (TEM) (Hitachi H-7000, Japan). Determination of the hydrodynamic size and zeta potential of the studied NP, in RPMI 1640 suspensions, were made using a NP analyzer SZ-100 (HORIBA Scientific) (DPSS laser 532 nm). Both PAA-coated and non-coated ION have a similar size distribution, with a mean particle size of 9.9 ± 2.3 nm and 10.1 ± 2.4 nm (mean ± SD) for the non-coated and PAA-coated ION, respectively. However, when the ION were dispersed in RPMI 1640 medium supplemented with fetal bovine serum, large hydrodynamic sizes [5166 ± 481 nm and 174 ± 65 nm (mean ± SEM) for the non-coated and PAA-coated ION, respectively], and low zeta potentials [-1.91 ± 0.35 mV and -3.02 ± 0.73 mV (mean ± SEM) for the non-coated and PAA-coated ION, respectively] were observed, which indicates that both types of NP tend to agglomerate when resuspended in RPMI 1640 medium, though in much higher intensity in the case of non-coated ION. Before dilutions, ION were sonicated for 5 min (P selecta ultrasonic bath, 50 Hz) to disrupt possible aggregates before the preparation of the samples.

2.2. Methods

2.2.1. Cell cultures

The procedure was performed as described in (Sousa et al., 2013): samples of 0.5 mL of whole blood were used for lymphocyte cultures in RPMI 1640 medium supplemented with 20% fetal bovine serum, 2 mM L-glutamine, 100 U/mL penicillin and 0.1 mg/mL streptomycin. The cultures were stimulated with 5 μg/mL phytohaemagglutinin and incubated at 37 °C with a 5% CO_2 atmosphere, for 24 h. In sequence, PAA-coated and non-coated ION (4, 20 and 100 μg/mL) were added to the lymphocyte cultures and the incubation proceeded for more 48 h. These concentrations are within those usually attained in biomedical applications [up to 70 μg/mL (Apopa et al., 2009)]. Simultaneously, it was performed an experiment to evaluate the genotoxic effect of ION in the presence of BLM. For this purpose, BLM (10 μg/mL) was added 1 h after the addition of the ION to lymphocyte cultures.

2.2.2. Isolation of human peripheral blood mononuclear cells by the gradient density centrifugation method

Following 72 h of culture, isolation of human peripheral blood mononuclear cells (PBMCs) was performed by the gradient density centrifugation method, as described in (Ngkelo et al., 2012) with slight adaptations: the tubes with the cells exposed to PAA-coated and non-coated ION (4, 20 and 100 μg/mL) were centrifuged at 890 × *g* for 10 min at 20 °C. Cell pellets were re-suspended in 3 mL of the centrifuged supernatant and placed on the top of 3 mL of Histopaque 1077 in a 14 mL polypropylene tube. After centrifugation at 890 × *g* for 30 min, at 20 °C, the layer corresponding to PBMCs was collected to a new polypropylene tube and PBS was added to wash the cells. The PBMC suspension was then centrifuged at 890 × *g* for 10 min, at 20 °C. Afterwards, the supernatant was decanted and new PBS was added to the tube and centrifuged at 890 × *g* for 10 min at 20 °C. This last step was repeated one more time. Cells were then re-suspended in PBS and counted using a neubauer chamber and an optic microscope (40×) in the presence of Türk's solution (the acetic acid of this solution hemolyzes the erythrocytes and the PBMCs are stained by the dye contained). The cell concentration was adjusted to 1×10^6 PBMCs/mL and, subsequently, the cells were used for cell cycle analysis by flow cytometry.

2.2.3. CD3 staining and cell cycle analysis by flow cytometry

Isolated PBMCs were sequentially labeled with anti-CD3 monoclonal mouse anti-human and anti-IgG polyclonal rabbit anti-mouse conjugated with FITC antibodies in order to label T lymphocytes. Cell staining for surface CD3 was performed using a two step-washing method, as previously described in detail (Lima et al., 2000). This method is based on the sequential use both of FITC-conjugated primary mouse anti-human CD3 monoclonal antibodies and FITC-conjugated secondary polyclonal rabbit anti-mouse immunoglobulins, a strategy that increases the FITC signal of CD3 positive cells without an appreciable increase in nonspecific staining. This procedure obviates difficulties imposed by the decrease of expression of cell surface antigens when cells are simultaneously stained for DNA, due to permeabilizing procedures. As a first step, cells were incubated with 10 μL of FITC-conjugated mouse anti-human anti-CD3 for 15 min at room temperature, protected from light, and washed twice in PBS. As a second step, 20 μL of FITC-conjugated rabbit anti-mouse immunoglobulins (Dako A/S, Glostrup, Denmark) were added and cells were incubated under the same conditions. Once this incubation period was completed, cells were washed once in PBS and then processed with the Coulter® DNA-Prep Reagent Kit (Beckman Coulter, Hialeah, FL), according to the manufacturer's instructions. Briefly, 100 μL of DNA Prep LPR reagent (to lyse red cells and permeabilize cell membranes) was added and vortexed for 8 s; after that, 2 mL of DNA-Prep stain (propidium iodide solution with RNAse) were added and vortexed for 10 s. Finally, the samples were incubated at 4 °C in the darkness for 15 min before acquisition.

2.2.3.1. Data acquisition and analysis. Data acquisition was carried out in an EPICS-XL-MCL flow cytometer (Beckman Coulter, Hialeah, FL, USA) equipped with a 15-mW air-cooled 488-nm argon laser, using the XL2 software program (Beckman Coulter, Hialeah, FL). Instrument alignment and standardization were performed daily and electronic compensation was used to remove spectral overlap. Samples were injected at a flow rate of 12 ± 3 μL/min. A normal blood sample was processed in parallel and the red fluorescence high voltage was adjusted to place the mean channel of the G0/G1 peak of normal blood lymphocytes at the channel 200 ± 10. Information was acquired and stored as list mode data for each staining. For cell cycle analysis, cell doublets were excluded and T lymphocytes were gated based on their positivity for CD3. Then, cell cycle distribution was analyzed using the Multicycle software (Phoenix Flow Systems, San Diego, CA).

2.2.4. Cytogenetic analysis

Cytogenetic analysis was performed as described in (Sousa et al., 2013): cells previously incubated with ION in the presence and absence of BLM (10 μg/mL) were harvested after 1 h incubation with colcemid (10 μg/mL), followed by hypotonic treatment with 75 mM KCl and fixation in a 1:3 solution of acetic acid:methanol. Chromosome preparations were made by the air drying method.

For each independent experiment, analysis of chromosome aberrations was performed by one scorer on 50 Giemsa-stained

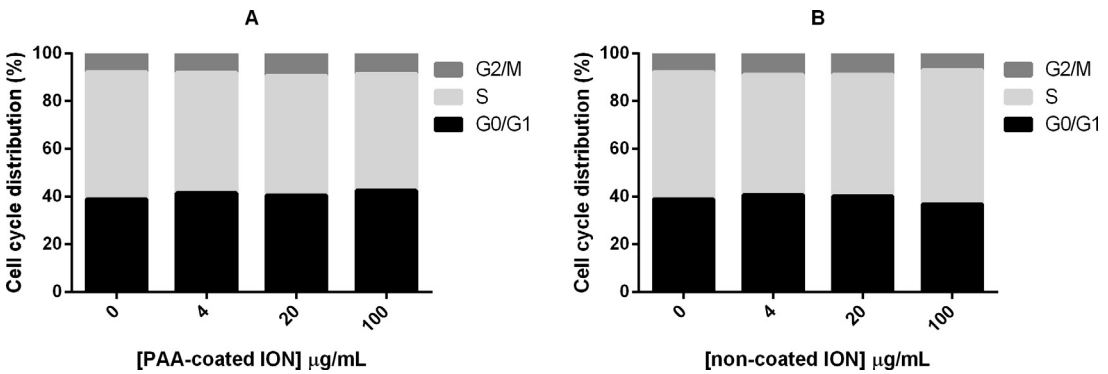

Fig. 1. Cell cycle distribution (expressed in percentage) following exposure to (A) PAA-coated and (B) non-coated ION (4, 20 and 100 μg/mL), at 37 °C, for 48 h. Values are given as mean of the percentages of T lymphocytes in the phases G0/G1, S and G2/M ($n \geq 7$).

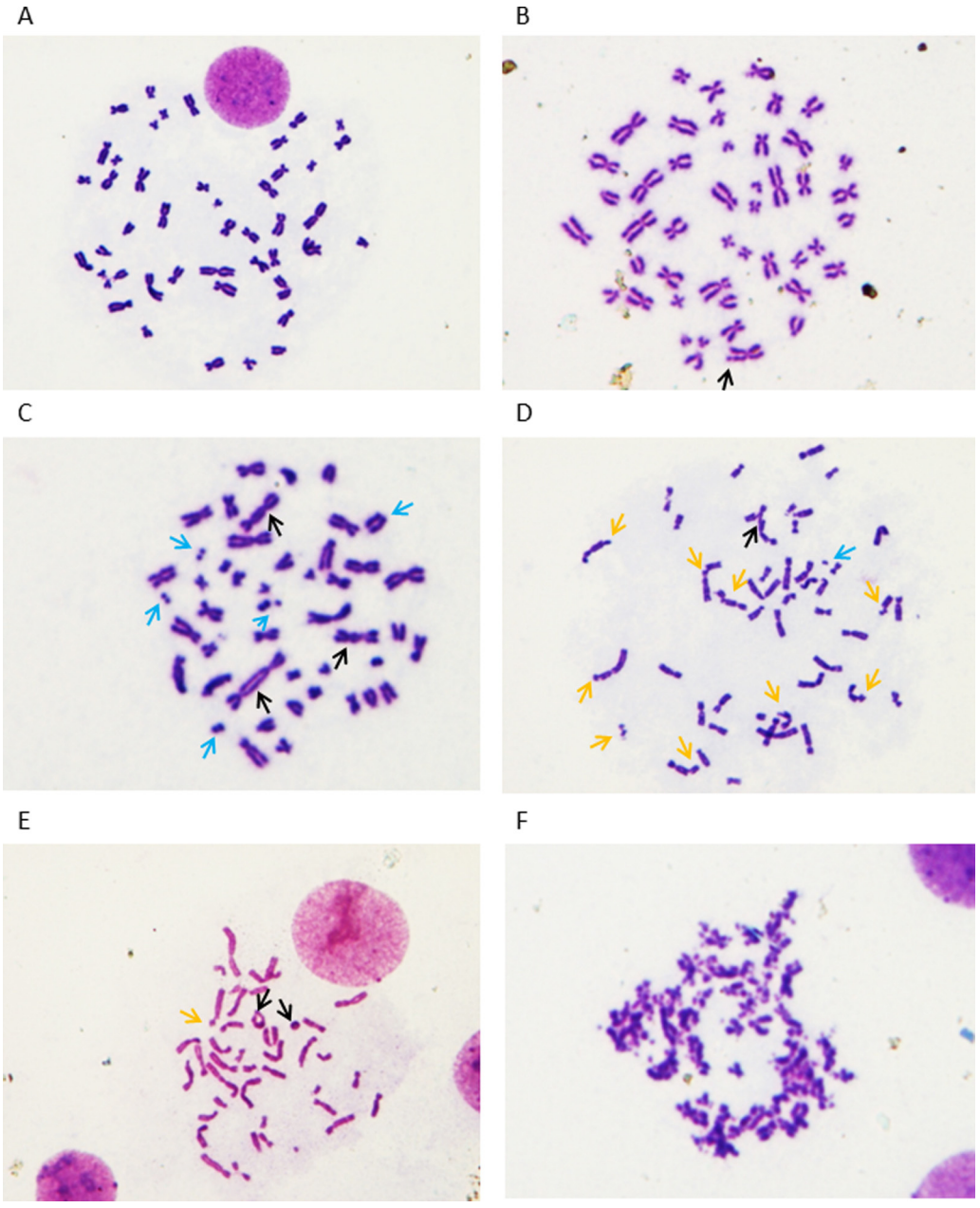

Fig. 2. Typical chromosomal aberrations observed in the present study (amplification 100×): metaphase without any chromosomal aberration (A); metaphase with a gap (B), indicated by a black arrowhead; metaphase with dicentric chromosomes and acentric fragments (C), indicated by black and blue arrowheads, respectively; metaphase with a figure, breaks and an acentric fragment (D), indicated by black, orange and blue arrowheads, respectively; metaphase with rings and a break (E), indicated by black and orange arrowheads, respectively; pulverized metaphase (F). (For interpretation of the references to color in this figure legend, the reader is referred to the web version of this article.)

metaphases from coded slides. To avoid bias in cell selection, consecutive metaphases that appeared intact, with sufficient well-defined chromosome morphology, were selected for study. Each cell was scored for chromosome number and the number and types of structural abnormalities. Achromatic areas less than a chromatid in width were scored as gaps while those wider than a chromatid were scored as breaks. Chromatid exchange configurations (like triradial and tetraradial figures), dicentric and ring chromosomes were scored as rearrangements. Gaps were excluded in the calculation of the chromosome breakage frequencies and rearrangements were scored as two breaks.

2.2.5. Statistical analysis

Results are expressed as the mean ± SEM (from at least seven individual experiments). Statistical comparison between groups was performed using the one-way analysis of variance, followed by Bonferroni's post hoc test using GraphPad Prism™ (version 6.0; GraphPad Software). *P* values lower than 0.05 were considered as statistically significant.

3. Results

3.1. CD3 immunofluorescent staining and cell cycle distribution

For a good knowledge of the cell cycle, it is important to reflect on its different phases. The period between mitoses is termed interphase. DNA replication occurs at a discrete time during interphase, termed DNA synthesis phase or S phase. The period between mitosis and the subsequent S phase is known as Gap 1 (G1), while the period between S phase and the following mitosis is

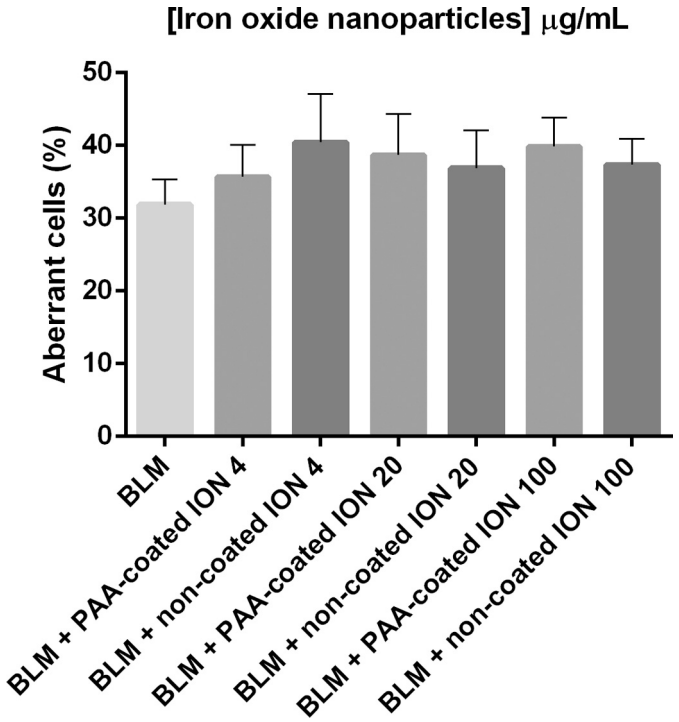

Fig. 3. Aberrant cells (expressed in percentage) in the presence of BLM (10 μg/mL) and: PAA-coated ION (4, 20 and 100 μg/mL) and non-coated ION (4, 20 and 100 μg/mL), at 37 °C, for 48 h. Values are given as mean ± SEM ($n = 12$).

Gap 2 (G2). Cells in a metabolically active state but not progressing to, or through DNA synthesis or cell division, are said to be quiescent or resting (G0). In the typical dividing eukaryotic cell, G1 phase lasts approximately 12 h, S phase 6–8 h, G2 phase 3–6 h, and mitosis about 30 min, although the exact length of each phase varies with cell type and growth conditions (Shackelford et al., 1999).

Cell cycle distribution of T lymphocytes exposed to PAA-coated and non-coated ION (4, 20 and 100 μg/mL) for 48 h at 37 °C was assessed by flow cytometry. It was verified that none of the ION tested had interference in the progression of cell cycle (Fig. 1A and B).

3.2. Cytogenetic effects

In human T lymphocyte cultures exposed to PAA-coated and non-coated ION (4, 20 and 100 μg/mL), no induction of genotoxicity was observed, as all the metaphases analyzed, in each culture condition, presented 46 chromosomes without any chromosomal aberration (Fig. 2A).

The possible cumulative effect of ION on BLM-induced lymphocyte cultures was also evaluated. For that purpose, human T lymphocytes were exposed to BLM at a pre-determined concentration that induces chromosomal aberrations, such as gaps (black arrowhead in Fig. 2B), breaks (orange arrowheads in Fig. 2D and E), acentric fragments (blue arrowheads in Fig. 2C and D), dicentric chromosomes (black arrowheads in Fig. 2C), rings (black arrowheads in Fig. 2E), figures (black arrowhead in Fig. 2D) and pulverized metaphases (Fig. 2F). In the BLM-induced cultures exposed to PAA-coated and non-coated ION (4, 20 and 100 μg/mL), although both ION showed some tendency to increase the genotoxicity of BLM, it did not reach significance, which allow us to conclude that, under the present experimental conditions, none of the studied ION potentiate the genotoxicity of BLM (Figs. 3 and 4, Tables 1 and 2).

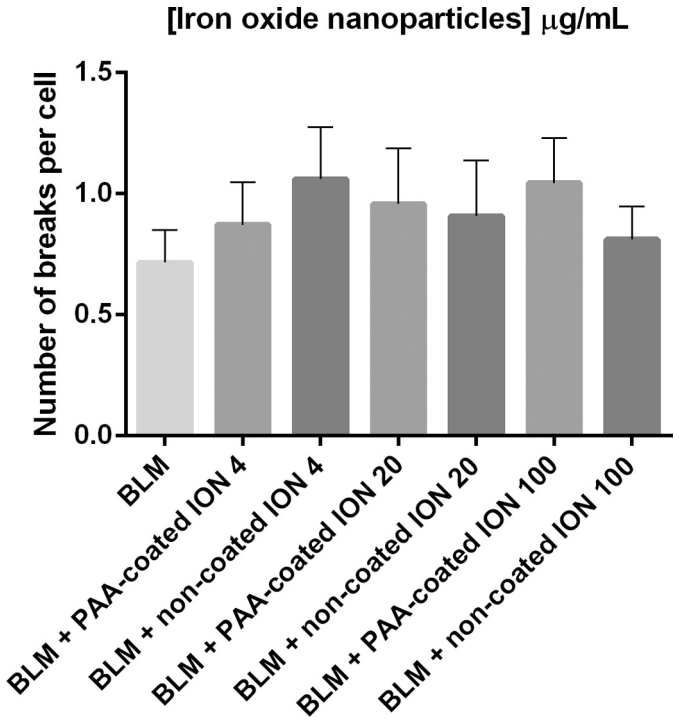

Fig. 4. Mean number of breaks per cell following exposure to BLM (10 μg/mL) and: PAA-coated ION (4, 20 and 100 μg/mL) and non-coated ION (4, 20 and 100 μg/mL), at 37 °C, for 48 h. Values are given as mean ± SEM ($n = 12$).

4. Discussion

This work was performed with the aim of evaluating the ability of PAA-coated and non-coated ION to induce genotoxicity in human T lymphocytes and to evaluate the possible cumulative effect with the iron-dependent clastogenic agent BLM. It was observed that, in isolated studies, the tested ION had no genotoxic effects, neither affected the cell cycle, nor affected significantly the clastogenicity of BLM.

Previous studies indicate that ION have genotoxic potential, as shown for Fe_2O_3 NP in human lung fibroblasts IMR 90 cells (Bhattacharya et al., 2009, 2012) and oleate-coated Fe_3O_4 NP in human peripheral lymphocytes (Magdolenova et al., 2013). However, in agreement with our study, there are also reports showing absence of genotoxicity, namely Fe_3O_4 NP in TK6 lymphoblastoid cells and human peripheral lymphocytes (Magdolenova et al., 2013) and γ-Fe_2O_3 NP, dextran-coated Fe_3O_4 NP and Fe_3O_4 NP in human B-lymphoblastoid MCL5 cells (Singh et al., 2012). Many factors may be involved in these differences, namely some particularities in the characteristics of ION, like size and coating, and its interaction with the different cells. For example, Magdolenova et al. (2013) found that oleate-coated Fe_3O_4 NP induced DNA damage in human peripheral lymphocytes and TK6 lymphoblastoid cells but Fe_3O_4 NP did not exert the same effect, which demonstrates, in this case, the influence of the coating on genotoxicity.

The mechanism by which BLM, a known antibiotic used in anticancer therapy, induces chromosome damage is through simultaneous binding to oxygen and redox-active transition metals, such as Fe^{2+}. The ternary complex of BLM with Fe^{2+} and oxygen binds to DNA, Fe^{2+} is oxidated to Fe^{3+} and a nucleophilic attack at the DNA desoxyribose C4′ position occurs, inducing this way breaks, gaps, dicentric chromosomes, rings and figures (Mir et al., 1996; Paika and Krishan, 1973). Therefore, as both ION used in this study are presented in the form of magnetite, where iron is

Table 1
BLM (10 μg/mL) and PAA-coated ION-induced chromosome instability in lymphocyte cultures from 12 individuals.

	% Aberrant cells				Number of breaks per cell			
Individuals	BLM	BLM + ION 4 μg/mL	BLM + ION 20 μg/mL	BLM + ION 100 μg/mL	BLM	BLM + ION 4 μg/mL	BLM + ION 20 μg/mL	BLM + ION 100 μg/mL
1	31	n.a.	n.a.	32	0.57	n.a.	n.a.	0.77
2	23	n.a.	n.a.	53	0.36	n.a.	n.a.	1.22
3	30	n.a.	n.a.	44	0.74	n.a.	n.a.	0.84
4	31	39	25	21	0.57	0.82	0.60	0.35
5	16	22	18	36	0.32	0.34	0.38	1.06
6	41	40	42	31	0.80	0.82	1.10	0.64
7	28	19	31	24	0.49	0.24	0.56	0.33
8	62	65	78	71	2.08	2.02	2.63	2.47
9	42	34	44	44	0.80	0.80	0.90	0.82
10	30	32	37	34	0.78	0.76	0.69	1.24
11	28	33	39	53	0.73	1.31	1.24	2.06
12	22	37	34	35	0.35	0.74	0.52	0.73
Mean ± SEM	32 ± 3	36 ± 4	39 ± 6	40 ± 4	0.7 ± 0.1	0.9 ± 0.2	1.0 ± 0.2	1.0 ± 0.2

n.a. not analyzed.

present as a mixture of Fe^{3+} and Fe^{2+} ions (Aranda et al., 2013), it was hypothesized that Fe^{2+} ions from ION could interact with BLM in the presence of oxygen, which would exacerbate its genotoxicity. However, although both ION showed some tendency to increase the genotoxicity of BLM, it did not reach significance, which allow us to conclude that, under the present experimental conditions, none of the studied ION potentiate the genotoxicity of BLM.

It is known that proper progression through the cell cycle is monitored by checkpoints that sense possible defects during DNA synthesis and chromosome segregation. Activation of these checkpoints induces cell cycle arrest through modulation of cyclin-dependent kinase (CDK) activity. Cell cycle arrest allows cells to properly repair eventual defects, thus preventing their transmission to the resulting daughter cells (Malumbres and Barbacid, 2009). Therefore, in conditions of oxidative stress and/or in the presence of agents that cause DNA damage, cells have the ability to arrest proliferation in G1 and G2 until the damage is repaired (AshaRani et al., 2009; Malumbres and Barbacid, 2009; Shackelford et al., 1999). In this study, we observed that none of the ION tested were able to interfere with the cell cycle. These data are in agreement with the ones obtained by Liu et al. (2011), who reported that dimercaptosuccinic acid-coated Fe_3O_4 NP have no effect on the cell cycle of THP-1 and RAW 264.7 cells. However, the opposite has also been described: Park et al. (2014b) reported that γ-Fe_2O_3 NP increased the proportion of RAW 264.7 cells in G1 phase. Additionally, dimercaptosuccinic acid-coated Fe_3O_4 NP increased the number of cells in G2/M phase in HepG2 hepatocytes (Liu et al., 2011). Consequently, the effect depends of the different characteristics of ION and cell type. For example, Park et al. (2014a) stated that, in a MH-S cell line, Fe_2O_3 NP increased the number of cells in the G1 phase, while Fe_3O_4 NP increased the number of cells in the G2/M phase, which reveals that different types of ION may influence cell cycle in a different manner.

5. Conclusion

From the results obtained in the present study, it can be concluded that the tested PAA-coated and non-coated ION are not direct genotoxic agents in human T lymphocytes, neither potentiate the genotoxicity of an iron-dependent clastogenic agent – BLM.

Conflict of interest

Authors declare no conflicts of interest concerning the present study.

Transparency document

The Transparency document associated with this article can be found in the online version.

Acknowledgements

Diana Couto acknowledges the FCT financial support for the PhD grant (SFRH/BD/72856/2010), in the ambit of "POPH – QREN – Tipologia 4.1 – Formação Avançada" co-sponsored by FSE and national funds of MCTES. Authors also greatly acknowledge the financial support given by Comissão de Bolsas e Prémios and

Table 2
BLM (10 μg/mL) and non-coated ION-induced chromosome instability in lymphocyte cultures from 12 individuals.

	% Aberrant cells				Number of breaks per cell			
Individuals	BLM	BLM + ION 4 μg/mL	BLM + ION 20 μg/mL	BLM + ION 100 μg/mL	BLM	BLM + ION 4 μg/mL	BLM + ION 20 μg/mL	BLM + ION 100 μg/mL
1	31	n.a.	n.a.	51	0.57	n.a.	n.a.	1.21
2	23	n.a.	n.a.	39	0.36	n.a.	n.a.	0.82
3	30	n.a.	n.a.	45	0.74	n.a.	n.a.	0.53
4	31	54	29	24	0.57	1.18	0.39	0.48
5	16	16	20	30	0.32	0.24	0.32	0.58
6	41	49	27	42	0.80	1.61	0.59	0.83
7	28	23	41	24	0.49	0.77	1.04	0.31
8	62	80	73	65	2.08	2.37	2.53	2.06
9	42	44	36	30	0.80	1.06	1.00	0.44
10	30	21	24	28	0.78	0.42	0.28	0.62
11	28	43	45	31	0.73	0.78	0.92	1.04
12	22	33	37	39	0.35	1.12	1.10	0.82
Mean ± SEM	32 ± 3	41 ± 7	37 ± 5	37 ± 4	0.7 ± 0.1	1.1 ± 0.2	0.9 ± 0.2	0.8 ± 0.1

n.a. not analyzed.

Departamento de Formação, Ensino e Investigação for Bolsa de Investigação Aplicada do Centro Hospitalar do Porto.

References

Apopa, P.L., Qian, Y., Shao, R., Guo, N.L., Schwegler-Berry, D., Pacurari, M., Porter, D., Shi, X., Vallyathan, V., Castranova, V., Flynn, D.C., 2009. Iron oxide nanoparticles induce human microvascular endothelial cell permeability through reactive oxygen species production and microtubule remodeling. Part. Fibre Toxicol. 6, 1.

Aranda, A., Sequedo, L., Tolosa, L., Quintas, G., Burello, E., Castell, J.V., Gombau, L., 2013. Dichloro-dihydro-fluorescein diacetate (DCFH-DA) assay: a quantitative method for oxidative stress assessment of nanoparticle-treated cells. Toxicol. In Vitro 27, 954–963.

AshaRani, P.V., Mun, G.L.K., Hande, M.P., Valiyaveettil, S., 2009. Cytotoxicity and genotoxicity of silver nanoparticles in human cells. ACS Nano 3, 279–290.

Azoulay, R., Olivier, P., Baud, O., Verney, C., Santus, R., Robert, P., Gressens, P., Sebag, G., 2008. USPIO (ferumoxtran-10)-enhanced MRI to visualize reticuloendothelial system cells in neonatal rats: feasibility and biodistribution study. J. Magn. Reson. Imaging 28, 1046–1052.

Bhattacharya, K., Davoren, M., Boertz, J., Schins, R.P., Hoffmann, E., Dopp, E., 2009. Titanium dioxide nanoparticles induce oxidative stress and DNA-adduct formation but not DNA-breakage in human lung cells. Part. Fibre Toxicol. 6, 17.

Bhattacharya, K., Hoffmann, E., Schins, R.F., Boertz, J., Prantl, E.M., Alink, G.M., Byrne, H.J., Kuhlbusch, T.A., Rahman, Q., Wiggers, H., Schulz, C., Dopp, E., 2012. Comparison of micro- and nanoscale Fe+3-containing (hematite) particles for their toxicological properties in human lung cells *in vitro*. Toxicol. Sci. 126, 173–182.

Cao, B., Qiu, P., Mao, C., 2013. Mesoporous iron oxide nanoparticles prepared by polyacrylic acid etching and their application in gene delivery to mesenchymal stem cells. Microsc. Res. Tech. 76, 936–941.

Cochran, D.B., Wattamwar, P.P., Wydra, R., Hilt, J.Z., Anderson, K.W., Eitel, R.E., Dziubla, T.D., 2013. Suppressing iron oxide nanoparticle toxicity by vascular targeted antioxidant polymer nanoparticles. Biomaterials 34, 9615–9622.

Couto, D., Freitas, M., Vilas-Boas, V., Dias, I., Porto, G., Lopez-Quintela, M.A., Rivas, J., Freitas, P., Carvalho, F., Fernandes, E., 2014. Interaction of polyacrylic acid coated and non-coated iron oxide nanoparticles with human neutrophils. Toxicol. Lett. 225, 57–65.

Ge, G., Wu, H., Xiong, F., Zhang, Y., Guo, Z., Bian, Z., Xu, J., Gu, C., Gu, N., Chen, X., Yang, D., 2013. The cytotoxicity evaluation of magnetic iron oxide nanoparticles on human aortic endothelial cells. Nanoscale Res. Lett. 8, 215.

Hoskins, C., Cuschieri, A., Wang, L., 2012. The cytotoxicity of polycationic iron oxide nanoparticles: common endpoint assays and alternative approaches for improved understanding of cellular response mechanism. J. Nanobiotechnol. 10, 15.

Hsiao, J.K., Chu, H.H., Wang, Y.H., Lai, C.W., Chou, P.T., Hsieh, S.T., Wang, J.L., Liu, H.M., 2008. Macrophage physiological function after superparamagnetic iron oxide labeling. NMR Biomed. 21, 820–829.

Iversen, N.K., Frische, S., Thomsen, K., Laustsen, C., Pedersen, M., Hansen, P.B., Bie, P., Fresnais, J., Berret, J.F., Baatrup, E., Wang, T., 2013. Superparamagnetic iron oxide polyacrylic acid coated γ-Fe_2O_3 nanoparticles do not affect kidney function but cause acute effect on the cardiovascular function in healthy mice. Toxicol. Appl. Pharmacol. 266, 276–288.

Jaloszynski, P., Kujawski, M., Czub-Swierczek, M., Markowska, J., Szyfter, K., 1997. Bleomycin-induced DNA damage and its removal in lymphocytes of breast cancer patients studied by comet assay. Mutat. Res. 385, 223–233.

Katsnelson, B., Privalova, L.I., Kuzmin, S.V., Degtyareva, T.D., Sutunkova, M.P., Yeremenko, O.S., Minigalieva, I.A., Kireyeva, E.P., Khodos, M.Y., Kozitsina, A.N., Malakhova, N.A., Glazyrina, J.A., Shur, V.Y., Shishkin, E.I., Nikolaeva, E.V., 2010. Some peculiarities of pulmonary clearance mechanisms in rats after intratracheal instillation of magnetite (Fe_3O_4) suspensions with different particle sizes in the nanometer and micrometer ranges: are we defenseless against nanoparticles? Int. J. Occup. Environ. Health 16, 508–524.

Kedziorek, D.A., Muja, N., Walczak, P., Ruiz-Cabello, J., Gilad, A.A., Jie, C.C., Bulte, J.W., 2010. Gene expression profiling reveals early cellular responses to intracellular magnetic labeling with superparamagnetic iron oxide nanoparticles. Magn. Reson. Med. 63, 1031–1043.

Kenzaoui, B.H., Bernasconi, C.C., Hofmann, H., Juillerat-Jeanneret, L., 2012. Evaluation of uptake and transport of ultrasmall superparamagnetic iron oxide nanoparticles by human brain-derived endothelial cells. Nanomedicine 7, 39–53.

Kumar, M., Singh, G., Arora, V., Mewar, S., Sharma, U., Jagannathan, N.R., Sapra, S., Dinda, A.K., Kharbanda, S., Singh, H., 2012. Cellular interaction of folic acid conjugated superparamagnetic iron oxide nanoparticles and its use as contrast agent for targeted magnetic imaging of tumor cells. Int. J. Nanomed. 7, 3503–3516.

Lee, R., Kim, Y.J., Lee, Y.J., Chung, H.W., 2004. The selective effect of genistein on the toxicity of bleomycin in normal lymphocytes and HL-60 cells. Toxicology 195, 87–95.

Lialiaris, T., Lyratzopoulos, E., Papachristou, F., Simopoulou, M., Mourelatos, C., Nikolettos, N., 2008. Supplementation of melatonin protects human lymphocytes *in vitro* from the genotoxic activity of melphalan. Mutagenesis 23, 347–354.

Liu, Y.X., Chen, Z.P., Wang, J.K., 2011. Systematic evaluation of biocompatibility of magnetic Fe_3O_4 nanoparticles with six different mammalian cell lines. J. Nanopart. Res. 13, 199–212.

Lima, M., Teixeira, M.A., Fonseca, S., Gonçalves, C., Guerra, M., Queirós, M.L., Santos, A.H., Coutinho, A., Pinho, L., Marques, L., Cunha, M., Ribeiro, P., Xavier, L., Vieira, H., Pinto, P., Justiça, B., 2000. Immunophenotypic aberrations DNA content and cell cycle analysis of plasma cells in patients with myeloma and monoclonal gammopathies. Blood Cells Mol. Dis. 26, 634–645.

Lunov, O., Syrovets, T., Buchele, B., Jiang, X., Rocker, C., Tron, K., Nienhaus, G.U., Walther, P., Mailander, V., Landfester, K., Simmet, T., 2010. The effect of carboxydextran-coated superparamagnetic iron oxide nanoparticles on c-Jun N-terminal kinase-mediated apoptosis in human macrophages. Biomaterials 31, 5063–5071.

Magdolenova, Z., Drlickova, M., Henjum, K., Runden-Pran, E., Tulinska, J., Bilanicova, D., Pojana, G., Kazimirova, A., Barancokova, M., Kuricova, M., Liskova, A., Staruchova, M., Ciampor, F., Vavra, I., Lorenzo, Y., Collins, A., Rinna, A., Fjellsbo, L., Volkovova, K., Marcomini, A., Amiry-Moghaddam, M., Dusinska, M., 2013. Coating-dependent induction of cytotoxicity and genotoxicity of iron oxide nanoparticles. Nanotoxicology 1–13.

Malumbres, M., Barbacid, M., 2009. Cell cycle, CDKs and cancer: a changing paradigm. Nat. Rev. Cancer 9, 153–166.

Mir, L.M., Tounekti, O., Orlowski, S., 1996. Bleomycin: revival of an old drug. Gen. Pharmacol. 27, 745–748.

Naqvi, S., Samim, M., Abdin, M., Ahmed, F.J., Maitra, A., Prashant, C., Dinda, A.K., 2010. Concentration-dependent toxicity of iron oxide nanoparticles mediated by increased oxidative stress. Int. J. Nanomed. 5, 983–989.

Newsholme, P., 2001. Why is L-glutamine metabolism important to cells of the immune system in health, postinjury, surgery or infection? J. Nutr. 131, 2515S–2522S (discussion 2523S-2514S).

Ngkelo, A., Meja, K., Yeadon, M., Adcock, I., Kirkham, P.A., 2012. LPS induced inflammatory responses in human peripheral blood mononuclear cells is mediated through NOX4 and Giα dependent PI-3kinase signalling. J. Inflamm. -Lond. 9, 1.

Paika, K.D., Krishan, A., 1973. Bleomycin-induced chromosomal-aberrations in cultured mammalian-cells. Cancer Res. 33, 961–965.

Park, E.J., Kim, H., Kim, Y., Yi, J., Choi, K., Park, K., 2010. Inflammatory responses may be induced by a single intratracheal instillation of iron nanoparticles in mice. Toxicology 275, 65–71.

Park, E.J., Umh, H.N., Choi, D.H., Cho, M.H., Choi, W., Kim, S.W., Kim, Y., Kim, J.H., 2014a. Magnetite- and maghemite-induced different toxicity in murine alveolar macrophage cells. Arch. Toxicol. 88, 1607–1618.

Park, E.J., Umh, H.N., Kim, S.W., Cho, M.H., Kim, J.H., Kim, Y., 2014b. ERK pathway is activated in bare-FeNPs-induced autophagy. Arch. Toxicol. 88, 323–336.

Poli, P., Aline de Mello, M., Buschini, A., Mortara, R.A., Northfleet de Albuquerque, C., da Silva, S., Rossi, C., Zucchi, T.M., 2002. Cytotoxic and genotoxic effects of megazol an anti-Chagas' disease drug, assessed by different short-term tests. Biochem. Pharmacol. 64, 1617–1627.

Schwartz, D., Rotter, V., 1998. p53-dependent cell cycle control: response to genotoxic stress. Semin. Cancer Biol. 8, 325–336.

Schwarz, S., Wong, J.E., Bornemann, J., Hodenius, M., Himmelreich, U., Richtering, W., Hoehn, M., Zenke, M., Hieronymus, T., 2012. Polyelectrolyte coating of iron oxide nanoparticles for MRI-based cell tracking. Nanomedicine 8, 682–691.

Shackelford, R.E., Kaufmann, W.K., Paules, R.S., 1999. Cell cycle control checkpoint mechanisms, and genotoxic stress. Environ. Health Perspect. 107, 5–24.

Shen, C.C., Liang, H.J., Wang, C.C., Liao, M.H., Jan, R., 2011. A role of cellular glutathione in the differential effects of iron oxide nanoparticles on antigen-specific T cell cytokine expression. Int. J. Nanomed. 6, 2791–2798.

Singh, N., Jenkins, G.J., Nelson, B.C., Marquis, B.J., Maffeis, T.G., Brown, A.P., Williams, P.M., Wright, C.J., Doak, S.H., 2012. The role of iron redox state in the genotoxicity of ultrafine superparamagnetic iron oxide nanoparticles. Biomaterials 33, 163–170.

Sousa, R., Ponte, F., Teixeira, S., Andrade, L., Goncalves, C., Barbot, J., Coutinho, J., Carvalho, F., Porto, B., 2013. Fosfomycin increases chromosome instability in lymphocytes from Fanconi Anemia patients. Mutat. Res. Genet. Toxicol. Environ. Mutagen. 754, 58–62.

Sun, S.L., Lo, Y.L., Chen, H.Y., Wang, L.F., 2012. Hybrid polyethylenimine and polyacrylic acid-bound iron oxide as a magnetoplex for gene delivery. Langmuir 28, 3542–3552.

Valois, C.R., Braz, J.M., Nunes, E.S., Vinolo, M.A., Lima, E.C., Curi, R., Kuebler, W.M., Azevedo, R.B., 2010. The effect of DMSA-functionalized magnetic nanoparticles on transendothelial migration of monocytes in the murine lung via a β_2 integrin-dependent pathway. Biomaterials 31, 366–374.

Vernole, P., Tedeschi, B., Caporossi, D., Maccarrone, M., Melino, G., Annicchiarico-Petruzzelli, M., 1998. Induction of apoptosis by bleomycin in resting and cycling human lymphocytes. Mutagenesis 13, 209–215.

Wu, J., Ding, T., Sun, J., 2012. Neurotoxic potential of iron oxide nanoparticles in the rat brain striatum and hippocampus. Neurotoxicology 34, 243–253.

Yu, M., Huang, S., Yu, K.J., Clyne, A.M., 2012. Dextran and polymer polyethylene glycol (PEG) coating reduce both 5 and 30 nm iron oxide nanoparticle cytotoxicity in 2D and 3D cell culture. Int. J. Mol. Sci 13, 5554–5570.

Zhang, Q.H., Wu, C.F., Duan, L., Yang, J.Y., 2008. Protective effects of total saponins from stem and leaf of *Panax ginseng* against cyclophosphamide-induced genotoxicity and apoptosis in mouse bone marrow cells and peripheral lymphocyte cells. Food Chem. Toxicol 46, 293–302.

Zhu, M.T., Feng, W.Y., Wang, B., Wang, T.C., Gu, Y.Q., Wang, M., Wang, Y., Ouyang, H., Zhao, Y.L., Chai, Z.F., 2008. Comparative study of pulmonary responses to nano- and submicron-sized ferric oxide in rats. Toxicology 247, 102–111.

II.4. THE BIODISTRIBUTION OF POLYACRYLIC ACID-COATED IRON OXIDE NANOPARTICLES IMPLIES A PRO-INFLAMMATORY EFFECT AND SOME DEGREE OF LIVER TOXICITY

Manuscript to be submitted for publication

The biodistribution of polyacrylic acid-coated iron oxide nanoparticles implies a pro-inflammatory effect and some degree of liver toxicity

Diana Couto[a], Marisa Freitas[a], Vera Marisa Costa[b], Renan Campos Chisté[a], Agostinho Almeida[a], M. Arturo Lopez-Quintela[c], José Rivas[d], Paulo Freitas[d], Paula Silva[e], Félix Carvalho[b*], Eduarda Fernandes[a*]

[a]UCIBIO/REQUIMTE, Laboratory of Applied Chemistry, Department of Chemical Sciences, Faculty of Pharmacy, University of Porto, Porto, Portugal
[b]UCIBIO/REQUIMTE, Laboratory of Toxicology, Department of Biological Sciences, Faculty of Pharmacy, University of Porto, Porto, Portugal
[c]Laboratory of Nanotechnology and Magnetism, Institute of Technological Research, IIT, University of Santiago de Compostela (USC), Spain
[d]International Iberian Nanotechnology Laboratory, Braga, Portugal
[e]Laboratory of Histology and Embryology, Institute of Biomedical Sciences Abel Salazar (ICBAS), University of Porto, Porto, Portugal

* **Corresponding authors:**
Eduarda Fernandes, PharmD; PhD
UCIBIO-REQUIMTE, Laboratory of Applied Chemistry
Department of Chemical Sciences
Faculty of Pharmacy, University of Porto, Porto, Portugal
Rua de Jorge Viterbo Ferreira n.º 228, 4050-313 Porto, Portugal
Phone: +351 220428675
Email: egracas@ff.up.pt

Félix Carvalho, PharmD; PhD
UCIBIO-REQUIMTE, Laboratory of Toxicology
Department of Biological Sciences
Faculty of Pharmacy, University of Porto, Porto, Portugal
Rua de Jorge Viterbo Ferreira n.º 228, 4050-313 Porto, Portugal
Phone: +351 220428600
Email: felixdc@ff.up.pt

Abstract

Iron oxide nanoparticles (IONs) have physical and chemical properties that render them useful in the development of new biomedical applications. Still, so far, *in vivo* safety studies of IONs with coatings with biomedical interest are still scarce. The aim of this study was, therefore, to provide a better clarification of the acute biological effects of polyacrylic acid (PAA)-coated IONs, by determining their biodistribution in several organs (liver, spleen, kidneys, brain, heart, testes, and lungs) and their putative pro-inflammatory and toxic effects. The biodistribution of PAA-coated IONs in several organs of the CD-1 mouse, the plasma cytokines, chemokine and aminotransferases levels, blood counts, oxidative stress parameters, adenosine triphosphate (ATP) and histologic features in liver, spleen and kidneys were evaluated 24 hours after an acute intravenous administration of PAA-coated IONs in magnetite form (8, 20 or 50 mg/kg). The obtained results showed that these IONs accumulate mainly in liver and spleen and, to a lesser extent, in the lungs. Although our data showed that PAA-coated IONs do not cause severe organ damage, an inflammatory process seems to be triggered *in vivo*, as evidenced by an increased neutrophils' and large lymphocytes' frequency in blood. Moreover, an accumulation of iron in liver and spleen macrophages was observed and hepatic lipid peroxidation was elicited, showing that these nanoparticles are able to induce oxidative stress. These effects need to be further investigated regarding the mechanisms involved and also the long term consequences of PAA-coated IONs.

Keywords: Iron oxide nanoparticles; biodistribution; inflammation; lipid peroxidation; histology; *in vivo* studies; CD-1 mice.

Abbreviations list

ALT – Alanine aminotransferase
AST – Aspartate aminotransferase
ATP – Adenosine triphosphate
BHT – Butylated hydroxytoluene
CK – Creatine kinase
DL – Detection limit
DTNB – 5,5'-Dithio-bis(2-nitrobenzoic acid)
GSH – L-glutathione reduced
GSHt – Total glutathione
GSSG – L-glutathione oxidized
H&E – Haematoxylin-eosin
IFN-γ – Interferon γ
IL – Interleukin
IONs – Iron oxide nanoparticles
i.p. - Intraperitoneal
i.v. – Intravenous
MAPK – Mitogen-activated protein kinase
MCP-1 – Monocyte chemoattractant protein-1
MDA – Malondialdehyde
NADPH – Reduced form of nicotinamide adenine dinucleotide phosphate
NPs – Nanoparticles
PAA – Polyacrylic acid
ROS – Reactive oxygen species
TAK1 – Transforming growth factor beta activated kinase
TBA – 2-Thiobarbituric acid
TNF-α – Tumor necrosis factor α

1. Background

The use of nanoparticles (NPs) is considered a promising strategy in the development of new biomedical applications, due to their distinctive physical and chemical properties [1]. Among the various types of NPs used for biomedical applications, iron oxide NPs (IONs) are one of the most common [2]. Several formulations of these NPs are used mainly for magnetic resonance imaging and diagnosis [1,3] and are presently being investigated in cancer treatment with the concurrent use of hyperthermia [4,5], and in inflammation imaging [1,3,6]. The human exposure to IONs is usually acute on resonance imaging, this procedure being often repeated throughout the patient's life [7,8].

So far the IONs available in the market are always coated, since coating is regarded as an improvement of these NPs biocompatibility. The most common coatings are based on dextran and its derivatives [9], though other coatings are being tested at this point. Recently, polyacrylic acid (PAA), an aqueous soluble polymer, has been shown to be a promising coating agent in gene delivery [10,11].

Despite the widespread use of IONs, safety issues are still a matter of debate. In fact, *in vitro* studies using different cellular models have reported that IONs with diverse coatings may cause increased production of reactive oxygen species (ROS), activation of inflammatory pathways, and cell death, among other adverse effects [12-14]. In our previous *in vitro* studies, we have demonstrated that PAA-coated IONs in magnetite form are able to trigger the production of ROS in human neutrophils, eliciting apoptosis in that cellular model [15]. We have also verified that the same PAA-coated IONs have the ability to induce cytokine production (interleukin - IL) IL-6, IL-8, IL-10, tumor necrosis factor α (TNF-α), interferon γ (IFN-γ) and IL-1β via transforming growth factor beta activated kinase (TAK1) and p38 mitogen-activated protein kinase (MAPK) activation in human blood cells [16]. Altogether, these results show that PAA-coated IONs have a pro-inflammatory potential that needs further investigation.

There are few *in vivo* studies performed so far with IONs to study their putative toxic effects. In mice, Fe_3O_4 NPs triggered hepatic and renal damage [17], whereas in humans the administration of IONs in magnetic resonance imaging caused some adverse effects, namely urticaria [7,18-20], diarrhea [18], allergic reactions [7], nausea [18,21], headache [18,19], back and chest pain [18,20], flush [20], dyspnea [20], vertigo [21], erythema [20], skin discoloration [22], pruritus [19,20] and vasodilatation [18]. Regarding PAA-coated IONs and to the best of our knowledge, there is only one *in vivo* study that evaluated in mice, the renofunctional and basic cardiovascular functions, 24 hours and 96 hours after a 10 mg/kg intravenous (i.v.) injection of PAA-coated γ-Fe_2O_3 IONs [23]. The

results obtained in that study suggest that these IONs do not affect kidney function but decrease blood pressure temporarily [23].

The aim of this work was to provide a better clarification of the acute effects of PAA-coated IONs, by determining their biodistribution in several organs (liver, spleen, kidneys, brain, heart, testes, and lungs) and putative pro-inflammatory and toxic effects following an acute i.v. administration in CD-1 mice. Histological analysis of liver, spleen and kidneys was done and general oxidative stress and energetic evaluations on liver and kidneys were also performed.

2. Materials and Methods

2.1. Materials

Isoflurane (Isoflo®) was obtained from Abbott Animal Health (USA). Iron standard for AAS (Trace CERT®, 1000 mg/L) and concentrated HNO_3 (TraceSELECT®, ≥69.0% w/w) were obtained from Fluka (France) and H_2O_2 solution (TraceSELECT® Ultra, ≥30% v/v) from Fluka (Italy). Ultrapure water (resistivity >18.2 MΩ.cm at 25ºC) was obtained from an arium®pro (Germany) water purification system. Sodium hydroxide, potassium bicarbonate and Histosec® pastilles (paraffin) were acquired from Merck (Germany). Ethanol was obtained from Panreac AppliChem (Darmstadt, Germany). BD™ Cytometric Bead Array (CBA) was acquired from BD Biosciences (USA). $HClO_4$, butylated hydroxytoluene (BHT), bovine serum albumin, 5,5'-dithio-bis(2-nitrobenzoic acid) (DTNB), β-nicotinamide adenine dinucleotide phosphate (β-NADPH), glutathione reductase, L-glutathione reduced (GSH), L-glutathione oxidized (GSSG) disodium salt, 2-vinylpyridine, 2-thiobarbituric acid (TBA), potassium phosphate monobasic, malondialdehyde (MDA), acetonitrile [high performance liquid chromatography (HPLC) grade], ammonium acetate (HPLC grade), adenosine triphosphate (ATP), luciferin and luciferase were obtained from Sigma Chemical Co (USA). RC DC Protein Assay kit was obtained from Bio-Rad® (California, USA). ABX Pentra reagents were purchased from HORIBA (Japan). Commercial 4% buffered formalin was purchased from Klinipath (Netherlands). Xylene was obtained from BDH - Prolabo (VWR International, Ireland).

2.2. Methods

2.2.1. Synthesis and characterization of the PAA-coated IONs

PAA-coated magnetite particles were obtained from Nanogap (Santiago de Compostela, Spain), and their preparation and physico-chemical characterization was performed as reported before [15]. Briefly, IONs "non-coated" magnetite particles preparation was based on the chemical co-precipitation of a mixture of Fe(II) and Fe(III) chloride salts (molar ratio 2:1) using NH_4OH in a degassed 1 M KCl aqueous solution at 60ºC. The dark precipitate was washed several times with deoxygenated water, and finally the particles were stored at pH 9.6 (well above their isoelectric point: 6.5). For the PAA-coated IONs, PAA [25% w/w with respect to the Fe(II) salt] was added to the reaction medium. PAA-coated IONs were characterized using transmission electron microscopy (Hitachi H-7000, Japan). Determination of the hydrodynamic size and zeta potential of NPs to be used, in 0.9% saline solution, were made using a nanoparticle analyzer SZ-100 (HORIBA Scientific) (DPSS laser 532 nm). PAA-coated IONs have a mean particle size of 10.1 ± 2.4 nm (mean ± SD). When the IONs were dispersed in physiological serum, a large hydrodynamic size 46.7 ± 12 nm was observed, and the zeta potential was -1.56 ± 0.45 mV.

2.2.2. Animals

Male mice (8 weeks) of CD-1 strain from Charles River laboratories (Barcelona, Spain), weighing 30-40 g were used in this study. Upon arrival, the animals were randomly housed in cages (each cage with 4 animals) and were maintained under a controlled environment [temperature 22.0 ± 2.0ºC, 40% humidity, and 12 hours light/dark cycles at the Institute for Biomedical Sciences Abel Salazar-University of Porto (ICBAS-UP) animal house facility]. The animals had *ad libitum* access to food and water and throughout the experimental period had permanent veterinary supervision.

All procedures were carried out to provide appropriate animal care, minimizing their suffering. Housing and experimental treatment of the animals were in accordance with the guidelines defined by the European Council Directive (2010/63/EU) transposed into Portuguese law (Decreto-Lei n.º 113/2013, de 7 de Agosto). Moreover, the experiments were performed with the approval of the Ethical Committee of the Faculty of Pharmacy, University of Porto (opinion nº 19/07/2014). Animals were allowed to adjust to the environmental conditions for 10 days, before starting the experiments.

2.2.3. Administration of PAA-coated IONs

Administration of PAA-coated IONs was performed through an i.v. injection in the tail vein by experienced veterinarians. All stock solutions of the NPs were prepared daily in sterile conditions and PAA-coated IONs were suspended in 0.9% saline solution. Four groups were created with 6 animals each: control; PAA-coated IONs 8 mg/kg; PAA-coated IONs 20 mg/kg; and PAA-coated IONs 50 mg/kg. The 0.9% saline solution was administered to control animals on the same schedule and at the same equivalent volume of PAA-coated IONs administration. Animal weight was assessed before and 24 hours after the i.v. administration and animals were sacrificed 24 hours after administration of PAA-coated IONs.

The use of IONs for imaging procedures has been reported to be between 2-7 mg/kg in humans [24,25]. Regarding the equivalence to the doses used in humans, the correlations were made according to the allometric scaling principles using the formula: *human dose (mg/kg) = animal dose (mg/kg) x (animal weight/human weight)*$^{1/4}$ [26]. In a 70 kg man, to whom 7 mg/kg was administered, the equivalent dose in mice (30 g) is ca. 49 mg/kg. Therefore, we are demonstrating the relevance of the present study, since we are using human pharmacological relevant doses.

2.2.4. Blood and organ collection

Animals were anesthetized and euthanized with isoflurane 24 hours after the PAA-coated IONs administration. Blood was immediately collected from the inferior vena cava. A drop of blood was used for smears, whereas the remaining blood was placed into EDTA Vacutainer® tubes. Subsequently, the blood was centrifuged at 920 *g*, 10 minutes, at 4ºC and plasma was collected and stored at -20ºC for posterior cytokine, total creatine kinase (CK), aspartate aminotransferase (AST) and alanine aminotransferase (ALT) levels. Immediately after sacrifice, the liver, spleen, kidneys, brain, heart, testes, and lungs were collected and weighted. The tail of the mouse was also collected.

For iron determination in mice organs, a small sample (approximately 200 mg) of tissue and the totality of the tail was collected. The possible contaminating blood of each organ was thoroughly washed away with ultrapure water and agitation. The organ samples were stored in decontaminated polypropylene tubes at 4ºC until analysis.

A portion of liver, spleen and kidney in control and 50 mg/kg PAA-coated IONs-treated animals was taken for histological processing and analysis, as described below.

The remaining liver and kidney tissue samples were homogenized in ice cold phosphate-buffered solution 0.1 M KH_2PO_4 pH 7.4 in an Ultra-Turrax® homogenizer and

processed as previously described [27]. An aliquot of the homogenates was placed in cold $HClO_4$ (5% final acid concentration), with 0.05% of antioxidant BHT and immediately frozen at -80ºC (for a maximum of one month) until MDA determination through HPLC. Another aliquot of the homogenates was treated with $HClO_4$ (5% final acid concentration) and centrifuged at 16000 *g* for 10 minutes at 4ºC. The resulting supernatant was separated and frozen at -80ºC for total glutathione (GSHt), GSSG and ATP determinations. The remaining homogenate was stored at -20ºC for protein determination.

2.2.5. Measurement of plasma biomarkers

CK, AST and ALT were determined using enzymatic assays in the apparatus ABX Pentra 400 with ABX Pentra reagents (HORIBA, Kyoto, Japan), according to the manufacturer's instructions.

2.2.6. Plasma cytokines and chemokine determination

Cytokines (IL-6, IL-10, IFN-γ, TNF-α, and IL-12p70) and chemokine monocyte chemoattractant protein-1 (MCP-1) were determined in plasma using a BD™ Cytometric Bead Array (BD Biosciences®), in accordance to manufacturer's instructions. Fluorescence signals for each sample were collected using BD Accuri™ C6 flow cytometer (California, USA) equipped with a 488 nm and a 640 nm lasers. Data were analyzed using FCAP Array™ software Version 3.0 (USA).

2.2.7. Differential leukocyte counts in peripheral blood smears

Blood smears were made on glass slides and air-dried. At least two blood smears were prepared per animal. The slides were stained using the Diff-Quik procedure, and a manual differential count of 100 leucocytes was performed under oil-immersion lens. Leukocyte nomenclature and morphology has been described previously for mouse [28] and it was followed in this study.

2.2.8. Iron determination in organs

Sample treatment and iron determination was performed as previously described [29]. Samples were placed in a dry oven (Spain) at 110°C until constant weight (ca. 24 hours). Dried samples were weighed and placed in the microwave oven digestion vessels, previously decontaminated with 10% (v/v) HNO_3 and thoroughly rinsed with

ultrapure water. Samples were digested using 2 mL of concentrated HNO_3 and 0.5 mL of H_2O_2 (except for tail, where 4 mL and 1 mL, respectively, were used). The sample digestion was performed in a mls 1200 mega microwave oven from Milestone (Italy) equipped with an HPR 1000/10 rotor using the following power (W)/time (minute) programme: 250/1, 0/2, 250/5, 400/5 and 600/5. After cooling, sample solutions were made up to 25 mL with ultrapure water (50 mL for tail samples) and stored in closed propylene tubes at 4°C until analysis. In each digestion batch (10 samples), a sample blank was also performed.

Iron determination was performed using a PerkinElmer (Germany) model 3100 atomic absorption spectrometer. An Intensitron™ (PerkinElmer) hollow cathode lamp was used as a light source (λ= 248.3 nm).

Calibration standards were prepared by diluting the commercial iron standard with 0.2% (v/v) HNO_3 solution. Calibration curves were obtained with five calibration standards with concentrations ranging from 0 to 4 mg/L. Data were expressed as organ iron (µg iron/g of organ).

2.2.9. Histological analysis

To assess the effect of PAA-coated IONs administration on liver, spleen and kidneys histology, basic histopathological analysis of the exposed animals to the highest concentration (50 mg/kg) was performed. In this study, liver was cut into ≈ 4 mm thick slabs and then a systematic selection was carried out and sampled pieces were processed for light microscopy. The spleen was cut in the midsagittal plane in two halves. The kidneys were divided in two equal parts: the cranial and caudal parts. Each half of both organs was then randomly selected for histological analysis. The organs were fixed in commercial 4% buffered formalin. After fixation (24 hours), the tissues were dehydrated through a series of graded ethanol solutions (70-99.8%), cleared in xylene, and impregnated and embedded in paraffin. Each organ was entirely sectioned (Microtome - Leica RM 2125) into thin sections (5 µm thick). For improving section adhesion, the sampled sections were mounted in silane coated microscope slides [Nuova Aptaca, Canelli (AT), Italy]. From each organ, the first section to be sampled was randomly selected. Four successive slides, with an equal number of sequential sections each, were set aside for posterior analysis. From then on every 5^{th} slides a group of 4 slides were chosen to histological analysis. This allowed for the analysis of the entire organ to check the existence of focal lesions. The sections were then stained according with the following scheme: 1 - Haematoxylin-eosin (H&E); 2 - Perl's Prussian blue; 3 - H&E; 4 - Masson's trichrome [30]. The Perl's reaction was the method used to identify iron.

2.2.10. Oxidative stress parameters

2.2.10.1. Glutathione assay

The GSHt and GSSG levels of tissue homogenates were determined by the DTNB-GSSG reductase recycling assay, as previously described [27]. For the quantification of GSSG, 10 µL of 2-vinylpyridine was added to the acidic supernatant and shaken for 1 hour in ice to block GSH. Then, the determination of GSSG was performed as described above for GSHt. The GSH was calculated using the following formula GSH = GSHt – 2 GSSG.

GSH and GSSG standard solutions (0-15 µM and 0-8 µM, respectively) were prepared in 5% $HClO_4$ and results were expressed as nmol/mg protein.

2.2.10.2. Lipid peroxidation

Lipid peroxidation was measured by HPLC quantification of MDA [27], with some modifications. Briefly, the acidic liver and kidney homogenates were centrifuged (16 000 *g*, 5 minutes, at 4ºC) and 200 µL of the resulting supernatant were incubated with 200 µL of TBA (0.8 % in water) for 60 minutes at 80ºC in a water bath. After cooling, 20 µL of the samples were injected into the HPLC system (Jasco, LC-2000 Plus, USA), equipped with quaternary pumps (PU-2089 Plus), an autosampler (AS-2057 Plus) and a fluorescence detector (FP-2020 Plus). MDA was separated on a C_{18} Synergi Hydro column (4 µm, 250 × 4.6 mm, Phenomenex), with a mobile phase consisting of (A) ammonium acetate aqueous solution (10 mM, pH 6.8) and (B) acetonitrile in the proportion 80/20 (v/v) in an isocratic mode at a flow rate of 1.0 mL/minute and at room temperature. The fluorescence detector was set at $\lambda_{excitation}$ = 525 nm and $\lambda_{emission}$ = 560 nm. MDA was quantified by comparison to external standards of MDA using seven-point analytical curves (0−3 µM, r^2>0.98), which was prepared at the same experimental conditions that all samples. The MDA content was expressed as picomol MDA/mg protein.

2.2.11. ATP measurement

ATP measurement in liver and kidney homogenates was performed by the luciferin/luciferase solution bioluminescence assay, as described before [31]: 150 µL of tissue homogenates were neutralized with 150 µL of 0.76 M $KHCO_3$ and centrifuged 16 000 *g*, 1 minute, at 4°C. The ATP levels were quantified after the reaction of 100 µL of

neutralized supernatant with luciferin/luciferase solution. ATP standards (0-10 μM) were prepared in 5% $HClO_4$. ATP intracellular levels were expressed in nmol/mg protein.

2.2.12. Protein determination

Protein content was determined with RC DC Protein Assay kit, according to the manufacturer's instructions. Bovine serum albumin prepared in NaOH 0.4 M (0-1.2 mg/mL) was used as standard.

2.2.13. Statistical analysis

Results are expressed as the mean ± SEM. Statistical comparison was made between control and PAA-coated IONs treated groups using the one-way analysis of variance (ANOVA), followed by Bonferroni's post hoc test using GraphPad Prism™ (version 6.0; GraphPad Software, USA). For body weight comparison within the same group of animals, between 0 and 24 hours after PAA-coated IONs administration, the paired t test was performed. P values lower than 0.05 were considered as statistically significant. Outliers were identified using the ROUT method (Q=1%).

3. Results

3.1. Plasma levels of CK increased, while AST or ALT were not altered after i.v. administration of PAA-coated IONs

As presented in table 1, no significant differences were found in plasma levels of AST or ALT from control mice (administered with 0.9% saline solution) and PAA-coated IONs (8, 20 or 50 mg/kg) treated mice. Only the levels of plasma CK for 8.0 mg/kg PAA-coated IONs group increased significantly when compared to control animals. The group of 20 mg/kg PAA-coated IONs also showed a tendency to increase, although without reaching statistical significance (table 1).

3.2. PAA-coated IONs did not cause any activation of plasma cytokines and chemokine MCP-1

Cytokines (IL-6, IL-10, IFN-γ, TNF-α, and IL-12p70) and chemokine MCP-1 were determined in plasma collected from control mice (administered with 0.9% saline solution) and PAA-coated IONs (8, 20 or 50 mg/kg) treated mice. It was observed that the PAA-

coated IONs did not cause any significant change in the levels of the tested cytokines and chemokine MCP-1, with their production being always residual for the control and the mice administered with PAA-coated IONs (data not shown).

3.3. The number of large lymphocytes and neutrophils augmented after administration of PAA-coated IONs

Differential leukocyte counts performed in blood of control mice (administered with 0.9% saline solution) and PAA-coated IONs (8, 20 or 50 mg/kg) treated mice revealed: (1) an increase in the neutrophils' frequency after the two highest concentrations of PAA-coated IONs; (2) the small lymphocytes' frequency was lower in the 50 mg/kg group; (3) the large lymphocytes' frequency increased, being almost the double for the concentration of 50 mg/kg, compared to the control group (table 2). No significant differences were observed for monocytes, eosinophils or basophils.

3.4. Administration of PAA-coated IONs led to a significant iron accumulation in liver, spleen and lung

Animals were weighed before and after 24 hours of PAA-coated IONs administration. After sacrifice, all collected organs were weighed. As it is seen on table 3, organ weights were not changed when compared to control animals.

In order to evaluate the biodistribution of PAA-coated IONs, iron levels were quantified in the liver, spleen, kidneys, brain, heart, testes, lungs and tail of control mice and PAA-coated IONs (8, 20 or 50 mg/kg) treated mice (figure 1). In treated animals, PAA-coated IONs accumulated mainly in the liver and spleen in the two highest PAA-coated IONs doses (20mg/kg and 50 mg/kg) and in the highest concentration in the lungs. One spleen value was undetectable with this method, therefore we replaced it for the value obtained with the formula: detection limit (DL)/$\sqrt{2}$, as previously described [32]. The calculated DL for iron in the spleen was 614 µg/g. Moreover, PAA-coated IONs showed a small tendency to accumulate in heart (figure 1), although without statistical significance. In contrast, these IONs did not show to accumulate in brain, kidneys nor testes (data not shown). In the tail, iron levels increased in a concentration-dependent manner, which suggests that some retention of PAA-coated IONs resulted from the i.v. administration.

3.5. Iron accumulates mostly in the periportal zone of the liver and in the red pulp of the spleen

Control animals showed normal liver histology. Iron-loaded Kupffer cells were found in exposed animals (figures 2A, B, C and D), whereas these were absent in animals not exposed to PAA-coated IONs (figures 2E and F). Due to iron presence, the cytoplasm of Kupffer cells was granular and golden brown on H&E staining (figure 2C). Exposed animals showed hepatic iron deposition, most marked in periportal region but present in all *acinus* zones. The histological examination using Perls' blue staining, confirmed this result (figures 2B and D). No hepatic collagen deposition, a marker of fibrosis and examined by histology Masson's trichrome staining, was detected. In some liver areas, mainly in periportal regions, clusters of early necrotic hepatocytes were observed. These early necrotic cells showed increased cytoplasmic eosinophilia (figure 3). All alterations detected were present in the whole organ.

Control animals exhibited normal spleen morphology on microscopic examination. Under light microscope, no apparent splenic alterations were observed in treated animals (50mg/kg-treated mice) on both H&E and Masson's trichrome staining's (figures 4A, B and C). No iron was detected by Perls' blue staining in the white pulp of both control and treated animals (figure 4D). When compared with the control mice (figure 4E), an increase in iron concentration was observed in splenic red pulp macrophages of animals in which PAA-coated IONs was administered (figure 4F). The iron was equally distributed by whole organ.

Histological examination of kidney sections from control and the 50 mg/kg group revealed a normal kidney organizational architecture. The usual renal morphological structures, such as corpuscles, proximal, distal, and collecting tubules were found in treated animals (figure 5). No morphologic alterations compatible, with any sort of kidney pathology, were observed (figure 5). No iron was detected in this organ in the two animal groups by the Perl's' blue staining.

3.6. Oxidative stress parameters

3.6.1. PAA-coated IONs did not cause any significant change in liver or kidney glutathione

GSSG and GSHt levels were determined in the liver and kidney in all groups of animals. Additionally, GSH and GSH/GSSG ratio were also calculated. It was observed

that PAA-coated IONs did not alter GSSG, GSH and GSHt levels nor GSH/GSSH ratio in mouse liver and kidney, even for the highest concentration tested (50 mg/kg) (table 4).

3.6.2. PAA-coated IONs caused hepatic lipid peroxidation at the highest tested concentration

MDA levels were measured in liver and kidney of control mice (administered with 0.9% saline solution) and mice previously administered with PAA-coated IONs (8, 20 or 50 mg/kg). It was clearly observed that PAA-coated IONs increased hepatic lipid peroxidation at the highest tested concentration (50 mg/kg) when compared to control values. In turn, PAA-coated IONs did not exert any significant effect in mouse kidney regarding lipid peroxidation (figure 6).

3.7. PAA-coated IONs did not affect hepatic or renal ATP levels

ATP measurement was assessed in liver and kidney of all groups tested. PAA-coated IONs showed some tendency to diminish ATP levels in mouse liver at the highest concentration tested (50 mg/kg), without reaching significance (table 4). In the kidney, PAA-coated IONs did not alter ATP levels when compared to control animals (table 4).

4. Discussion

This work was undertaken to assess the biodistribution of PAA-coated IONs in several organs of CD-1 mice (liver, spleen, kidneys, brain, heart, testes, and lungs) and putative pro-inflammatory and toxic effects following an acute i.v. administration of these NPs. For this purpose, a time-point of 24 hours was selected. As major findings, it was observed that: 1) PAA-coated IONs showed to accumulate in the liver, spleen and lungs; 2) the PAA-coated IONs treated animals showed significant iron accumulation in macrophages mostly in the periportal zone of the hepatic *acinus* and in the splenic red pulp; 3) no significant cytokine activation occurred, although PAA-coated IONs caused significant changes both in the blood levels of neutrophils and in activated lymphocytes; 4) PAA-coated IONs caused hepatic lipid peroxidation that was accompanied by early necrosis; 5) liver and kidney levels of glutathione and ATP were not affected by PAA-coated IONs.

AST and ALT are parenchymal intracellular enzymes released into systemic circulation when there is hepatocellular and cardiac injury, usually involving necrosis [33]. No significant differences were found in plasma levels of AST or ALT from both control

and PAA-coated IONs treated mice, thus suggesting that these NPs did not cause any substantial liver or heart necrotic damage. However, the histological examination of the highest IONs concentration tested (50 mg/kg) showed foci of early necrotic cells. Whether this small number of cells did not largely contribute to a significant change of aminotransferase plasma levels or if the cells have not yet released their content are two valid hypotheses. On the other hand, the plasma CK levels for 8.0 mg/kg PAA-coated IONs increased significantly when compared to control values. CK constitutes a marker of muscle damage [34]. The 20 mg/kg and 50 mg/kg PAA-coated IONs treated groups also showed a tendency to higher CK levels, however without reaching statistical significance. In fact, it has been described that changes in the values of serum CK after muscular damage follow a pattern where there is a rapid release of CK subsequently an injury and also a fast plasma clearance, making plasma values return to basal normal values in mice in less than 24 hours [34]. Therefore, it is possible that, for the highest concentrations, plasma CK values had already decreased to normal range or were decreasing to normal values at 24 hours after PAA-coated IONs administration. However, the mechanisms behind the CK alteration caused by PAA-coated IONs are yet to be elucidated.

Given that some IONs are described to act on defense cells and inflammatory pathways [15,16,35], these aspects were evaluated on the present study. An increase in the number of neutrophils as well as in the large lymphocytes occurred for the highest dose of PAA-coated IONs tested (50 mg/kg). Since neutrophils constitute the first line of innate host defense against pathogens and associated acute inflammations [36] and that small lymphocytes, when activated, transform into large lymphocytes [37], the increase number of these cells may be indicative of an inflammatory process elicited by PAA-coated IONs. During the inflammatory cascade, several mediators may be produced and cytokines may exert pivotal roles in those processes. Since lymphocytes, as well as neutrophils, are widely described as being cytokine producers [38,39], the putative effect of PAA-coated IONs in several plasma cytokine levels, such as IL-6, IL-10, IFN-γ, TNF-α and IL-12p70 and chemokine MCP-1 was evaluated. Despite IONs-induced increase of large lymphocytes' and neutrophils in the highest dose tested, there was no effect on the levels of plasma cytokines/chemokine. We have recently shown, *in vitro*, that PAA-coated IONs (4 μg/mL) were able to extensively activate the production of several cytokines in human blood after a 24 hours incubation period [16]. *In vivo* cytokines suffer a rapid turnover and elimination, therefore the half-life of most cytokines is usually minutes *in vivo*, while *in vitro*, as there is a lack of renal and hepatic clearance, the half-life of cytokines is substantially longer [40]. We also hypothesize that, although rapid cytokine turnover can occur *in vivo*, the pharmacokinetic features of NPs implies the need for a longer extent of plasma exposure when compared to the *in vitro* studies. Cytokine signal

activation perhaps is in need of more time and therefore lymphocytes activation had not yet reflected in cytokine levels increase. In fact, Chen and colleagues reported that 72 hours after non-coated Fe_3O_4 NPs acute administration to ICR mice (0-51.4 mg/kg), the levels of IFN-γ, IL-2 and IL-10 increased [41]. Although one could advocate for coating differences regarding the previously mentioned study, in our previous *in vitro* study, we demonstrated that the extensive activation of the cytokines was independent of the existence of coating in our IONs [16]. Therefore, the exposure time seemed to be of the essence for a putative cytokine production *in vivo*. To verify the accuracy of our methodologies *in vivo*, lipopolysaccharide was administered in different doses [5 and 15 mg/kg intraperitoneal (i.p.)] and exposition times (2 or 4 hours) in CD-1 mice. The blood collected was used as a positive control, as lipopolysaccharide showed to cause increase in cytokines and the chemokine (unpublished results).

The biodistribution in several organs was also studied herein. IONs mainly accumulated in liver, spleen and lungs. Iron is largely stored in ferritin, particularly in the cells of the liver, spleen and bone marrow, the former organs being involved in the iron recycling of aged red cells through macrophages phagocytosis [42]. The PAA-coated IONs were taken up by macrophages in the liver (Kupffer cells) and spleen, confirming that these IONs have specific uptake by the monocyte–macrophage system [9]. Histology of liver slices (Perl's staining) confirms the presence of Prussian blue positive stained cells mainly in contact with main hepatic portal branches. IONs were also removed from the circulation by macrophages found in the red pulp of the spleen. A similar pattern of accumulation was also observed in a previous work, where Fe_3O_4 NPs coated with amphiphilic polymers containing carboxylic acid (total of 20 mg/kg in two i.v. injections 24 hours apart) mainly accumulated in the liver and spleen, followed by lungs and kidneys of Kunming mice [43]. Almost all organs contain iron *in vivo*, but the most highly ferruginous organs are the liver and spleen, while the lungs also contain considerable amounts of iron. In ICR mice given 600 mg/kg Fe_3O_4 magnetic NPs by intragastric administration, the iron lung levels peaked at 6 hours and then decreased steadily after Fe_3O_4 magnetic NPs administration [44]. Actually, we have observed that, for the highest dose tested (50 mg/kg) of PAA-coated IONs, an iron accumulation in the lungs occurred. Since the lungs have a very rich resident macrophages population that is reported to be able to phagocyte particles from the circulating blood [45], we believe that these macrophages were able to ingest the circulating PAA-coated IONs, as it happens for the liver and spleen.

No significant differences were observed in iron content in the kidneys of either controls or PAA-coated IONs treated animals. In fact, in the work of Wang and colleagues [44], the iron content in the kidneys of Fe_3O_4 magnetic NPs treated mice remained slightly above the background level during the entire observation period (up to 10 days after

administration), indicating that renal excretion of iron is modest. Also in our study, we have shown that PAA-coated IONs do not significantly cross the blood brain barrier, while others have observed that albumin-coated γ-Fe_2O_3 NPs (ca. 25 mg/kg, administrated i.p.) were able to cross blood brain barrier in Swiss mice, reaching a maximum iron concentration at the end of 48 hours [46]. In another study performed by Wang and colleagues [44], Fe_3O_4 magnetic NPs also crossed the blood barrier, although the underlying mechanisms were not determined. The different coatings seem determinant for the IONs distribution in these animal models.

Metal-containing NPs raise toxicity concerns because they can be quickly cleared from the blood by the reticuloendothelial system and can remain in organs, such as the liver and spleen, for prolonged periods of time [44,47]. Moreover, when a foreign body is internalized by phagocytes, an inflammatory process is triggered and production of inflammatory mediators and ROS may occur [48]. We have demonstrated *in vitro* that these PAA-coated IONs induce ROS production [15]. It is also known that oxidative stress is involved in hepatic and renal damage elicited by IONs *in vivo* [17]. In fact, MDA levels were increased in the mouse liver for the highest tested dose (50 mg/kg) when compared with control animals. To the best of our knowledge, this is the first time that PAA-coated IONs are reported to trigger MDA production *in vivo*. We hypothesize that this ROS generation occurred due to PAA-coated IONs internalization by liver phagocytes, which results in their activation with subsequent production of reactive species. The results obtained by Ma *et al* [17] also showed that Fe_3O_4 NPs were capable of increasing MDA production in mice liver (20 mg/kg i.p., once daily, for a week). Whether the observed lipid peroxidation in the present work can lead to the necrotic foci observed at the highest tested concentration is to be investigated. However, those necrotic foci were not sufficient to cause a considerable ALT and/or AST plasma increase or hepatic ATP changes in comparison to control animals.

No significant differences were observed regarding hepatic GSH or GSSG levels. Ma and co-workers observed a significant decrease in GSH in Kunming mouse liver and kidney after daily 40 mg/kg i.p. administrations of Fe_3O_4 NPs for a week [17]. The cumulative higher dose certainly affected the cytosolic redox of these animals. Herein, no lipid peroxidation or GSH status alteration occurred in the kidney possibly because these PAA-coated IONs had no significant renal accumulation.

The obtained results in this pre-clinical study with PAA-coated IONs showed that these IONs accumulate mainly in liver and spleen and, to a lesser extent, in the lungs. Although our data showed that PAA-coated IONs do not cause severe organ damage, an inflammatory process seems to be triggered *in vivo*, as evidenced by an increased neutrophils' and large lymphocytes' frequency in blood. Moreover, an accumulation of

PAA-coated IONs in liver phagocytes was observed and hepatic lipid peroxidation was elicited showing that these NPs are able to induce oxidative stress. These effects need to be further investigated regarding the mechanisms involved and also the long term consequences of PAA-coated IONs exposure.

5. Acknowledgements

We greatly acknowledge Drª. Laura Pereira for her assistance in the plasma determinations and Celeste Resende for her assistance in the histological procedures. We acknowledge Professor José Alberto Duarte for allowing the use of his lab installations and the Veterinarians in the ICBAS for their assistance in the animals' administration and treatment. This work received financial support from the European Union (FEDER funds through COMPETE) and FCT (Fundação para a Ciência e Tecnologia) through project Pest-C/EQB/LA0006/2013. The work also received financial support from the European Union (FEDER funds) under the framework of QREN through Project NORTE-07-0124-FEDER-000066. Diana Couto, Marisa Freitas and Vera M. Costa acknowledge the FCT financial support for the PhD and Pos-doc grants (SFRH/BD/72856/2010, SFRH/BPD/76909/2011 and SFRH/BPD/63746/2009, respectively), in the ambit of "POPH - QREN - Tipologia 4.1 - Formação Avançada" co-sponsored by FSE and national funds of MCTES.

6. Bibliography

[1] Weinstein JS, Varallyay CG, Dosa E, Gahramanov S, Hamilton B, Rooney WD, et al. Superparamagnetic iron oxide nanoparticles: diagnostic magnetic resonance imaging and potential therapeutic applications in neurooncology and central nervous system inflammatory pathologies, a review. J Cerebr Blood F Met 2010;30(1):15-35.

[2] Shubayev VI, Pisanic TR, 2nd, Jin S. Magnetic nanoparticles for theragnostics. Adv Drug Deliver Rev 2009;61(6):467-77.

[3] Farrell BT, Hamilton BE, Dosa E, Rimely E, Nasseri M, Gahramanov S, et al. Using iron oxide nanoparticles to diagnose CNS inflammatory diseases and PCNSL. Neurology 2013;81(3):256-63.

[4] Maier-Hauff K, Rothe R, Scholz R, Gneveckow U, Wust P, Thiesen B, et al. Intracranial thermotherapy using magnetic nanoparticles combined with external beam radiotherapy: Results of a feasibility study on patients with glioblastoma multiforme. J Neuro-Oncol 2007;81(1):53-60.

[5] Maier-Hauff K, Ulrich F, Nestler D, Niehoff H, Wust P, Thiesen B, et al. Efficacy and safety of intratumoral thermotherapy using magnetic iron-oxide nanoparticles combined with external beam radiotherapy on patients with recurrent glioblastoma multiforme. J Neuro-Oncol 2011;103(2):317-24.

[6] Alkins R, Burgess A, Ganguly M, Francia G, Kerbel R, Wels WS, et al. Focused ultrasound delivers targeted immune cells to metastatic brain tumors. Cancer Res 2013;73(6):1892-99.

[7] Ross RW, Zietman AL, Xie W, Coen JJ, Dahl DM, Shipley WU, et al. Lymphotropic nanoparticle-enhanced magnetic resonance imaging (LNMRI) identifies occult lymph node metastases in prostate cancer patients prior to salvage radiation therapy. Clin Imag 2009;33(4):301-5.

[8] Ito A, Honda H, Kobayashi T. Cancer immunotherapy based on intracellular hyperthermia using magnetite nanoparticles: a novel concept of "heat-controlled necrosis" with heat shock protein expression. Cancer Immunol Immun 2006;55(3):320-8.

[9] Corot C, Robert P, Idee JM, Port M. Recent advances in iron oxide nanocrystal technology for medical imaging. Adv Drug Deliver Rev 2006;58(14):1471-504.

[10] Cao B, Qiu P, Mao C. Mesoporous iron oxide nanoparticles prepared by polyacrylic acid etching and their application in gene delivery to mesenchymal stem cells. Microsc Res Techniq 2013;76(9):936-41.

[11] Sun SL, Lo YL, Chen HY, Wang LF. Hybrid polyethylenimine and polyacrylic acid-bound iron oxide as a magnetoplex for gene delivery. Langmuir 2012;28(7):3542-52.

[12] Dan M, Scott DF, Hardy PA, Wydra RJ, Hilt JZ, Yokel RA, et al. Block copolymer cross-linked nanoassemblies improve particle stability and biocompatibility of superparamagnetic iron oxide nanoparticles. Pharm Res 2013;30(2):552-61.

[13] Ahamed M, Alhadlaq HA, Alam J, Khan MA, Ali D, Alarafi S. Iron oxide nanoparticle-induced oxidative stress and genotoxicity in human skin epithelial and lung epithelial cell lines. Curr Pharm Design 2013;19(37):6681-90.

[14] Liu Y, Chen Z, Gu N, Wang J. Effects of DMSA-coated Fe_3O_4 magnetic nanoparticles on global gene expression of mouse macrophage RAW264.7 cells. Toxicol Lett 2011;205(2):130-9.

[15] Couto D, Freitas M, Vilas-Boas V, Dias I, Porto G, Lopez-Quintela MA, et al. Interaction of polyacrylic acid coated and non-coated iron oxide nanoparticles with human neutrophils. Toxicol Lett 2014;225(1):57-65.

[16] Couto D, Freitas M, Porto G, Lopez-Quintela MA, Rivas J, Freitas P, et al. Polyacrylic acid-coated and non-coated iron oxide nanoparticles induce cytokine activation in human blood cells through TAK1, p38 MAPK and JNK pro-inflammatory pathways. Arch Toxicol 2014; DOI 10.1007/s00204-014-1325-4.

[17] Ma P, Luo Q, Chen J, Gan Y, Du J, Ding S, et al. Intraperitoneal injection of magnetic Fe_3O_4-nanoparticle induces hepatic and renal tissue injury via oxidative stress in mice. Int J Nanomed 2012;7:4809-18.

[18] Anzai Y, Piccoli CW, Outwater EK, Stanford W, Bluemke DA, Nurenberg P, et al. Evaluation of neck and body metastases to nodes with Ferumoxtran 10-enhanced MR imaging: Phase III safety and efficacy study. Radiology 2003;228(3):777-88.

[19] Hudgins PA, Anzai Y, Morris MR, Lucas MA. Ferumoxtran-10, a superparamagnetic iron oxide as a magnetic resonance enhancement agent for imaging lymph nodes: A phase 2 dose study. Am J Neuroradiol 2002;23(4):649-56.

[20] Keller TM, Michel SC, Frohlich J, Fink D, Caduff R, Marincek B, et al. USPIO-enhanced MRI for preoperative staging of gynecological pelvic tumors: preliminary results. Eur Radiol 2004;14(6):937-44.

[21] Mack MG, Balzer JO, Straub R, Eichler K, Vogl TJ. Superparamagnetic iron oxide-enhanced MR imaging of head and neck lymph nodes. Radiology 2002;222(1):239-44.

[22] McCauley TR, Rifkin MD, Ledet CA. Pelvic lymph node visualization with MR imaging using local administration of ultra-small superparamagnetic iron oxide contrast. J Magn Reson Imaging 2002;15(4):492-7.

[23] Iversen NK, Frische S, Thomsen K, Laustsen C, Pedersen M, Hansen PB, et al. Superparamagnetic iron oxide polyacrylic acid coated γ-Fe_2O_3 nanoparticles do not affect kidney function but cause acute effect on the cardiovascular function in healthy mice. Toxicol Appl Pharm 2013;266:276-88.

[24] Kooi ME, Cappendijk VC, Cleutjens KB, Kessels AG, Kitslaar PJ, Borgers M, et al. Accumulation of ultrasmall superparamagnetic particles of iron oxide in human atherosclerotic plaques can be detected by *in vivo* magnetic resonance imaging. Circulation 2003;107(19):2453-8.

[25] Qiu D, Zaharchuk G, Christen T, Ni WW, Moseley ME. Contrast-enhanced functional blood volume imaging (CE-fBVI): Enhanced sensitivity for brain activation in humans using the ultrasmall superparamagnetic iron oxide agent ferumoxytol. Neuroimage 2012;62(3):1726-31.

[26] Hayes AW. Principles and methods of toxicology. CRC Press; 2001.

[27] Dores-Sousa JL, Duarte JA, Seabra V, Bastos ML, Carvalho F, Costa VM. The age factor for mitoxantrone's cardiotoxicity: Multiple doses render the adult mouse heart more susceptible to injury. Toxicology 2015;329:106-19.

[28] Bolliger AP, Everds NE. Hematology of laboratory rodents: mouse (*Mus musculus*) and rat (*Rattus norvegicus*). In: D. J. Weiss and K. J. Wardrop. Schalm's Veterinary Hematology. 2010. p. 852-62.

[29] Ramos P, Santos A, Pinto NR, Mendes R, Magalhaes T, Almeida A. Iron levels in the human brain: A post-mortem study of anatomical region differences and age-related changes. J Trace Elem Med Bio 2014;28(1):13-7.

[30] Bancroft JD, Gamble M. Theory and practice of histological techniques. 6th edn. London: Churchill Livingston; 2008.

[31] Rossato LG, Costa VM, Dallegrave E, Arbo M, Dinis-Oliveira RJ, Santos-Silva A, et al. Cumulative mitoxantrone-induced haematological and hepatic adverse effects in a subchronic *in vivo* study. Basic Clin Pharmacol 2014;114(3):254-62.

[32] Croghan C, Egeghy PP. Methods of dealing with values below the limit of detection using Sas. Southern SAS User Group, St. Petersburg, FL. September 22-24, 2003.

[33] Huang XJ, Choi YK, Im HS, Yarimaga O, Yoon E, Kim HS. Aspartate aminotransferase (AST/GOT) and alanine aminotransferase (ALT/GPT) detection techniques. Sensors-Basel 2006;6(7):756-82.

[34] Marunak SL, Leiva L, Denegri MEG, Teibler P, de Perez OA. Isolation and biological characterization of a basic phospholipase A_2 from *Bothrops jararacussu* snake venom. Biocell 2007;31(3):355-64.

[35] Zhu MT, Wang B, Wang Y, Yuan L, Wang HJ, Wang M, et al. Endothelial dysfunction and inflammation induced by iron oxide nanoparticle exposure: Risk factors for early atherosclerosis. Toxicol Lett 2011;203(2):162-71.

[36] Freitas M, Porto G, Lima JL, Fernandes E. Isolation and activation of human neutrophils *in vitro*. The importance of the anticoagulant used during blood collection. Clin Biochem 2008;41(7-8):570-5.

[37] Portnoi D, Freitas A, Holmberg D, Bandeira A, Coutinho A. Immunocompetent autoreactive lymphocytes B are activated cycling cells in normal mice. J Exp Med 1986;164(1):25-35.

[38] Cassatella MA. The production of cytokines by polymorphonuclear neutrophils. Immunol Today 1995;16(1):21-6.

[39] Johnson AH. The host response to grafts and transplantation immunology. In: J. P. Kreier. Infection, resistance, and immunology. New York: Taylor & Francis; 2002. p. 212.

[40] Remick DG. Cytokines and cytokine receptors: principles of action. In: Z. Kronfol. Cytokines and mental health. Kluwer Academic Publishers; 2003. p. 8-9.

[41] Chen BA, Jin N, Wang J, Ding J, Gao C, Cheng J, et al. The effect of magnetic nanoparticles of Fe_3O_4 on immune function in normal ICR mice. Int J Nanomed 2010;5:593-9.

[42] Linder MC. Mobilization of stored iron in mammals: A review. Nutrients 2013;5(10):4022-50.

[43] Yang L, Kuang H, Zhang W, Aguilar ZP, Xiong Y, Lai W, et al. Size dependent biodistribution and toxicokinetics of iron oxide magnetic nanoparticles in mice. Nanoscale 2015;7(2):625-36.

[44] Wang J, Chen Y, Chen B, Ding J, Xia G, Gao C, et al. Pharmacokinetic parameters and tissue distribution of magnetic Fe_3O_4 nanoparticles in mice. Int J Nanomed 2010;5:861-66.

[45] Brain JD. Mechanisms, measurement, and significance of lung macrophage function. Environ Health Persp 1992;97:5-10.

[46] Estevanato L, Cintra D, Baldini N, Portilho F, Barbosa L, Martins O, et al. Preliminary biocompatibility investigation of magnetic albumin nanosphere designed as a potential versatile drug delivery system. Int J Nanomed 2011;6:1709-17.

[47] Almeida JP, Chen AL, Foster A, Drezek R. *In vivo* biodistribution of nanoparticles. Nanomedicine-UK 2011;6(5):815-35.

[48] Gomes A, Fernandes E, Lima JLFC, Mira L, Corvo ML. Molecular mechanisms of anti-inflammatory activity mediated by flavonoids. Curr Med Chem 2008;15(16):1586-605.

Figure legends

Figure 1. Iron biodistribution (liver, spleen, tail, lungs and heart) in CD-1 mice administered with PAA-coated IONs (0, 8, 20 or 50 mg/kg, i.v.) 24 hours before. ***p<0.001, **p<0.01 and *p<0.05 when compared to control (mice administered with 0.9% saline solution). Data are expressed as organ iron (µg iron/g of organ). Values are given as mean ± SEM (n = 6).

Figure 2. Light micrographs of paraffin sections from mouse liver stained with haematoxylin-eosin (A, C and E) and Perl's Prussian blue (B, D and F). No iron was detected in control animals with both stainings (E and F). In animals exposed to PAA-coated IONs (A, B, C and D), iron-loaded Kupffer cells (thin arrows) in sinusoids (thick arrows - endotheliocytes) were observed. Under lower magnification, it is possible to detect the abundance of the iron in the liver of treated animals both with haematoxylin-eosin (A) and with Perl's Prussian blue (B). Boxed area in A is shown at higher magnification on image below (C), where it is possible to observe that, with this staining, the Kupffer cell cytoplasm has a granular and golden brown appearance. Binucleate hepatocytes (bH) are common in the mice.

Figure 3. Light micrographs of paraffin sections from liver of mice exposed to PAA-coated IONs stained with haematoxylin-eosin. Under lower magnification (A) clusters of the early necrotic hepatocytes (eNH) were identified by an increase of eosinophilia. Boxed area is shown at higher magnification on the right (B). At this magnification, it is possible to observe a local distribution pattern of eosinophilic hepatocytes and also the presence of iron-loaded Kupffer cells (thin arrows).

Figure 4. Mice spleen. With Masson's trichrome staining (A, B and C), both control and PAA-coated IONs mice spleens showed a normal morphology (A), with a smaller proportion of red pulp (R). In mice, the splenic red pulp (B) is a major site of myeloid, erythroid hyperplasia and megakaryocytic hyperplasia (Meg - megakaryocyte). As shown in C, the white pulp (W) is a lymphoid area consisting of sheaths of lymphoid cells composed primarily of T cells (T) around the central arteriole (A). No iron was detected in white pulp with the Perls' blue staining, both in control and treated animals (50 mg/kg) (D). When compared with the control (E), the splenic red pulp had a great amount of iron-laden macrophages in treated animals (50 mg/kg) (F).

Figure 5. Kidney of mice exposed to PAA-coated IONs stained with Masson's trichrome. No histopathologic alterations were found in mice kidney after the treatment. Abbreviations are: PT – Proximal tubule; DT – Distal tubule; AT – Afferent arteriole; RSC - Renin-secreting cell; VP – Vascular polar; C – Renal corpuscle; BS – Bowman's space; BC - Bowman's capsule; P - Podocytes.

Figure 6. MDA evaluation in liver and kidney of CD-1 mice administered with PAA-coated IONs (0, 8, 20 or 50 mg/kg) 24 hours before. ***$p<0.001$ when compared to control (mice administered with 0.9% saline solution). Data are expressed as pmol MDA/mg protein. Values are given as mean ± SEM ($n \geq 5$).

Figure 1

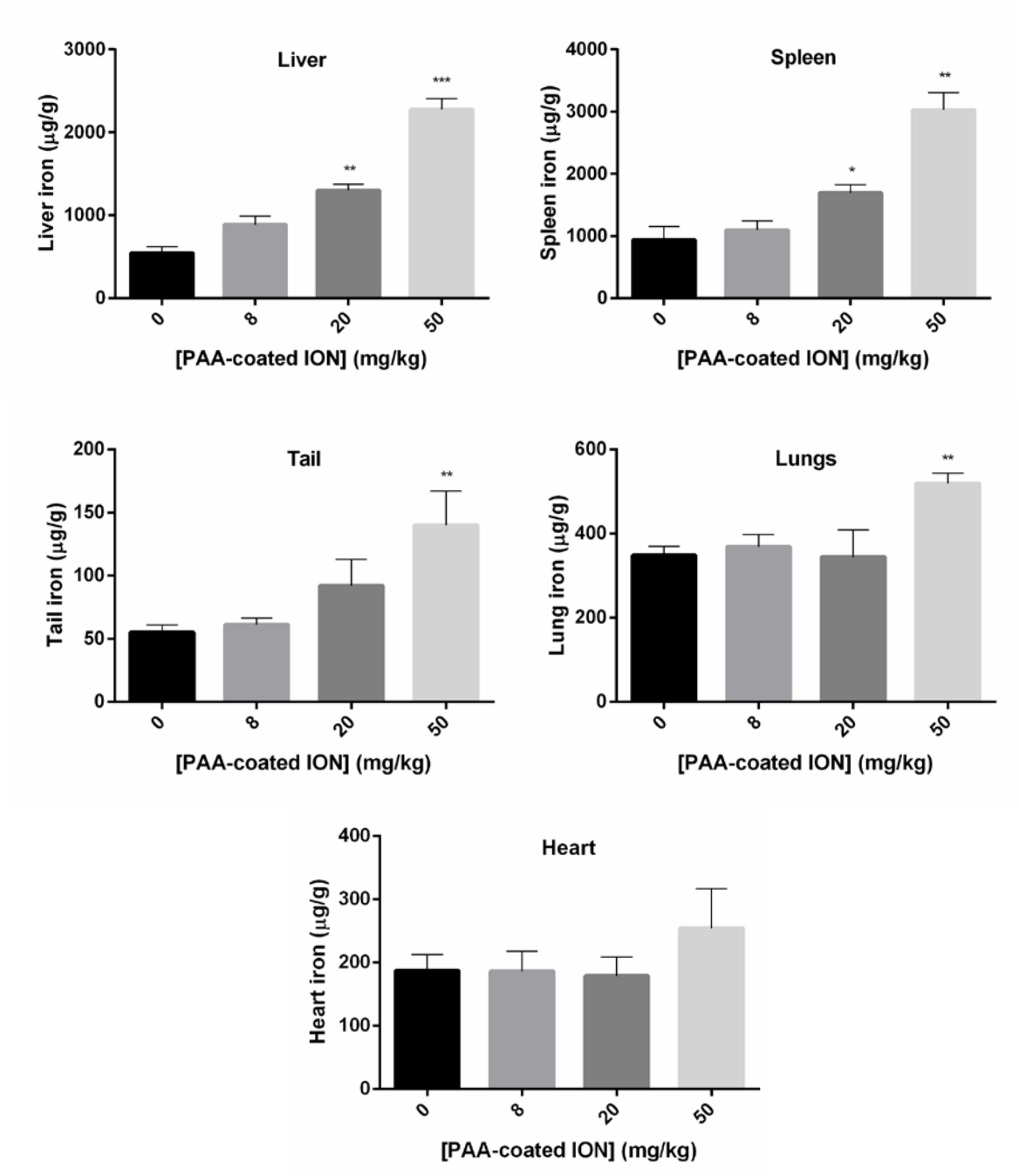
Liver
Liver iron (µg/g)
3000
2000
1000
0
**
***
0
8
20
50
[PAA-coated ION] (mg/kg)
Spleen
Spleen iron (µg/g)
4000
3000
2000
1000
0
*
**
0
8
20
50
[PAA-coated ION] (mg/kg)
Tail
Tail iron (µg/g)
200
150
100
50
0
**
0
8
20
50
[PAA-coated ION] (mg/kg)
Lungs
Lung iron (µg/g)
600
400
200
0
**
0
8
20
50
[PAA-coated ION] (mg/kg)
Heart
Heart iron (µg/g)
400
300
200
100
0
0
8
20
50
[PAA-coated ION] (mg/kg)

Figure 2

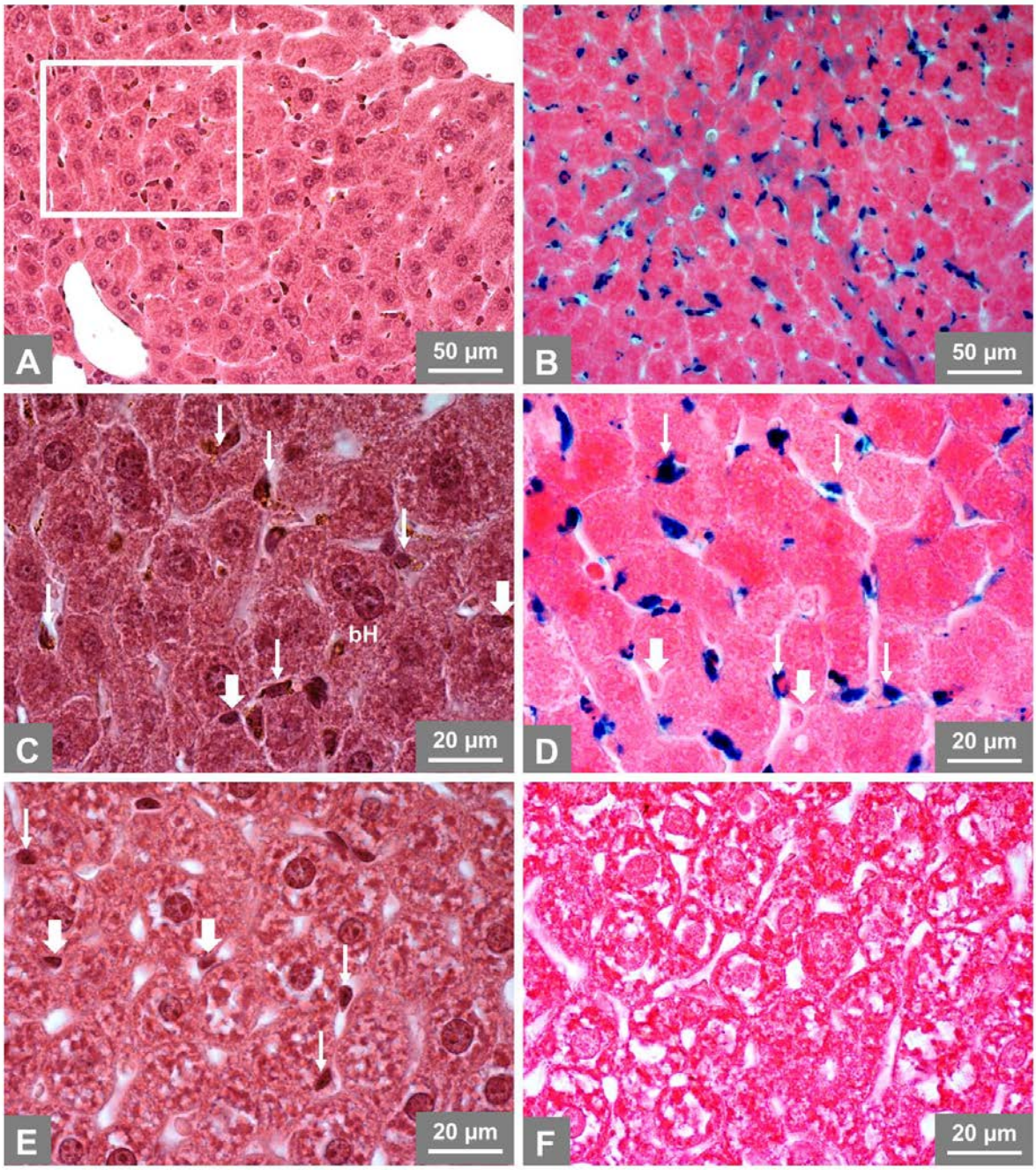

Figure 3

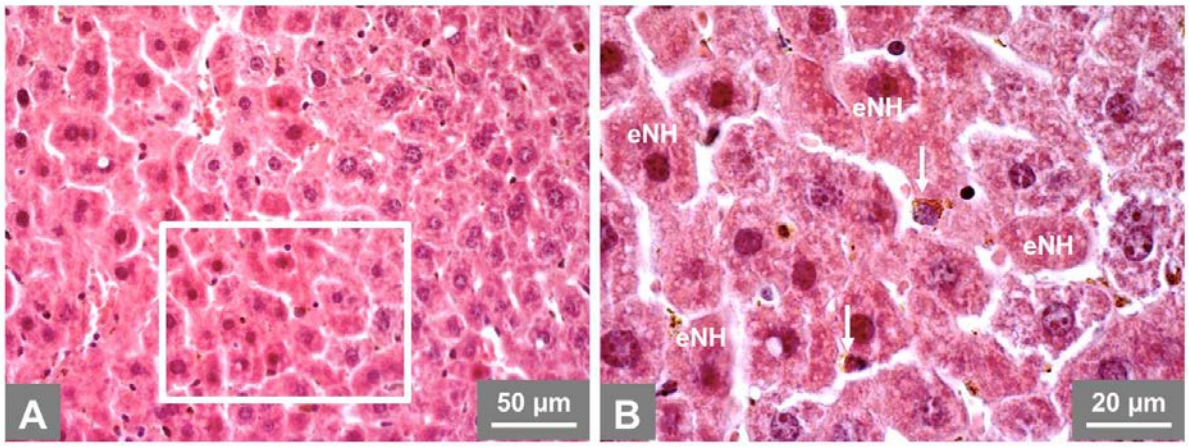

Figure 4

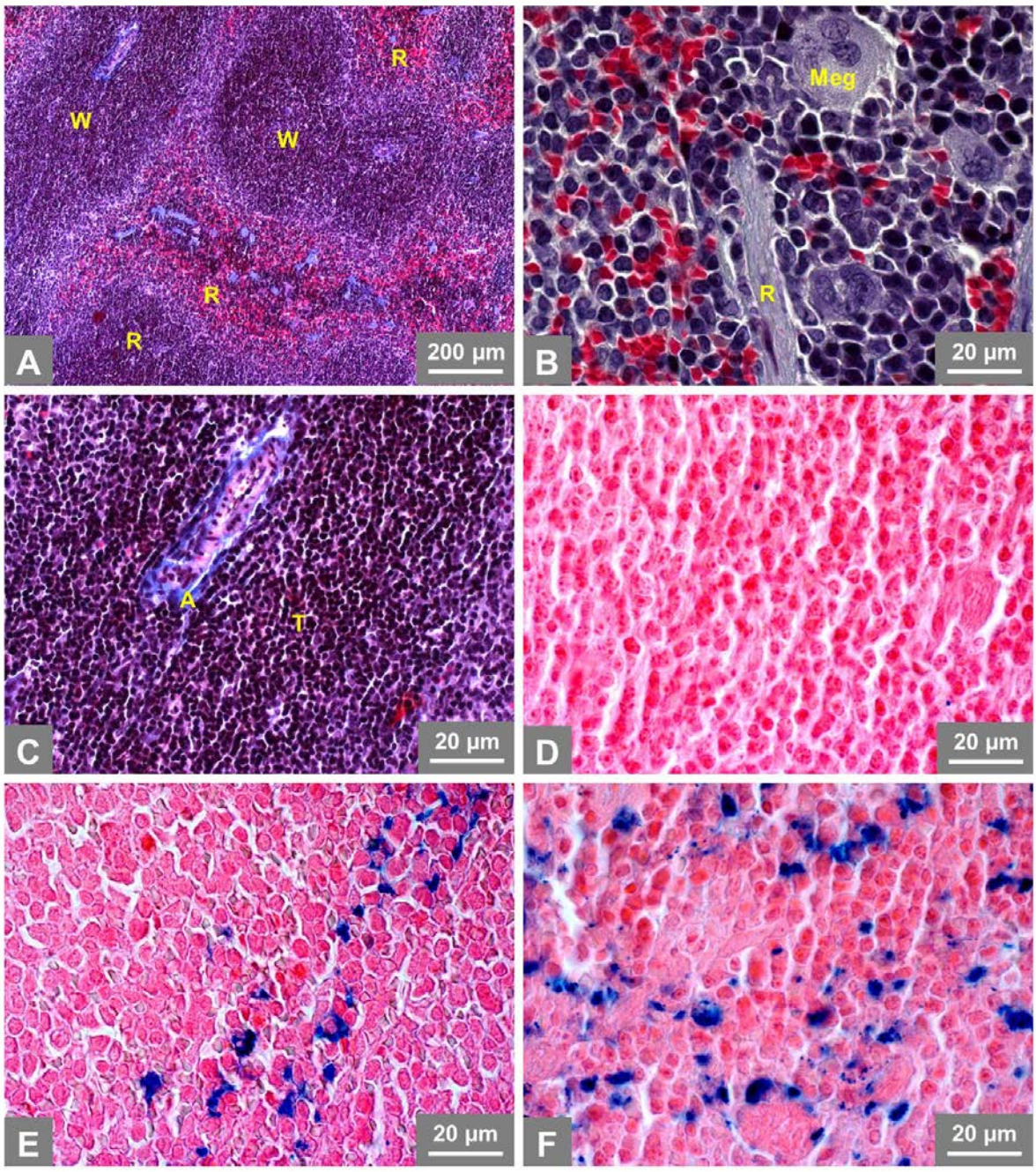

Figure 5

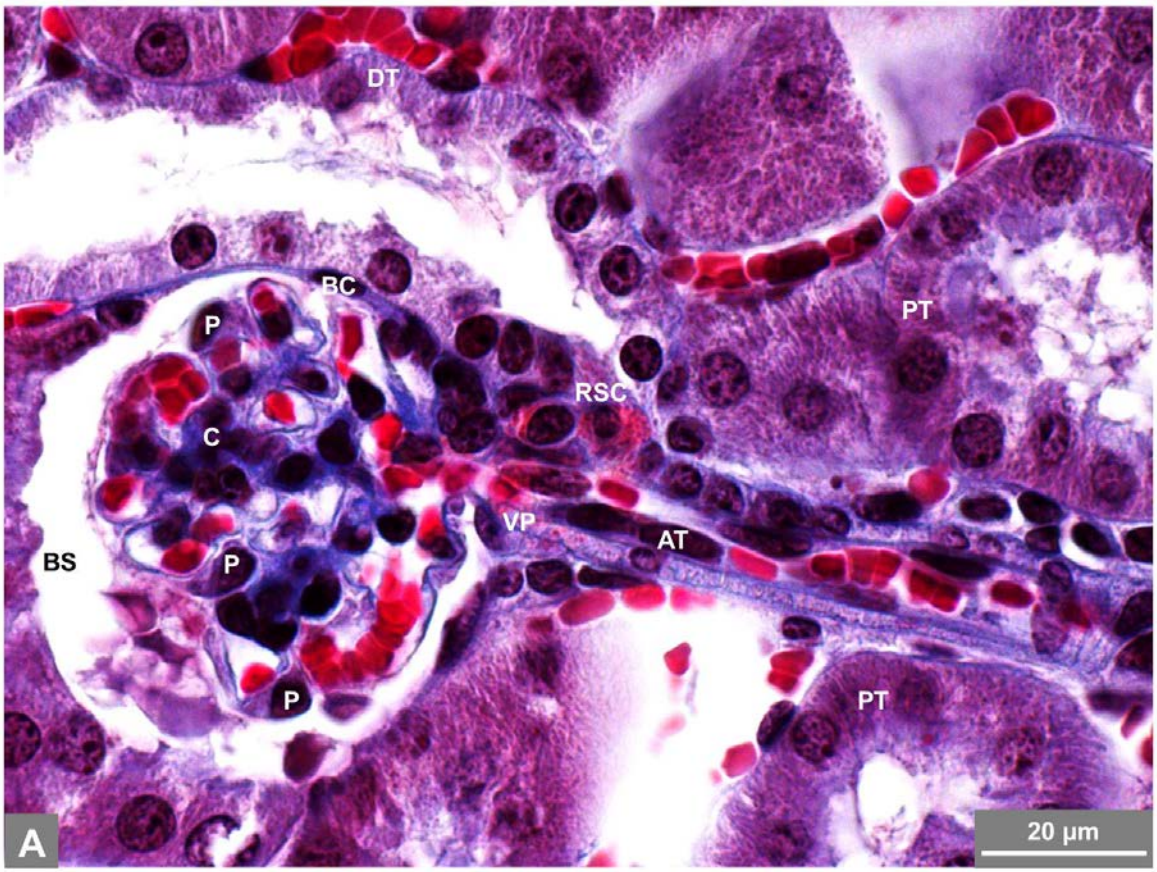

Figure 6

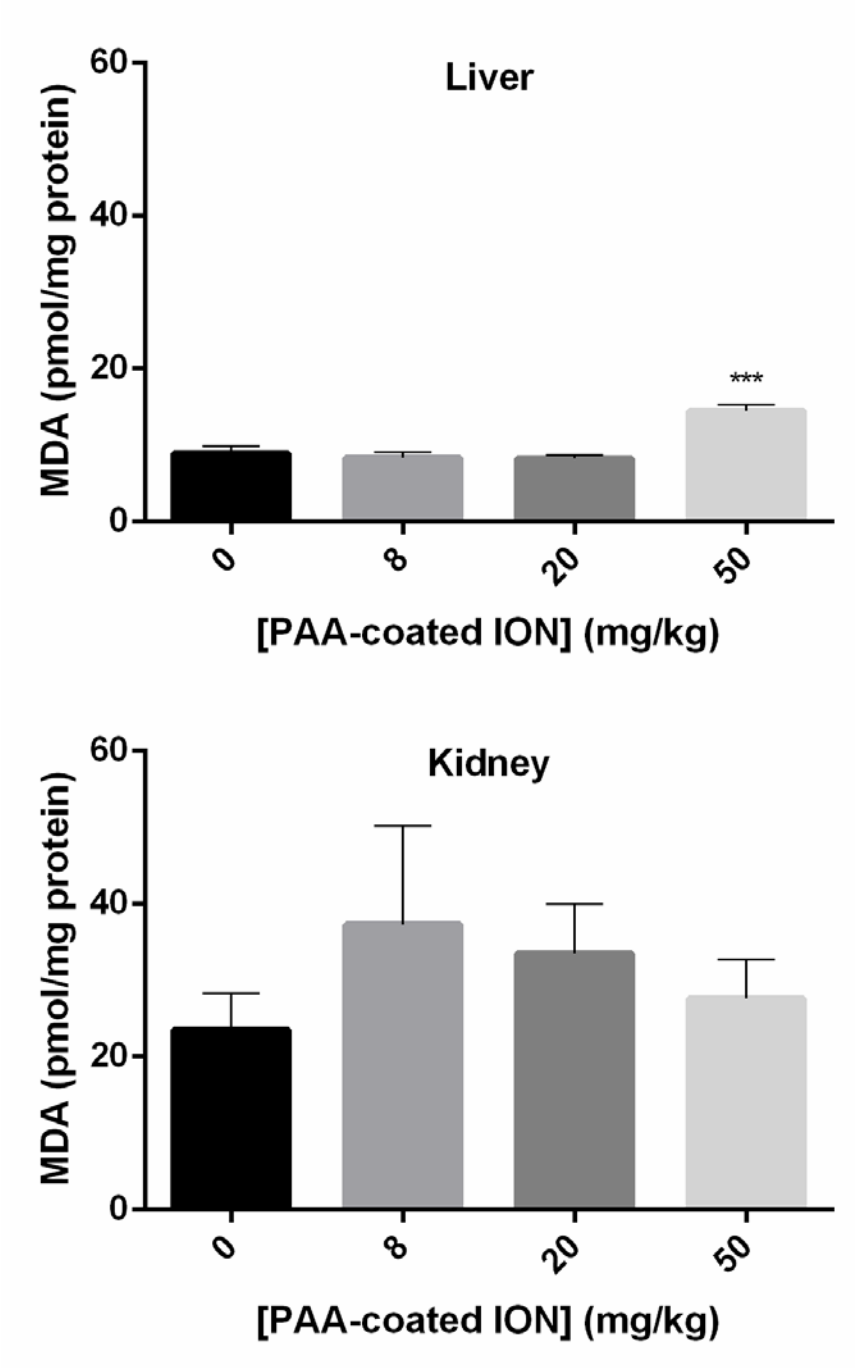
Liver
MDA (pmol/mg protein)
60
40
20
0
***
0
8
20
50
[PAA-coated ION] (mg/kg)
Kidney
MDA (pmol/mg protein)
60
40
20
0
0
8
20
50
[PAA-coated ION] (mg/kg)

Table 1. Plasma levels of AST, ALT and total CK in CD-1 mice exposed to PAA-coated IONs (0, 8, 20 or 50 mg/kg).

	Groups			
	0 mg/kg	8 mg/kg	20 mg/kg	50 mg/kg
AST (U/L)	66.8 ± 17.3	50.7 ± 8.1	45.8 ± 8.5	38.8 ± 3.5
ALT (U/L)	32.4 ± 5.4	33.0 ± 3.5	22.8 ± 1.9	25.3 ± 2.2
CK (U/L)	58.5 ± 6.3	124.3 ± 22.6*	88.0 ± 6.9	81.7 ± 13.2

Values are presented as mean ± SEM, n = 4 to 6 per group. *p<0.05 when compared to control (mice administered with 0.9% saline solution).

Table 2. Leukocyte differential counts for mice injected with PAA-coated IONs (0, 8, 20 or 50 mg/kg).

Leukocytes (%)	Groups			
	0 mg/kg	8 mg/kg	20 mg/kg	50 mg/kg
Neutrophils	12.0 ± 0.6	15.8 ± 0.8	18.7 ± 0.8**	21.2 ± 2.0****
Small Lymphocytes	75.5 ± 0.7	68.2 ± 2.4	68.8 ± 2.6	60.0 ± 2.5***
Large Lymphocytes	8.5 ± 1.5	11.2 ± 2.6	10.2 ± 2.5	16.8 ± 1.4*
Monocytes	3.0 ± 1.0	4.3 ± 0.4	2.2 ± 0.7	2.0 ± 0.9
Eosinophils	0.3 ± 0.2	0.0 ± 0.0	0.0 ± 0.0	0.0 ± 0.0
Basophils	0.7 ± 0.3	0.5 ± 0.3	0.2 ± 0.2	0.0 ± 0.0

Values are presented as mean ± SEM, n = 6 per group. ****p<0.0001, ***p<0.001, **p<0.01 and *p<0.05 when compared to control (mice administered with 0.9% saline solution).

Table 3. Body and organs weight of CD-1 mice administered with PAA-coated IONs (0, 8, 20 or 50 mg/kg).

Parameters	Groups			
	0 mg/kg	8 mg/kg	20 mg/kg	50 mg/kg
0 hours				
Body weight (g)	34.50 ± 0.62	32.83 ± 0.40	33.33 ± 0.99	33.50 ± 1.18
24 hours				
Body weight (g)	34.33 ± 0.61	32.75 ± 0.79	32.83 ± 1.11	33.00 ± 1.03
Liver weight/total weight ratio (%)	6.55 ± 0.29	6.65 ± 0.15	6.30 ± 0.15	6.46 ± 0.31
Spleen weight/total weight ratio (%)	0.38 ± 0.01	0.39 ± 0.02	0.39 ± 0.02	0.41 ± 0.04
Lungs weight/total weight ratio (%)	0.52 ± 0.02	0.51 ± 0.01	0.51 ± 0.02	0.51 ± 0.04
Kidneys weight/total weight ratio (%)	1.60 ± 0.92	1.77 ± 0.06	1.63 ± 0.08	1.81 ± 0.05
Brain weight/total weight ratio (%)	1.28 ± 0.06	1.27 ± 0.03	1.36 ± 0.05	1.47 ± 0.07
Heart weight/total weight ratio (%)	0.39 ± 0.01	0.38 ± 0.02	0.41 ± 0.01	0.40 ± 0.01
Testes weight/total weight ratio (%)	0.52 ± 0.01	0.59 ± 0.04	0.58 ± 0.03	0.62 ± 0.05

Values are presented as mean ± SEM, n = 6 per group.

Table 4. GSHt, GSSG, GSH, ATP levels and GSH/GSSG ratio of CD-1 mice exposed to PAA-coated IONs (0, 8, 20 or 50 mg/kg).

Parameters	Groups							
	Liver				Kidneys			
	0 mg/kg	8 mg/kg	20 mg/kg	50 mg/kg	0 mg/kg	8 mg/kg	20 mg/kg	50 mg/kg
GSHt (nmol/mg protein)	44.06 ± 4.60	46.18 ± 4.73	46.92 ± 3.90	48.19 ± 3.81	7.18 ± 1.98	7.30 ± 1.99	7.55 ± 1.73	7.78 ± 1.51
GSSG (nmol/mg protein)	1.16 ± 0.09	1.20 ± 0.08	1.34 ± 0.10	1.32 ± 0.14	0.12 ± 0.04	0.11 ± 0.02	0.11 ± 0.02	0.12 ± 0.02
GSH (nmol/mg protein)	41.74 ± 4.42	43.79 ± 4.60	44.24 ± 3.78	45.54 ± 3.58	6.93 ± 1.92	7.08 ± 1.95	7.33 ± 1.69	7.54 ± 1.47
GSH/GSSG ratio	35.54 ± 1.37	36.49 ± 2.57	33.32 ± 2.56	35.04 ± 2.03	54.11 ± 9.41	56.47 ± 8.70	65.26 ± 5.19	62.86 ± 8.05
ATP (nmol/mg protein)	7.92 ± 1.12	6.90 ± 1.02	7.22 ± 1.01	5.38 ± 0.70	1.43 ± 0.39	1.42 ± 0.38	1.22 ± 0.19	1.64 ± 0.18

Values are presented as mean ± SEM, n = 6 per group.

CHAPTER III

INTEGRATED DISCUSSION AND CONCLUSIONS

III.1. INTEGRATED DISCUSSION

Iron oxide nanoparticles (IONs) are endowed with unique physicochemical properties that enable its use in several biomedical applications. However, like any other drug or compound intended for human use, the safety of IONs needs to be clearly established, and all potential biological/adverse effects well studied. The studies assessing the effect of IONs on the cells of immune system, namely neutrophils, lymphocytes, monocytes, are still scarce and some of them have given contradictory results. Moreover, the biological effects of IONs with some coatings that are described as promising for some biomedical applications, namely polyacrylic acid (PAA), require further pre-clinical examination. Therefore, we felt the need to deepen the knowledge existing so far in this area.

We started our studies evaluating the interaction of PAA-coated and non-coated magnetite IONs in human neutrophils, given that these cells are the most abundant leukocytes in blood and constitute the first line of innate host defense against pathogens and associated acute inflammations [1]. In this first study, the ability of these IONs to induce oxidative burst was studied, given that neutrophils, when activated, produce reactive oxygen species (ROS) and reactive nitrogen species (RNS), mainly through the activation of the enzyme nicotinamide adenine dinucleotide phosphate (NADPH) oxidase [1]. It was verified that PAA-coated and non-coated IONs were able to trigger oxidative burst in human neutrophils. IONs-induced oxidative burst was inhibited by diphenyleneiodonium chloride (DPI), a NADPH oxidase inhibitor, demonstrating that IONs-induced oxidative burst occurs via NADPH activation. IONs are believed to induce redox cycling and catalytic chemistry via the Fenton reaction [2]. Our study, however, demonstrates that IONs also have the ability to activate NADPH oxidase. Although the hypothesis that IONs could be able to activate NADPH oxidase has been raised previously [3], this was, to the best of our knowledge, the first study showing the involvement of NADPH oxidase in the production of ROS induced by IONs.

As it is known that ROS may interfere with cell death pathways, namely by triggering mitochondrial dysfunction and consequent cytochrome c release [4] or by downregulating antiapoptotic proteins related to extrinsic and intrinsic apoptotic pathways [5,6], the effect of these IONs on neutrophils' cell death pathways was also evaluated. Although we observed that both IONs studied (PAA coated and non-coated IONs) do not induce necrosis, we observed that they are able to interfere with the natural apoptotic

course of neutrophils. However, PAA-coated and non-coated magnetite IONs revealed to trigger opposite responses regarding this process: while PAA-coated IONs demonstrated to increase apoptosis, non-coated IONs showed to inhibit and/or delay the apoptotic process. Two of the apoptotic pathways are the mitochondrial-mediated or intrinsic and the receptor-mediated or extrinsic. In mitochondrial-mediated or intrinsic apoptosis, a loss in membrane potential occurs and the consequent release of soluble factors into the cytosol, such as cytochrome c and apoptosis inducing factor (AIF), as well as Smac/Diablo takes place [7]. Cytochrome c forms a complex with a cytosolic protein named apoptosis protease-activating factor 1 (Apaf 1) to activate caspase 9 [7]. Receptor-mediated or extrinsic pathway is triggered by the activation of death receptors such as those activated by Fas ligand, tumor necrosis factor (TNF)-related apoptosis-inducing ligand or TNF. The activation of these receptors results in the formation of the death-inducing signaling complex composed by the Fas-associated death domain (FADD) and procaspase 8 and caspase 8 is activated [8]. In both pathways, the initiator caspases (caspase 8 in extrinsic and caspase 9 in intrinsic pathway) activate downstream effector caspases, mainly caspase 3, by proteolytic induction of its inactive zymogen form. Effector caspases cleave cytoplasmic and nuclear components, and promote deoxyribonucleic acid (DNA) degradation and cell dismantling, which converges in the demise of the cell [8]. In order to find out on which apoptotic pathway(s) IONs are interfering, caspases 3, 8 and 9 activities were measured. PAA-coated IONs increased all these caspases activities, while non-coated IONs decreased only caspases 3 and 9. These data led us to conclude that PAA-coated IONs are able to induce apoptosis via intrinsic and extrinsic pathways, while non-coated IONs exert their inhibitory effect only via intrinsic pathway. Given that p53 is reported to be activated by DNA damage resulting from ROS and RNS production [9], and may trigger apoptosis, typically via mitochondrial pathway but also via receptor-mediated pathway [10], we hypothesized that apoptosis could be also triggered in response to p53 activation due to ROS and RNS production. Our results showed, for the first time, that PAA-coated IONs were able to activate p53 in neutrophils in part of the individuals tested. Therefore, under the experimental conditions of this study, p53 activation does not seem to be essential to trigger apoptosis, given that apoptotic process was increased for all donors tested with PAA-coated IONs, while p53 activation occurred only for one part of the donors.

The interactions between the cell and IONs are determined by the physicochemical properties of the nanoparticles (NPs) surface, namely surface charge, hydrodynamic radius, agglomeration status, among others [11,12]. Consequently, PAA

coating will determine new interactions with the neutrophils, altering this way their properties and changing their effects. Visually, using optic microscopy, it was possible to observe that PAA reduce the aggregation phenomenon, highly visible in non-coated IONs and less visible in PAA-coated IONs. Therefore, it is possible that the aggregation state of the non-coated IONs may have perturbed the apoptotic process, while the PAA-coated IONs, well dispersed in the cytoplasm, could be able to activate cellular machinery, promoting a cellular response.

The aim of our second work was to evaluate the effect of our IONs on cytokine production in human blood cells given that, after arrival of the neutrophils to the inflammation site, other inflammatory cells belonging to blood, namely lymphocytes, are activated, which results in an exacerbated cytokine production [13]. The results obtained showed us that both IONs studied were able to induce the release of the cytokines tested [IL-1β, TNF-α, IL-6, IL-8, interferon gamma (IFN-γ) and IL-10] by human blood cells, in the following decreasing order of extent, for PAA-coated IONs IL-6 > IL-8 > TNF-α > IFN-γ > IL-1β > IL-10 and for the non-coated IONs IL-8 > IL-6 > IL-1β > IFN-γ > TNF-α > IL-10. These cytokines are known to mediate inflammatory reactions, as indicated by cytokines produced and/or associated with Th1 cells, such as IFN-γ, TNF-α, IL-1β and IL-8, and also by their involvement in B cell activation and differentiation (Th2), such as IL-6 and IL-10 [14,15]. Some previous studies have already reported that IONs are able to induce cytokine production in different cells [16,17]. However, these studies did not establish a correlation between the cytokines produced and the inflammatory pathways that may be behind their activation. Therefore, we used inhibitors of the most relevant pathways [c-Jun-N-terminal kinase (JNK), p38 mitogen-activated protein kinase (MAPK), nuclear factor kB (NF-kB), activator protein 1 (AP-1) and transforming growth factor beta activated kinase (TAK1)], in order to find out which of those were able to inhibit cytokine induction triggered by IONs. By doing that, we were able to verify that TAK1 and p38 MAPK inhibitors were able to inhibit the production of all the cytokines tested, which led us to conclude that IONs studied activate TAK1 and p38 MAPK, inducing this way cytokine production. Moreover, JNK inhibitor also provoked a decrease of IFN-γ, IL-8 and TNF-α production, which demonstrates that JNK pathway induction by IONs is also directly involved in the production of these cytokines. AP-1 and NK-kB inhibitors, however, did not inhibit cytokine production, having in some cases even increased cytokine production. However, this does not mean that AP-1 and NF-kB are not involved in IONs-induced cytokine production. As it was previously referred, in the presence of inhibitors of these pathways, a negative feedback mechanism may occur, thereby enhancing or prolonging

TAK1 activation [18]. Moreover, as it is known, TAK1 is competent for activation of mitogen activated protein kinase kinase (MKK) 3, 6 and other kinases, and its activation indirectly results in p38 MAPK and JNK activation [18] and p38 MAPK and JNK activate some members of AP-1 family that lead to the production of the above mentioned cytokines [19,20]. Therefore, one may postulate that AP-1 is probably indirectly involved in the IONs-induced cytokine production. Likewise, TAK1 has also the ability to activate the NF-kB pathway [21], and therefore this pathway is also indirectly activated by IONs. It is important to mention that, given that both IONs studied (PAA-coated and non-coated IONs) showed to be able to activate cytokine production at a similar extent, although with some small variations in the production of each cytokine individually, PAA coating did not show to be able to alter the interaction of non-coated IONs with the immune system cells of the blood, and their ability to activate inflammatory pathways. In our first work, although we had concluded that these IONs had opposite effects concerning apoptosis, they had similar effects concerning ROS production by human neutrophils. In fact, inflammatory processes and ROS production in neutrophils are correlated. When neutrophils infiltrate sites of injury by responding to chemical cues elicited by proinflammatory cytokines and chemokines produced by monocytes, neutrophils, lymphocytes and other cells of the immune system, they produce ROS and RNS that can directly induce DNA base oxidation and deamination and can indirectly lead to base alkylation via lipid peroxidation [22,23].

Therefore, the aim of our third work was to evaluate the genotoxicity of PAA-coated and non-coated IONs in human T lymphocytes, given that these cells have the important role of stimulating macrophage and B-lymphocyte activities mainly via production of regulatory cytokines [24] and present a high rate of division [25]. The results obtained showed that both IONs studied are not genotoxic to human T lymphocytes, not triggering the occurrence of chromosomal aberrations. Although there are studies reported in the literature that are in accordance with our study [26,27], some studies have already reported that IONs provoke genotoxicity in several cells [28,29]. The fact that different cells and/or cellular lines were used in these above mentioned cases, may have contributed to the differences in the results. It is known, as it was previously mentioned, that cell cycle arrest allows cells to properly repair eventual defects, thus preventing their transmission to the resulting daughter cells [30]. Indeed, in the presence of DNA damage, cells have the ability to arrest proliferation in G1 and G2 until the damage is repaired [30]. Consequently, we also evaluated the effect of IONs on the cell cycle. The results obtained show that PAA-coated and non-coated IONs did not have any effect on cell cycle, which

leads us to conclude that the absence of genotoxicity in human T lymphocytes is not related to cell cycle arrest and repair of eventual defects.

It is known that bleomycin (BLM), a known antibiotic used in anticancer therapy, with clastogenic properties, exerts a synergistic effect with other xenobiotics concerning genotoxic promotion [31]. Given that BLM induces chromosome damage through simultaneous binding to oxygen and redox-active transition metals, such as Fe^{2+}, as previously mentioned [32], and as both IONs used in this study are presented in the form of magnetite, where iron is present as a mixture of Fe^{3+} and Fe^{2+} ions [33], we considered that it would be important to evaluate the ability of IONs to interact with this clastogenic agent, exacerbating its genotoxicity. Our results demonstrated that, although both IONs showed some tendency to increase the genotoxicity of BLM, this increase was not statistically significant, which allow us to conclude that none of the studied IONs potentiate the genotoxicity of BLM under the experimental conditions in which the study was performed.

Given that our PAA-coated and non-coated IONs had demonstrated relevant toxicological and inflammatory data *in vitro*, we felt it was important to verify if these relevant results could be reproducible *in vivo*. For this purpose, PAA-coated IONs were administered intravenously to male CD-1 mice with 8 weeks and their biodistribution and effects on organs were evaluated 24 hours after. The reason why only PAA-coated IONs were chosen for *in vivo* studies was that, when IONs are used for biomedical purposes, they are always coated in order to prevent aggregation [34]. Moreover, we had already verified in our three previous works that non-coated IONs have a great tendency to aggregate and this aggregation could potentially lead to embolism after intravenous administration [35].

In order to ascertain if PAA-coated IONs were able to cause liver, heart or muscle damage, alanine aminotransferase (ALT), aspartate aminotransferase (AST) and creatine kinase (CK) were determinated in blood. The results revealed that PAA-coated IONs did not trigger ALT or AST alterations while, for CK, there were an increase for the lowest concentration tested. As it was previously mentioned, AST and ALT are parenchymal intracellular enzymes released into systemic circulation when there is hepatocellular and cardiac injury, usually involving necrosis [36]. Therefore, this result may lead us to conclude that the IONs studied did not cause hepatic and cardiac injury. However, when hepatic histological studies were performed, it was revealed that foci of early necrotic cells were found. The explanation found for this fact was that these cells probably had not time

to release their content and, consequently, the enzymes ALT and AST, until the moment the sacrifice occurred. Concerning CK, as this enzyme is a marker of muscle damage [37], its increase revealed that some muscular damage may have occurred. The reason why this increase occurred only for the lowest concentration, not having been observed an increase in a concentration-dependent manner, remains to be elucidated.

Given that in our first work we had verified that PAA-coated IONs were able to trigger ROS production by human neutrophils and in our second work we had verified that these IONs were able to trigger cytokine production through inflammatory pathways activation, we considered that evaluating the pro-inflammatory potential of the same IONs *in vivo* was of utmost importance. Therefore, differential leukocytes counts, as well as cytokine production, in the whole blood, were evaluated. The cytokines here evaluated, accordingly to the cytokines evaluated in our second work, are equally cytokines that mediate inflammatory reactions, IFN-γ, TNF-α and IL-12p70 being involved in Th1 responses and IL-6, IL-10 and monocyte chemoattractant protein-1 (MCP-1) in Th2 responses [14,38]. The results obtained showed that, comparatively to control mice, PAA-coated IONs-treated animals presented an increase in neutrophils and large lymphocytes. Given that, as previously referred, neutrophils constitute the first line of innate host defense against pathogens and associated acute inflammations [1] and that small lymphocytes, when activated, transform into large lymphocytes [39], this increase put in evidence the existence of an inflammatory process. However, contrarily to what had happened *in vitro*, there was not an increase in cytokine production *in vivo*. This does not mean that cytokine production in the presence of IONs did not occur. In fact, it is described that, once the cytokines are produced, they are rapidly cleared: the half-life of most cytokines is usually minutes *in vivo*, while *in vitro*, as there is lack of the renal and hepatic clearance mechanisms, the half-life of cytokines is substantially greater [40]. Therefore, at the end of 24 hours, it is possible that, *in vivo*, the cytokines produced by PAA-coated IONs had been already metabolized and eliminated and, for this reason, they were not detected as it had occurred *in vitro*. However, we also raised the hypothesis that the exposure time necessary to trigger cytokine production *in vivo* may be superior to the time observed *in vitro* and, therefore, cytokine production may have not occurred until the 24 hours of study, occurring at a later time point. Further studies at several exposure times would be necessary in order to prove these hypotheses.

Besides evaluation of the PAA-coated IONs capacity to induce necrotic damage and inflammatory processes, the biodistribution of the studied IONs indicated that they accumulated essentially in liver, spleen and, to a lesser extent, in lung. In fact, these

results were expected since, as it was previously referred, liver is the major site of iron storage, the site of synthesis for major proteins of iron metabolism and a regulator of iron traffic into the body [41]. It is, also, together with spleen, the major organ responsible for the recycling of iron [42]. This last fact may explain why PAA-coated IONs have also accumulated in the spleen. Regarding lung, we hypothesize that this accumulation occurred due to the capacity of lung macrophages to ingest particles from the circulating blood [43]. As macrophages are cells involved in inflammatory process, with functions in antigen presentation, phagocytosis and immunomodulation through production of cytokines and growth factors [22], the accumulation of these IONs in lung revealed a relationship with a possible pro-inflammatory process. Moreover, in our histological studies in liver, an accumulation of iron was observed in Kupffer cells of PAA-coated IONs-treated animals as well as a cytoplasmic eosinophilia in early necrotic cells, which, again, put in evidence the occurrence of an inflammatory process. Additionally, histological studies in spleen revealed an increase in iron concentration in splenic red pulp of PAA-coated IONs-treated animals. Given that red pulp is a blood filter that removes foreign material and contains also macrophages actively phagocytic [44], the accumulation of the IONs studied in the spleen played favourably with the hypothesis that PAA-coated IONs accumulate in organs rich in phagocytic cells.

In fact, and as it was previously mentioned, when a foreign body is internalized by phagocytes, an inflammatory process is triggered with inflammatory mediators and ROS production [45]. Moreover, and as we had previously demonstrated *in vitro* in our first work that these IONs induce ROS production in human neutrophils, oxidative stress parameters, such as malondialdehyde (MDA), reduced glutathione (GSH) and oxidized glutathione (GSSG) levels were evaluated in liver and kidney, due to the role of these organs in metabolization and excretion, respectively. In liver, an increase in MDA levels was observed in PAA-coated IONs-treated mice, which suggested the occurrence of ROS formation in this organ and consequent macromolecules attack by these ROS, namely lipids containing carbon-carbon double bonds, leading to formation of lipid hydroperoxides, which form MDA, among others, as secondary products [46]. However, the observed ROS production was not enough to produce alterations in GSH and GSSG.

In kidney, neither MDA nor GSH and GSSG levels were altered in PAA-coated IONs-treated mice. Moreover, in histological and biodistribution studies performed in kidney, we observed that the studied IONs do not accumulate in this organ and, for this reason, they do not exert any adverse effect.

As it is known that oxidative damage may impair adenosine triphosphate (ATP) production [47], we decided that it was important to evaluate ATP production. ATP levels were not significantly affected by PAA-coated IONs, although a decrease tendency in the liver was found. Therefore, *in vivo*, although an inflammatory process has been put in evidence, with consequent internalization of the studied IONs by phagocytes of the liver, spleen and lung, the oxidative damage seems to have been limited, not having caused severe damage to cell organelles, such as mitochondria.

We finish this dissertation mindful of having contributed to a better understanding of the biological effects triggered by IONs but also certain that much more studies are required for a greater awareness of their consequences when they are used for biomedical purposes.

III.2. CONCLUSIONS

- From the results obtained in this dissertation, it may be concluded that:
- *In vitro,* PAA-coated and non-coated IONs:

  - induced oxidative burst in human neutrophils through NADPH oxidase activation;
  - PAA-coated IONs induced intrinsic and extrinsic apoptotic pathways, while non-coated IONs inhibited and/or delayed intrinsic apoptotic pathway in human neutrophils;
  - activated directly TAK1, JNK and p38 MAPK pathways, inducing thereby the production of the cytokines IL-1β, TNF-α, IL-6, IL-8, IFN-γ and IL-10 in human whole blood;
  - did not induce an increase in chromosomal aberrations nor in the cell cycle of human T lymphocytes, not being therefore genotoxic;
  - did not increase the genotoxic behavior of BLM.

- *In vivo*, the acute administration of PAA-coated IONs:

  - accumulated in phagocytic cells in the periportal zone of the liver and in splenic red pulp as well as in the lung;
  - induced an increase in neutrophils' and large lymphocytes' frequency and a slight increase in CK levels in mouse blood;
  - did not induce alterations in AST, ALT and in the cytokines IL-6, IL-10, IFN-γ, TNF-α and IL-12p70 and chemokine MCP-1 levels in mouse blood;
  - induced an increase in MDA levels in mouse liver but not in mouse kidney;
  - do not induce alterations in GSSG, GSH and ATP levels nor in the GSH/GSSG ratio in mouse liver and kidney.

As a final conclusion, the IONs studied revealed the ability to influence cell death processes and activate inflammatory pathways *in vitro* and *in vivo*, showing also a certain ability to cause liver toxicity *in vivo*. The results obtained in this study suggest that caution should be taken when these IONs are used for biomedical purposes and should constitute a starting point to further *in vitro* and *in vivo* studies, in order to determine more precisely the toxicological potential of these IONs and avoid nefarious consequences to the human health.

III.3. REFERENCES

[1] Freitas M, Lima JL, Fernandes E. Optical probes for detection and quantification of neutrophils' oxidative burst. A review. Anal Chim Acta 2009;649(1):8-23.

[2] Shubayev VI, Pisanic TR, 2nd, Jin S. Magnetic nanoparticles for theragnostics. Adv Drug Deliver Rev 2009;61(6):467-77.

[3] Radu M, Munteanu MC, Petrache S, Serban AI, Dinu D, Hermenean A, et al. Depletion of intracellular glutathione and increased lipid peroxidation mediate cytotoxicity of hematite nanoparticles in MRC-5 cells. Acta Biochim Pol 2010;57(3):355-60.

[4] Circu ML, Aw TY. Reactive oxygen species, cellular redox systems, and apoptosis. Free Radical Bio Med 2010;48(6):749-62.

[5] Moungjaroen J, Nimmannit U, Callery PS, Wang LY, Azad N, Lipipun V, et al. Reactive oxygen species mediate caspase activation and apoptosis induced by lipoic acid in human lung epithelial cancer cells through Bcl-2 down-regulation. J Pharmacol Exp Ther 2006;319(3):1062-69.

[6] Wang LY, Azad N, Kongkaneramit L, Chen F, Lu YJ, Jiang BH, et al. The Fas death signaling pathway connecting reactive oxygen species generation and FLICE inhibitory protein down-regulation. J Immunol 2008;180(5):3072-80.

[7] Chen F, Shi X. Intracellular signal transduction of cells in response to carcinogenic metals. Crit Rev Oncol Hemat 2002;42(1):105-21.

[8] Franco R, Sanchez-Olea R, Reyes-Reyes EM, Panayiotidis MI. Environmental toxicity, oxidative stress and apoptosis: menage a trois. Mutat Res 2009;674(1-2):3-22.

[9] Simbula G, Columbano A, Ledda-Columbano GM, Sanna L, Deidda M, Diana A, et al. Increased ROS generation and p53 activation in a-lipoic acid-induced apoptosis of hepatoma cells. Apoptosis 2007;12(1):113-23.

[10] Amaral JD, Xavier JM, Steer CJ, Rodrigues CMP. The role of p53 in apoptosis. Discov Med 2010;45:145-52.

[11] Ayala V, Herrera AP, Latorre-Esteves M, Torres-Lugo M, Rinaldi C. Effect of surface charge on the colloidal stability and *in vitro* uptake of carboxymethyl dextran-coated iron oxide nanoparticles. J Nanopart Res 2013;15(8):1874.

[12] Hoskins C, Cuschieri A, Wang L. The cytotoxicity of polycationic iron oxide nanoparticles: Common endpoint assays and alternative approaches for improved understanding of cellular response mechanism. J Nanobiotechnology 2012;10:15.

[13] Mocsai A. Diverse novel functions of neutrophils in immunity, inflammation, and beyond. J Exp Med 2013;210(7):1283-99.

[14] Oreja-Guevara C, Ramos-Cejudo J, Aroeira LS, Chamorro B, Diez-Tejedor E. TH1/TH2 Cytokine profile in relapsing-remitting multiple sclerosis patients treated with Glatiramer acetate or Natalizumab. Bmc Neurol 2012;12:95.

[15] Babu S, Nutman TB. Proinflammatory cytokines dominate the early immune response to filarial parasites. J Immunol 2003;171(12):6723-32.

[16] Park EJ, Kim H, Kim Y, Yi J, Choi K, Park K. Inflammatory responses may be induced by a single intratracheal instillation of iron nanoparticles in mice. Toxicology 2010;275(1-3):65-71.

[17] Ban M, Langonne I, Huguet N, Goutet M. Effect of submicron and nano-iron oxide particles on pulmonary immunity in mice. Toxicol Lett 2012;210(3):267-75.

[18] Clark AR, Dean JL. The p38 MAPK pathway in rheumatoid arthritis: A sideways look. Open Rheumatol J 2012;6:209-19.

[19] Karin M. The regulation of AP-1 Activity by mitogen-activated protein-kinases. J Biol Chem 1995;270(28):16483-86.

[20] Kikuchi T, Hagiwara K, Honda Y, Gomi K, Kobayashi T, Takahashi H, et al. Clarithromycin suppresses lipopolysaccharide-induced interleukin-8 production by human monocytes through AP-1 and NF-kB transcription factors. J Antimicrob Chemoth 2002;49(5):745-55.

[21] Craig R, Larkin A, Mingo AM, Thuerauf DJ, Andrews C, McDonough PM, et al. p38 MAPK and NF-kB collaborate to induce interleukin-6 gene expression and release. Evidence for a cytoprotective autocrine signaling pathway in a cardiac myocyte model system. J Biol Chem 2000;275(31):23814-24.

[22] Beckmann N, Cannet C, Babin AL, Ble FX, Zurbruegg S, Kneuer R, et al. *In vivo* visualization of macrophage infiltration and activity in inflammation using magnetic resonance imaging. Wiley Interdiscip Rev Nanomed Nanobiotechnol 2009;1(3):272-98.

[23] Meira LB, Bugni JM, Green SL, Lee CW, Pang B, Borenshtein D, et al. DNA damage induced by chronic inflammation contributes to colon carcinogenesis in mice. J Clin Invest 2008;118(7):2516-25.

[24] Newsholme P. Why is L-glutamine metabolism important to cells of the immune system in health, postinjury, surgery or infection? J Nutr 2001;131(9 Suppl):2515S-22S; discussion 23S-4S.

[25] Lialiaris T, Lyratzopoulos E, Papachristou F, Simopoulou M, Mourelatos C, Nikolettos N. Supplementation of melatonin protects human lymphocytes *in vitro* from the genotoxic activity of melphalan. Mutagenesis 2008;23(5):347-54.

[26] Freyria FS, Bonelli B, Tomatis M, Ghiazza M, Gazzano E, Ghigo D, et al. Hematite nanoparticles larger than 90 nm show no sign of toxicity in terms of lactate dehydrogenase release, nitric oxide generation, apoptosis, and comet assay in murine alveolar macrophages and human lung epithelial cells. Chem Res Toxicol 2012;25(4):850-61.

[27] Guichard Y, Schmit J, Darne C, Gate L, Goutet M, Rousset D, et al. Cytotoxicity and genotoxicity of nanosized and microsized titanium dioxide and iron oxide particles in Syrian hamster embryo cells. Ann Occup Hyg 2012;56(5):631-44.

[28] Magdolenova Z, Drlickova M, Henjum K, Runden-Pran E, Tulinska J, Bilanicova D, et al. Coating-dependent induction of cytotoxicity and genotoxicity of iron oxide nanoparticles. Nanotoxicology 2013;1-13.

[29] Bhattacharya K, Hoffmann E, Schins RF, Boertz J, Prantl EM, Alink GM, et al. Comparison of micro- and nanoscale Fe^{+3}-containing (hematite) particles for their toxicological properties in human lung cells *in vitro*. Toxicol Sci 2012;126(1):173-82.

[30] Malumbres M, Barbacid M. Cell cycle, CDKs and cancer: a changing paradigm. Nat Rev Cancer 2009;9(3):153-66.

[31] Lee R, Kim YJ, Lee YJ, Chung HW. The selective effect of genistein on the toxicity of bleomycin in normal lymphocytes and HL-60 cells. Toxicology 2004;195(2-3):87-95.

[32] Mir LM, Tounekti O, Orlowski S. Bleomycin: Revival of an old drug. Gen Pharmacol 1996;27(5):745-8.

[33] Aranda A, Sequedo L, Tolosa L, Quintas G, Burello E, Castell JV, et al. Dichloro-dihydro-fluorescein diacetate (DCFH-DA) assay: A quantitative method for oxidative stress assessment of nanoparticle-treated cells. Toxicol Vitro 2013;27(2):954-63.

[34] Roohi F, Lohrke J, Ide A, Schutz G, Dassler K. Studying the effect of particle size and coating type on the blood kinetics of superparamagnetic iron oxide nanoparticles. Int J Nanomed 2012;7:4447-58.

[35] Müller RH, Böhm B. Nanosuspensions. In: R. H. Müller, S. Benita and B. Böhm. Emulsions and nanosuspensions for the formulation of poorly soluble drugs. Stuttgart: Medpharm GmbH Scientific Publishers; 1998. p. 170.

[36] Huang XJ, Choi YK, Im HS, Yarimaga O, Yoon E, Kim HS. Aspartate aminotransferase (AST/GOT) and alanine aminotransferase (ALT/GPT) detection techniques. Sensors-Basel 2006;6(7):756-82.

[37] Marunak SL, Leiva L, Denegri MEG, Teibler P, de Perez OA. Isolation and biological characterization of a basic phospholipase A_2 from *Bothrops jararacussu* snake venom. Biocell 2007;31(3):355-64.

[38] Gu L, Tseng S, Horner RM, Tam C, Loda M, Rollins BJ. Control of T_H2 polarization by the chemokine monocyte chemoattractant protein-1. Nature 2000;404(6776):407-11.

[39] Portnoi D, Freitas A, Holmberg D, Bandeira A, Coutinho A. Immunocompetent autoreactive lymphocytes B are activated cycling cells in normal mice. J Exp Med 1986;164(1):25-35.

[40] Remick DG. Cytokines and cytokine receptors: principles of action. In: Z. Kronfol. Cytokines and mental health. Kluwer Academic Publishers; 2003. p. 8-9.

[41] Anderson GJ, Frazer DM. Hepatic iron metabolism. Semin Liver Dis 2005;25(4):420-32.

[42] Zhang AS, Enns CA. Iron homeostasis: Recently identified proteins provide insight into novel control mechanisms. J Biol Chem 2009;284(2):711-15.

[43] Brain JD. Mechanisms, measurement, and significance of lung macrophage function. Environ Health Persp 1992;97:5-10.

[44] Cesta MF. Normal structure, function, and histology of the spleen. Toxicol Pathol 2006;34(5):455-65.

[45] Gomes A, Fernandes E, Lima JL, Mira L, Corvo ML. Molecular mechanisms of anti-inflammatory activity mediated by flavonoids. Curr Med Chem 2008;15(16):1586-605.

[46] Ayala A, Munoz MF, Arguelles S. Lipid peroxidation: Production, metabolism, and signaling mechanisms of malondialdehyde and 4-hydroxy-2-nonenal. Oxid Med Cell Longev 2014;2014:360438.

[47] Liang HY, Van Remmen H, Frohlich V, Lechleiter J, Richardson A, Ran QT. Gpx4 protects mitochondrial ATP generation against oxidative damage. Biochem Biophys Res Co 2007;356(4):893-98.